Surface and Interface Science at the Atomic Scale

2006 Program Meeting

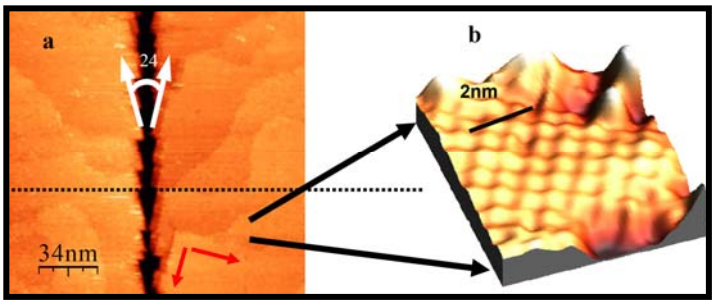

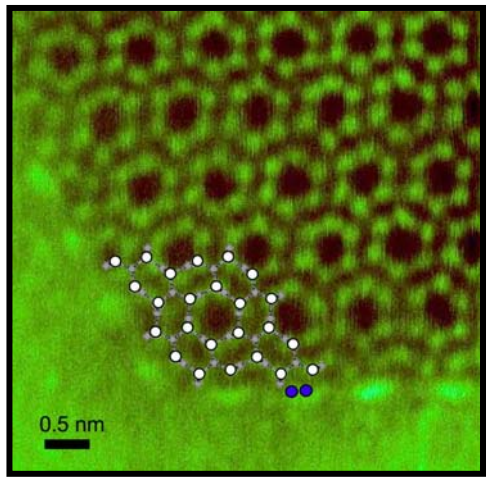

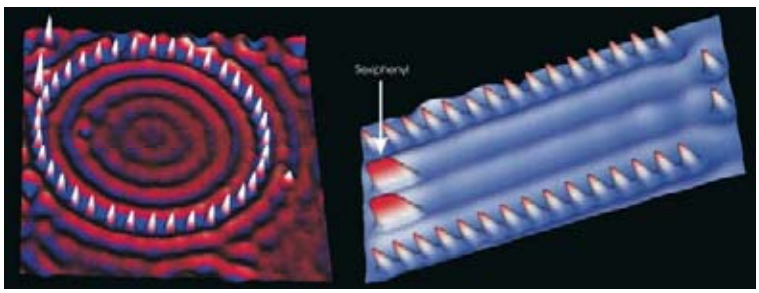

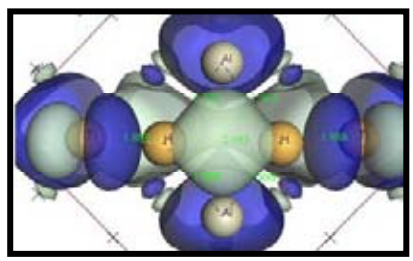

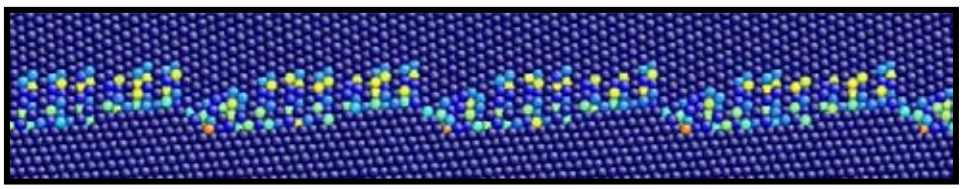

Airlie Conference Center
Warrenton, Virginia
October 29 - November 1, 2006

Office of Basic Energy Sciences

Division of Materials Sciences and Engineering

Office of Science
U.S. DEPARTMENT OF ENERGY

Cover

Top left: A $SrTiO_3$ bicrystal grain boundary intersecting the (100) surface which is in a R5xR5 reconstruction (see enlargement). The surface potential at the boundary is imaged directly with scanning surface potential microscopy. [courtesy Dawn Bonnell, U. Penn.]

Top right: Atomic resolution Z-contrast image of a Si_3N_4 grain, oriented along the [0001] zone axis, with a hexagonal edge showing the interface with Lu_2O_3. Si, N and Lu atoms are shown schematically in white, gray and blue circles, respectively. [courtesy N. D. Browning, UC Davis and LLNL, J.-C. Idrobo, ORNL and Vanderbilt, and A. Ziegler, Max-Planck Institute for Biochemistry]

Center left: The circular quantum corral and the linear electron resonator are built using individual silver atoms extracted locally with a scanning tunneling microscope tip manipulation on a Ag(111) surface at liquid helium temperatures. The circular corral is used for the investigations of detailed atom movement mechanisms during single atom manipulation. The linear electron resonator is used for the transport of sexiphenyl molecules. Here, the two sexiphenyl molecules are positioned at the left end of the resonator to shoot them toward two target atoms located at the right end using scanning tunneling microscope tip. [Courtesy: Saw-Wai Hla, Ohio University]

Center right: Structure of a catalytic Ti-Al surface complex predicted by first-principles theory to be highly active in the dissociative chemisorption of molecular hydrogen (H_2), a key step in hydrogen storage reactions. Shown in light and dark blue is the highest occupied molecular orbital (HOMO) of the Ti-Al surface/hydrogen system in its final structure after H_2 adsorption and spontaneous dissociation of the H-H bond. [Courtesy Peter Sutter, BNL]

Bottom: Atomistic simulation of a tilt grain boundary in gold. The atomic steps possess dislocation content that accommodates coherency strains across the interface. Because the coherency strain controls the step spacing, the boundary inclination is coupled to the mechanism of strain relief. [courtesy Doug Medlin, SNL]

This document was produced under contract number DE-AC05-06OR23100 between the U.S. Department of Energy and Oak Ridge Associated Universities.

Foreword

This volume highlights the scientific content of the 2006 Program Meeting on Surface and Interface Science at the Atomic Scale (SISAS) sponsored by the Division of Materials Sciences and Engineering (DMS&E) in the Office of Basic Energy Sciences (BES) of the U. S. Department of Energy (DOE). This is the first Program Meeting based on the SISAS research theme and will highlight the atomic-scale microscopy and spectroscopy studies of surfaces and interfaces in combination with theory. Electron microscopy and scanning probe microscopy are the main techniques emphasized in the Structure and Composition of Materials core research activity (CRA) for the fundamental understanding of atomic, electronic, and magnetic structures of materials. Integrated theory and experiment are needed in understanding these complex structures. While the majority of the principal investigators (PIs) at this meeting are from the Structure and Composition of Materials CRA, this meeting is broadly participated by PIs from several DMS&E research program areas including Experimental Condensed Matter Physics, Physical Behavior of Materials, X-Ray and Neutron Scattering, Materials Chemistry and Synthesis and Processing Science. The 2006 meeting is organized around the following research topics as reflected in the agenda: atomistic structure and processes at surfaces and interfaces, complex oxides and alloys, grain boundaries, defects, nanostructured materials, and new directions in probing local phenomena by electron microscopy and scanning probe microscopy.

The purpose of this Program Meeting is to bring together researchers funded by BES in this important research area, to facilitate the exchange of new results and research highlights, to foster new ideas and collaborations among the participants, and to identify needs of the research community. The meeting will also help DMS&E in assessing the state of the program, charting future directions and identifying programmatic needs. Since this is the inaugural program meeting in this area, feedback from the participants will be greatly appreciated.

I gratefully acknowledge the contributions of all meeting participants for their investment of time and for their willingness to share their ideas and research results. The dedicated efforts of the Meeting Chairs, Dawn Bonnell and Steve Pennycook, in organizing the meeting are sincerely appreciated. Thanks also go to Pete Tortorelli for assembling the book of abstracts, and to Sophia Kitts from the Oak Ridge Institute of Science and Education and Christie Ashton from DMS&E for taking care of the logistical aspects of the meeting.

Jane G. Zhu
Division of Materials Sciences and Engineering
Office of Basic Energy Sciences
Office of Science
U.S. Department of Energy

U. S. Dept of Energy
Office of Basic Energy Sciences
First DMS&E Program Meeting on
Surface and Interface Science at the Atomic Scale

October 29 – November 1, 2006

Sunday, October 29

3:00 – 6:00 pm Registration

5:00 – 6:00 pm Reception (No Host)

6:00 – 7:00 pm ***** Dinner *****

7:30 pm *Welcome and Introductory Remarks*
Jane Zhu
Program Manager, Structure and Composition of Materials

7:35 pm *Welcome and Overview of DMSE programs*
Harriet Kung
Director, Division of Materials Science and Engineering

Invited Talks
Chair: Steve Pennycook, ORNL

8:00 – 8:30 pm George Crabtree, ANL
Science and Materials for Energy: Challenges and Opportunities

8:30 -- 9:10 pm Manfred Rühle, MPI
Future Directions in Electron Microscopy

9:10 – 9:50 pm Flemming Besenbacher, University of Aarhus
Frontiers in Scanning Probe Microscopy

Monday, October 30

7:00 – 8:00 a.m. Breakfast

Session I Atomistic Structure and Processes at Surfaces
Chair: Dawn Bonnell, U. Penn

8:30 – 9:00 am Norman Bartelt, SNL
Kinetic Pathways to Nanoscale Self Assembly on Surfaces

9:00 -- 9:30 am Miquel Salmeron, LBNL
Atomic Scale Mechanical and Chemical Properties of Surface

9:30 – 10:00 pm Laurence Marks, Northwestern
Combined Experimental and Theoretical Studies of Oxide Surfaces

10:00 – 10:30 am ***** Break *****

Session II Complex Oxides
Chair: Ward Plummer, ORNL/UTK

10:30 – 11:00 am Sergei Kalinin, ORNL
Interaction of Order Parameters and Energy Dissipation in Strongly Correlated Oxides

11:00 – 11:30 am J.C. Séamus Davis, Cornell
Atomic Scale Visualization of Complex Electronic Quantum Matter in Transition Metal Oxides

11:30 – 12:00 Noon Aharon Kapitulnik, Stanford
Local Studies of Correlated Electron Materials

12:00 Noon –1:00 pm ***** Lunch *****

1:00 – 4:00 pm **Time for Interactions & Discussions**

4:00 – 6:00 pm ***Poster Session I***

6:00 – 7:00 pm ***** Dinner *****

Session III Surfaces and SPM
Chair: Jim Horwitz, DOE

7:00 – 7:30 pm Michael Tringides, Ames
Understanding and Controlling the Self-Organization of Nanostructures

7:30 -- 8:00 pm Raffi Budakian, UIUC
Three-Dimensional Sub-Surface Imaging of Single Spins Using Magnetic Resonance Force Microscopy

8:00 – 8:30 pm Lian Li, UWM
Toward the Realization of Room Temperature Ferromagnetic Semiconductors: A Spin-Polarized STM study

8:30 – 9:00 pm Lukas Novotny, U. Rochester
Near-Field Raman Spectroscopy of Carbon Nanotubes

9:00 – 11:00 pm ***Continuation of Poster Session I***

Tuesday, October 31

7:00 – 8:00 a.m. Breakfast

Session IV Grain Boundaries, Defects and Interfaces
Chair: Uli Dahmen, LBNL

8:15 – 8:45 am Yimei Zhu, BNL
Understanding the Electronic and Magnetic Structure of Advanced Materials

8:45 – 9:15 am Amanda Petford-Long, ANL
The Role of Interface Chemistry and Structure on Properties of Oxide Thin Film Heterostructures

9:15 – 9:45 am Nigel Browning, UC Davis
Materials Properties at Internal Interfaces: Fundamental Atomic Issues

9:45 – 10:15 am ***** Break *****

Session IV –continued
Chair: Vasek Vitek, U. Penn

10:15 – 10:45 am Wai-Yim Ching, U. Missouri
Electronic Structure and Properties of Complex Ceramics and Their Microstructures

10:45 – 11:15 am Emmanuelle Marquis, SNL
Finite Size Effects on Grain Boundary Structures and Precipitation Composition

11:15 – 11:45 am Mark Asta, UC Davis
Computational Investigations of Crystal-Melt Interfaces in Metals and Alloys

11:45 – 12:00 Noon Tof Carim, DOE
BES Scientific User Facilities for Investigating the Structure and Composition of Materials

12:00 Noon –1:00 pm ***** Lunch *****

1:00 – 4:00 pm **Time for Interactions & Discussions**

4:00 – 6:00 pm ***Poster Session II***

6:00 – 7:00 pm ***** Dinner *****

Session V Nanostructured materials

7:00 – 7:30 pm Susanne Stemmer, UCSB
Microstructural Origins of the Dielectric Behavior of Ferroelectric Thin Films

7:30 -- 8:00 pm Martha McCartney, ASU
Nanoscale Imaging of Electrostatic and Magnetic Fields

8:00 – 8:30 pm Jim Zuo, UIUC
Quantitative Electron Nanocrystallography

8:30 – 9:00 pm Kit Bowen, JHU
Toward the Development of Cluster-Based Materials

9:00 – 11:00 pm ***Continuation of Poster Session II***

Wednesday, NOVEMBER 1

7:00 – 8:00 am Breakfast

Session VI New Directions in Probing Local Phenomena
Chair: Jane Zhu, DOE

8:15 – 8:45 am Geoffrey Campbell, LLNL
Complex Transient Events in Materials Studied with Nanosecond Electron Microscopy

8:45 – 9:15 am Chong-Yu Ruan, MSU
Ultrafast Dynamics at Nano-Interfaces

9:15 – 9:45 am John Spence, ASU
Nanocrystallography

9:45 – 10:15 am ***** Break *****

10:15 – 10:45 am Saw-Wai Hla, Ohio U.
Single Atom and Molecule Manipulation and Its Application to Nanoscience and Technology

10:45 – 11:15 am Dawn Bonnell, U. Penn
Beyond Structure: Pushing Property Probes to Atomic Dimensions

11:15 – 11:45 am Steve Pennycook, ORNL
Watching Atoms Work: New Views of Materials through Aberration-Corrected STEM

11:45 – 12:00 Noon Closing Remarks
Dawn Bonnell and Steve Pennycook, Meeting Chairs
Jane Zhu, Meeting Organizer

12:00 Noon ***** Lunch and Adjourn *****
(Optional Box Lunches Available)

POSTER SESSION I
Monday, October 30, 2006

P-I.1
Imaging Molecules and Active Sites for Oxide-Supported Nanocatalysts
Baddorf, Dag, Kalinin, Meunier, Mullins, Overbury, Zhou

P-I.2
Experimental and Theoretical Studies of Alloyed Semiconductor Surfaces
Bickel, Modine, Pearson, **Mirecki-Millunchick**

P-I.3
Epitaxial Multifunctional Oxide Heterostructures
Chandrasekhar, Eom

P-I.4
Fundamental Investigations of Candidate Ferromagnetic Oxide Semiconductors
Chambers, Droubay, Kaspar, Wang, Heald, Shutthanandan, McCready

P-I.5
Filtered Electron Backscatter Diffraction
Deal, Hooghan, **Eades**

P-I.6
In-Situ Synchrotron X-Ray Studies of Interfacial Reactions
Eastman

P-I.7
New Magnetic Behavior of Nanostructures
Gai, Shen

P-I.8
Microscopic Subsurface Characterization of Layered Magnetic Materials using Low Temperature Magnetic Resonance Force Microscopy
Hammel

P-I.9
Atomistic Basis for Surface Nanostructure Formation
Kellogg, Feibelman, **Swartzentruber**, Bartelt

P-I.10
Hydrogen interactions with surface alloys of simple and transition metals
Roland Stumpf

P-I.11
Towards Quantitative Understanding of Strain Induced Nano-Scale Self-Assembly from Atomic-Scale
Feng Liu

P-I.12
Atomistic Transport Mechanisms in Revisible Complex Metal Hydrides
Sutter, Muckerman, Chabal

P-I.13
First Principles and Atomistic Simulation Studies of Surfaces
Wang, **Ho**

P-I.14
Multiscale Atomistic Simulation of Metal-Oxygen Surface Interactions: Methodological Development, Theoretical Investigation, and Correlation with Experiments
J. Yang

P-I.15
Phase Reconstruction and Vector Field Electron Tomography
Tandon, Phatak, **De Graef**

P-I.16
Surface evolution caused by sub-surface defect dynamics
Kevin McCarty, John Pierce and Norm Bartelt

P-I.17
Surface self-organization caused by dislocation networks
Konrad Thürmer and Norman Bartelt

POSTER SESSION II
Tuesday, October 31, 2006

P-II.1
Determining the Origins of Electronic States in Semiconductor Nanostructures
Goldman, Johnson

P-II.2
Using Plasmon Peaks in Electron Energy-Loss Spectroscopy to Determine the Physical and Mechanical Properties of Nanoscale Materials
J. Howe

P-II.3
An Integrated Computational and Experimental Study of the Dynamics of Grain Boundaries in Impure Systems
Mendelev, Liu, **Kramer**

P-II.4
Crystal-Melt Interfaces and Selection at Extreme Rates
Napolitano, Trivedi, Mendelev, Kramer

P-II.5
Bulk and Thin Film Alloys for Structural, Electronic and Energy Related Applications
Radmilovic, **Dahmen**

P-II.6
Ion Beam Irradiation Effects in Pyrochlore and Murataite Ceramics
Ewing, Wang, Lian

P-II.7
Electron Diffraction Determination of Nanoscale Structures
Parks, Xing, Li

P-II.8
Electron Microscopy of Materials
Pennycook, Varela, Lupini, Borisevich

P-II.9
Atomistic Studies of Deformation and Fracture in Materials with Mixed Metallic and Covalent Bonding:
V. Vitek

P-II.10
Atomic and Electronic Structure of Polar Oxide Interfaces
Gajdardziska-Josifovska, Weinert, Chambers

P-II.11
Engineering and Characterizing Nanoscale Multilayers
Yang, Ji, **Chang**

P-II.12
Structure and Bonding at Surfaces, Interfaces, and Low-Dimensional Solids
J. Zuo

P-II.13
First Principles Studies of Intergranular Films in Ceramics
Painter, Averill

P-II.14
Transient states during rapid chemical reactions in multilayer thin films studied with nanosecond electron microscopy
Judy S. Kim, Thomas LaGrange, **Geoffrey H. Campbell**, Nigel D. Browning, and Wayne E. King

P-II.15
Pb Nanoprecipitates in Al: Magic-Shape Effects Due to Elastic Strain
John Hamilton, Uli Dahmen and Francois Leonard

P-II.16
Accommodation of Grain Boundary Coherency Strain by Interfacial Disconnections
Doug Medlin

P-II.17
Reversal behavior of patterned ferromagnetic elements
M. Schofield, M. Beleggia, J. Lau, L. Huang, V.V. Volkov, **Y. Zhu**

P-II.18
On Calculating the Magnetic State of Nanostructures
G. Malcolm Stocks

Table of Contents

Session IV: Grain Boundaries, Defects, and Interfaces

Session V: Nanostructured Materials

Session VI: New Directions in Probing Local Phenomena

Research Summaries

Session I

Atomistic Structure and Processes at Surfaces

Surface Dynamics

Norman C. Bartelt, John C. Hamilton, Konrad Thürmer, and Kevin F. McCarty
Sandia National Laboratories, Livermore, CA 94550

Program Scope

A long-standing goal of surface science has been to develop the ability to predict how surface morphology and composition evolve during, for example, epitaxial growth. We are still far from this goal. Despite improved understanding of the general mechanisms governing surface morphology and composition, quantitatively connecting even the observed nanoscale evolution (never mind macroscopic) of any particular surface to individual atomic events is still very challenging. The difficulty is that surface structure and surface diffusion are far from simple – the energy landscape of diffusing atoms is complicated and usually the result of very delicate energy balances. Our approach to solving these sorts of problems is to use state-of-the-art, real-time microscopy to quantitatively characterize the time dependence of carefully defined, fairly simple, nanoscale surface features. We then write down statistical mechanical equations of motion that describe this evolution and relate the parameters of these models to atomic processes using statistical mechanics and density functional theory (DFT) calculations.

Our work is largely focused on addressing four general, important, scientific issues where very basic gaps exist in the understanding of kinetic pathways: 1) Film wetting and de-wetting. Thin solid films are often thermodynamically unstable; free energy can be lowered by forming 3D crystals on the surface and exposing either the bare substrate or a thin wetting layer. Despite de-wetting's ubiquity and the fairly thorough general understanding of the driving forces for de-wetting, the kinetic, atomic mechanisms by which it happens are largely unknown.[A] 2) Bulk/surface exchange. At high temperature, the time dependence of surface morphology can be controlled by bulk diffusion. This possibility, which was recognized at least since Mullins' work in the 1950's,[B] has been indirectly inferred by measurements of the decay rate of corrugated surfaces. However, the atomic mechanisms of the mass exchange between the bulk and the surface have not been systematically studied. 3) Surface self-assembly. That surfaces with two phases can lower their free energy by forming domains with periodic patterns is now well known.[C] However, these domain patterns have been convincingly observed only in a few systems. A severe constraint on self-assembly on crystalline surfaces is dynamics -- for (nanoscale) ordered patterns to form, a large fraction of the surface atoms must collectively arrange themselves. Again, the atomic mechanisms of surface diffusion are so numerous that its effect on self-assembly has not been systematically explored. 4) Oxide surfaces and metal oxidation. Finally, we focus on understanding the dynamical processes that occur on oxide surfaces and as metal surfaces are oxidized. The multicomponent materials (compounds) of these systems frequently exhibit variable composition, an additional complexity. We explore the little-understood role of point and extended defects (which allow composition changes, enable bulk/surface mass diffusion, and can accommodate oxide film strain) in controlling oxide surface structure and oxidation mechanisms.

Recent Progress

Film wetting and de-wetting Often films do not uniformly wet their substrates at equilibrium. Instead, 3D islands form, exposing the bare substrate or a very thin wetting layer. Because of the energetic cost of creating steps, a large free-energy barrier restricts thickening of any island by new-layer nucleation.[A] How this barrier is avoided to allow 3D growth to occur was a puzzle. Using low-energy electron microscopy (LEEM) to directly observe how 3D islands form (Fig. 1), we discovered that film de-wetting can occur through a remarkably simple but previously unrecognized mechanism that avoids having to nucleate new film layers.[1] In the presence of substrate steps, islands thicken by migrating down the staircase of substrate steps. Because the islands maintain a flat top, islands get one layer thicker each time they extend across a descending

substrate step, without having to nucleate a new layer. Indeed, without substrate steps, the nucleation barrier is not surmounted and 3D islands do not form.[2] We have exploited the mechanism of "downhill migration" to produce uniform arrays of metal cylinders by controlling the substrate topography prior to film deposition using a focused ion beam (FIB) to machine small holes in the substrate.[3]

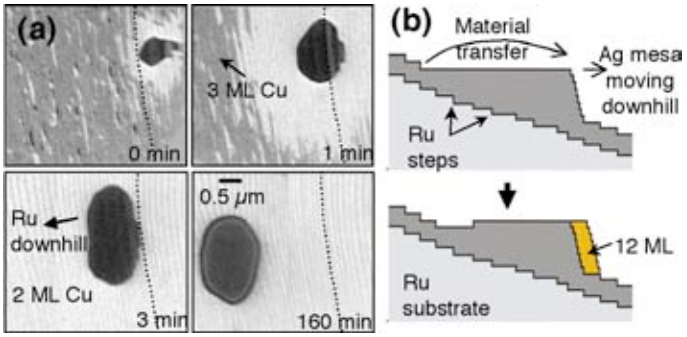

Fig. 1. A 3D island forming without new-layer nucleation by downhill migration process. (a). The Cu island moves about 2 μm down the stair case of substrate steps in the LEEM images. Initial location of island's leading edge marked with dashed line. (b) Schematic illustration of the process.

Bulk/surface exchange We have followed our first short report of the direct observation of the mass exchange between the bulk and the surface of NiAl with detailed studies of the process.[4, 5] Since this work showed that mass exchange occurred only near surface steps (not on the intervening terraces), we now know that the surface is not a spatially uniform sink and source of vacancies, as assumed in the classic continuum theories of Mullins.[A] Since then, other studies have also directly shown the importance of bulk/surface exchange in surface self-diffusion of metals.[D] We have also explored the role of bulk/surface exchange in the surface phase transitions and crystal growth of the model non-stoichiometric oxide TiO_2 (also see below).[6]

Surface self-assembly We have discovered a new mechanism that can stabilize nanometer-dimension patterns on a surface.[7, 8] Scanning tunneling microscopy (STM) images obtained during the self-assembly revealed that holes in a thin film organized into a regular hexagonal array by the motion and reactions of dislocations within the film. By analyzing the thermal vibrations of the hole array, we established that the array is stabilized by a dislocation network that interconnects the holes (Fig. 2). This mechanism of self-assembly and stabilization is distinct from the commonly invoked (but often not rigorously proven) mechanism that balances bulk elasticity against surface stress.[C] However, in both our new and the old mechanisms, rapid mass transport is needed for self-assembly to occur. We have shown that enhanced mass transport occurs by quite different processes in the various self-assembling systems we have studied -- transport by dislocation motion in Ag films on Ru, but via the fast diffusion of Cu through a Pb overlayer in the remarkable Pb/Cu system.[9-13] (The latter work is in collaboration with Gary Kellogg and co-workers in Sandia/New Mexico.) Moreover, mass transport can be greatly accelerated by "chemical" means, as we recently showed for Cu diffusion enhanced by S.[14]

Oxide surfaces and metal oxidation Our work on oxide surfaces and metal oxidation has shown that bulk/surface exchange (e.g., in TiO_2, as discussed above) is important and can lead to various forms of self-assembly. In particular, we have found that oxidation of NiAl can produce aligned rods of nanometer-dimension width.[15] Real-time observations of the rod formation reveal they grow vertically layer-by-layer. In addition to the rod-forming oxide phase, we have investigated the dynamics of Al_2O_3 formation on NiAl(110). LEEM observations reveal that translational domains (called antiphase domains in the literature) are created within isolated alumina islands as they grow or are annealed.[16] Thus, the domains do not originate when islands with displaced lattices impinge, as frequently assumed in models of film growth. Rather, even though the planar defects that bound the translation-related domains cost energy, the misfit dislocations that terminate the domain boundaries form to lower the film's strain energy.[17, 18]

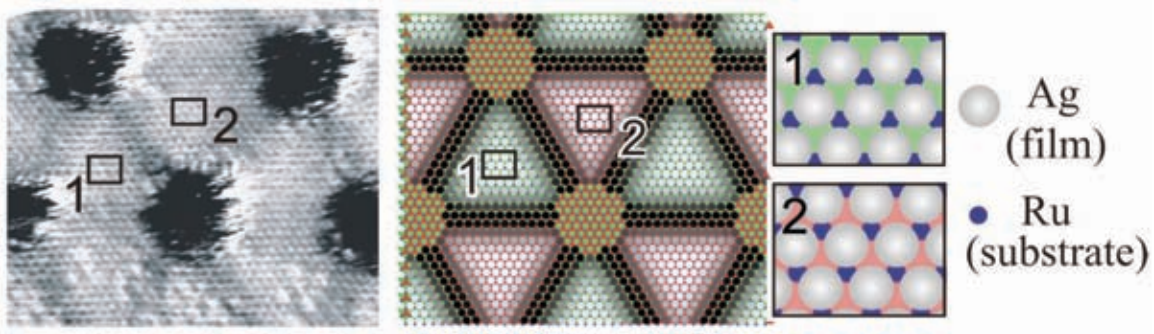

Fig. 2. Left: Atomically resolved STM image of the hole-array structure in Ag films on Ru induced by S, right: corresponding unit cell used in a Frenkel-Kontorova model. The inserts 1 and 2 show the different stacking in the two types (green and red) of triangular building blocks separated by Shockley partial dislocations.

Future Plans

Self-assembly and de-wetting Our future work will explore the interrelationships between de-wetting and self-assembly,[19] and on understanding the mechanisms of enhanced surface diffusion needed to achieve the latter. We have recently found that both Cr and Au can self-organize into long, narrow "wires" on the W(110) surface. The Cr wires are 3D (e.g., multilayer thick) and form when a thick film de-wets. Preliminary observation suggests that the mechanism of Cr wire formation is distinct from the downhill-migration pathway of de-wetting discussed above. In contrast, the Au wires are 2D (one Au atom thick) and appear to form near a structural phase transition in the Au overlayer. Finally, we will explore self-assembly and de-wetting in an important molecular crystal system, H_2O on Pt(111). In addition to the obvious importance of knowing the structure of water next to crystalline materials, understanding the mechanisms of H_2O bonding to metals presents a formidable challenge to 1st principles calculations.[E] In preliminary work, we find that bilayer films of water on Pt forms contain ordered vacancy arrays, an unanticipated result. Furthermore, for the first time, we have observed complete water multilayers using STM and tracked the coarsening of 3D islands. We will use this data to measure the rate of diffusion of water molecules on ice.

Bulk/surface exchange Another situation where bulk/surface exchange is important is when an impurity species segregates from the bulk to the surface.[20] We have started to investigate segregation in a well-characterizable model system: carbon segregating to a ruthenium surface[21] to form graphene, i.e., one-atom-thick sheets of graphitic carbon. To fully understand the energetics and kinetics of the segregation process, we have developed a new method (based on monitoring changes in electron reflectivity) to measure the spatial concentration of the mobile carbon adatoms that co-exist with the condensed carbon (i.e., the graphene) and the bulk carbon.[22] We will be able to simultaneously measure the adatom concentration and the local rate of island formation on a surface. We also intend to investigate the role of bulk/surface exchange in the surface structure and composition of an oxide, $SrTiO_3$, which has more complex bulk defects than previously studied systems.

Oxide surfaces and metal oxidation A key question is how size affects the thermodynamic stability of various structures and phases. This question is particularly important in film systems, where the interface energy and/or film's strain energy may significantly alter the stability of the system. We are exploring whether the thermodynamic stability (i.e., the Gibbs free energy) of nanometer-dimension oxide islands can be determined by measuring the temperature/O_2 pressure at which the islands neither shrink nor grow. Our preliminary analysis suggests that this method allows the relative energetic stability of competing surfaces phases to be accurately determined and compared to predictions of DFT calculations.

References

[A] W. W. Mullins and G. S. Rohrer, Nucleation barrier for volume-conserving shape changes of faceted crystals, J. American Ceramic Society **83**, 214 (2000).

[B] W. W. Mullins, Flattening of a nearly plane solid surface due to capillarity, J. Appl. Phys. **30**, 77 (1959).

[C] F. Rosei, Nanostructured surfaces: Challenges and frontiers in nanotechnology, Journal of Physics: Condensed Matter **16**, S1373 (2004).

[D] M. Ondrejcek, W. Swiech, G. Yang, and C. P. Flynn, Crossover from bulk to surface diffusion in the fluctuations of step edges on Pt(111), Philosophical Magazine Letters **84**, 69 (2004).

[E] P. J. Feibelman, Partial dissociation of water on Ru(0001), Science **295**, 99 (2002).

DOE Sponsored Publications 2004-2006

[1] W. L. Ling, T. Giessel, K. Thurmer, R. Q. Hwang, N. C. Bartelt, and K. F. McCarty, Crucial role of substrate steps in de-wetting of crystalline thin films, Surface Science **570**, L297 (2004).

[2] F. E. Gabaly, S. Gallego, C. Munoz, L. Szunyogh, P. Weinberger, C. Klein, A. K. Schmid, K. F. McCarty, and F. de la Figuera, Imaging Spin Reorientation Transitions in Consecutive Atomic Co layers on Ru(0001), Physical Review Letters **96**, 147202 (2006).

[3] K. F. McCarty, Deterministic positioning of three-dimensional structures on a substrate by film growth, Nano Letters **6**, 858 (2006).

[4] K. F. McCarty, J. A. Nobel, and N. C. Bartelt, Surface dynamics dominated by bulk thermal defects: The case of NiAl(110), Physical Review B **71**, 085421 (2005).

[5] B. Poelsema, J. B. Hannon, N. C. Bartelt, and G. L. Kellogg, Bulk-surface vacancy exchange on Pt(111), Applied Physics Letters **84**, 2551 (2004).

[6] K. F. McCarty and N. C. Bartelt, Crystal growth rate limited by step length - the case of oxygen-deficient TiO_2 exposed to oxygen, Journal of Crystal Growth **270**, 691 (2004).

[7] K. Thurmer, C. B. Carter, N. C. Bartelt, and R. Q. Hwang, Self-assembly via adsorbate-driven dislocation reactions, Physical Review Letters **92**, 106101 (2004).

[8] K. Thurmer, R. Q. Hwang, and N. C. Bartelt, Surface self-organization caused by dislocation networks, Science **311**, 1272 (2006).

[9] M. L. Anderson, N. C. Bartelt, P. J. Feibelman, B. S. Swartzentruber, and G. L. Kellogg, The effect of embedded Pb on Cu diffusion on Pb/Cu(111) surface alloys, Surface Science **600**, 1901 (2006).

[10] R. van Gastel, N. C. Bartelt, and G. L. Kellogg, Reversible shape transition of Pb islands on Cu(111), Physical Review Letters **96**, 036106 (2006).

[11] G. L. Kellogg and N. C. Bartelt, Surface-diffusion-limited island decay on Rh(001), Surface Science **577**, 151 (2005).

[12] F. Leonard, N. C. Bartelt, and G. L. Kellogg, Effects of elastic anisotropy on the periodicity and orientation of striped stress domain patterns at solid surfaces, Physical Review B **71**, 045416 (2005).

[13] R. van Gastel, N. C. Bartelt, P. J. Feibelman, F. Leonard, and G. L. Kellogg, Relationship between domain-boundary free energy and the temperature dependence of stress-domain patterns of Pb on Cu(111), Physical Review B **70**, 245413 (2004).

[14] W. L. Ling, N. C. Bartelt, K. Pohl, J. de la Figuera, R. Q. Hwang, and K. F. McCarty, Enhanced self-diffusion on Cu(111) by trace amounts of S: chemical-reaction-limited kinetics, Physical Review Letters **93**, 166101 (2004).

[15] J. P. Pierce and K. F. McCarty, Self-assembly and dynamics of oxide nanorods on NiAl(110), Physical Review B **71**, 125428 (2005).

[16] K. F. McCarty, J. P. Pierce, and C. B. Carter, Observing that translation domains form to relieve strain in a thin alumina film on NiAl(110) Applied Physics Letters **88**, 141902 (2006).

[17] F. El Gabaly, W. L. W. Ling, K. F. McCarty, and J. de la Figuera, The importance of threading dislocations on the motion of domain boundaries in thin films, Science **308**, 1303 (2005).

[18] W. L. Ling, N. C. Bartelt, K. F. McCarty, and C. B. Carter, Twin boundaries can be moved by step edges during film growth, Physical Review Letters **95**, 166105 (2005).

[19] W. L. Ling, J. C. Hamilton, K. Thürmer, G. E. Thayer, J. de la Figuera, R. Q. Hwang, N. C. Bartelt, C. B. Carter, and K. F. McCarty, Herringbone and Triangular Patterns of Dislocations in Ag, Au, and AgAu Alloy Films on Ru(0001), Surface Science **600**, 1735 (2006).

[20] P. Y. Hou and K. F. McCarty, Surface and interface segregation in β-NiAl with and without Pt addition,, Scripta Materialia **54**, 937 (2006).

[21] J. de al Figuera, J. M. Puerta, J. I. Cerda, F. E. Gabaly, and K. F. McCarty, Determining the structure of Ru(0001) from low-energy electron diffraction of a single terrace, Surface Science **600**, L105 (2006).

[22] J. de al Figuera, N. C. Bartelt, and K. F. McCarty, Electron reflectivity measurements of Ag adatom concentrations on W(110), Surface Science, in press (2006).

Atomic Scale Mechanical and Chemical Properties of Surfaces (2001-2006)

Miquel Salmeron. Lawrence Berkeley National Laboratory.

1. Purpose

The purpose of this project is to provide an understanding of the fundamental physical and chemical processes governing the tribological properties of surfaces (adhesion, friction, wear), and to determine the role of surface films (wetting layers, lubricants) in modifying these properties. Over the last few years we have concentrated in identifying and studying elementary energy dissipation processes that take place between two solids or between solid and liquid surfaces in contact. The surfaces studied included metals (Au, Pd, Ru, Cu, Pt), metal quasiycrystals (Al-Ni-Co), and minerals (mica, SiO_2, TiO2, Fe_2O_3). Important surface films studied include organic monolayers (SAM), as well as atoms and simple molecules such as oxygen, hydrogen, CO and water.

Instrumentation used in our studies includes Scanning Tunneling and Atomic Force Microscopy (STM, AFM), a host of surface characterization techniques (Auger, XPS, LEED, x-ray absorption and emission (XAS, XES), and surface sensitive optical techniques such as Second Harmonic and Sum Frequency Generation (SHG, SFG). In many cases we have developed new instrumentation, as required to accomplish our goals. Some of these instruments, including the STM have found their way into the commercial sector (RHK technologies, is the only US manufacturer of STM, based our original LBNL design). Other instruments include the High Pressure Photoelectron Spectrometer (HPPES) that makes possible to acquire XPS, and absorption spectra while the sample is under gas environments in the torr pressure range. Several companies are now developing and selling instruments based on our design (published in the Review of Scientific Instruments).

We measure forces using the AFM and the Surface Forces Apparatus (SFA).

2. Accomplishments

1) Organic self-assembled monolayers containing long alkane chains respond to applied pressure by distortions of the molecules of several well characterized types. At low pressures (1-100 MPa) gauche defects are produced at the end groups of the molecules, where steric encumbrances are not a major problem, as determined by SFG in the SFA. At higher pressures (0.1-10 GPa) internal shear processes occur leading to rigid tilts of the molecular backbones. To tilt the molecules slide past each other in discrete steps following the periodicity of the methylene groups in the chains.

2) Repeated sliding over a surface above some critical load leads to the production of point defects (vacancies). Accumulation of vacancies beyond some concentration leads to the collapse of entire atomic layers of the material leading up to wear.

3) The interaction of water with SAM films of alkyl -silanes, and -amines results in penetration of water to the substrate through defects. This changes the structural properties of the molecular film.

4) The friction force depends on the sliding velocity in a manner that depends on the chemical nature of the contacting surfaces. When the interface contains species capable of forming a network of H-bonds (OH, NH, COOH terminated surfaces) friction decreases with velocity. When no networks of connected molecules can form (CH_3, dry SiO_2, mica, etc.) friction increases with velocity.

5) We developed AFM non-contact imaging methods that make possible the study of soft and delicate surfaces, including liquid films. With it we studied wetting properties at the nanoscale, which is of fundamental importance in tribology, chemistry, environmental sciences and biology. The technique is based on the electrical forces between an ac-biased tip and the surface. We have shown the formation ordered of water films, the spreading of nanometer thin films of various liquids, including sulfuric acid, salt solutions, glycerol and liquid crystals.

6) With the newly developed HPXPS we have obtained the first well characterized isotherms and isobars of water on several oxide surfaces, including Cu(110), TiO_2, SiO_2 and Fe_2O_3.

7) Using STM we have shown that even very small amounts of surface impurities (<1%), either at the surface or buried below the first atomic layer have an enormous influence of the chemical properties of the surface.
8) We have studied the condensation and growth of water on Pd(111) and Ru(0001) with STM at temperatures from 4K to near 300K and determined the diffusion constants of water monomers. We have shown that diffusion of small clusters (dimers, trimers and tetramers) is orders of magnitude faster than monomers.
9) We have shown that diffusion of water is greatly enhanced when the scissor and stretching modes of the molecule are excited (using tunneling electrons from the STM tip to address individual water molecules).
10) We have shown that the growth and structure of water films is dominated by the H-bonding of the molecules and have shown the strong driving force that the formation of saturated H-bonds exerts on the growth.
11) We have determined diffusion constants, ordered structures, dissociation and reactions of several small molecules including H_2, O_2 and CO. Strong repulsive interactions between H and O leads to the compression of O structures upon addition of H. In contrast there is an attractive interaction between pairs of CO molecules. We have shown that the steps are important reaction centers for the formation of water from H and O on Pd(111).
12) We have found that dissociation of H2 on Pd(111) requires at least three adjacent vacancies where Pd atoms with no contact with H can be found.
13) We have found large friction anisotropy in Al-Ni-Co quasicrystal surfaces cut parallel to the decagonal axis. This surface has the peculiar property of being periodic in one direction and aperiodic in the perpendicular direction. Friction was found to be a factor of 8 lower in the aperiodic direction. We proposed that phonon excitation is less effectively in the aperiodic direction due to the formation of many gaps.
14) We have discovered an interesting correlation between friction and electronic density. Using a nearly intrinsic n-type Si substrate with patterned lines of highly doped p stripes, we could induce charge accumulation or depletion in the p regions, by simple application of a bias voltage to our conductive TiN coated tip. In accumulation the p regions showed an increase in the friction force, while no such change was observed in the low doping density n-regions, or in the p regions in depletion.

*3. Future plan*s

We will continue our studies of elementary excitations in atoms and molecules, in the form of vibration quanta and electronic transitions, using STM. The purpose is: a) to determine the vibration and electronic structure of atoms and molecules, and to determine how this structure depends on the location of the molecule on the surface such as near a step, an impurity atom, or the vicinity of another similar molecule; b) how the energy of the excitation is dissipated into other modes (vibration, librations and translations) and substrate excitations. The goal is to obtain the most fundamental information about surface reactions, and how energy is dissipated in friction.

We plan to continue our studies of water growth and wetting phenomena at the nanometer scale on a variety of surfaces including metals, oxides, ionic solids and organic surfaces to understand the molecular origin of hydrophillicity and hydrophobicity. Principal techniques will be STM, AFM and HPPES.

We will complete the construction of a new low temperature AFM (4K) for studies of surface forces and force spectroscopy on single atoms and molecules. In particular we aim at understanding the origin of molecular interaction forces in relation to their electronic structure. This instrument will also be used for studies of the structure of water and other molecules on insulating surfaces.

4. Publications from this project (2004-2006):

The role of intermolecular and molecule-substrate interactions in dertermining the structure and and stability of alkanethiols on Au(111). E. Barrena, E. Palacios-Lidón, C. Munuera, X. Torrelles, S. Ferrer, U. Jonas, M. Salmeron and C. Ocal. J. Am. Chem. Soc. 126, (1) 385 (2004).

Novel Water overlayer growth on Pd(111) characterized with STM and DFT. J. Cerda, A. Michaelides, M.L. Bocquet, P.J. Feibelman, T. Mitsui, M. Rose, E. Fomin, and M. Salmeron. Phys. Rev. Lett. 93, (11) 6101 (2004).

When Langmuir is too simple: H_2 dissociation on Pd(111) at high coverage. N. Lopez, Z. Lodziana, F. Illas and M. Salmeron. Phys. Rev. Lett. 93, 6103 (2004).

Diffusion and pair interactions of CO molecules on Pd(111). T. Mitsui, M. K. Rose, E. Fomin, D.F. Ogletree and M. Salmeron. Phys. Rev. Lett. 94, (03) 6101 (2005).

Dielectric Properties of Self-Assembled Layers of Octadecylamine on Mica in Dry and Humid Enviornments. J.J. Benitez, E. Diez-Pérez, F. Sanz and Miquel Salmeron. J. Chem. Phys. 123, 104706 (2005).

Elastic and Inelastic deformation of ethylene-passivated 10-fold decagonal Al-Ni-Co quasicrystal surface. J.Y. Park, D.F. Ogletree, C.J. Jenks, P.A. Thiel and M. Salmeron. Phys. Rev. B. 71, 144203 (2005).

The origin of contrast in STM images of oxygen on Pd (111) and its dependence on tip structure and tunneling parameters. J.M. Blanco, C. González, P. Jelínek, J. Ortega, F. Flores, R. Pérez, M. Rose, M. Salmeron, J. Méndez, J. Wintterlin and G. Ertl. Phys Rev. B. 71, 113402 (2005).

In situ study of water induced segregation of bromide in bromide-doped sodium chloride by Scanning Polarization Force Microscopy. S. Ghosal, A. Verdaguer, J.C. Hemminger and M. Salmeron. J. Phys. Chem. A 109, 4744-4749 (2005).

Electron Spectroscopy of Aqueous Solution Interfaces Reveals Surface Enhancement of Halides: Implications for Atmospheric Chemistry. S. Ghosal, J.C. Hemminger, H. Bluhm, B.S. Mun, E.L.D. Hebenstreit, G. Ketteler, D.F. Ogletree, F. Requejo and M. Salmeron. Science 307, 563 (2005).

High Frictional Anisotropy of Periodic and Aperiodic Directions on a Quasicrystal Surface. J.Y. Park, D.F. Ogletree, M. Salmeron, R.A. Ribeiro, P.C. Canfield, C.J. Jenks and P.A. Thiel. Science 309, 1354 (2005).

Sensing dipole fields at atomic steps with combined scanning tunneling and force microscopy. J.Y. Park, G.M. Sacha, M. Enachescu, D.F. Ogletree, R.A. Ribeiro, P.C. Canfield, C.J. Jenks, P.A Thiel, J.J. Sáenz and M. Salmeron. Phys. Rev. Lett. 95, 136802 (2005).

Atomic Scale coexistence of Periodic and quasiperiodic order in a 2-fold Al-Ni-Co decagonal quasicrystal surface. J.Y. Park, D. F. Ogletree, M. Salmeron, R.A. Ribeiro, P.C. Canfield, C. J. Jenks, and P.A. Thiel, Phys. Rev. B. 72, 220201R (2005).

Kinetic Effects in the Self-Assembly of Pure and Mixed Tetradecyl and Octadecylamine Molecules on Mica. J.J. Benitez and M. Salmeron. Surf. Sci. 600, 1326-1330 (2006).

The Molecular Structure of Water at Interfaces: Wetting at the Nanometer Scale. A.Verdaguer, G.M. Sacha, H. Bluhm, M. Salmeron. Chem. Rev. 106, 1478-1510 (2006).

The Electronic Structure of ensembles of Gold nanoparticles: size and proximity effects. H. Liu, B.S. Mun, G. Thornton, S.R. Isaacs, Y-S. Shon, D.F. Ogletree, and M. Salmeron. Phys. Rev. B. 72, 155430 (2005).

In situ Spectroscopic Study of the Oxidation and Reduction of Pd(111). G. Ketteler, D.F. Ogletree, H. Bluhm, H. Liu, E.L.D. Hebenstreit, M. Salmeron. J. Am. Chem. Soc. 127, 18269 (2005).

Initial stages of water adsorption on NaCl (100) studied by Scanning Polarization Force Microscopy. A. Verdaguer, G.M Sacha, D.F. Ogletree and Miquel Salmeron. J. Chem. Phys. 123, 124703 (2005).

Vibrationally assisted diffusion of H_2O and D_2O on Pd(111). Evgeny Fomin, Mous Tatarkhanov, Toshi Mitsui, Mark Rose, D.F. Ogletree and Miquel Salmeron. Surf. Sci. 600, 542 (2006).

Electronic control of friction in silicon pn junctions. J.Y. Park, D. F. Ogletree. P.A. Thiel and M. Salmeron. Science. 313, 186 (2006).

Velocity dependence of friction and hydrogen bonding effects. J. Chen, I. Ratera, J.Y. Park, and M. Salmeron. Phys. Rev. Lett. 96, 236102 (2006).

New Methods for Atomic Structure Determination of Nanoscale Materials

Laurence D. Marks
L-marks@northwestern.edu
Department of Materials Science and Engineering,
Northwestern University, Evanston, IL 60201

Program Scope

For many years transmission electron microscopy has been powerful in determining the positions of atoms. In many respects if we knew the positions of the electrons (charge density) we would not need to know where the atoms are. The scope of this program is to try and determine the positions of atoms with high precision in nanostructures, and going beyond this to find the charge density. Elements of this work are experimental, but an emerging effort is to combine experiment with density functional calculations (DFT) particularly for oxide surfaces in a synergistic effort with students and postdocs become experts in both. A "grand challenge" is to try and develop predictive rules for oxide surface structures.

Recent Progress

The work on code for direct methods (edm)[1] is now almost complete. Some minor details remain, for instance finishing up the interface for a CBED simulation package (MBFIT) from Prof. Kenji Tsuda (Tohoku University, Sendai, Japan) and finishing a public cvs. This has been a success, with the process of going from diffraction data to a structure solution speeded up by a factor of 10-100.

Work on precession diffraction has also been a success. The PhD thesis of Chris Own (http://www.numis.northwestern.edu/Research/Current/precession.shtml) as well as an instrumentation paper[2] have been quite widely used as a basic introduction to the technique as well as a guide for implementing it. Work on some of the details of the theory of precession diffraction is continuing, with a multislice analysis[3], some applications[4] as well as how precession could be applied in a Cs-corrected instrument[5] accepted for publication and a two-beam analysis[6] being written up. In progress is a more systematic analysis of how the precession scan angle effects the intensities of kinematically-forbidden/dynamically-allowed, the effects of bonding on precession intensities and research (joint with D. Van-Dyck, Antwerp) to try and obtain a closed form expression going beyond a two-beam Blackmann solution.

The precession technique is now moving beyond the development phase into widespread application. A commercial unit (Nanomegas, http://www.nanomegas.com) is now available and there are ~12 precession cameras around the world, with this number fairly rapidly increasing. With the final construction of two Northwestern units this fall (one at Northwestern, one at the University of Illinois Champaign-Urbana) research on this topic within this grant will probably be de-emphasized.

Research into the possibility of imaging bonding effects using transmission electron microscopy has moved forward. One theoretical paper on the magnitude of the change in contrast in bulk materials has appeared[7], and a second for defects[8] has been

submitted. The later is particularly interesting since it appears to be much *easier* to observe charge density effects at a defect than in a bulk material. Interestingly it is also significantly easier to observe the effects of bonding in one of the new Cs corrected instruments.

Future Plans

Our initial investigation into the effects of bonding in bulk materials is looking very promising, although it is still early in this work. Collaborations are underway with Prof. A. Kirland (Oxford) and H. Lichte (Triebenberg Laboratory) to try and observe the effects experimentally; we are also trying to observe them ourselves using our UHV transmission electron microscope. We are also working to exploit a methodology for parameterizing the bulk charge density[9] which we recently used to produce the first three-dimensional analysis of a surface charge density[10] for other problems, for instance to investigate the possible effects of bonding on the imaginary coefficient of the potential of silicon due to thermal vibrations. It is currently too early to say whether we can experimentally determine bonding effects at defects or not.

Beyond this, one thing which has become clear recently is the utility of having a strong theoretical DFT component within the group at Northwestern directly coupled with both theoretical and experimental electron diffraction work, particularly for surfaces. Over the last few years the PI has developed some expertise in DFT calculations particularly with the Wien2k code[11], both as a user and as a developer. For instance the main minimizer used in this code was contributed by the PI, some changes to the mixer are also part of the main code as well as a utility for initializing the minimization[12]. There is now a reasonable level of expertise with students and postdocs doing both the experimental work as well as the DFT calculations. The intention in the future is to shift some of the DOE supported research in this direction to support this effort.

An example of this is two ongoing pieces of work. The first is the structure of the (001) $LaAlO_3$ surface. This is an interesting problem because per surface 1x1 cell one has to have fractional extra charges to accomplish charge neutrality unlike most other (polar) surfaces. Experimental work under different funding (DOE-ICEP) determined that there was a $\sqrt{5}x\sqrt{5}$ R26 reconstruction; we then used the edm code developed under this program to solve the structure and the postdoc supported on this program (B. Deng) has performed DFT calculations to model the structure in three-dimensions as well as understand the mechanism of charge redistribution. The structure is surprisingly simple consisting of a single lanthanum vacancy per surface unit cell. The combination of DFT with the experimental results indicate that the primary mechanism of charge compensation is by increased covalency at the surface coupled with a highly delocalized fractional hole and expulsion of the hard cation (lanthanum) which is less able to form covalent bonds.

The second piece of work is a 3x3 reconstruction of the $SrTiO_3$ (111) surface. Experimental data was obtained under different funding (DOE-ICEP), again solved using the edm software. This work is in collaboration with Dr. M. Castell (Oxford) who has used STM to image the surface. The postdoc supported on this project both performed the DFT to obtain the three-dimensional structure as well as simulated the STM images which are exceedingly close to the experimental results. Somewhat similar to the $LaAlO_3$ surface the hard cation (strontium) is lost from the surface, but there are much more

substantial rearrangements than this. Loss of the strontium from one layer gives a charge-compensated structure which would have severely under-coordinated titanium atoms; this is then covered by an additional layer with a composition of stoichiometric TiO_2. Rather than adopting the normal octahedral arrangement, the co-ordination of the titanium at the surface is reduced to either 5-fold or 4-fold. This allows for increased covalency by reducing the Ti-O bond lengths which would not be possible due to the non-bonded oxygen repulsions (see [13]) if a full octahedral co-ordination was retained. The final structure is dramatically different from a simple bulk, and with 19 unique positions is one of the largest surface structures solved to date.

A "grand challenge" is to be able to obtain enough information about oxide surfaces so that one can generate rules which allow for the prediction of what structures will form under different conditions. If we can achieve this then it will become plausible to design new types of catalyst supports, as well as new type of supports for thin film growth or dielectric layers. While we are still some distance from being able to do this, some parts of such rules are starting to become clear, for instance the role of increased covalency, non-bonded oxygen repulsions and the role of hard (or soft) ions in terms of their ability to form covalent bonds near the surface. Experiments are clearly important for this, and our tools of direct methods coupled with transmission electron diffraction are rather powerful for solving structures. However this needs to be done coupled with theoretical analyses where there are still many unresolved issues such as the question of whether the so-called "surface intrinsic error"[14] is relevant for oxide surfaces, and problems such as LDA methods apparently working well for simple oxides surface energies such as for MgO (001) where they agree with quantum monte-carlo[15] whereas GGA appears at the moment to be relatively bad.

References

1 R. Kilaas, L. D. Marks, and C. S. Own, Ultramicroscopy **102**, 233 (2005).

2 C. S. Own, L. D. Marks, and W. Sinkler, Review of Scientific Instruments **76** (2005).

3 C. S. Own, W. Sinkler, and L. D. Marks, Acta Crystallographica **In Press** (2006).

4 C. S. Own, W. Sinkler, and L. D. Marks, Ultramicroscopy **106**, 114 (2006).

5 C. S. Own, W. Sinkler, and L. D. Marks, Ultramicroscopy **In Press** (2006).

6 C. S. Own, W. Sinkler, and L. D. Marks, Acta Crystallographica **In preparation** (2006).

7 B. Deng and L. D. Marks, Acta Crystallographica Section A **62**, 208 (2006).

8 B. Deng and L. D. Marks, Ultramicroscopy **Submitted** (2006).

9 L. D. Marks, J. Ciston, B. Deng, et al., Acta Crystallographica Section A **62**, 309 (2006).

10 J. Ciston, L. D. Marks, R. Feidenhans'l, et al., Physical Review B (Condensed Matter and Materials Physics) **74**, 085401 (2006).

11 P. Blaha, K. Schwartz, G. K. H. Madsen, et al., *An Augmented Plane Wave + Local Orbitals Program for Calculating Crystal Properties* (Karlheinz Schwarz, Techn. Universit¨at Wien, Austria, 2001).

12 J. Rondinelli, D. Bin, and L. D. Marks, Computational Materials Science **Submitted** (2006).
13 O. Warschkow, M. Asta, N. Erdman, et al., Surface Science **573**, 446 (2004).
14 A. E. Mattsson and D. R. Jennison, Surface Science **520**, L611 (2002).
15 Alf, D., and M. J. Gillan, Journal of Physics: Condensed Matter **18**, L435 (2006).

DOE Sponsored Publications 2004-2006

1. Own, C.S., W. Sinkler, and L.D. Marks, *Multislice Simulation of Precession Diffraction II: Reduction using Lorentz and other Corrections.* Acta Crystallographica, 2006. **In preparation**.
2. Rondinelli, J., D. Bin, and L.D. Marks, *Enhancing structure relaxations for first-principles codes: an approximate Hessian approach.* Computational Materials Science, 2006. **Submitted**.
3. Merkle, A. and L.D. Marks, *A dislocation drag model for friction.* Tribology Letters, 2006. **Submitted**.
4. Deng, B. and L.D. Marks, *Charge Defects Glow in the Dark.* Ultramicroscopy, 2006. **Submitted**.
5. Sinkler, W., C.S. Own, and L.D. Marks, *Application of a 2-beam model for improving the structure factors from precession electron diffraction intensities.* Ultramicroscopy, 2006. **In Press**.
6. Own, C.S., W. Sinkler, and L.D. Marks, *Multislice Simulation of Precession Diffraction I: Method and comparison with experiment.* Acta Crystallographica, 2006. **In Press**.
7. Own, C.S., W. Sinkler, and L.D. Marks, *Prospects for Aberration Corrected Precession Diffraction.* Ultramicroscopy, 2006. **In Press**.
8. Own, C.S., W. Sinkler, and L.D. Marks, *Rapid structure determination of a metal oxide from pseudo-kinematical electron diffraction data.* Ultramicroscopy, 2006. **106**(2): p. 114-122.
9. Marks, L.D., et al., *Fitting valence charge densities at a crystal surface.* Acta Crystallographica Section A, 2006. **62**: p. 309-315.
10. Deng, B. and L.D. Marks, *Theoretical structure factors for selected oxides and their effects in high-resolution electron-microscope (HREM) images.* Acta Crystallographica Section A, 2006. **62**: p. 208-216.
11. Own, C.S., L.D. Marks, and W. Sinkler, *Electron precession: A guide for implementation.* Review of Scientific Instruments, 2005. **76**(3).
12. Kilaas, R., L.D. Marks, and C.S. Own, *EDM 1.0: Electron direct methods.* Ultramicroscopy, 2005. **102**(3): p. 233-237.
13. Own, C.S., A.K. Subramanian, and L.D. Marks, *Quantitative analyses of precession diffraction data for a large cell oxide.* Microscopy and Microanalysis, 2004. **10**(1): p. 96-104.

Session II

Complex Oxides

Interaction of Order Parameters and Energy Dissipation in Strongly Correlated Oxides by Scanning Probe Microscopy

S.V. Kalinin, A.P. Baddorf, J.F. Wendelken, and E. W. Plummer
(sergei2, baddorfap, wendelkenjf)@ornl.gov, eplummer@utk.edu

Postdocs and students: B.J. Rodriguez, S. Jesse, J. Shin, J. Zhou

Materials Science and Technology Division, Oak Ridge National Laboratory, Oak Ridge, TN 37831

Program scope

Interactions between multiple order parameters including ferroelectric polarization, magnetization, and strain, and lattice properties underpin the beautiful physics of multiferroic materials and strongly-correlated oxides. The key goal of this program is to develop an understanding of the atomistic mechanisms of the coupling between multiple order parameters, establish roles of surfaces, interfaces, and structural defects, and ultimately probe low-level excitations and quasiparticles such as phonons, plasmons, polaritons and magnons, on the nanometer and atomic length scales. This goal is being accomplished through the synergistic effort involving (a) development of advanced Scanning Probe Microscopies capable of probing order parameter interactions and energy dissipation, (b) capabilities for *in-situ* growth and characterization of pristine oxide surfaces, and (c) theoretical framework for data interpretation. These developments are exemplified by the strain – polarization coupling in ferroelectric materials, role of local defects on polarization switching (Landauer paradox), energy dissipation probing in SPM, and polarization-dependent tunneling in ultrathin ferroelectric films.

Recent Progress

Imaging local polarization dynamics and switching centers in ferroelectrics: Strong coupling between polarization and electromechanical response allows using the latter as a functional basis of nanoscale probing of polarization distribution and switching processes in ferroelectrics. In Piezoresponse Force Microscopy, application of periodic electric bias to a conductive tip in contact with the surface results in surface displacement, detected by standard AFM electronics. The amplitude of the response is directly proportional to local polarization. This approach can be directly extended to probe local polarization dynamics. The probe concentrates an electric field to a nanoscale volume of material (dia. ~10 nm), and induces local domain formation [Fig. 1]. Simultaneously, the probe detects the onset of nucleation and the size of a forming domain via detection of the electromechanical response of the material to a small AC bias.[1] Thus obtained local hysteresis loops contain the information on the domain nucleation and growth processes.

In Switching Spectroscopy PFM, the hysteresis loops are acquired at each point of the image, and analyzed to yield 2D maps of coercive and nucleation biases, imprint, work of switching and switchable polarization. This achievement is

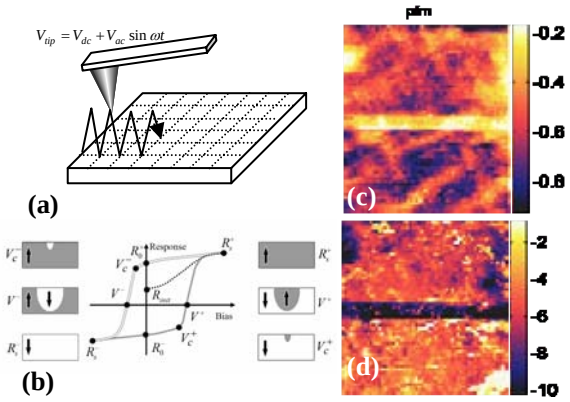

Fig. 1. Mapping origins of Landauer paradox on the nanoscale. (a) In SS-PFM, hysteresis loops are acquired at each point and analyzed to yield 2D maps of switching parameters. (b) Domain evolution at the different stages of hysteresis loop. SS-PFM (a) piezoresponse and (d) nucleation bias maps for epitaxial PZT film (sample by M. Alexe, Max Plank). Bright dots correspond to nucleation centers responsible for Landauer paradox.

made possible *by the 2 order of magnitude* increase in data acquisition speed that allowed reducing the time for a single loop acquisition from 30 s to ~100 ms. Maps of switching behavior can be correlated with surface structure and morphology. In particular, we have observed (a) internal distributions of work of switching in ferroelectric nanodots, (b) polarization pinning at step edges and grain boundaries, and (c) the role of local defects on polarization dynamics. In many cases, the hysteresis loops in the vicinity of defects were found to possess intricate fine structure formed due to the interaction of nascent domains with strain fields of the defect.

One of the key issues in ferroelectric applications is the mechanisms for polarization switching processes under the action of an electric field. Landauer[2] has demonstrated that experimentally observed fields required for polarization switching correspond to unphysically large values (~10^5 kT) for the activation energy for nucleation. This necessitated postulating the presence of switching centers having defined spatial and energy distributions at which nucleation is initiated. SS-PFM allows localizing and probing these individual nucleation centers. We noted that the onset of nucleation occurs at the point in the electromechanical hysteresis loop where the curve deviates from a constant value. As in the macroscopic case, the presence of defects lowers the nucleation bias. Hence, a map of local nucleation voltages represents the spatial and energy distribution of local switching centers, providing direct insight into the origins of Landauer paradox [Fig. 1 (d)].

Energy dissipation measurements in Scanning Probe Microscopy. Energy transfer between the tip and the surface in SPM provides the fundamental information on local dissipative behavior. Examples include magnetic dissipation due to tip-induced domain wall motion and phonon emission in Magnetic Force Microscopy, electrical losses due to the movement of depletion regions in Electrostatic Force Microscopy and Kelvin Probe Force Microscopy, and dissipation due to formation and breaking of a single chemical bond or excitation of conformational molecular degrees of freedom in Non-Contact AFM.[3,4] The existing approaches for mapping energy dissipation processes in force-based SPM are based on the detection of changes in the dynamic behavior of the cantilever as it interacts with the surface in constant frequency[5] and frequency tracking modes.[6] The data analysis in all dissipation SPMs to date is based on an assumption of a constant driving force. While approximately correct for acoustic driving of the cantilever, this assumption is no longer correct for SPMs with position-dependent electrical, mechanical, magnetic, or electromechanical excitation, severely limiting applicability of SPM to study coupling phenomena.

We have developed an approach based on an adaptive, digitally synthesized signal that excites a band of frequencies over a selected frequency range simultaneously (Fig. 2). By accessing a finite region of the Fourier space of the system centered at the resonance, the energy dissipation can de determined directly from the *Q*-factor of the cantilever. This avoids the limitations of existing SPM techniques that are limited to a single frequency in the Fourier space. While in its infancy, we have demonstrated applicability of this band excitation approach for mapping energy dissipation in mechanical and electromechanical probes, including loss processes during ferroelectric domain formation, mapping viscoelastic behavior on surfaces, and evolution of dynamic behavior of

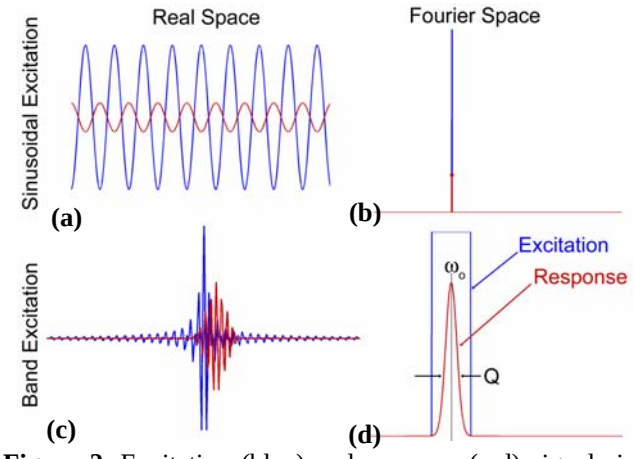

Figure 2. Excitation (blue) and response (red) signals in standard SPM techniques in (a) time domain and (b) Fourier domain. Excitation (blue) and response (red) signals in band-excitation (BE) SPM in (c) time domain and (d) Fourier domain. In BE, the system response is probed in the specified frequency range (e.g. encompassing a resonance), as opposed to a single frequency in conventional SPMs.

the probes during force-distance curve acquisition.

A UHV based system referred to as the **Nanotransport system** has been developed for *in-situ* growth (Pulsed Laser Deposition with RHEED control) and characterization of oxide thin films and incorporates facilities for electron spectroscopy (XPS and Auger), diffraction probes (LEED) and SPM (STM and NC-AFM). Shown in Fig. 3 is an example of atomic-resolution STM image of $SrRuO_3$ (100) surface grown by PLD, demonstrating ordered defect rows. The preliminary results on growth of ferroelectric $BaTiO_3/SrRuO_3$ ultra thin films and polarization-dependent tunneling have been obtained

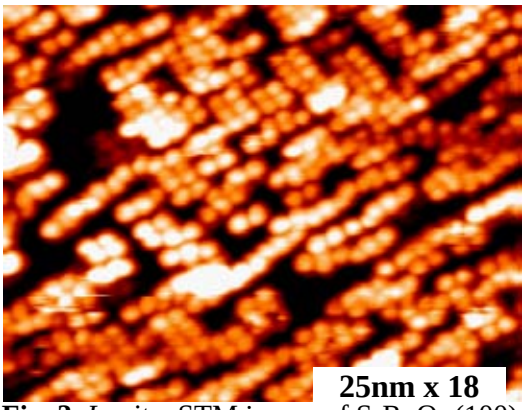

Fig. 3. *In-situ* STM image of $SrRuO_3$ (100) measured at RT with -1.535 V tip bias

Future plans

Understanding of fundamental physical phenomena on strongly-correlated oxide surfaces necessitates a synergistic effort that involves (a) *in-situ* studies of grown or cleaved surfaces free of chemisorbed species, (b) development of stable UHV platforms optimized for cross-coupled measurements [i.e. low cross-talk between driving and response signals] operating in the broad temperature and magnetic field ranges, and (c) advanced software and hardware for fast data acquisition and processing beyond conventional contact or NC-AFM. Our research effort specifically addresses these directions, as delineated below.

Physics of low-dimensional ferroelectric materials. Combination of advanced growth capabilities in the Nanotransport system, in-situ surface characterization tools, with conventional (STM) and advanced SPM techniques will allow to find the answers for the long-standing fundamental questions in ferroelectric materials, including

- The role of the surface on ferroelectric behavior, including both intrinsic factors such as antiferrodistortive transitions,[7] and adsorbate and surface chemistry mediated phases,[8,9,10]
- Ferroelectric behavior in low dimensional systems, including ordering and stability of ferroelectric phases,[11,] and existence of recently predicted toroidal polarization states,[12] by PFM spectroscopy
- Polarization dependent tunneling through *in-situ* grown ultrathin ferroelectric films using combined PFM and STM
- Surface metal-insulator transitions mediated by polarization charge in ferroelectrics and heterostructures.
- Interplay between magnetic and ferroelectric order parameters results in multiferroic materials such as Bi_2FeCrO_6 and titanate/manganite heterostructures using combination of PFM and spin-polarized STM

Advanced SPM methods for probing order parameter couplings (including PFM, magnetostrictive force microscopy, etc) and energy dissipation measurements will be implemented on the UHV VT AFM-STM system (Omicron) and further developed for incorporation on low-T high field AFM/STM platform. By using a tip having defined atomic, electronic, and magnetic structure we will be able to probe the non-conservative interactions and quantum coupling between the tip atom and the surface. These measurements as a function of external parameter such as tip-surface bias, magnetic field, or tip-surface separation will provide the information on the quasiparticle generation and energy spectra. This task will be developed in collaboration with theory groups to develop a theoretical framework for data interpretation accounting for near-field geometry of the probe that will affect permitted dissipation channels. More generally, observation and mapping of the force- and

current fluctuations of the cantilever under defined driving conditions allows direct insight into statistical physics of the tip surface system through the fluctuation-dissipation theorem. From the fluctuation data and more complex statistical processing, dynamic processes in material such as low-frequency molecular vibrations, dynamic polar nanoregions in relaxor ferroelectrics and their evolution at Burns and Curie temperatures, stripe and charge-ordered region dynamics in manganites can be extracted. Specifically, we aim to address:

- Structural and electronic properties of phase ordered regions in complex manganites and the dynamic behavior under mechanical and magnetic stimuli, providing information on the interplay between lattice, spin, and charge degrees of freedom
- Nanoscale phase separation and polarization dynamics in relaxor ferroelectrics imaged through acoustic and piezoresponse modes and fluctuation imaging
- Coupling between magnetic and ferroelectric behavior in multiferroic systems and interaction of these order parameters at surfaces, domain walls, etc.
- Unusual coupling between polarization and electronic behavior in materials such as $LuFe_2O_4$ and $PbVO_4$

DOE-sponsored publications 2004-2006:
In total, ~25 peer-reviewed papers (2 Phys. Rev. Lett.), 1 patent disclosure submitted.

1. B.J. RODRIGUEZ, S. JESSE, and SERGEI V. KALININ, *Electromechanical Imaging in Liquid Environment*, Phys. Rev. Lett. **96**, 237602 (2006).

2. S. JESSE, H.N. LEE, and SERGEI V. KALININ, *Quantitative Mapping of Switching Behavior in Piezoresponse Force Microscopy*, Rev. Sci. Instr. **77**, 073702 (2006).

3. S. V. KALININ, S. JESSE, J. SHIN, A.P. BADDORF, H.N. LEE, A. BORISEVICH, and S.J. PENNYCOOK, *Resolution, Information Limit, and Contrast Transfer in Piezoresponse Force Microscopy*, Nanotechnology, **17**, 3400 (2006).

4. J. SHIN, S.V. KALININ, H.N. LEE, H.M. CHRISTEN, R.G. MOORE, E.W. PLUMMER, and A.P. BADDORF, *Surface Stability of Epitaxial* $SrRuO_3$ *Thin Films*, Surf. Sci. **581**, 118 (2005).

5. SERGEI V. KALININ, A.L. GRUVERMAN, J. SHIN, A.P. BADDORF, E. KARAPETIAN, and M. KACHANOV, *Nanoelectromechanics of Polarization Switching by Piezoresponse Force Microscopy*, J. Appl. Phys. **97**, 074305 (2005),

References

[1] S. Jesse, H.N. Lee, and Sergei V. Kalinin, Rev. Sci. Instr. **77**, 073702 (2006).

[2] R. Landauer, J. Appl. Phys. **28**, 227 (1957).

[3] W. Denk and D.W. Pohl, Appl. Phys. Lett. **59**, 2171 (1991).

[4] T. D. Stowe, T. W. Kenny, D. J. Thomson, and D. Rugar, Appl. Phys. Lett. **75**, 2785 (1999).

[5] J.P. Cleveland, B. Anczykowski, A.E. Schmid, and V.B. Elings, Appl. Phys. Lett. **72**, 2613 (1998).

[6] T.R. Albrecht, P. Grütter, D. Horne, and D. Rugar, J. Appl. Phys. **69**, 668 (1991).

[7] A. Munkholm, S.K. Streiffer, M.V. Ramana Murty, J.A. Eastman, C. Thompson, O. Auciello, L. Thompson, J.F. Moore, and G.B. Stephenson, Phys. Rev. Lett. **88**, 016101 (2002).

[8] D.D. Fong, A.M. Kolpak, J.A. Eastman, et al. Phys. Rev. Lett. **96**, 127601 (2006).

[9] A.G. Zembilgotov, N.A. Pertsev, H. Kohlstedt, and R. Waser, J. Appl. Phys. **91**, 2247 (2002)

[10] C.H. Ahn, K.M. Rabe KM, and J.M. Triscone, Science **303**, 488 (2004).

[11] M. Dawber, K.M. Rabe, J.F. Scott, Rev. Mod. Phys. **77**, 1083 (2005).

[12] I.I. Naumov, L. Bellaiche L, and H.X. Fu, Nature **432**, 737 (2004)

Atomic Scale Visualization of Complex Electronic Quantum Matter in Transition Metal Oxides

JC Séamus Davis, LASSP, Physics Department, Cornell University, Ithaca, NY 14850, USA. ***Email:*** jcdavis@ccmr.cornell.edu

Program Scope

Development and Application of Novel SI-STM Techniques for Cuprate Studies

In recent years, we have developed novel applications of SI-STM specifically for use in studies of atomic-scale electronic structure of cuprates, manganites, ruthenates or other transition metal oxide materials. For example, energy-resolved local density of states (*LDOS*) imaging was introduced to cuprate studies [1]. In this technique, measurement of the STM tip-sample differential tunneling conductance $g(\vec{r},V) \equiv dI/dV\big|_{\vec{r},V}$ at locations $\vec{r}$ and sample bias voltage *V*, yields an spatial image of the local-density-of-states $LDOS(\vec{r},E)$ at energy E (because $LDOS(\vec{r},E=eV) \propto g(\vec{r},V)$). We introduced[2] the superconducting energy *gap-map* technique in which superconducting energy-gap variations $\Delta(\vec{r})$ can be imaged with atomic resolution. Another technique that we introduced to cuprate studies[3] is Fourier transform scanning tunneling spectroscopy (*FT-STS*). Here, the $\vec{q}$ -vectors of spatial modulations in $g(\vec{r},E)$ are determined from the locations of peaks in $g(\vec{q},E)$, the Fourier transform magnitude of $g(\vec{r},E)$. This technique has proven particularly valuable by virtue of its exceptional capability[4,5] to relate the atomic-scale $\vec{r}$ -space electronic structure to that in $\vec{k}$ -space. This year, we introduced direct imaging of dopant atoms and demonstrated the effects of dopants on the superconducting electronic structure[6]. Among the results achieved:

Impact of Individual Impurity Atoms on Electronic Structure of Cuprates:

We studied effects of individual Zn and Ni impurity atoms substituted at the Cu site in $Bi_2Sr_2CaCu_2O_{8+\delta}$ including the four-fold symmetric quasi-particle 'impurity-state' aligned with the d-wave gap nodes[7,8].

Nanoscale Electronic Disorder $\Delta(\vec{r})$ ***at Gap Energy in*** $Bi_2Sr_2CaCu_2O_{8+\delta}$:

We studied the doping dependence of superconducting energy gap-maps in $Bi_2Sr_2CaCu_2O_{8+\delta}$. Intense disorder, with gap values ranging from 20meV→65meV between distinct ~3nm domains, was discovered[9,10].

Cuprate Fourier Transform Scanning Tunneling Spectroscopy: We imaged energy-dispersive modulations of $LDOS(E,\vec{r})$ in $Bi_2Sr_2CaCu_2O_{8+\delta}$. Within a scattering-induced quasiparticle interference model they yield elements of the $\vec{k}$ -space electronic structure in agreement with photoemission[11,12]. This is a fascinating new tool to relate real-space to momentum-space electronic structure. It should work equally well at very high fields where ARPES is impossible.

Magnetic Field Induced 'Checkerboard' Modulations at Cuprate Vortex Cores:

By atomically registered subtraction of *LDOS* images measured with/without magnetic field, we discovered that the pseudogap-like conductance spectrum exhibits

associated ~$4a_0$ 'checkerboard' incommensurate low-energy *LDOS*-modulations in regions proximate to each vortex core[13].

'Checkerboard' Electronic Crystal State in Lightly Doped $Ca_{2-x}Na_xCuO_2Cl_2$:

In the very lightly doped cuprate, $Ca_{2-x}Na_xCuO_2Cl_2$**,** we discovered an almost V-shaped energy gap supporting non-dispersive conductance modulations with $4a_0 \times 4a_0$ 'checkerboard' correlations.[14]

Millikelvin SI-STM studies of p-wave Sr_2RuO_4:

Atomic-resolution millikelvin SI-STM was used to study the spectrum of quasiparticle states and electronic structure of vortex cores in p-wave superconducting Sr_2RuO_4.[15]

Impact of Individual Dopant Atoms on Cuprate Electronic Structure:

We identified electronic impurity states at E = -0.96eV as produced by the oxygen dopant atoms. These states were strongly correlated with $\Delta(\vec{r})$ disorder and also the primary scattering centers for quasiparticle interference. Thus, nanoscale electronic disorder of $Bi_2Sr_2CaCu_2O_{8+\delta}$ originates at impurity-states generated by the oxygen dopant atoms. Finding local effects of individual dopant atoms with this technique will be of wide utility in new materials created by chemical doping.

Recent Progress

Atomic-scale structure of the Cuprate Electronic 'Cluster Glass' State in $Ca_{1.8}Na_{0.12}CuO_2Cl_2$ and $Bi_2Sr_2Dy_{0.2}Ca_{0.8}Cu_2O_{8+\delta}$

The quantum mechanical state of holes doped into the CuO_2 plane is critical to understanding formation of high temperature superconductivity in cuprates. We apply new techniques of atomic resolution of spectral weight transfer mapping to study two HTS materials of very different crystal structure We identify primary atomic scale spatial variations on oxygen atoms. We show that these valence states are form a glass containing nano-electronic domains or 'clusters' which appear to be are bond centered nano-stripes. These data provide the first images of the pervasive electronic 'cluster' glass state of cuprates, and our first looks at the geometry and internal electronics structure of the electronic 'cluster' or nano-stripes.

Future Plans

In the short term, we plan SI-STM studies of the doping dependence of superconducting energy gap using FT-STS, the dependence of superconducting energy gap on nanoscale variations of crystal unit cell dimensions in $Bi_2Sr_2CaCu_2O_8$, a search for the "checkerboard" modulations in $Bi_2Sr_2CaCu_2O_8$, and direct imaging of the metamagnetic transition in $Sr_3Ru_2O_7$.

References

1 E.W. Hudson, S. H. Pan, A. K. Gupta, K-W Ng, and J.C. Davis, Quasi-Particle Scattering Resonances in $Bi_2Sr_2CaCu_2O_{8+d}$, Science 285, 88 (1999)

2 V. Madhavan et al., Bull. Amer. Phys. Soc. 45, 416 (2000).

3 J. E. Hoffman, E.W. Hudson, K. M. Lang, V. Madhavan, H. Eisaki, S. Uchida, and J.C. Davis, A

four unit cell periodic pattern of quasiparticle states surrounding vortex cores in $Bi_2Sr_2CaCu_2O_{8+d}$, Science 266, 455 (2002).

[4] J. Hoffman, K. McElroy, D-H Lee, K.M. Lang, H Eisaki, S. Uchida, and J. C. Davis, Imaging Quasiparticle Interference in $Bi_2Sr_2CaCu_2O_{8+d}$, Science 297 1148 (2002).

[5] K. McElroy, R. W. Simmonds, J. E. Hoffman, D.-H. Lee, J. Orenstein, H. Eisaki, S. Uchida & J.C. Davis, Relating atomic scale electronic phenomena to wave-like quasiparticle states in superconducting $Bi_2Sr_2CaCu_2O_{8+d}$ Nature 422, 520 (2003).

[6] K. McElroy, Jinho Lee, J. A. Slezak, D.-H. Lee, H. Eisaki, S. Uchida, & J. C. Davis, Atomic-Scale Sources and Mechanism of Nanoscale Electronic Disorder in $Bi_2Sr_2CaCu_2O_{8+\delta}$ Science **309**, 1048 (2005).

[7] Imaging the Effects of Individual Zinc Impurity Atoms on Superconductivity in $Bi_2Sr_2CaCu_2O_{8+d}$, S.H. Pan, E.W. Hudson, K.M. Lang, H. Eisaki, S. Uchida, and J.C. Davis, *Nature* 403, 746 (2000)

[8] Interplay of magnetism and high-T_c superconductivity at individual Ni impurity atoms in $Bi_2Sr_2CaCu_2O_{8+\delta}$. Hudson, E.W., *et al*. *Nature* 411, 920-924 (2001).

[9] Microscopic electronic inhomogeneity in the high-temperature superconductor $Bi_2Sr_2CaCu_2O_{8+d}$ S. H. Pan, J. O'Neil, R.L. Badzey, C. Chamon, H. Ding, J. R. Englebrecht, Z. Wang, H. Esiaki, S. Uchida, A. Gupta. K-W Ng, E. W. Hudson K.M. Lang and J. C. Davis, *Nature* 413 *282 (2001).*

[10] Imaging the granular structure of high-T_c superconductivity in underdoped $Bi_2Sr_2CaCu_2O_{8+d}$. K. M. Lang, V. Madhavan, J. Hoffman, E.W. Hudson, H. Eisaki, S. Uchida, and J.C. Davis, Nature 415, 412 (2002).

[11] Imaging Quasiparticle Interference in $Bi_2Sr_2CaCu_2O_{8+d}$" J. Hoffman, K. McElroy, D-H Lee, K.M. Lang, H Eisaki, S. Uchida, and J. C. Davis, Science **297** 1148 (2002).

[12] Relating atomic scale electronic phenomena to wave-like quasiparticle states in superconducting $Bi_2Sr_2CaCu_2O_{8+d}$ K. McElroy, R. W. Simmonds, J. E. Hoffman, D.-H. Lee, J. Orenstein, H. Eisaki, S. Uchida & J.C. Davis" Nature **422**, 520 (2003).

[13] A four unit cell periodic pattern of quasiparticle states surrounding vortex cores in $Bi_2Sr_2CaCu_2O_{8+d}$ J. E. Hoffman, E.W. Hudson, K. M. Lang, V. Madhavan, H. Eisaki, S. Uchida, and J.C. Davis, Science **266**,455 (2002).

[14] A 'checkerboard' electronic crystal state in Lightly Hole-Doped $Ca_{2-x}Na_xCuO_2Cl_2$" T. Hanaguri, C. Lupien, Y. Kohsaka, D.-H. Lee, M. Azuma, M. Takano, H. Takagi, & J. C. Davis. Nature **430**, 1001 (2004).

[15] Millikelvin-STM Studies of the Temperature- and Field-dependence of the Quasiparticle Spectrum of Superconducting Sr_2RuO_4 , C. Lupien , B. Barker, S. Dutta, Y. Maeno and J.C. Davis. Cond/mat 0503317

Local studies of correlated electron materials

AHARON KAPITULNIK
aharonk@stanford.edu
Geballe Laboratory for Advanced Materials, Stanford University, Stanford, CA 94305

PROGRAM SCOPE

The discovery by Bednorz and Müller (1986) of high temperature (high-T_c) superconductivity in copper oxides (cuprates) had an enormous impact on almost all aspects of research in strongly correlated electron systems in general, and superconductivity in particular. Soon after this discovery, a whole range of novel superconducting, magnetic and metallic states were discovered. New pairing mechanisms associated with novel broken symmetries have been the highlight of the field. Recent progress in the field both, theoretically and experimentally, suggests that local phenomena at the nanometer scale are the key to the novel behavior. The electrons have a very strong propensity to microscopically phase separate and to self-organize in patterns of lower-dimension [1, 2, 3, 4, 5, 6].

The scope of our program is to study nanoscale ordering, competition and transition phenomena in complex materials, by choosing several model systems and using several novel techniques. We use Sr_2RuO_4 [7] as a model system for strongly correlated oxide material in which magnetism and superconductivity are intimately present resulting in possible unconventional superconductivity with possible broken time-reversal symmetry. We use layered rare earth tellurides as model systems for interplay between itinerant electrons and charge density waves [8, 9, 10]. This is a topic of intense debate in recent years in other systems such as high-temperature superconductors [11]. Its "clean" occurrence in the layered rare earth tellurides make them an ideal model system. We use Tl-doped PbTe as a model system for the development of local correlations and superconductivity through disproportionation of certain heavy ions [12, 13]. That this may contribute to (i.e. enhance) pairing interactions in the cuprate superconductors is now an established fact; however, the complexity of the cuprates make the study of these effects in isolation unfavorable. Finally we use underdoped cuprates as model systems for doping the AFM ground state in strongly correlated systems near the emergence of superconductivity [14, 15].

RECENT PROGRESS

Nature of the Gap Inhomogeneities in BSCCO

The density of electronic states in nearly optimally doped $Bi_2Sr_2CaCu_2O_{8+\delta}$ in zero field is studied using STM. Focusing on the superconducting gap, we find patches of what appear to be two different phases in a background of some average gap, one with a relatively small gap and sharp large coherence peaks and one characterized by a large gap with broad weak coherence peaks. We compare these spectra with calculations of the local density of states for a simple phenomenological model in which a $2\xi_0 \times 2\xi_0$ patch with an enhanced or suppressed d-wave gap amplitude is embedded in a region with a uniform average d-wave gap. It would be natural to identify the large gap regions as being more representative of the electronic structure of underdoped cuprates and the small gap regions more representative of overdoped cuprates, both influenced by some "average gap" background. However, decreasing x also leads to a rapid decrease of T_c and the superfluid

density, which implies that a large pairing field alone is insufficient to characterize the features of the electronic structure which reflect the approach to the Mott insulator [18].

High Resolution Polar Kerr Effect Measurements of Sr_2RuO_4: Evidence for Broken Time Reversal Symmetry in the Superconducting State

The possible existence of time-reversal-symmetry (TRS) breaking has considerable implications for understanding superconductivity of Sr_2RuO_4. Thus, establishing the existence of this effect, and in particular in the bulk without relying on imperfections and defects (e.g. by using muon spin relaxation measurements) is of utmost importance. The challenge is therefore to couple to the TRS-breaking part of the order parameter to demonstrate the effect unambiguously. To this end we constructed a high precision Sagnac interferometer with a zero-area Sagnac loop. This allowed us to measure polar Kerr effect with unprecedented sensitivity of 100 nanorad/$Hz^{1/2}$ with 10 μW incident power, down to 0.5 K [16]. We observed non-zero Kerr rotations as big as 65 nanorad appearing below T_c in large domains [17]. Our results imply a broken time reversal symmetry state in the superconducting state of Sr_2RuO_4, similar to 3He-A.

STM Studies of the CDW state of $TbTe_3$

RTe_3 is a family of layered compounds (R = rare earth) where an incommensurate Charge Density Wave (CDW) opens a large gap (200-400meV) in optimally nested regions of the Fermi Surface (FS), whereas other sections with poorer nesting remain ungapped. In collaboration with Ian Fisher's and ZX Shen's groups at Stanford, we performed high resolution STM studies of $TbTe_3$. The topography of this system clearly reveals the CDW ordering. Fourier transform of the topography revealed different peaks which could be identified as the atomic ordering of the underlying lattice, the fundamental CDW ordering peak and interactions between the two. High-bias topography could be used to find the fundamental peaks [19].

FUTURE PLANS

We plan to continue our studies in all three directions described above. First, we plan to continue our studies on the nature of the inhomogeneities in high-Tc. In particular, the recent work of Wakimoto *et al.* [20] who used neutron scattering to study magnetic excitations on overdoped $La_{2-x}Sr_xCuO_4$ reinforces the model we first presented in our recent work [18] of phase separation in the overdoped cuprates. We therefore plan to continue with a parallel study of similar compositions in BSCCO samples.

Second, our discovery of broken time reversal symmetry in Sr_2RuO_4 opens new opportunities for similar discoveries in other systems. $PrOs_4Sb_12$, and $(TMTSF)_2ClO_4$ are the first systems that we will try. Also, we will embark on the study of the chirality domain structure and its synamics dynamics in these systems.

Finally, we plan to extend our studies of commensurability in CDW systems of the TbTe3 variety to other rare earth on the Tb site.

BIBLIOGRAPHY

References

[1] V.J. Emery, S.A. Kivelson, and H.Q. Lin, Phys. Rev. Lett. 64, 475 (1990).

[2] U. Low , V. J. Emery, K. Fabricius, and S. A. Kivelson, Phys. Rev. Lett. 72, 1918 (1994).

[3] Subir Sachdev, Quantum magnetism (Lecture Notes in Phys. Vol.645); p.381-432, condmat/0401041.

[4] S. Sachdev, Rev. Mod. Phys. 75, 913-932 (2003).

[5] Y. Imry and S.-K. Ma, Phys. Rev. Lett. 35, 1399 (1975).

[6] E. Shimshoni, A. Auerbach and A. Kapitulnik, Phys. Rev. Lett. 80, 3352 (1998).

[7] A.P. Mackenzie and Y. Maeno, Rev. Mod. Phys. 70, 657 (2003).

[8] J. Voit et al., Science 290, 501 (2000).

[9] A. Audouard et al., Phys. Rev. B 50, 12726 (1994).

[10] P. A. Goddard et al., Synthetic Metals 120, 783 (2001).

[11] S. A. Kivelson, E. Fradkin, V. Oganesyan, J. M. Tranquada, A. Kapitulnik, and C. Howald, Rev. Mod. Phys. 75, 1201-41 (2003).

[12] T.H. Geballe and B.Y. Moyzhes, Physica C 341-348, 1821-1824 (2000).

[13] V. Oganesyan, S. Kivelson,T. Geballe and B.Y. Mozyhes, Phys. Rev. B 65, 1725041-4 (2002).

[14] E. W. Carlson, V. J. Emery, S. A. Kivelson, and D. Orgad, Review chapter to appear in The Physics of Conventional and Unconventional Superconductors ed. by K. H. Bennemann and J. B. Ketterson (Springer-Verlag), cond-mat/0206217.

[15] P.A. Lee, Annales Henri Poincare 4, suppl.2, p.S529-S537 (2003).

[16] Jing Xia, Peter T. Beyersdorf, M. M. Fejer, and Aharon Kapitulnik, Appl. Phys. Lett. 89, 062508 (2006)

[17] Jing Xia, Maeno Yoshiteru,Peter T. Beyersdorf, M. M. Fejer, and Aharon Kapitulnik, Submitted to Phys. Rev. Lett. (2006), cond-mat/0607539.

[18] A. C. Fang, L. Capriotti, D.J. Scalapino, S.A. Kivelson, and A. Kapitulnik, Phys. Rev. Lett. 96, 017007 (2006).

[19] A. Fang, N. Ru, K.Y. Shin, I.R. Fisher, and A. Kapitulnik, Scanning Tunneling Spectroscopy of $TbTe_3$, manuscript in preparation.

[20] S. Wakimoto, K. Yamada, J. M. Tranquada, C. D. Frost, R. J. Birgeneau, and H. Zhang, "Disappearance of high-energy spin excitations in overdoped $La_{2-x}Sr_xCuO_4$," condmat/0609155.

DOE Sponsored Publications in 2002-2006:

[1] "Coexistence of periodic modulation of quasiparticle states and superconductivity in $Bi_2Sr_2CaCu_2O_{8+\delta}$," C. Howald, H. Eisaki, N. Kaneko, and A. Kapitulnik, Proceedings of the National Academy of Sciences of the United States of America 100 (2003), 9705.

[2] "Periodic Density of States Modulations in Superconducting $Bi_2Sr_2CaCu_2O_{8+\delta}$," C. Howald, H. Eisaki, N. Kaneko, M. Greven and A. Kapitulnik, Physical Review B 67, 014533 (2003).

[3] "How to detect fluctuating order in the high-temperature superconductors," S. A. Kivelson, E. Fradkin, V. Oganesyan, J. M. Tranquada, A. Kapitulnik, and C. Howald, Rev. Mod. Phys. 75 (2003), 1201-41.

[4] "Periodic Coherence Peak Height Modulations in Superconducting $Bi_2Sr_2CaCu_2O_{8+\delta}$," A. Fang, C. Howald, N. Kaneko, M. Greven and A. Kapitulnik, Phys. Rev. B 70 (2004), 214514.

[5] "STM Studies of Near-Optimal Doped $Bi_2Sr_2CaCu_2O_{8+\delta}$," A. Kapitulnik, A. Fang, C. Howald, and M. Greven, J. Phys. Chem. Solids 67 (2006), 344-9.

[6] "Gap Inhomogeneity-Induced Electronic States in Superconducting $Bi_2Sr_2CaCu_2O_{8+\delta}$," A. C. Fang, L. Capriotti, D.J. Scalapino, S.A. Kivelson, and A. Kapitulnik, Phys. Rev. Lett. 96 (2006), 017007.

[7] "What is local about the local density of states?," R. Jamei, J. Robertson, E-A. Kim, A. Fang, A. Kapitulnik, and S.A. Kivelson, Submitted to Phys. Rev. B (2006), cond-mat/0608318.

[8] "High Resolution Polar Kerr E ect Measurements of Sr_2RuO_4: Evidence for Broken Time Reversal Symmetry in the Superconducting State," Jing Xia, Maeno Yoshiteru, Peter T. Beyersdorf, M. M. Fejer, Aharon Kapitulnik, Submitted to Phys. Rev. Lett. (2006), cond-mat/0607539.

[9] "Distinguishing Patterns of Charge Order: Stripes or Checkerboards," John A. Robertson, Steven A. Kivelson, Eduardo Fradkin, Alan C. Fang, Aharon Kapitulnik, Submitted to Phys. Rev. B (2006), cond-mat/0602675.

Session III

Surfaces and SPM

Understanding and controlling the self-organization of nanostructures

Michael C. Tringides, M. Hupalo and M.Yakes
tringides @ameslab.gov, hupalo@ameslab.gov, myakes @iastate.edu
Ames Laboratory and Iowa State University

I. **Program scope**

The growth of self-organized low dimensional structures is based on finding novel, robust ways to control their dimensions and geometry. If such control is achievable it would be possible to "tune" the structure electronic properties to specific technological applications, because their electronic structure (i.e. the confined energy levels etc) depends on their size. The scope of our program is to discover novel routes to this self organization on the nanoscale and to understand the key physical processes (i.e. diffusion, coarsening, nucleation etc.) controlling their formation and stability. Two complementary techniques, Scanning Tunneling Microscopy (STM) and High Resolution SPA-LEED are used for structure characterization. In collaboration with theoretical groups worldwide we aim to attain a better understanding of the structure energetic stability and the controlling kinetic barriers. The ultimate goal is to use this information to grow in a predictable way custom-made nano materials of uniform selectable dimensions.

II. Recent progress

IIa. Coarsening kinetics on Si(111)-(7x7)

We have studied the coarsening kinetics of the uniform height Pb islands on Si(111) as a function of flux rate and coverage[1]. We have found that the island coarsening is not described by the classical Gibbs Thompson analysis. Such classical analysis defines island stability in terms of island curvature, so smaller islands have higher probability to evaporate. Instead, we found that island decay time is a function of both size and height with unstable height Pb islands (i.e. even height islands) decaying unusually fast (irrespectively of their lateral size). These results were obtained with two complementary techniques, locally with STM (as seen in fig.1 for coarsening on the 7x7) and with surface X-ray scattering (in collaboration with the μ-cat team at Argonne Advanced Photon Source).

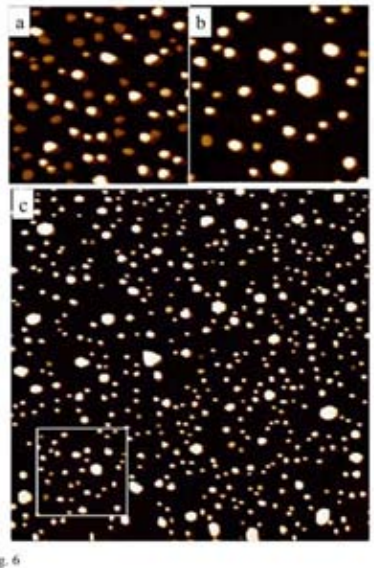

Fig. 6

Fig, 1 Coarsening experiments:(a) initially an 250x250nm^2 area showing a mixture of stable (7-layer ,bright color) and unstable(4-layer, brown color) islands. (b)8 hours later an 250x250nm^2 area shown and outlined at the bottom of (c) a bigger 1000x1000nm^2 area. Most of the 4-layer convert to 7-layer islands

While we know that the formation of the uniform height Pb/Si(111) islands is related to Quantum Size Effects (QSE i.e., how the energy of the confined electrons depends on island size)), it is still not clear what are the key kinetic processes controlling island growth. First-principles calculations in collaboration with the local theory group (Wang, Ho) were used to calculate the kinetic barriers[2]. Very low diffusion barriers were found for diffusion on top of Pb(111), with the diffusion barrier for stable islands higher than the one for unstable Pb islands. This variation accounts for the novel second layer nucleation morphology i.e. islands grow in height from rings nucleated at the island perimeter.

In collaboration with a Czech group[3] we have modeled the island growth with Monte Carlo simulations. A complex potential energy surface(PES) can reproduce the observed island ring morphology within the deposition time. The barriers of the PES are dictated by the fast island completion and the unusual second layer ring morphology. Classical nucleation predicts that nucleation would start randomly anywhere on the island instead at the island perimeter, contrary to the observations.

IIb.Controlling more than one dimension

With STM and SPA-LEED we found that Pb deposited on Si(111)--In (4x1) at 180K forms nanowires of uniform 4-layer height and uniform width of $5w_0$ (where w_0 =1.33nm is the width of the 4x1 unit cell)[4]. This is due to the combined effect of QSE and the anisotropic strain potential of the substrate[5] and shows that it is possible to control two of the island dimensions (i.e. height and width). In addition this preferred height is unusually stable because it is unchanged even after annealing to room temperature; which is surprising because of the typically low QSE energies (less than ~50meV). These low QSE energies lead in other systems after annealing to island decay and broadening of the height distribution below room temperature.

IIc.2-d equilibrium physics

With SPA-LEED and STM we have measured the temperature T vs coverage θ phase diagram of the dense Si(111)-Pb-α√3x√3 phase (close to θ=4/3ML), which has been controversial [6]. Conflicting phase assignment of different symmetry have been given in the literature for the same (T,θ) region[7,8]. This is because at low temperatures numerous linear phases form, a realization of a "Devil's Staircase"(DS) due to long range interactions[6]. With annealing these phases transform into the so called Hexagonal Incommensurate (HIC) and Striped Incommensurate(SIC) phases (as shown in fig.2). In collaboration with Zaluska Kotur (Polish Academy of Sciences) and Gortel (Alberta) we have explained the surprising rapid formation of the numerous DS phases at low temperature by showing that the diffusion coefficient in a system with long range interactions has strong maxima at all DS phases[9]. These new results about kinetics are relevant in other systems where long range interactions are important[10, 11].

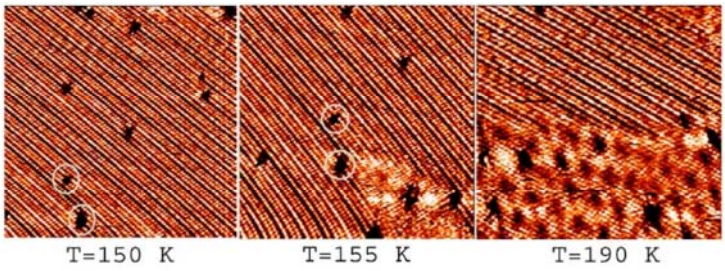

Fig.2 The phase transition with temperature observed in a 43x43nm^2 area in Si(111)-Pb α(√3x√3) showing at 150K a linear DS phase. After annealing to 190K there is coexistence between the linear DS and HIC phases.

In collaboration with Chvoj(Czech Academy of Sciences) we have organized the International Workshop on Physics and Technology of Thin Films (IWTF2) held in Prague June 2006 Details are on http://www.fzu.cz/activities/workshops/iwtf2

IV. Future Plans

IVa. Non-classical coarsening

Although QSE in Pb/Si(111) control island height selection many questions are open. As described earlier in IIIa QSE affect not only the energetics, but also modify the kinetic barriers. We will extend our previous coarsening studies on a different interface (Si(111)- Pb(√3x√3) to measure how stable islands evolve from unstable ones. We will test whether similar non-classical effects hold as on Si(111)-(7x7). We will measure other kinetic barriers (i.e. step edge barrier which controls interlayer diffusion) to test how they depend on island stability. The collaboration on these questions will continue both with the X-ray group of the μ-cat and the local theorists. A novel picture of nucleation emerges in systems when QSE operate which shows that in such systems self -organization is possible at low temperatures (against conventional wisdom, except fro growth on Si(111)-In(4x1)).

Since the Pb islands are metastable and in most cases decay at temperatures less than room temperature we will search for ways to modify the kinetic barriers that control the island height with the use of surfactants (adsorbed gases i.e. oxygen , hydrogen) similar to way surfactants have been used to modify 3-dimensional growth to layer-by-layer growth[12]. We expect surfactants will raise the step edge barrier and suppress the transfer of atoms from the surrounding area to the island top and thus extend island stability,

After the role of QSE both on energetics and kinetics are well understood the search for similar self-organization in other metal/semiconductor systems (i.e. In, Sn, Al on Si(111) and Si(100)) will be easier.

IVb. Exploring 1-d physics on Si(111)-In(4x1)

In collaboration with A. Kaminski(Ames) we will carry out angle resolved photoemission measurements on the uniform height Pb islands grown on In(4x1) to search for lateral quantization in the photoemission spectra (since as found a year ago the island width is constant $5w_0$) and to understand why the selected height 4-layer on the In(4x1) is so stable.

The adsorption of submonolayer Pb amount $\theta<0.2$ML on the anisotropic Si(111)-(4x1) substrate will be used to study the physics of 1-d electronic systems[13]. From preliminary results the adsorption of the Pb atoms on top of the Si(111)-In(4x1) chains is not random but there are preferred adatom separations indicating the presence of indirect interactions. The Pb adatom separation is an odd multiple of the lattice constant and suppresses the low-temperature In-(4x2) charge density wave (CDW) known to form on this surface, indicating a strong antiphase interference between adatom interaction o and CDW of the In(4x1) Si(111). We plan to explore further the physics in 1-d systems.

IVc. 2-dimensional equilibrium physics

Other metals (In,Sn ,etc) will be deposited on the Pb/Si(111)-$\alpha\sqrt{3}x\sqrt{3}$ to test if linear DS phases also formed as in the case of Pb deposition. With the Czech theory group we will deduce the Hamiltonian that can reproduce the T-θ phase diagram for the Pb system and the non-monotonic dependence of the transition temperature on coverage .

References

1. C. Joeffrey R. Feng, E.H. Conrad, M Hupalo, P. Ryan, C. Kim, P.F. Miceli, M. C. Tringides *Phys. Rev. Let.* 96 106105 (2006)
2. T.L. Chan , M.Hupalo, M.C. Tringides, C. Z. Wang K.H.Ho *Phys. Rev. Let.* 96 226102 (2006)
3. Z. Kuntova, Z. Kuntova, M. Hupalo, Z. Chvoj M. C. Tringides *Surf. Sci.* (in press)
4. M. Hupalo and M.C.Tringides *Phys. Rev B Rapid Comm.* 75 041405 R 2006
5 F. Liu, C. Li, M.G. Lagally, *Phys. Rev. Lett.* **87**, 126103 (2001).
6 S. Stepanovskyy *et. al. Surf. Sci.* 600 1417 (2006)
7 A. Petkova, J. Wollschläger, H. -L. Günter and M. Henzler, *Surf. Sci*. **471** 11-20 (2000).
8. I.S. Hwang et al. *Phys. Rev. Let*. 93 106101(2004)
9 M.Hupalo, M.Yakes, M. Zaluska-Kotur, Z. Gortel and M.C.Tringides *Phys. Rev. Let.* (submitted)
10 R. Plass et al., *Nature (*London) 412, 875 (2001)
11 S. C. Erwin, C. Stephen Hellberg, *Surf. Sci.* 585 L171 (2005)
12 M.Horn-von Hoegen and A. Golla, *Phys. Rev. Lett.* **76**, 2953 (1996).
13 J. N. Crain *at al*., *Phys. Rev. B 69*, 125401 (2004).

Publications 2004-2006

1. “Self organization at finite temperature of the “devil’s staircase in Pb/Si(111)” M. Yakes, V. Yeh, M. Hupalo, and M.C. Tringides *Phys. Rev. B*, **69,** 224103 (2004)
2. “Quantum Well Dimension and Energy Level Determination in Pb/Si(111)-7x7” V.Yeh, M.Hupalo, E.H. Conrad, and M.C. Tringides *Surf. Sci.*, **23,** 551/1-2 (2004)
3. “Low Temperature Formation of the Pb/Si(111) ‘Devil's Staircase’” V. Yeh , M. Yakes, M. Hupalo, and M.C. Tringides *Surf. Sci.*, **562**, 238 (2004).
4. “Wetting Layer Transformation from Pb Nanocrystals Grown on Si(111)” R. Feng, E.H. Conrad, M.C. Tringides, C. Kim, and R.F. Miceli *Appl. Phys. Lett*., **85**, 3866 (2004).
5.“The Evolution of the Structure of Quantum Size Effects of Pb Nanocrystals on Si(111)-7x7” R. Feng, E.H. Conrad, C. Kim, R.F. Miceli, and M.C. Tringides *Physica B* 357 175 (2005)
6.“Limitations of the thermodynamic Gibbs-Thompson analysis of nano-island decay” Z. Kuntova , Z. Chvoj, V. ŠSima and M.C. Tringides *Phys. Rev. B* 71 125415 (2005)

7."Fluctuations and Growth Phenomena in Surface Diffusion" M.C. Tringides and M.Hupalo In *Diffusion in Condensed Matter*, J. Karger, P. Heitjans, and R. Haberlandt, editors. Vieweg, Braunschweig/Wiesbaden, Germany, 2005 (invited).

8."Novel Diffusion pathways in low temperature self-organization of Nanostructrues" M.C.Tringides. M.Hupalo. M. Yakes *Physica A* 357 216 (2005)

9.Comment on the paper M.H. Upton et al., M.C. Tringides and M. Hupalo *Phys. Rev. Lett.*, ***93*** *026802 (2004)*

10. "Interface relaxation and electronic corrugation in the Pb/Si(111)-Pb-$\alpha\sqrt{3}x\sqrt{3}$"M. Hupalo, V. Yeh, T.L.Chan C. Z. Wang, K.M.Ho and M.C.Tringides *Phys. Rev. B* 71 193408 (2005)

11. "Self-Organization and Geometry Control of Pb Islands Grown on Anisotropic Substrates" M. Hupalo and M.C.Tringides *Phys. Rev B Rapid Comm*. 75 041405 R 2006

12. "The dense α-$\sqrt{3}x\sqrt{3}$ Pb/Si(111) phase: a comprehensive STM and SPA-LEED study of ordering, phase transitions and interactions" S. Stepanovsky[*], M. Yakes, V. Yeh[**], M.Hupalo and M. C. Tringides *Surface Science 600 1417 (2006)*

13. "Impact of Interface Relaxation on the Nanoscale Corrugation in Pb/Si(111) Islands" T.L. Chan, C.Z. Wang, M. Hupalo, M.C. Tringides, W.C. Lu, and K.M. Ho *Surf. Sci. Lett*. 600 179 (2006)

14. "Quantum size effect on the diffusion barrier and growth morphology on Pb/Si(111)" TL.Chan , C. Z. Wang.M.Hupalo MC.Tringides and K. M.Ho *Phys. Rev. Let.* 96 226102 (2006)

15. "Novel nucleation mechanisms driven by Quantum Size Effects" R. Feng, E.H. Conrad, M. C. Tringides, M Hupalo, P. Ryan, C. Kim, P.F. Miceli *Phys. Rev. Let.* 96 106105 (2006)

16. "Non-classical kinetics processes and morphologies in QSE driven growth in Pb/Si(111)" Z. Kuntova, M. Hupalo, Z. Chvoj and M. C. Tringides *Surf. Sci*. (in press)

17 "The Growth of Pb Nanocrystals on Si(111)7x7: Quantum Size Effects" C. A. Jeffrey, R. Feng, E. H. Conrad, P. F. Miceli, C. Kim, M. Hupalo, M. C. Tringides and P. J. Ryan *Physica A* (in press)

18. Low temperature ultra fast mobility in systems with long range repulsive interactions: Pb/Si(111)M.Hupalo, M.Yakes, M. Zaluska-Kotur, Z. Gortel and M.C.Tringides *Phys. Rev. Let.* (submitted)

19. "Bilayer ring second layer nucleation morphology in Pb/Si(111)-7x7" Z. Kuntova, M. Hupalo, Z. Chvoj and M. C. Tringides *Phys. Rev. B* (submitted)

20. "Interplay Between Indirect Interaction and Charge Density Wave in Pb adsorbed In(4x1)-Si(111)". M. Hupalo, T.-L. Chan, C. Z. Wang, K.-M. Ho, and M. C. Tringides *Phys. Rev. Let.* (submitted)

21. "Ultrafast kinetics in Pb/Si(111) from the collective spreading of the wetting layer" M. Hupalo and M. C. Tringides *Phys. Rev. B* (submitted)

Three-Dimensional Sub-Surface Imaging of Single Spins Using Magnetic Resonance Force Microscopy

Raffi Budakian, Trevis Crane, Joonho Jang, Xu Wang, Xin Zhao
Frederick Seitz Materials Research Laboratory, University of Illinois at Urbana-Champaign, Urbana, IL 61801

Program Scope

Magnetic resonance force microscopy (MRFM) is an emerging technique that combines magnetic resonance and force microscopy to manipulate and detect sub-surface spins with nanometer spatial resolution and ultra-high sensitivity. Recent MRFM measurements have demonstrated single electron spin sensitivity by detecting the spin of individual defects in silica with 25 nm lateral spatial resolution located as much as 100 nm below the surface.[1] The primary goal of this research program is to advance the state of the art in MRFM detection to enable three-dimensional imaging and chemical characterization of defects and dopant atoms in buried interfaces. In addition to imaging, MRFM has also been used to measure the local spin-lattice relaxation rate of small spin ensembles.[2] By combining single spin imaging and local spin-lattice relaxation measurements, quantitative information can be gained regarding the dynamics of the lattice near the spin. Nanometer scale imaging and spectroscopic characterization at the single spin level can further our understanding of materials at the atomic scale and facilitate the development of advanced materials.

Recent Progress

MRFM was originally proposed as a technique for direct three-dimensional imaging of proteins.[3, 4] Since its initial proposal in 1992,[3] the sensitivity of MRFM detection has increased by more than 10^7 . Recently, MRFM has been used to image a single electron spin,[1] making it the most sensitive technique for direct spin detection currently available. Some of the key factors that has made this advance possible are understanding the spin decoherence mechanisms in the presence of large field gradients,[5-7] engineering cantilevers that suppress cantilever induced spin relaxation,[8] and implementing measurement protocols for detecting the $\sqrt{N}$ statistical imbalance in small spin ensembles.[9] These advances have enabled the detection of single electron spins from sub-surface paramagnetic defects in SiO_2 ,[1] the realization of ultra long spin relaxation times during measurement exceeding 1 s,[9] and the real-time control of small spin ensembles through active feedback.[2] By building upon these advances, MRFM may become a characterization tool to advance areas of broad practical and scientific interest including imaging defects and dopants in buried interfaces and manipulation of spins for quantum information processing.

The most sensitive MRFM measurements have been obtained from silica samples containing low concentrations of E' centers[10] (paramagnetic silicon dangling bonds). In these measurements, the concentration of defects was low enough that, for most scan locations, the resonant slice did not contain any spins. Figure 1A shows the signal from an isolated electron spin obtained by laterally scanning the tip approximately 100 nm

over the surface of the sample. The 25 nm lateral spatial resolution is consistent with the oscillation amplitude of the cantilever during measurement.

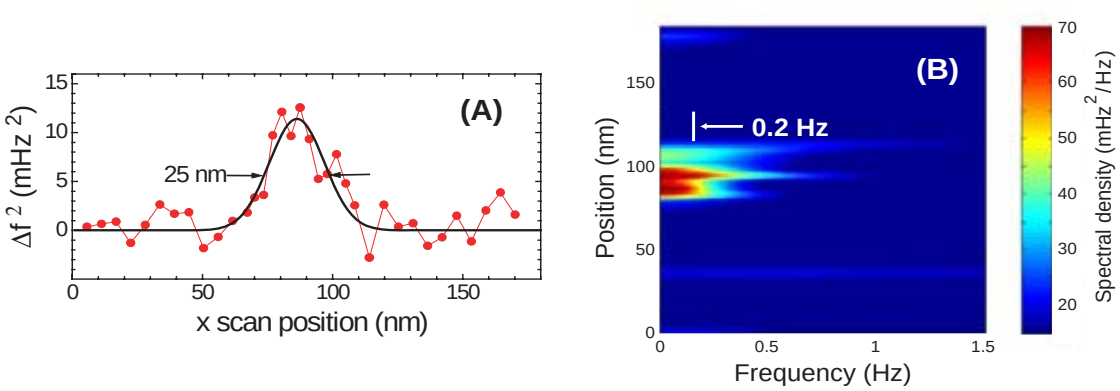

Figure 1: Single spin data from E' centers in SiO_2. (A) The 1D lateral scan displays the integrated spin signal from an isolated electron spin. (B) False color image showing the spectral density of the spin signal as a function of position. The data indicate a highly coherent spin signal having a relaxation time of $\tau_m = 1/2\pi\Delta\nu \approx 760$ ms.

In addition to the signal amplitude, the spin coherence was also measured as a function of position. Figure 1B shows the signal's spectral density at each scan location. When the spin is centered in the resonant slice, the signal has the narrowest bandwidth, corresponding to $\Delta\nu = 0.21$ Hz or spin relaxation times of $\tau_m = 760$ ms.

Future Plans

While this result marks a major milestone in MRFM detection, significant progress must be made before MRFM detection can be applied to single-spin imaging and quantum measurement. Under current operating conditions, the spin signal must be averaged for 4 hours to detect a single spin with 90% fidelity. For rapid imaging to be possible, understanding how the measurement times scale with the experimental parameters is essential. Because the instantaneous sign of the spin signal is not known, the signal power rather than the signal amplitude must be averaged. In the low signal to noise limit, the measurement times scale quadratically with the power SNR

$$t_{meas} \propto \frac{S_F^2}{\tau_m (\mu_s G)^4}.$$

Here, S_F is the power spectral density of force noise fluctuations, and μ_s is the magnetic moment of the spin and G is the field gradient from the tip. The strong dependence of t_{meas} on G means that even modest increases in the field gradient and reduction in force noise can significantly reduce measurement times.

A key technical challenge will be to increase the field gradients from the MRFM probe tips. Currently, the best magnetic tips (i.e. tips that produce the highest field

gradients and lowest spin relaxation rates) are fabricated by attaching a micron size rare earth magnetic particle to the end of the cantilever and shaping it down to 100-200 nm diameter using a Focused Ion Beam (FIB). It is thought that the high energy gallium ions used the FIB process produce a damaged layer of magnetization around the particle. Since the spins in the damaged shell lack the crystalline anisotropy of the bulk, the field gradient near the tip is diminished. In future experiments, the tips will be sputtered with low energy (< 500 eV) Ar or Xe ions after the FIB procedure to remove the damaged region and increase field gradients.

The cantilever is at the heart of ultrasensitive force detection. To facilitate rapid imaging and quantum measurement of single spins, ultra-sensitive cantilevers are currently being developed which are expected to approach sub-attonewton force sensitivity. The new cantilever design incorporates a superconducting quantum interference device (SQUID) in order to provide high sensitivity displacement detection. SQUID based detection should permit much lower cantilever temperatures to be realized than currently used optical detection techniques. Consequently, the thermal fluctuations experienced by the cantilever should be much less, thus increasing the force detection sensitivity.

In addition to more sensitive cantilevers, new spin detection techniques will be implemented to reduce the fluctuations experienced by the cantilever near the surface. Minimizing surface fluctuations is essential to sensitive spin detection in two key respects. First, lower force fluctuations directly result in smaller dissipation, lower force noise and higher SNR values. Second, lower surface noise should permit closer operation between the tip and the surface and enable higher filed gradients to be realized.

In future experiments, fluctuations near the surface will be minimized by (1) *in-situ* heating of the surface to reduce adsorbed atoms/molecules that could be mobile and (2) eliminating static charge by coating the surface with a thin layer of gold. In addition, a new protocol will be implemented that should permit spin detection at the thermal limit of the cantilever.[11] By realizing the thermal limit and by minimizing surface dissipation the surface noise S_F is expected to reduce by $10\times$ or more which would decrease measurement times by $100\times$. This improvement, in addition to the increased field gradients, should enable detection times to decrease by more than $25,000\times$ which would make both quantum measurement and three dimensional single-spin imaging a reality.

References

[1] D. Rugar, R. Budakian, H. J. Mamin, et al., *Nature* **430**, 329 (2004).

[2] R. Budakian, H. J. Mamin, B. W. Chui, et al., *Science* **307**, 408 (2005).

[3] J. A. Sidles, *Phys. Rev. Lett.* **68**, 1124 (1992).

[4] J. A. Sidles, J. L. Garbini, and K. J. Bruland, *Rev. Mod. Phys.* **67**, 249 (1995).

[5] G. P. Berman, V. N. Gorshkov, D. Rugar, et al., *Phys. Rev. B* **68**, 094402 (2003).

[6] D. Mozyrsky, I. Martin, D. Pelekhov, et al., *Appl. Phys. Lett.* **82**, 1278 (2003).

[7] B. C. Stipe, H. J. Mamin, C. S. Yannoni, et al., *Phys. Rev. Lett.* **87**, 277602 (2001).

[8] B. W. Chui, in *Technical digest of the 12th Int. Conf. on Solid-State Sensors and Actuators (Transducers'03)* (IEEE, Piscataway, 2003), pp. 1120.

[9] H. J. Mamin, R. Budakian, B. W. Chui, et al., *Phys. Rev. Lett.* **91**, 207604 (2003).

[10] J. G. Castle, D. W. Feldman, P. G. Klemens, et al., *Phys. Rev.* **130**, 577 (1963).

[11] R. Budakian, H.J. Mamin, and D. Rugar, publication to appear in *Appl. Phys. Lett.* (2006).

Publication List 2004-2006

1. R. Budakian, H.J. Mamin, and D. Rugar, Suppression of spin diffusion near a micron-size ferromagnet. *Phys. Rev. Lett.* **92**, 037205 (2004).

2. D. Rugar, R. Budakian, H. J. Mamin, and B.W. Chui, Single spin detection by magnetic resonance force microscopy. *Nature* **430**, 329 (2004).

3. R. Budakian, H. J. Mamin, B.W. Chui, and D. Rugar, Creating order from random fluctuations in small spin ensembles. *Science* **307**, 408 (2005).

4. H. J. Mamin, R. Budakian, B. W. Chui, and D. Rugar, Magnetic resonance force microscopy of nuclear spins: Detection and manipulation of statistical polarization. *Phys. Rev. B* **72**, 024413 (2005).

5. R. Budakian, H.J. Mamin, and D. Rugar, Spin manipulation using fast cantilever phase reversals. Accepted for publication in *Appl. Phys. Lett.* (2006).

Toward the Realization of Room Temperature Ferromagnetic Semiconductors: A Spin-polarized STM Study

Lian Li
lianli@uwm.edu
Physics Department, University of Wisconsin, Milwaukee, WI 53211

Program Scope

Diluted ferromagnetic semiconductors are a new class of semiconductors that exhibit long-range ferromagnetic ordering when alloyed with a few percent of a transition metal such as Mn [1]. They are being investigated for fabricating semiconductor spin devices that explore the use of electron *spin* to process information [2]. Challenges remain, however, in synthesizing a homogenous material with Curie temperature above 300 K for practical applications. This program aims to study the interactions between transition metal impurities and their host semiconductors at the atomic scale with a combined experimental and theoretical approach using spin polarized scanning tunneling microscopy/spectroscopy and first principles calculations.

Our first specific goal is to investigate the exchange coupling between the impurity spins and host conduction or valance bands. Using spin-polarized STM, local differential conductivity (*dI/dV*) imaging, and first principles calculations, we focus on the incorporation of transition metals on the growth surfaces of III-nitride and arsenide, e.g. GaN(0001); as well as cleaved surfaces of these materials, e.g. GaAs (110). The first case is directly related to the incorporation of magnetic dopants during growth, while the later case is more representative of the properties of the dopant incorporated in the bulk of these semiconductors. The second goal is to develop local differential magnetic conductivity $\frac{dI}{dm_T}(\vec{r}_T, V)$ imaging that provides spatially resolved mapping of magnetization $m_S(\vec{r}_T, E_F + eV)$. The third goal is to investigate the electronic and magnetic properties of ferromagnetic semiconductors at the onset of ferromagnetic ordering, using spin-polarized STM, *dI/dV* and dI/dm_T imaging. Knowledge gained from these studies will be critical to elucidate the nature of the interactions between the magnetic dopant and host semiconductors at the atomic scale, which holds the key to the realization of room temperature ferromagnetic semiconductors.

Recent Progress

1. Atomic resolution view of Mn incorporation on GaN(0001) by STM

A metallic pseudo-1x1 (denoted "1x1") surface of GaN(0001) is composed of more than two additional monolayers (ML) of Ga on top of the Ga-terminated GaN, and is often found on films grown under Ga-rich conditions [3]. The presence of the Ga adlayer offers new subsurface diffusion channels for lateral adatom transport during GaN MBE [4,5]. For the first part of this program, we have carried out a detailed study of the Mn adsorption on the "1x1" surface. Presented in Fig. 1 are STM images of the "1x1" surface after Mn adsorption. On the large scale, triangular islands of contrasting brightness are observed (Fig. 1(a)). The atomic resolution image of the region marked by a green box reveals a perfectly ordered (1x1) structure (Fig. 1(b)) [6]. On the other hand, the region marked by a white box exhibits a slightly disordered ($\sqrt{3}\times\sqrt{3}$)

reconstruction. Regions of contrasting brightness exist randomly. Interestingly, the (√3×√3) geometry is preserved across the boundaries.

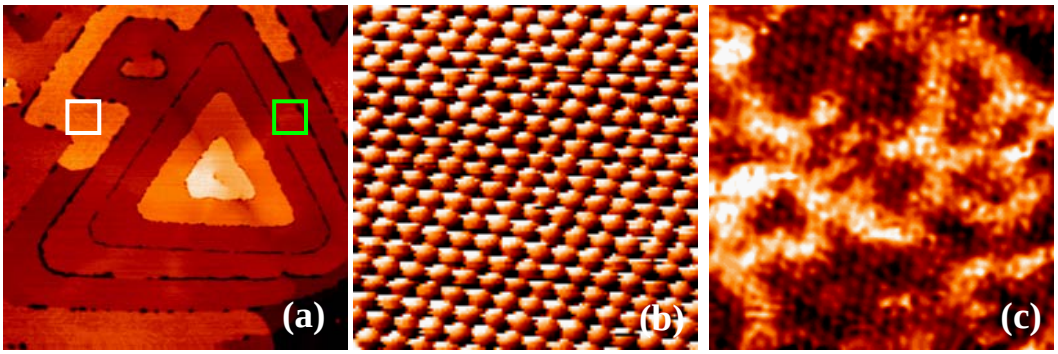

Fig. 1 (a) STM image of the GaN(0001) surface after Mn deposition (450x450nm^2, V_t=-0.5V, and I_t=0.1nA); (b) close-up of the "1x1" region in green box (4x4 nm^2, V_t=-1.1V, and I_t=0.1nA); and (c) close-up of the (√3×√3) region in white box (12x12nm^2, V_t=-0.2V, and I_t=0.75nA).

2. *First principles calculations of Mn substitution on GaN(0001)*

Spin-resolved density of states (DOS) for the surface Mn and Ga have been calculated using the Full-potential Linearized Augmented Plane Wave (FLAPW) method [7], as shown in Fig. 2. A total magnetic moment of ~2.6 μ_B/Mn is found. This behavior is exactly as one would expect from a localized (magnetic) impurity in a free-electron like material (virtual bound state). The widths of the bands (~1.5 eV) show that there are still significant Mn-Ga interactions.

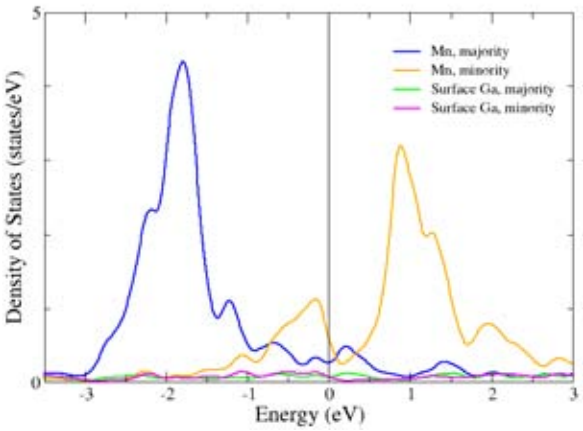

Fig. 2 Calculated spin-resolved DOS for Mn and Ga on the "1x1" surface with Mn substituting the top Ga.

a. Charge DOS of Mn on GaN(0001)

To better illuminate the STM observations, spatially resolved DOS around the Fermi level, ρ_F, have been calculated for the "1x1" surface without and with (Fig. 3(a)) Mn. A higher density of charge is found at the Mn atom substituted for a top layer Ga.

Based on the calculations, a structural model for the (√3×√3) reconstruction is proposed as shown in Fig. 3(b): the Mn substitution of Ga freezes the Ga motion in adlayer of the "1x1", hence the extra Ga atoms of the top layer Ga "pop up" above the top

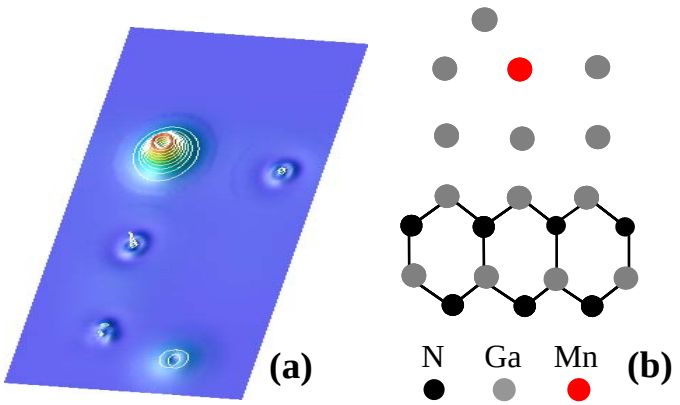

Fig. 3 (a) Calculated charge DOS of the "1x1" at Fermi level with Mn substituting a top layer Ga. (b) Ball-and-stick model of the (√3×√3).

layer to reside at the T_4 sites, forming the ($\sqrt{3}\times\sqrt{3}$) reconstruction. Due to the higher density of states at Mn sites, the regions that contain the incorporated Mn would give rise to the bright features observed in the STM image in Fig. 2(b).

b. Spin-resolved DOS of Mn on GaN(0001)

We have also calculated the spin-resolved DOS for Mn incorporation on the pseudo (1x1), as shown in Fig. 4. Clearly, the spin densities in the occupied and unoccupied states are almost completely reversed, and should manifest in the enhanced contrast in spin polarized STM, facilitating their detection by spin-polarized *dI/dV* imaging.

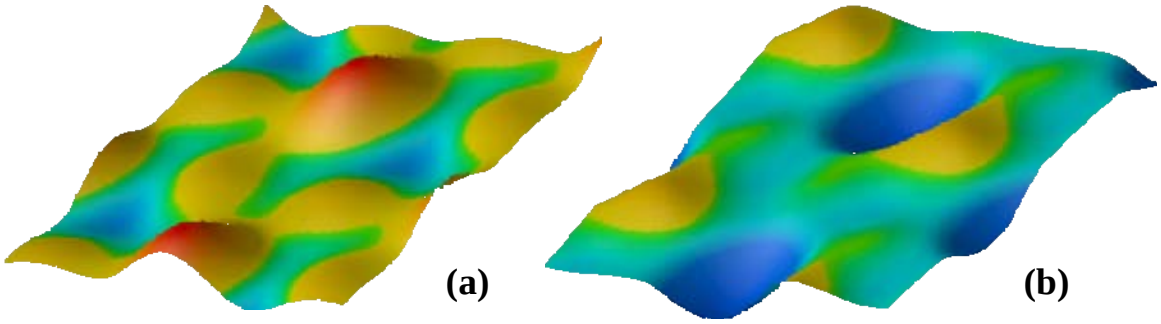

Fig. 4 Calculated (a) occupied and (b) unoccupied spin DOS of the Mn:GaN "1x1".

Future Plans

The immediate plan is to fabricate magnetic tips that are W coated with Fe and/or other magnetic material such as Cr and Mn using a tip annealing apparatus that we constructed recently. Spin-polarized *dI/dV* imaging of the Mn incorporated GaN(0001) surfaces will then be carried out. The experiments will be guided and compared to the calculated spin-polarized DOS presented above.

Next we will investigate the electronic and magnetic properties of Mn incorporation on the cleaved surfaces of GaN and GaAs. The lack of surface states on these surfaces, such as GaAs(110), make them good candidates for the investigation of properties of the magnetic dopant incorporated in the bulk of these semiconductors. GaAs and GaN samples will be cleave *in situ*, and Mn adsorption on the cleaved surfaces will be investigated by spin-polarized imaging and spectroscopy. Comparison between Mn incorporation in these two materials will be interesting as Mn is a shallow acceptor in GaAs where as in GaN it introduces deep acceptor level. Theoretical calculations of the electronic and magnetic properties in these two scenarios will be especially illuminating in interpreting experimental results.

References

1. T. Dietl, H. Ohno, F. Matsukura, J. Cibert, and D. Ferrand, "Zener model description of ferromagnetism in zinc-blende magnetic semiconductor", Science **287**, 1019 (2000).
2. S. A. Wolf, D. D. Awschalom, R. A. Buhrman, J. M. Daughton, S. von Molnar, M. L. Roukes, A. Y. Chtchelkanova, and D. M. Treger, "Spintronics: A spin-based electronics vision for the future", Science **294**, 1488 (2001).
3. J. E. Northrup, J. Neugebauer, R. M. Feenstra, and A. R. Smith, "Structure of GaN(0001): The laterally contracted Ga bilayer model", Phys. Rev. B **61**, 9932 (2000).

4. J. Neugebauer, T. K. Zywietz, M. Scheffler, J. E. Northrup, H. Chen, R. M. Feenstra, "Adatom kinetics on and below the surface: The existence of a new diffusion channel", Phys. Rev. Lett. **90**, 056101 (2003).
5. S. T. King, M. Weinert, and L. Li, "Atomic structure of the metastable GaN 'ghost' islands and a mechanism for their conversion", Phys. Rev. Lett. (submitted, Aug. 22, 2006).
6. M. L. Harland and L. Li, "Observation of standing waves at steps on the GaN(0001) pseudo 1x1 surface by scanning tunneling spectroscopy at room temperature", Appl. Phys. Lett. (in press).
7. M. Weinert, E. Wimmer, and A. J. Freeman, Phys. Rev. B **26**, 4571 (1982).

DOE Sponsored Publications in 2005-2006

1. *"Atomic Structure of the Metastable GaN "Ghost" Islands and a Mechanism for Their Conversion"*, S. T. King, M. Weinert, and L. Li, Phys. Rev. Lett. (submitted, Aug. 22, 2006).
2. *"Observation of Standing Waves at Steps on the GaN(0001) Pseudo 1x1 Surface by Scanning Tunneling Spectroscopy at Room Temperature"*, M. L. Harland and L. Li, Appl. Phys. Lett. (in press).

Near-Field Raman Spectroscopy of Carbon Nanotubes

(Annual Report, DOE Grant No. DE-FG02-05ER46207)

Lukas Novotny, University of Rochester, The Institute of Optics, Rochester, NY 14627

1 Program Scope

In this project we study local defects and dopants in carbon nanotubes, as well as their interaction with the local environment. Detection and characterization of structural and electronic properties of carbon nanotubes relies on spectroscopic techniques with high spatial resolution. While optical spectroscopy is a powerful technique for the study of structural and chemical properties of materials its resolution is traditionally limited by diffraction to $\approx \lambda/2$. This is typically more than one order of magnitude larger than the characteristic length-scale of most nanoscale systems. To overcome this limitation, we have developed a near-field optical technique based on the well-known effect of surface enhanced Raman scattering (SERS) [1, 2]. A sharp laser-irradiated metal tip localizes and enhances the optical field at its apex thereby creating a nanoscale light source. The metal tip is brought in close proximity to a sample surface and Raman scattered light is collected and assigned to the momentary tip position. By raster scanning the tip, a high-resolution, chemically specific map of the sample surface can be recorded.

Figure 1 shows a typical data set recorded on a semiconducting single-walled carbon nanotube (SWNT). The spatial resolution is roughly 15 nm as indicated in (A). for every image pixel a full Raman scattering spectrum is recorded (B). The image contrast in (A) is obtained by integrating the recorded spectra over a spectral range and assigning to the resulting value a color. In the example shown in Figure 1 the spectral integration range is indicated by the vertical yellow stripe. (C) shows the Raman scattering strength as a function of the distance between tip and nanotube.

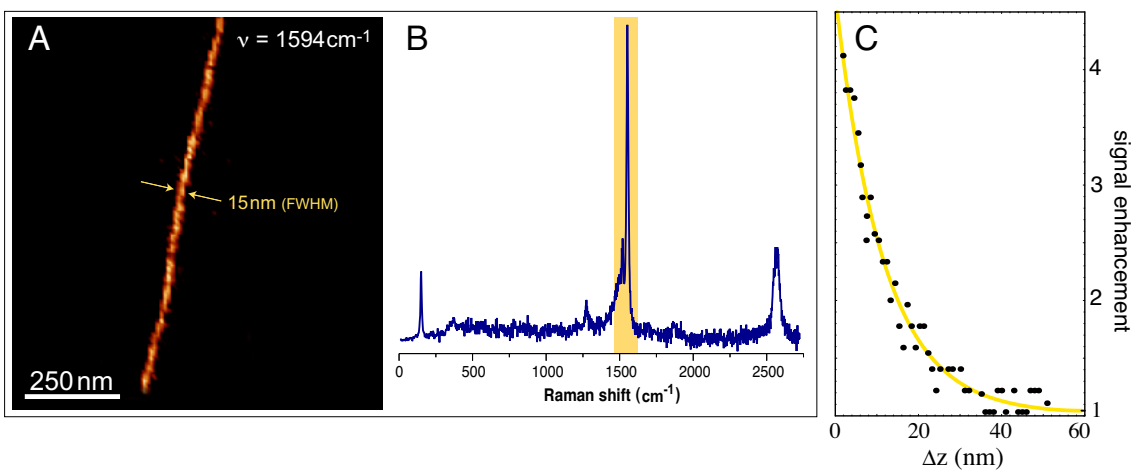

Figure 1: *Near-field Raman imaging of single-walled carbon nanotubes. The spatial resolution of 15nm in (A) is entirely defined by the tip sharpness. This image has been recorded by raster-scanning the sample underneath the laser-irradiated metal tip and integrating, for each image pixel, the photon counts that fall into a narrow spectral bandwidth centered around the G-line at* $\nu = 1594\ cm^{-1}$ *(indicated by the yellow stripe in B). (B) Raman scattering spectrum recorded on top of the nanotube, (C) Enhancement of the G-line signal as a function of tip-sample distance. The yellow line is an exponential fit with a 13nm decay length.*

2 Recent Progress

In the first year of this project we have completed the experimental setup and began first near-field Raman studies of SWNTs. A schematic of the setup is shown in Fig. 2. The light source is a combination of a Dye Laser (Coherent 699) and a Titanium-Sapphire laser (Coherent 899-01) both pumped by a solid state Nd:YAG laser (Coherent Verdi 8W). This laser system provides narrow line continuous-wave operation in the wavelength range $532 - 940\,\mathrm{nm}$. It allows us to excite individual nanotubes resonantly into their excitonic states and also excite the band-to-band transitions E_{11} an E_{22}.

Before the laser beam is sent into a modified inverted fluorescence microscope (Nikon TE300, existing), it is externally converted to a radially polarized mode to ensure a strong longitudinal field component at the laser focus. After entering the inverted microscope the laser beam is reflected by a dichroic beam-splitter and focused by a microscope objective on the sample surface. A sharp gold tip, held above the sample surface in close proximity, is centered onto the focal spot and maintained there by use of a sensitive shear-force feedback system. The locally scattered field is collected by the same objective lens, filtered by the combination of the dichroic filter and interference filters, and detected by either a photon-counting avalanche photodiode or a combination of a spectrograph and a liquid nitrogen cooled CCD. The sampleis mounted on a $40 \times 40 \mu m$ closed-loop scan-bed and raster-scanned in the horizontal plane. The control electronics consists of a modified controller for scanning tunneling microscopy. It is used for controlling the scan-bed, tip height regulation, and image acquisition. The entire setup is placed inside a light-free, acoustically damped enclosure located on a floating optical table.

The gold tips needed for the experiments are produced by electrochemical etching and optionally modified by focused ion beam milling. The shape and material of the tips is being optimized for strong field enhancement. The access to a high resolution scanning electron microscope (LEO,

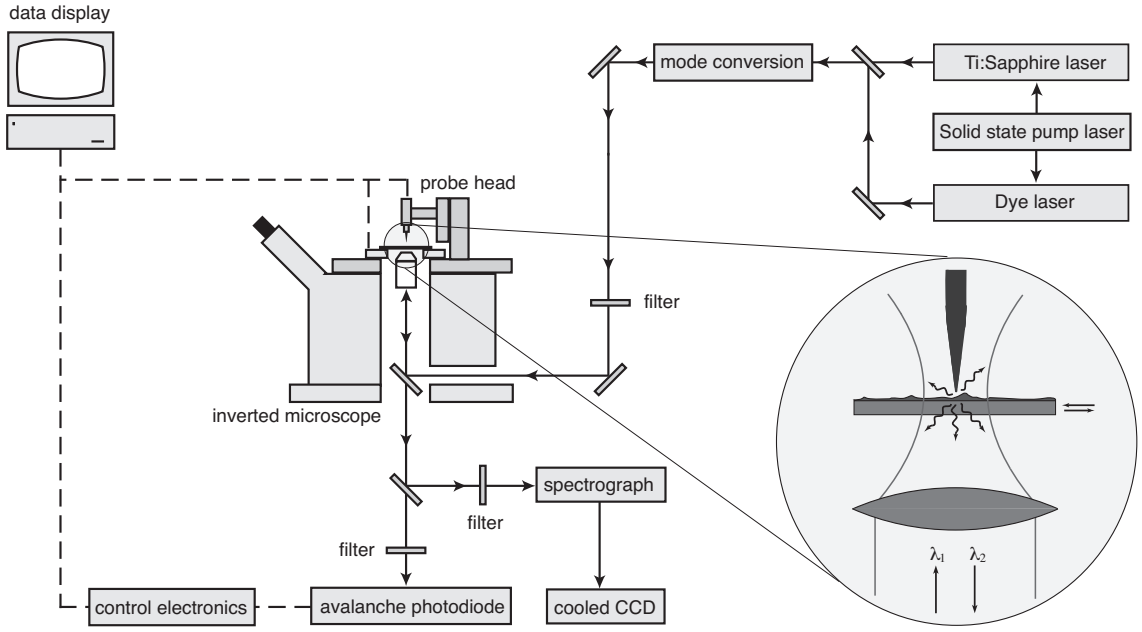

Figure 2: Schematic of the experimental setup. The optical path is represented by solid lines, electronic signals are represented by dashed lines. See text for details.

Gemini) at the Institute of Optics helps greatly in this optimization process. The metal tip is maintained within $1-2nm$ above the sample surface by using a tuning-fork feedback mechanism. A highly sensitive pre-amplification allows operation with interaction forces of $10pN$ between tip and sample. Forces in this range do not damage the soft metal tips.

We have made measurements using carbon nanotubes produced by different methods: 1) arc-discharge, 2) HiPco, and 3) CVD. Our measurements have revealed that the measured Raman modes on arc-discharge and HiPco tubes are often spatially localized whereas they appear continuously distributed along CVD grown nanotubes [3]. We tentatively assign this observation to defects in the tube structure. Currently we are in the process of generating intentional defects using local oxygen plasma etching induced by the tip potential. This will allow us to image the same nanotube before and after introducing defects. The comparison will allow us to quantitatively investigate to what extent the individual Raman modes are perturbed by local defects. Also, this procedure will allow us to study the effect of exciton localization in nanotubes [4, 5].

As shown in Fig. 3 we have established first evidence that certain phonon modes tend to localize near defects. The data set shows a different Raman modes along a single CVD grown nanotube. The nanotube is surrounded by many catalyst particles which are clearly visible in the simultaneously recorded topographic image (not shown). The nanotube winds around a particularly large catalyst particle giving rise to a local perturbation. While the radial breathing mode (RBM) is largely unaffected by this local interaction other modes, such as the D band or the intermediate frequency mode (IFM) show up only near the defect (circled red). In a defect-free planar graphite sheet the D-band does not exist. The necessary momentum balance needed to generate D-band scattering can only be accomplished through defects in the graphite structure. We expect similar D-band origins for carbon nanotubes and our preliminary results support this hypothesis.

3 Future Plans

We intend to establish quantitative relationships between defects and localization of phonon modes. For this purpose we will grow uniform carbon nanotubes by CVD and then use local voltage pulses

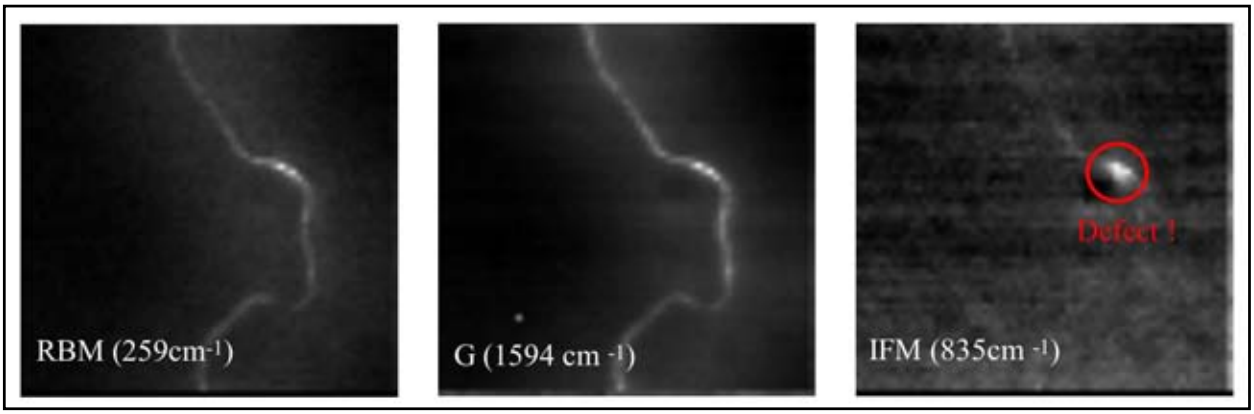

Figure 3: *Demonstration of defect localization in carbon nanotubes using near-field Raman scattering. The images show a single-walled carbon nanotube imaged at different vibrational frequencies. The image size is 1μm x 1μm and the resolution is better than 15nm. The radial breathing mode frequency (RBM) determines the tube structure (n,m)=(8,5) and its diameter d=0.9nm. The defect-mediated intermediate frequency mode (IFM) indicates that the tube has a local defect, most likely induced by a catalyst particle.*

applied to the metal tip to induce local defects in the tube structure. This approach will allow us to quantitatively compare the Raman signatures before and after the tube has been structurally modified.

References:

[1] A. Hartschuh, E. J. Sanchez, X. S. Xie, and L. Novotny, "High-resolution near-field Raman microscopy of single-walled carbon nanotubes," *Phys. Rev. Lett.*, vol. 90, 95503, 2003.

[2] A. Hartschuh, M. R. Beversluis, A. Bouhelier, and L. Novotny, "Tip-enhanced optical spectroscopy," *Phil. Trans. R. Soc. Lond. A*, vol. 362, pp. 807–819, 2004.

[3] N. Anderson, A. Hartschuh, S. Cronin, and L. Novotny, "Nanoscale vibrational analysis of single-walled carbon nanotubes," *J. Am. Chem. Soc.*, vol. 127, pp. 2533-2537, 2005.

[4] A. Hartschuh, H. N. Pedrosa, L. Novotny, and T. D. Krauss, "Simultaneous fluorescence and Raman scattering from single carbon nanotubes," *Science*, vol. 301, pp. 1354–1356, 2003.

[5] A. Hartschuh, H. Qian, A. J. Meixner, N. Anderson, and L. Novotny, "Nanoscale optical imaging of excitons in single-walled carbon nanotubes," *Nano Lett.* vol. 5, pp. 2310–2313, 2005.

[6] A. Hartschuh, H. Qian, A. J. Meixner, N. Anderson, and L. Novotny "Tip-enhanced optical spectroscopy of single-walled carbon nanotubes," in *Advances in Nano-Optics and Nano-Photonics, Vol 1: Tip Enhancements*, S. Kawata and V. M. Shalaev (eds.), Elsevier, in print, 2006.

[7] A. Hartschuh, H. Qian, A. J. Meixner, N. Anderson, and L. Novotny "Tip-enhanced optical spectroscopy for surface analysis in biosciences," *Surface and Interface Analysis* in print, 2006.

Publications [6], [7] resulted from the current budget period (since May 15, 2005).

Session IV

Grain Boundaries, Defects, and Interfaces

Understanding the Electronic and Magnetic Structure of Advanced Materials

Y. Zhu, R.F. Klie, M.A. Schofield, V.V. Volkov, M. Beleggia and L. Wu
zhu@bnl.gov, klie@bnl.gov, schofield@bnl.gov, volkov@bnl.gov, beleggia@bnl.gov, ljwu@bnl.gov
Brookhaven National Laboratory, Upton, NY 11973

Program Scope

The research focus of this program is on exploring nanoscale phenomena that control the functionality of technologically important materials having significant relevance to the DOE's energy mission. It includes two major areas of research: 1) electronic structure, structural defects and interfaces in strongly correlated electron systems; and 2) magnetic structure and nanoscale magnetism. The emphasis is on understanding the relationship between structure and properties, and the underlying mechanisms of the complex physical behaviors of a wide range of functional materials including high-temperature superconductors (HTS). Advanced quantitative electron microscopy techniques, such as coherent electron diffraction, atomic imaging, electron spectroscopy, and phase retrieval methods are extended to study these materials. Experiments are closely coupled with structural modeling and theory. Although electron scattering and electron microscopy are the primary tools, complementary methods such as synchrotron x-ray and neutron scattering are also used.

Recent Progress

In the area of strongly correlated electron systems, we studied $CaCu_3Ti_4O_{12}$, a perovskite oxide that exhibits a prodigiously high dielectric constant (~10^5) for a non-ferroelectric over a wide range of temperature and frequency.[1] Using quantitative electron diffraction and extended x-ray absorption fine structure (EXAFS) spectroscopy, we studied the valence electron distribution and revealed nanoscale disorder in the system, involving Cu-Ca substitutions. Density Functional Theory (DFT) calculations showed that when Cu occupies the Ca site in the insulating matrix, the region becomes metallic due to orbital degeneracy and yields the mystifying dielectric behavior.

Grain boundaries and interfaces often define the functionality of a material or a device. Our latest study on interfaces was the direct observation of the correlated behavior of charge, spin and orbital ordering of $LaMnO_3/SrMnO_3$ superlattices. The digitally synthesized thin films (in collaboration with researchers at ANL and UIUC) represent a model system to understand correlated behavior and emergent phenomena at an ideal mixed-valence interface.[2] Although both $LaMnO_3$ (Mn^{3+}) and $SrMnO_3$ (Mn^{4+}) are antiferromagnetic insulators at low temperature, when synthesized to a superlattice structure $(LaMnO_3)_8/(SrMnO_3)_4$, the system undergoes an antiferromagnetic to ferromagnetic transition at 225K with significant change in resistivity. Using atomic Z-contrast imaging, column-by-column electron energy-loss spectroscopy (EELS) and electron holography in the temperature regime between 86-300K, we were able to directly measure the local hole concentration, the Mn valence and total magnetization moment across the interfaces associated with the magnetic transition. We revealed, for the first time, the interplay between spin, charge and orbital ordering that occurs at the

interface on an atomic scale. We found that the mixed-valence phase emerging near the interface and penetrating about one nanometer from $SrMnO_3$ into the $LaMnO_3$ layer is responsible for the interfacial ferromagnetic ordering via a double exchange mechanism. The observed ferromagnetically ordered phase at the interface was confirmed by DFT calculations. We proposed a model for the interfacial ferromagnetic state and a hopping mechanism for coupling charge mobility and the emergent magnetism.

Another area where we have made significant progress recently is on nanoscale magnetism. We studied the magneto-static and -dynamic behavior of individual ferromagnetic elements with various sizes and shapes using in-situ magnetization techniques, Lorentz microscopy and electron holography. These elements can be considered as magnetic building blocks with different ground states (e.g., "0" and "1") under different applied fields, thus are very important to the high-density data-storage technology. Our progress includes fabrication of Permalloy and Co film-elements with square, ellipse, circle, and tear-drop shapes and understanding their magnetic hysteresis and reversal behavior. The success was built on our instrumentation development, including a home-made UHV e-beam deposition system and sample stages with a Hall-sensor to measure local field as well as with Helmholtz coils and a Piezo controlled magnetic tips (a scanning-tunneling-microscope based stage) to apply local fields. The experimental observations were directly compared with micromagnetics simulation using the Landau-Lifshitz-Gilbert equation to understand the magnetostatics and dynamic behavior of the magnetic building blocks.

Future Planes

Our previous studies on Ca-doped $YBa_2Cu_3O_7$ bi-crystals indicate that the grain boundary transport properties are strongly affected by the electronic state and charge transfer due to the local lattice strain surrounding the interfacial dislocation cores.[3] Furthermore, the study of $LaMnO_3/SrMnO_3$ superlattices reveals a striking dependence of conductivity on the magnetic state at the heterogeneous interfaces. While we are making progress, fundamental understanding of interfacial phenomena such as hole accumulation, spin ordering and transport remains seriously inadequate. Future advances in grain boundary engineering and electronic and spintronic devices demand a better understanding of these interfacial properties and phenomena.

To address these challenging issues, we will continue to investigate homogeneous and heterogeneous interfaces in strongly correlated systems. With our unique nano-probe capabilities ranging from atomic imaging and spectroscopy to electron holography, we can identify not only the interfacial atomic arrangement, but also the distribution of charge, the electrostatic and magnetic potential and their dependence on temperature and applied field. Corresponding macroscopic measurements such as transport and magneto-optic properties will be carried out. In addition to the study of $(LaMnO_3)_{2m}/(SrMnO_3)_m$, we will study the hetero-interfaces between HTS and non-HTS oxide multi-layer films and junctions synthesized by Ivan Bozovic at BNL with his state-of-the-art MBE system. We will focus on the emergent interfacial characteristics such as atomic layer sequence, interfacial strain, local charge inhomogeneity and transfer, and magnetic order across the superconducting transition temperature in order to shed light on the competition between

lattice, charge, spin and orbital degrees of freedom at the interfaces, as well as their relation to the superconductivity.

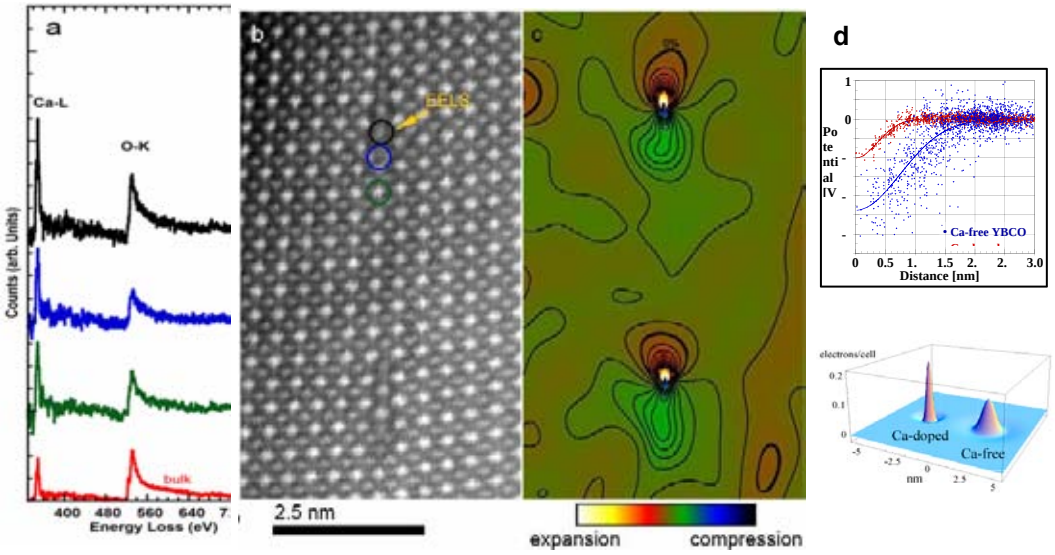

An example of interface study. (a) Column-by-column EELS from the dislocation core marked in (b); (b) STEM image of a Ca-doped 4º [001] tilt boundary in YBCO bi-crystal; (c) strain map of the dislocation cores based on geometric phase analysis, color scale indicates relative strain; and (d) electrostatic potential and space charge of the dislocation core with and without Ca doping measured by electron holography.

In the area of nano-magnetism, we will focus on magnetodynamics of domain and vortex nucleation and evolution, their relation to structural defects, and magnetization reversal and switching behavior as a function of field and temperature in artificially designed model systems to resolve fundamental questions in nanomagnetism. Amongst the numerous issues facing the data-storage industry today is the insufficient knowledge regarding the effects of long-range magnetostatic interactions in determining the magnetic and thermal responses in arrays of magnetic elements. With our theoretical developments, we can evaluate the minimum energy state of the system for a given set of external parameters. For example, we found that some systems composed of macro-spins, i.e. magnetic elements below the single domain critical size showing a quasi-uniform magnetization topography, undergo a shape-induced magnetic phase transition. Below a critical combination of aspect ratios and distances, a system of three equilaterally-spaced magnetic disks will change abruptly from an overall closure domain state, with zero net magnetization, to a dipolar ferromagnetic state with a net magnetization that depends on the interaction strength between the elements.[4] Our goal is to experimentally verify these theoretical predications and to fully understand the low-energy states and switching process of magnetic elements with different shapes and sizes, and the interaction with their neighbors under a magnetically frustrated environment.

References

(1) C.C. Homes et al., *Science* **293**, 673 (2001).
(2) A. Ohtomo et al., *Nature*, **419** 378 (2002).
(3) R.F.Klie et al., *Nature*, **435**, 475 (2005).
(4) M. Beleggia et al., *App. Phys. Lett.*, **87**, 202504 (2005).

DOE Sponsored Publications in 2005

1. *Intersecting Basal Plane and Prismatic Stacking Fault Structures and Their Formation Mechanism in GaN*, J. Bai, X.Huang, M.Dudley, B.Wagner, R.Davis, L.Wu, E. Sutter, Y. Zhu, B.Skromme, *J. Appl. Phys*. **98**, 063510 (2005).
2. *Shape-induced ferromagnetic ordering in a triangular array of magnetized disks*, M. Beleggia, S. Tandon, Y. Zhu and M. De Graef,. *Appl. Phys. Lett*. **87**, 202504-202506 (2005).
3. *General magnetostatic shape-shape interactions*, M.Beleggia and M.De Graef. *J. Mag. Mag. Mat.* **285**, L1(2005).
4. *Nanoscale magnetic phase imaging and induction mapping using advanced electron microscopy techniques*, M. Beleggia and Y. Zhu, chapter 7 in "Modern techniques for characterizing magnetic materials", Ed. Y. Zhu, (Kluwer academic, 2005).
5. *Demagnetization factors for elliptic cylinders*, M. Beleggia, M. De Graef, Y.T. Millev, D.A. Goode and G. Rowlands,. *J. Phys. D: Appl. Phys*. **38**, 3333-3342 (2005).
6. *Phase diagram for magnetic nano-rings*, M. Beleggia, J.W. Lau, M.A. Schofield, Y. Zhu, S. Tandon, and M. De Graef.. *Mag. Mater*, **301**, 131-146 (2005).
7. *Inversion of two-band superconductivity at the critical electron doping of (Mg,Al)B_2*, L. D. Cooley, A.J. Zambano, A.R. Moodenbaugh, R.F. Klie, Z.C. Zhen, Y. Zhu, *Phys. Rev. Lett.* **95** 267002 (2005).
8. *Electron optical phase shifts by Fourier methods: analytical versus numerical calculations*, P.F. Fazzini, G. Pozzi, M. Beleggia, *Ultramicroscopy*, **104**, 193-205 (2005).
9. *Formation and oxidation state of CeO_{2-x} nanotubes*, W.Han, L.Wu and Y.Zhu, *J.Am.Chem.Soc*.,**127** 12814 (2005).
10. *Growth of anatase films on vicinal and flat LaAlO3 (110) substrates by oxygen plasma assisted molecular beam epitaxy*, W. Gao, R.F. Klie, E.I. Altman, *Thin Solid Films* **485**(1-2), 115-125 (2005).
11. *Growth and Characterization of Model Oxide Catalysts*, W. Gao, M. Li, R.F. Klie, and E.I. Altman, *J. Elect. Spectr*. **150** (2-3), (2005).
12. *In-situ Formation of Ultrathin Ge Nanobelts Bonded with Nanotubes*, Wei-Qiang Han, Lijun Wu, Yimei Zhu and Myron Strongin, *Nano Lett.* **5** 1419 (2005).
13. *Quasi-Continuous Growth of Ultralong Carbon Nanotube Arrays*, B. H. Hong, J. Y. Lee, T. Beetz, Y. Zhu, P. Kim, and K.S. Kim, *J. Am. Chem. Soc*., **127** 15336 (2005).
14. *Step-Controlled Strain Relaxation in the Vicinal Surface Epitaxy of Nitrides*, X. R. Huang, J. Bai, M. Dudley, B. Wagner, R. F. Davis, and Y. Zhu, *Phys. Rev. Lett.* **95**, 086101 (2005).
15. *Direct Imaging of Cooperative Doping Mechanisms at Grain Boundaries in Ca-doped $YBa_2Cu_3O_{7-\delta}$*, R. F.Klie, J. Buban, M.Varela, A.Franceschetti, C.Jooss, Y. Zhu, S.T.Pantelides, S.J.Pennycook, *Nature* **435**, 475-478 (2005).
16. *Atomic Resolution Electron Energy-Loss Spectroscopy*, R. F. Klie, I. Arslan, N. D. Browning, *J. Elect. Spectr*., **143** (2-3), 107-117 (2005).
17. *Atomic resolution STEM analysis of defects and interfaces in ceramic materials*, R. F. Klie and Y. Zhu, Review article, *Micron*, **36** 219-231 (2005).
18. *Atomic structure of epitaxial $SrTiO_3$-GaAs (001) heterojunctions*, R. F. Klie and Y. Zhu, E.I. Altman, and Y. Liang, *Appl. Phys. Lett.* **87**, 143106 (2005).
19. *Direct correlation of reversal rate dynamics to domain configurations in micronsized Permalloy elements*, J. W. Lau, M. Beleggia, M. A. Schofield, G. F. Neumark, and Y. Zhu, *J. Appl. Phys*., **97** 10E702 (2005)
20. *Electron-beam patterning with sub-2nm line-edge roughness*, M. Malac, R. Egerton, M. Freeman, J. Lau, Y. Zhu, and L. Wu, *J. Vacuum Sci. Tech. B* **23** (1), 271 (2005).
21. *Electrical Characterization of Single GaN Nanowires*, E. Stern, G. Cheng, E. Cimpoiasu, R.F. Klie, S. Guthrie, J. Klemic, I. Kretzschmar, E. Steinlauf, D. Turner-Evans, E. Broomfield, J. Hyland, R. Koudelka, T. Boone, M. Young, A. Sanders, R. Munden, T. Lee, D. Routenberg, and M. A. Reed, *Nanotechnology*, in press.
22. *BaF_2 post-deposition reaction process for thick YBCO films*, M. Suenaga, V. F.Solovyov, L. Wu, H.Wiesmann and Y. Zhu, chapter in: *Second-generation HTS conductors*, A.Goyal Ed, Kluwer Academic, pp. 135-148 (2005).
23. *Assembly and Interaction of Au/C Core-Shell Nanostructures: In-Situ Observation in the Transmission Electron Microscope*, E. Sutter, P. Sutter, and Y. Zhu, *Nano Lett*. **5**, 2092 (2005).
24. *Martensitic phase transformation of isolated HfO_2, ZrO_2 and $Hf_xZr_{1-x}O_2$ ($0<x<1$) nanocrystals*, J. Tang, F. Zhang, P. Zoogman, J. Fabbri, S. Chan, Y. Zhu, L. E. Brus, and M. L. Steigerwald, *Adv .Func. Mater*, **15** (10) 1-8 (2005).
25. *Defect structure of the high-dielectric-constant perovskite $CaCu_3Ti_4O_{12}$*, L. Wu, Y. Zhu, S. Park, S. Shapiro, and G. Shirane, *Phys. Rev. B*, **71**, 014118 (2005).
26. *Enhanced Flux Pinning in YBCO Films by Nano-Scaled Substrate Surface Roughness*, Z. Ye, W. D. Si, Q. Li, Y. Hu, P. D. Johnson, and Y. Zhu, *Appl. Phys. Lett*. **87** 122502 (2005).
27. *Searching for higher superconducting transition temperature in strained MgB2 using first principles calculations*, J. Zheng, and Y. Zhu, *Phys. Rev. B*, in press.
28. On *the sensitivity of electron- and x-ray-scattering factors to valence charge distributions*, J. Zheng, L. Wu, Y. Zhu, and J. W. Davenport, *J. of Appl. Crystallography*, **38**, 648–656 (2005).

The role of interface chemistry and structure on properties of oxide thin film heterostructures

A K Petford-Long, O Auciello, J Eastman, S Nakhmanson and S K Streiffer
Petford.long@anl.gov, auciello@anl.gov, jeastman@anl.gov, nakhmanson@anl.gov, streiffer@anl.gov
Materials Science Division, Argonne National Laboratory, Argonne, IL 60439

Program Scope

The goal of the program is to advance our understanding of the importance of interfacial contributions to novel phenomena exhibited by thin film oxide heterostructures. Our research program is structured around three thematic areas. Firstly, to understand growth dynamics in the synthesis of complex oxide films, including competition between the growing composition and stress development and the formation of interfaces in heterostructures. Additionally to understand the role of interface and surface modification in controlling factors such as domain behavior in ferroelectric thin films. Secondly, to understand the mechanisms by which the properties of an oxide thin film are changed/modified when in contact with another material, through effects such as mechanical confinement (in three-dimensions), charge transfer and band structure modification. Thirdly, to develop a full understanding of the dynamic response of ferroic nanostructures. While macroscopic theories of domain dynamics have been validated for bulk materials, these theories do not always properly describe the observed phenomena (switching speeds, activation energies, etc.) for thin films or nanopatterned structures. This includes the physics underlying reversal domain nucleation and domain wall velocity in ferroelectrics, and ferromagnetic magnetization reversal mechanisms in patterned oxide heterostructures.

Recent progress

In Situ X-Ray Studies of MOCVD Pb(Zr,Ti)O_3 Growth An ongoing objective of our program has been to build up a detailed understanding of complex oxide thin film growth processes, particularly in the context of metalorganic chemical vapor deposition (MOCVD). Utilizing our unique facility developed on APS beamline 12ID-D for in situ probing of materials processing in real time (in collaboration with G.B. Stephenson), we have observed variation in the Zr:Ti ratio during MOCVD growth of Pb(Zr,Ti)O_3 (PZT) on $SrTiO_3$ substrates, correlated with relaxation of epitaxial strains. Strain-coupled composition variation has been observed in semiconductor systems,[i] but has not previously been seen in complex oxide systems. Our previous studies on $PbTiO_3$/$SrTiO_3$ found ferroelectricity for films with thickness as small as 1.2 nm,[ii] motivating us to examine the behavior of more complex alloys, where local chemical heterogeneity is expected to give rise to new physics as dimensions are reduced. The film initially grew lattice-matched to the $SrTiO_3$ substrate, but began relaxing and evolving in composition at a thickness of ~22.5 nm. The behavior can be qualitatively explained as follows. For a coherently and compressively strained film, Zr, which is large relative to Ti, has low incorporation efficiency into the growing film given the gas phase Zr/Ti precursor ratio of 0.10. As the film relaxes, there is a smaller energy penalty for Zr incorporation. Resulting in an increase in the Zr concentration at the growth interface, even though the growth conditions remain the same. Note that good reproducibility of these results and absence of composition changes for growth onto relaxed films after interruption indicates that this is indeed a real effect.

In-situ TEM studies of vortex behavior in exchange-biased magnetic dots and of tunneling mechanisms
We are using in-situ Lorentz TEM and holography to probe the *local* domain structure in magnetic and ferroelectric heterostructures.[iii] There is considerable interest in the dynamics of magnetic vortices in patterned magnetic nanostructures, both in single layers[iv,v] and in exchange-biased systems.[vi] We are carrying out initial studies of exchange-biased IrMn/NiFe magnetic dots containing magnetic vortices, as a precursor to studying vortex behavior in magnetic tunnel junction heterostructures. We have observed a complicated reversal mechanism with the nucleation and subsequent annihilation of single or double

vortices, as a function of angle between the field and the exchange bias direction, in addition to motion of the vortices by a viscous mechanism involving motion of the pinned and unpinned ends of the vortex at different applied field values. Micromagnetic simulations (collaboration with O. Heinonen, Seagate Technology) show the vortex to move at an angle to IrMn/NiFe interface, which is not seen for single layer NiFe dots. We have also developed a novel nanobiasing TEM holder that is allowing us to bring a sharp tip into contact with the top surface of a thin tunnel junction structure in order that the local I-V curve can be measured at the same time as cross-section TEM images are recorded of the same area.

Biomatter-Polarizable Ferroelectric Interfaces The interaction of surface polarization with charged/polar entities across an interface presents a unique method for nanostructure assembly on surfaces, for example of biomolecules, but an understanding of the interface between biomatter and polarizable ferroelectric film surfaces is vital. Recent initial research involving a collaboration with M. Firestone (Materials Science Division) and L Ocola (Center for Nanoscale Materials) have demonstrated that the surface of ferroelectric $PbZr_xTi_{1-x}O_3$ (PZT) films can be functionalized using silane chemistry.[vii] The formation of a chemisorbed monolayer on the PZT surface upon exposure to the silane chemistry can subsequently be used to covalently attach a wide variety of biomolecules. Combinatorial phage display methods were used in the initial research to identify a circularly constrained heptapeptide sequence, ISLLHST, that strongly associates with the perovskite ferroelectric PZT surface. The affinity and selectively of binding to polycrystalline MOCVD deposited PZT thin films supported on $Si/SiO_2/Pt$ substrates were determined by titration and immunofluorescence microscopy. Ferroelectric properties were evaluated by measurement of the P-E hysteresis loop on unmodified and phage bound PZT thin films and showed no degradation of properties by the aqueous functionalization process.

Future work

We intend to continue to develop our unique in-situ X-ray analysis/ MOCVD growth facilities to manipulate film strain using composition and substrate-induced constraints. One of our scientific goals will be analysis of coupled phase transitions between structural and functional degrees of freedom. The most common phase transitions in perovskite-structured compounds occur due to cooperative motions of oxygen octahedra,[viii] that result in coupled tilts or rotations of the oxygen octahedral framework known as tilt transitions, which have a profound impact on properties.[ix] Despite the importance of these rotational or tilt transitions, the physics of size effects and the effect of mechanical constraint are poorly understood in comparison to displacive/ordering transitions. Moreover, tilt transitions compete with other instabilities such as those inducing ferroelectricity,[x] and changes in constraint could therefore strongly modify phase transition behavior in important ways. Little experimental data exist, but some predictions for $SrTiO_3$, have been made using mean field theory. Phenomenological calculations for a (100) $SrTiO_3$ film,[xi] show that ferroelectric phase transitions and tilt transitions are predicted to be functions of the mechanical boundary conditions. The domain structures that form will be strongly impacted by the mechanical and electrical boundary conditions of the film, and these will be studied using X-ray diffraction analysis. The use of size and boundary conditions to change the relative stability of tilted structures offers the opportunity to engineer new materials with improved dielectric and piezoelectric response.

Our studies of the effect of interfaces on electronic phenomena are being expanded to include a range of heterostructures in which the ferroic behavior of one or more layers (and its interfaces) influences the behavior of the heterostructure as a whole. One of the heterostructures that we intend to study combines the novel mechanical, physical and transport properties of piezoelectric and diamond films. Addition of the diamond layers enables the tunability of the piezoelectric properties to be extended beyond what could be achieved simply be changing the thickness of the PZT film. The nanocrystalline diamond layers show very high Young modulus hardness and fracture strength, and our goal will be to understand the dynamic mechanical behavior of PZT-ultrananocrystalline diamond (UNCD) hybrid heterostructures, building on our previous studies of thin film oxides and nanocarbon materials.[xii] The

behavior of the piezoelectric material depends critically on its mechanical confinement and thus a good understanding of the oxide/nanocarbon interface is needed, together with mechanisms by which this can be controlled, such as the use of a thermodynamically stable TiAl layer as an excellent diffusion barrier[xiii] to achieve oxide-nanocarbon integration.

We will also concentrate on understanding the phenomenon of quantum tunneling across a thin oxide barrier layer and of the role that microstructure and local chemistry play. We will then be able to make predictions about the nanoscale features that control the tunneling mechanisms, whether these be spin–independent tunneling, or spin-dependent tunneling between magnetic layers.[xiv] We will do this via a combination of experiment and theory: local transport measurements at the nanometer scale, high spatial resolution structural and chemical analysis using atom probe and TEM, and electronic structure calculations. We intend that our research will enable realistic band structure models of the shape and height of the tunnel barriers to be created. We are interested in a range of systems, but magnetic tunnel junction structures with MgO tunnel barriers, are of particular interest because of the very high room temperature tunnel magnetoresistance (TMR) values that they exhibit[xv] which is attributed to coherent tunneling across the barrier.[xvi] MgO-based tunnel junctions with CoFeB and CoFe ferromagnetic layers will form the basis for our initial studies.

Our studies of domain behavior in ferroic materials using TEM and X-ray scattering are also continuing and will be concentrating on laterally confined heterostructures: interactions in layered magnetic nanostructures, nanoscale ferroelectric structures and nanocomposite multiferroic nanostructures.

---

[i] D M Wood and A Zunger, Phys. Rev. B. **40**, 4062 (1989) and references thererin

[ii] D D Fong , G B Stephenson, S K Streiffer, J A Eastman, O Auciello, P H Fuoss, and C Thompson, Science **304**, 1650-1653 (2004).

[iii] Ch 4, A K Petford-Long and J N Chapman, and Ch 5, M R McCartney, R E Dunin-Borkowski and D J Smith in *Magnetic Microscopy of Nanostructures* (eds. H Hopster and H P Oepen, Springer, 2005).

[iv] T Shinjo, T Okuno, R Hassdorf, K Shigeto and T Ono, Science 289 (2000) 930

[v] K Yu Guslienko, W Scholz, R W Chantrell and V Novosad, Phys. Rev. B 71, 144407 (2005)

[vi] K S Buchanan, K Yu Guslienko, S-B Choe, A Doran, A Scholl, S D Bader and V Novosad, J. Appl. Phys. 97, 20H503 (2005).

[vii] B D Reiss, G Bai, O Auciello, L E Ocola, M A Firestone, Appl. Phys. Lett **88**, 083903 (2006).

[viii] P M Woodward, Acta Crystallogr. B, Struct. Sci. **B53**, 44 (1997). P M Woodward, Acta Crystallogr. B, Struct. Sci. **B57**, 725 (2001).

[ix] C A Randall, R Eitel, B Jones, T R Shrout, D I Woodward, I M Reaney, J. Appl. Phys. **95,** 3633 (2004).

[x] E.g. R. Seshadri and N. A. Hill, Chem. Mat. **13**, 2892 (2001).

[xi] Private communication, Yulan Li, Los Alamos National Laboratory, and L.Q. Chen, Penn State.

[xii] A R Krauss, O Auciello, D M Gruen, A Jayatissa, A Sumant, J Tucek, D Mancini, N Moldovan, A Erdemir, D Ersoy, M N Gardos, H G Busmann, E M Meyer, M Q Ding, Diamond and Related Materials **10**, 1952 (2001).

[xiii] A M Dhote, O Auciello, D M Gruen and R Ramesh, Appl. Phys. Lett. **79,** 800 (2001).

[xiv] E Y Tsymbal, O N Mryasov and P R LeClair, J. Phys.: Cond. Matt. 15, R109 (2003).

[xv] S Yuasa, T Nagahama, A Fukishima, Y Suzuki and K Ando, Nat. Mater. 3, 868 (2004).

[xvi] W H Butler, X G Zhang, T C Schulthess and J M MacLaren, Phys. Rev. B 63, 055416 (2001).

DOE-sponsored publications 2004–2006

"Science and Technology of High Dielectric Constant Thin Films and Materials Integration for Application to High Frequency Devices", O. Auciello, S. Saha, D. Y. Kaufman, S. K. Streiffer, W. Fan, B. Kabius, J. Im, P. Baumann, J. Electroceram. **12 (1-2)**, 119-131 (2004)

"Ferroelectric Domain Structures in $SrBi_2Nb_2O_2$ Epitaxial Thin Films: Electron Microscopy and Phase-Field Simulations", Y. L. Li, L. Q. Chen, G. Asayama, D. G. Schlom, M. A. Zurbuchen, S. K. Streiffer, J. Appl. Phys. **95(11)**, 6332-6340 (2004)

"Ferroelectric Domain Structures in $Sr_2Bi_2Nb_2O_9$ Epitaxial Thin Films: Electron Microscopy and Phase-Field Simulations", Y. L. Li, L. Q. Chen, G. Asayama, D. G. Schlom, M. A. Zurbuchen, S. K. Streiffer, J. Appl. Phys. **95 (11)**, 6332 (2004)

"Ferroelectricity in Ultrathin Perovskite Films", D. D. Fong, G. B. Stephenson, S. K. Streiffer, J. A. Eastman, O. Auciello, P. H. Fuoss, C. Thompson, Science **304**, 1650-1653 (2004)

"Room-Temperature Ferroelectricity in Strained $SrTiO_3$" J. H. Haeni, P. Irvin, W. Chang, R. Uecker, P. Reiche, Y. L. Li, S. Choudhury, W. Tian, M. E. Hawley, B. Craigo, A. K. Tagantsev, X. Q. Pan, S. K. Streiffer, L. Q. Chen, S. W. Kirchoefer, J. Levy, D. G. Schlom, Nature **430**, 758 (2004)

"Thermal Transport in Nanofluids", J. A. Eastman, S. R. Phillpot, S. U. S. Choi, P. Keblinski, Annual Review of Materials Research **34**, 219-246 (2004)

"The Influence of Time, Temperature, and Grain Size on Indentation Creep in High Purity Nanocrystalline and Ultra-Fine Grain Copper", K. Zhang, J. A. Eastman, J. R. Weertman, Appl. Phys. Lett. **85 (22)**, 5197 (2004)

"Low Temperature Growth of Ultrananocrystalline Diamond", X. Xiao, J. Birrell, J.E. Gerbi, O. Auciello and J.A. Carlisle, J. Appl. Phys. **96**, 2232-2239 (2004)

"In Situ Synchrotron X-Ray Studies of Ferroelectric Thin Films", D. D. Fong, J. A. Eastman, G. B. Stephenson, P. H. Fuoss, S. K. Streiffer, C. Thompson, O. Auciello, J. Synchrotron Rad. **12**, 163-167 (2005)

"Direct Structural Determination in Ultrathin Ferroelectric Films by Analysis of Synchrotron X-Ray Scattering Measurements", D. D. Fong, C. Cionca, Y. Yacoby, G. B. Stephenson, J. A. Eastman, P. H. Fuoss, S. K. Streiffer, C. Thompson, R. Clarke, R. Pindak, E. A. Stern, Phys. Rev. B **71**, 144112 (2005)

"Order-Disorder Behavior in $KNbO_3$ and $KNbO_3/KTaO_3$ Solid Solutions and Superlattices by Molecular-Dynamics Simulations", S. R. Phillpot, M. Sepliarsky, S. K. Streiffer, M. G. Stachiotti, R. L. Migoni, J. Mater. Sci., **40 (12)**, 3213-3217 (2005)

"Materials Science and Fabrication Processes for a New MEMS Technology Based on Ultrananocrystalline Diamond Thin Films", O. Auciello, J. Birrell, J.A. Carlisle, J.E. Gerbi, and X. Xiao, B. Peng, and H.D. Espinosa, J. of Physics: Condensed Matter, **vol. 16 (**16), R539-R552 (2004)

"Thermionic Field Emission from Nanocrystalline Diamond-Coated Silicon Tip Arrays", J. M. Garguilo, F. A. M. Koeck, R. J. Nemanich, X. C. Xiao, J. A. Carlisle, O. Auciello, Phys. Rev. **B 72**, 165404 (2005)

"Multiferroic Composite Ferroelectric-Ferromagnetic Films", M. A. Zurbuchen, T. Wu, S. Saha, J. Mitchell, S. K. Streiffer , Appl. Phys. Lett. **87,** 232908 (2005)

"A New Hybrid $Ti_xAl_{1-x}O_y$ Gate Dielectric Layer for Next Generation Ultra-High Capacitance Density CMOS Gates", O. Auciello, W. Fan, B. Kabius, S. Saha, and J.A. Carlisle, C. Lopez and E.A. Irene, R.A. Baragiola, Appl. Phys. Lett **86** (2005)

"Identification of Peptides for the Surface Functionalization of Perovskite Ferroelectrics", B. D. Reiss, G.-R. Bai, O. Auciello, L. E. Ocola, and M. A. Firestone, Appl. Phys. Lett. **88,**) 083903 (2006)

"In-situ TEM studies of magnetisation reversal processes in magnetic nanostructures", A K Petford-Long, T J Bromwich, A Kohn, V Jackson, T Kasama, R E Dunin-Borkowski and C A Ross, *Mater. Res. Soc. Symp. Proc.* **907E**, 0907-MM04-01.1 (2006)

"Remanent magnetic states and interactions in nano-pillars", T J Bromwich, T Kasama, R K K Chong, R E Dunin-Borkowski, A K Petford-Long, O Heinonen and C A Ross, *Nanotechnology* **17**, 4367 (2006).

"Relaxor Ferroelectricity in Strained Epitaxial $SrTiO_3$ Thin Films on $DyScO_3$ Substrates", M. D. Biegalski, D. G. Schlom, S. Trolier-McKinstry, S. K. Streiffer, W. Chang, S. W. Kirchoefe, R. Uecker, P. Reiche, Appl. Phys. Lett. (submitted, 2006)

"Stabilization of Monodomain Polarization in Ultrathin $PbTiO_3$ Films", D. D. Fong, A. M. Kolpak, J. A. Eastman, S. K. Streiffer, P. H. Fuoss, G. B. Stephenson, C. Thompson, D. M. Kim, K. J. Choi, C. B. Eom (Univ. Wisconsin-Madison), I. Grinberg, A. M. Rappe, Phys. Rev. Lett. (accepted, 2006)

"Identification of Peptides for the Selective Surface Modification of Perovskite Ferroelectrics", B. D. Reiss (MSD/CNM), G.-R. Bai, O. Auciello, L. E. Ocola, M. A. Firestone, Appl. Phys. Lett. **88**, 083903 (2006)

"The formation mechanism of aluminium oxide tunnel barriers", A Cerezo (univ. of Oxford), A K Petford-Long, D J Larson, S Pinitsoontorn, E W Singleton, J. Mater. Sci. (in Press, 2006).

Materials Properties at Internal Interfaces: Fundamental Atomic Issues

N. D. Browning (nbrowning@ucdavis.edu)
Department of Chemical Engineering and Materials Science, University of California-Davis, 1 Shields Ave, Davis. CA 95616

Program Scope

The goal of this research program is to investigate the fundamental changes in atomic and electronic structure occurring at interfaces and defects in nanostructured materials, and to determine the effect that these changes have on the properties. This research utilizes recent developments in scanning transmission electron microscopy (STEM); monochromators and aberration correctors to push the spatial resolution for imaging to ~0.1nm and the energy resolution for spectroscopy to ~0.2eV. As these advanced capabilities provide a level of characterization far beyond traditional methods, one of the main aims of this program has been to evaluate their applicability to a wide range of materials science problems. In particular, these methods have been used to investigate the effect of size, shape and composition on the local band structure of quantum dots and the effect of impurity/vacancy segregation to dislocations, interfaces and grain boundaries in semiconductors. Many of these projects have been/will be supported by ab-initio density functional theory calculations, to link the unique atomic scale measurements from the microscope with the fundamental materials properties.

Recent Progress

One of the first results obtained using the STEM methods illustrates how a range of rare-earth atoms bond to the interface between the intergranular oxide phase and the matrix grains in an advanced silicon nitride ceramic. In particular, it was found that each rare-earth atom bonds to the interface at a different location, depending on atom size, electronic configuration and the presence of oxygen at the interface. This essential information is the key factor to understanding the origin of the mechanical properties in these ceramics and will enable precise tailoring in the future to critically improve the materials performance in wide-ranging applications. A summary of the results is shown in figure 1. Further work in partnership with the University of Illinois at Chicago has shown that non-stoichiometry appears to change the energetics of the surface formation, indicating that the growth conditions and presence of oxygen play an important role in determining how the particular interface structures form in this material.

Further use of high spatial resolution imaging and EELS capabilities were highlighted by a study of mixed dislocations in GaN. Here the complexity of the atomic arrangement in the core was imaged directly for the first time using an aberration corrected (STEM). In addition to being present as a full core structure, the mixed dislocation was observed to decompose into partial dislocations separated by a stacking fault only a few unit cells in length. The generation of this stacking fault appears to be impurity driven and its presence is consistent with theoretical predictions.

Most of the work on the use of EELS in this program has been in the development of the monochromated electron beam in the Tecnai F20 as part of the user program at the National Center for Electron Microscopy (NCEM). The advantage of the monochromator is that the zero loss peak can be accurately subtracted from the spectrum

and precise low-loss (valence-loss) EELS analysis performed. One example application for materials science is the use of valence electron energy-loss spectroscopy (VEELS) to measure the energy gaps of individual quantum dots (QDs). The gap energies of a series of CdSe QDs measured by VEELS reveal the expected quantum confinement effect; the gap energy increases with decreasing particle size. However, the values derived from these first VEELS measurements of single QDs are larger than values commonly measured by optical spectroscopy. As standard optical methods lack the spatial resolution to probe individual nanoparticles, the particle-size distribution influences the optical response. The results suggest that the impact of the particle-size distribution accounts for the discrepancy between the energy-gap values derived from VEELS of single QDs and from optical methods of ensembles of QDs (Figure 2).

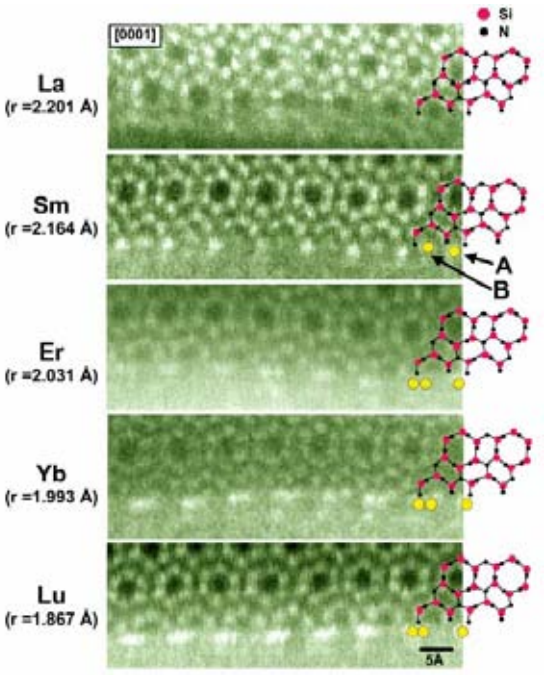

Fig. 1. images of La-, Sm-, Er-, Yb, and Lu-doped Si_3N_4, the matrix grain is oriented along the [0001] zone axis such that the open Si_3N_4 crystal structure is clearly visible at the atomic level and its prismatic plane faces the amorphous intergranular phase. The images confirm a unique feature in that they show how the Si_3N_4 crystal structure ends at the interface with the intergranular phase, namely with open hexagonal rings. The atoms attach in the form of atomic columns oriented normal to the image plane, which contributes to their strong Z-contrast. Two distinct atom positions, A and B, can be identified along the interface.

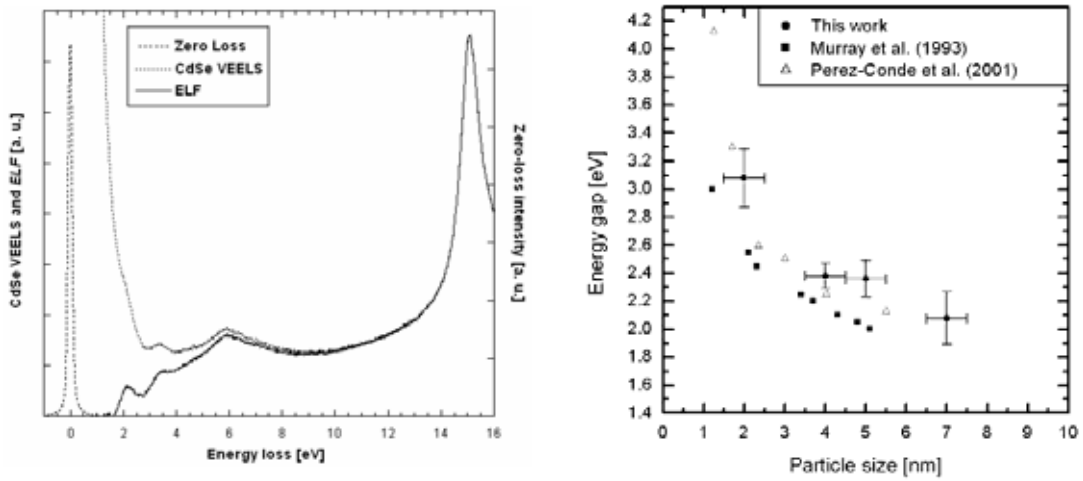

Fig. 2. (a) Low-loss spectrum from a CdSe particle (dotted), the zero-loss peak (dashed) and the energy-loss function (full) (b) Measurement of band-gap as a function of size for a series of CdSe quantum dots compared to theory and optical measurements [1,2].

The analysis of the band-gaps by EELS highlighted the need to fully understand the effect of QD shape. In collaboration with the University of Cambridge, tomography has been used to quantify the 3-D shape of QDs. In particular, tomographic methods have been used to reconstruct the structure of Sn QDs in a Si matrix from a series of Z-contrast images taken at different tilt angles (Figure 3). In this work, the first ever ~1nm^3 spatial resolution reconstructions show that the nucleation and growth of alpha phased QDs follows a coating of voids in the Si matrix (Stranski-Krastanow growth inside a constrained nanosystem). As the dots exceed a few nanometers, they transform to the beta phase and take on new shapes (from cuboctahedral to rectangular parallelepiped).

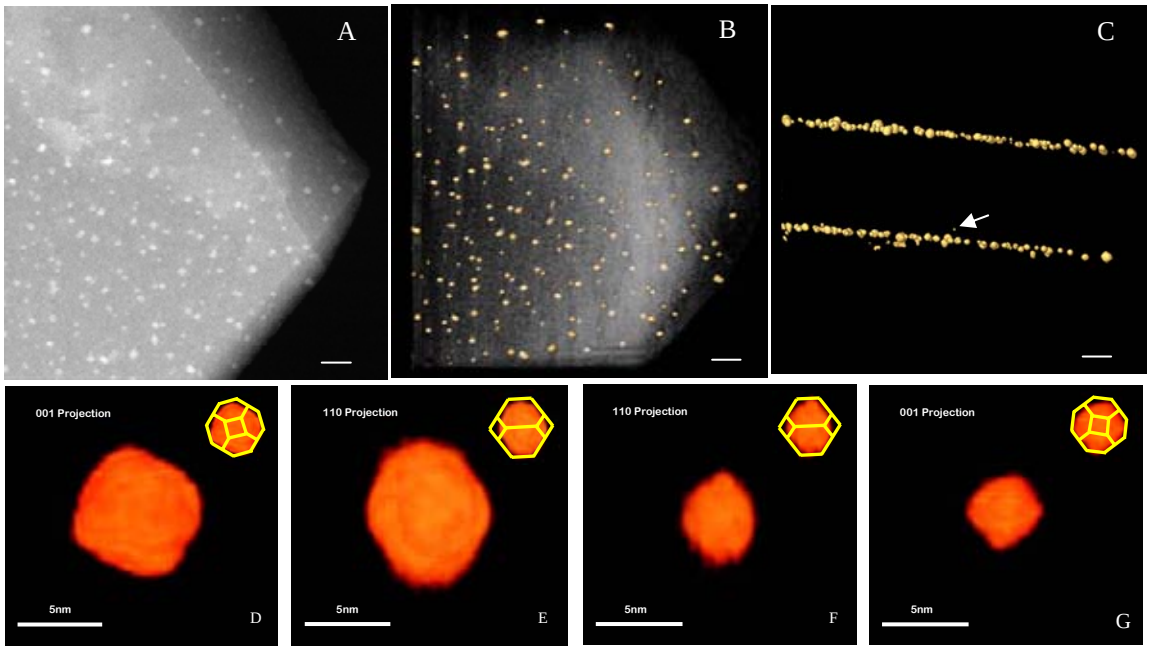

Fig.3. (A) Z-contrast image of the Sn/Si quantum dot system. (B) Reconstruction of the whole volume showing the QDs in yellow. (C) Cross section of figure (B), showing two layers of embedded QDs, and one small QD between the layers. (D) A reconstruction of a 7nm in-layer QD, with inset showing good agreement with a truncated octahedron shape. (E) The same dot in cross section. (F) and (G) present the out-of-layer 3.5nm QD showing a non-uniform structure caused by the constrained Stranski-Krastanow growth.

Future Plans

The results obtained from the analysis so far indicate that the STEM methods can provide fundamental information on the atomic scale properties of interfaces and defects. However, although the indications are clear that vacancies and impurities (i.e. point defects) play a large role in determining the properties, there has been no facility to modify the interfaces in the microscope, i.e. evaluate how a dynamic flux of point defects modifies the properties. Future work will observe the interaction of vacancies and impurities with interfaces and defects by using a unique in-situ stage to modify the point defect concentration in the vicinity of extended structural features. Furthermore, developments currently underway will allow these aberration corrected/monochromated methods to also be applied to organic materials and in particular to evaluate the behavior of inorganic-organic interfaces with atomic spatial resolution.

References

[1] C. B. Murray, D. J. Norris, M. G. Bawendi, *J. Am. Chem. Soc.* **115**, 8706 (1993)
[2] J. Pérez-Conde & A. K. Bhattacharjee, *Phys. Rev. B.* **63**, 2453181 (2001)

DOE Sponsored Publications 2004-2006

"Using EELS to Observe Composition/Electronic Structure Variations at Dislocations in GaN", I. Arslan , A. Bleloch, E. A. Stach, S. Ogut,' N. D. Browning, in press *Phil Mag.*

"Interfacial structure in silicon nitride sintered with lanthanide oxide", C. Dwyer, A. Ziegler, N. Shibata, G. B. Winkelman, R. L. Satet, M. J. Hoffmann, M. K. Cinibulk, P. F. Becher, G. S. Painter, N. D. Browning, D. J. H. Cockayne, R. O. Ritchie, and S. J. Pennycook, in press *J. Materials Science*

"Atomic Resolution Defect Analysis in the STEM", I. Arslan and N. D. Browning, *Microscopy Research and Techniques* **69**, 330-342 (2006)

"Orientation-dependent grain growth in a bulk nanocrystalline alloy during the uniaxial compressive deformation", G. J. Fan, Y. D. Wang, L. F. Fu, H. Choo, G. Ren, P. K. Liaw, and N. D. Browning, *Applied Physics Letters* 88, 171914 (2006)

"Grain growth in a bulk nanocrystalline Co alloy during tensile plastic deformation", G. J. Fan, L. Fu, D. C. Qiao, H. Choo, P. K. Liaw and N. D. Browning, *Scripta Materialia* 54, 2137-2141 (2006)

"Observation of semi-crystalline intergranular films in Si_3N_4 ceramics", A. Ziegler, J. C. Idrobo, M. K. Cinibulk, C. Kisielowski, N. D. Browning and R. O. Ritchie, *Applied Physics Letters* **88**, 141919 (2006)

"Ab-initio structural energetics of b-Si_3N_4 Surfaces", J. C. Idrobo, H. Iddir, S. Ogut, A. Ziegler, N. D. Browning, R. O. Ritchie, *Physical Review B* **72**, 24130 (R) (2005)

"Distortion and segregation in a dislocation core region with atomic resolution ", X. Xu, S.P. Beckman, P. Specht, E.R. Weber, D.C. Chrzan, I. Arslan, R. P. Erni, N. D. Browning, A. Bleloch, C. Kisielowski, *Phys. Rev. Letts.* **95**, 145501 (2005)

"Embedded nanostructures revealed in 3-D", I. Arslan, T. J. Yates, P. A. Midgley & N. D. Browning, *Science* **309**, 2195-2198 (2005)

"Atomic resolution EELS", R. F. Klie, I. Arslan & N. D. Browning, *J. Electron Spectroscopy***143**, 105-115 (2005)

"Carriers of the astronomical 2175 Å extinction feature", J. Bradley, Z. Dai, R. Erni, N. Browning, G. Graham, P. Weber, J. Smith, I. Hutcheon, H. Ishii, S. Bajt, C. Floss and F. Stadermann, *Science* **307**, 244-247 (2005)

"The Atomic and Electronic Structure of Mixed and Partial Dislocations in GaN", I. Arslan, A. Bleloch, E. A. Stach, N. D. Browning, *Phys. Rev. Letts.* **94**, 025504 (2005)

"The Effect of the Crystal-Intergranular Phase Interface on the Fracture Toughness of Silicon Nitride Ceramics", A. Ziegler, J. C. Idrobo, R. L. Satet, M. J. Hoffmann, M. K. Cinibulk, C. Kisielowski, N. D. Browning, R. O. Ritchie, *Science***306**, 1768-1770 (2004)

"The electronic and superconducting properties of oxygen ordered MgB_2 compounds of the form $Mg_2B_3O_x$", J-C. Idrobo, S. Ogut, T. Yildirim, R. F. Klie and N. D. Browning, *Phys. Rev. B* 70, 172503 (2004).

Title: Electronic structure and properties of complex ceramics and their microstructures

Wai-Yim Ching, Chingw@umkc.edu
Department of Physics, University of Missouri-Kansas City
Kansas City, Missouri 64110

Program Scope

This program consists of large-scale *ab initio* and broad-ranged computational efforts to study the structure and properties of complex ceramics and their microstructures. The project takes advantage of the rapidly growing computing power and the state-of-the-art computational methods such that we can now apply to much larger and more complex systems than ever before. It enables us to explore, investigate, and verify the structure/properties relationship for complex microstructures in ceramics including grain boundaries, intergranular glassy films (IGF), defects, surfaces and interfaces. More over, it allows us to perform theoretical experiments with precisely controlled conditions, which would be rather difficult to do in real laboratory experiments. Current emphasizes are on the elastic and mechanical properties of IGF models in silicon nitrides, grain boundaries in alumina. The electronic structure and spectroscopic properties of novel materials and configurations are also covered under this program. These investigations are carried out in close collaboration with experimental groups.

Recent Progress

(A) *Structure and Properties of intergranular glassy films in β-Si_3N_4.*

We have made significant progress in studying the structure and properties of intergranular glassy films (IGF) in Si_3N_4, one of the most common but least understood microstructure in structural ceramics. We have built large atomistic models [1], performed accurate ab initio relaxations, calculated the electronic structures [1,2], and performed theoretical tensile experiments [2,3]. We showed that rare-earth doping can enhance the mechanical properties of IGF. (see Fig.1). For the first time, the complex nonlinear deformation of IGF under tensile stress was revealed. (see Fig. 2) This work is at full speed with more calculations on different IGF models with different crystalline orientations and compositions in progress.

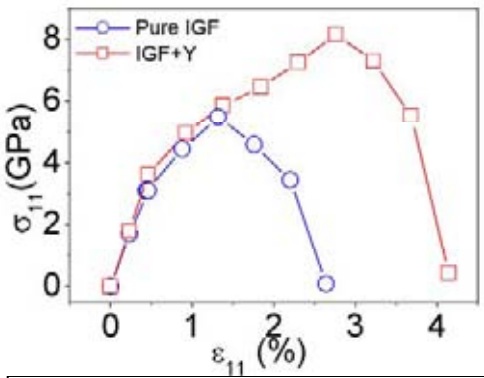

Fig. 1: Stress vs strain data from theoretical tensile experiment. Y-doped IGF has a much larger maximum stress. (ref.2)

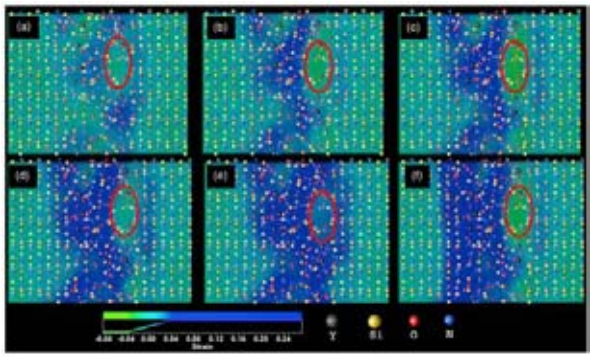

Fig. 2: Strain field diagram in Y-doped IGF for strain of (a) 0.5%; (b) 0.9%; (c) 2.3%; (d) 2.7%; (e) 3.1%; (f) 3.7%. Note the nonlinear behavior even at low strain and in the bulk crystal region. (ref.2)

(B) Grain boundary models in alumina

Several grain boundary models (GB) in alumina have been carefully studied [4,5,6]. This includes the ∑7, ∑37 and ∑31 models. Based on the calculated electronic structure and bonding, an explanation for the increase in creep resistance by adding rare earth elements in alumina has been provided. This so-called "Y-effect" is basically due to the enhanced bonding

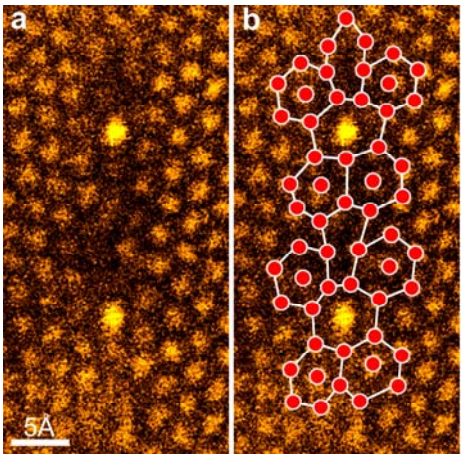

Fig. 3) Left: Z-contrast STEM image of a y-doped Σ31 GB. Rigt: atomic column arrangement of the same image. The geometry was verified by the ab initio calculations [ref. 6].

of Y with O due to the participation of Y-4d electrons and the semi-core Y-4p electrons. International collaboration with an experimental group at the University of Tokyo resulted in the full elucidation of Y doping in the ∑31 GB, showing the presence of the Y at the center of a 7-member ring of Al columns [6]. (See Fig.3) Additional calculations on the electronic structures of these GB models are currently in progress.

(C) Study of novel and complex materials, and development of computational techniques

We have made great progress in the study of Fe-doped TiO_2 [7], a very promising room temperature ferromagnetic material for spintronics applications. We have showed explicitly the role played by the O-vacancy in the ferromagnetism of Fe-doped TiO_2. Other work on novel materials include spinel nitrides (started in previous grant) [8,9], Binding in biomaterials such as vitamin B_{12} molecules [10] and simplified DNA models [11]. Due to the complexity and the size of the systems we investigate, efficient data analysis and visualization tool become an important part of the research project. Special scripts and programs were written to improve the efficency of data transfer, conversion and analysis, especially for data obtained from the DOE-managed supercomputing center NERSC. The two main computational codes, OLCAO and VASP are both under continuing refinement to meet the new challenge.

Futures Plans

(A) Investigation of the IGF models in Si_3N_4 and grain boundary models in Al_2O_3

This will be our major effort in the coming years since great progress has already been made. Our group is clearly at the leading edge for modeling the mechanical and electronic properties of complex ceramics microstructures at the *ab initio* level. We will carry out theoretical experiments on shear and compression in addition to tensile deformation. Different and larger IGF models (up to 1200 atoms) with prismatic planes will be constructed. For both IGF and GBs in alumina, different levels of dopant concentrations and distribution patterns and their effect on the electronic and mechanical properties will be critically evaluated. Spectroscopic properties of these large IGF and grain boundary models will be planed in collaboration with experimentalists as a viable means of characterizating these microstructures.

(B) Electronic and spectroscopic properties of complex ceramics

We continue to maintain our major effort on the complex ceramic crystals. There are important ceramic systems such as mullites [12] with little or no information on their electronic structure and spectroscopic properties. The main obstacle is that many of these ceramic crystals have partial site occupations or disorders. We will study the electronic structure, bonding and optical properties of multi-component ceramic systems such as Ca-Al-O, γ-Al_2O_3, Si-Al-O, and Mg-Si-O and their extension to oxynitrides in order to facilitate the interpretations of many experimental data. In a longer time frame, we will start *ab initio* calculations of phonon spectra in some of these crystals with the aim to calculate the Gibb's free energy G(V,T) in ceramic crystals. These calculations will be helpful in obtaining parameters needed in modeling processing in ceramic materials at high temperatures.

(C). Surfaces and interface modeling of ceramics

We plan to start surface and interface modeling in bioceramic crystals. This is a very complex task that requires careful planning. We have the right tools and experience to make it a very worthy project. Some promising results have already been obtained for the surface model of fluoroapatite and hydrxyapatites crystals [13]. (see Fig. 5). At a later stage, interfaces with water will be investigated.

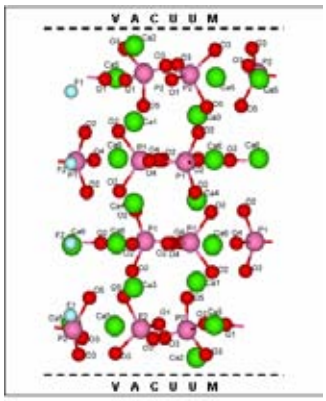

Another novel idea for interface studies is to model the two-phase system, crystallites of Si with different shapes (cubic, spherical, trigonal, etc) embedded in a matrix of a-SiO_2 glass (liquid phase). The goal is to obtain data via accurate first-principles calculations on the effect of crystal size, shape and orientations on the mechanical and electronic properties. Such data are currently unavailable. A large number of large-scale calculations will be carefully designed and systematically carried out.

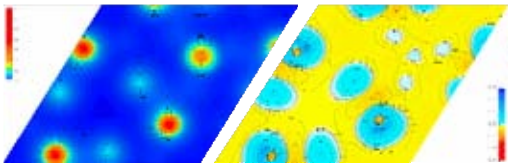

Fig. 5 Top rifgt: Relaxed structure of (001) surface in FAP. Large relaxations of surface atoms were observed. Lower right: Total charge density ρ(r) and the difference charge density Δρ(r) for a near-surface plane. It shows that the surface is mostly positively charged as indicated by red to yellow color.

References

[1] Paul Rulis, Jun Chen, Lizhi Ouyang and W.Y. Ching, Xiaotao Su, S.H. Garofalini, Phys. Rev. B71, 235317-1-10 (2005).
[2] J. Chen, P. Rulis, L. Ouyang, A. Misra, and W.Y. Ching, Phys. Rev. Lett. 95, 256103-07 (2005).
[3] W. Y. Ching, Jun Chen, Paul Rulis, Lizhi Ouyang, and Anil Misra, J. Materials Science (accepted and in press, 2006).
[4] Jun Chen, Y.-N. Xu, Paul Rulis, Lizhi Ouyang, and W.Y. Ching, Acta Materialia, 53 [2], 403-410 (2005).
[5] Jun Chen, L. Ouyang, and W.Y. Ching, Acta Materialia, 53 [15], 4111-4120 (2005).
[6] J. Buban, K. Matsunaga, J. Chen, N. Shibata, W.Y. Ching, T. Yamamoto, Y. Ikuhara, Science, 311, 212-215 (2006).
[7] Jun Chen, Paul Rulis, Lizhi Ouyang, S. Satpathy, and W.Y. Ching, submitted to Phys. Rev. Lett.
[8] W.Y Ching and Paul Rulis, Phys. Rev. B73, 045202-1-9 (2006).
[9] A. Zerr, R. Riedel,T.Sikine, T.Lowther, W.Y. Ching, and I.Tanaka, Advanced Materials (in press, 2006).
[10] Lizhi Ouyang, P. Rulis, W.Y. Ching, M. Slouf, G. Nardin and L. Randaccio, Spectrochimica Acta A, 61(7), 1647-1652 (2005).
[11] J.B. MacNaughton, A. Mowes, J.S. Lee, S.D. Wetting, H.-B. Kraatz, L. Ouyang, W.Y. Ching and E.Z. Kurmaev, J. Phys. Chem. 110(32), 15742-15748 (2006).
[12] *Mullite*, edted by H. Schneider and S. Komaneni, Wiley-VCH Verlag Gmbh & Co, KGaA, Wienheim, Germany (2005).
[13] Hongzhi Yao, P. Rulis, and W.Y. Ching, to be published.

DOE Sponsored Publications in 2004-2006

1). L. Ouyang, H. Yao, S. Richey, Y.-N. Xu and **W.Y. Ching**, "On the crystal structure and optical Properties of $YSiO_2N$", Phys. Rev. B69, 094112-1-6 (2004).
2). L. Ouyang, P. Rulis, **W.Y. Ching**, G. Nardin, and L. Randaccio, "Electronic Structure and Bonding in Adenosylcobalamin", Inorg. Chem. 43 (4), 1235-1241 (2004).
3). R. Ahujal, J.M. Osorio-Guillenl, J. S. de Almeidal, B. Holml, **W.Y. Ching**, B. Johansson, "Electronic and optical properties of γ-Al_2O_3 from ab-initio theory", J. Phys.:Condens. Matter 16, 2891-2900, (2004).
4). Lizhi Ouyang and **W.Y. Ching**," Electronic structure and dielectric properties of gate material: $(ZrO_2)_x(SiO_2)_{1-x}$", J. Appl. Phys, 95 (12) 7918-7924 (2004).
5). P. Rulis, **W.Y. Ching** and M. Kohyama, "ab-initio ELNES/XANES spectral calculation of polar and non-polar grain boundary models in β-SiC", Acta Materialia, 52[10], 30009-18 (2004).

6). **W. Y. Ching**, P. Rulis, and Y. Chen, "Xanes/Elnes: "A Powerful Tool for Interface Characterization of Electronic Materials," p. 137-149 *in Interfaces in Electronic Ceramics,* L. Cook, D. Misra, S. Mukhopadhyay, W. Wong-Ng, O. Leonte, K. Sundaram, editors, The Electrochemical Society, Pennington, NJ, 325 pp (2005). P137-149.
7). T. Mizoguchi, I. Tanaka, S. Yoshioka, M. Kunisu, T. Yamamoto, and **W.Y. Ching**, "First-principles calculations of ELNES/XANES of selected wide gap materials: dependence on crystal structure and orientation", Phys. Rev. B70, 045103 (2004).
8). **W.Y. Ching**, L. Ouyang, Hongzhi Yao and Y.-N. Xu, "Electronic Structure and Bonding in the Y-Si-O-N quaternary Crystals", Phys. Rev. B70, 085105-118 (2004)
9). S. Leitch, A. Moewes, L. Ouyang, **W.Y. Ching**, T. Sekine, "Properties of non-equivalent sites and band gap of spinel-phase silicon nitride using soft X-ray spectroscopy", J. Phys.: Condens. Matter 16, 6469-6476 (2004).
10). Paul Rulis, Lizhi Ouyang, and **W.Y. Ching**, "Electronic Structure and Bonding in Calcium Apatite Crystals: Hydroxyapatite, Fluorapatite, Chlorapatite, and Bromapatite", Phys. Rev. B70, 155104 (2004).
11). Jun Chen, Yong-Nian Xu, Paul Rulis, Lizhi Ouyang**,** and **W.Y. Ching** "Ab-initio tensor experiments on Y-doped Σ=3 grain boundary in α-Al_2O_3", Acta Materialia, 53 [2], 403-410 (2005).
12). Lizhi Ouyang, P. Rulis, **W.Y. Ching**, M. Slouf, G. Nardin and L. Randaccio, "Electronic structure and bonding in Hydroxl-cobalamin", Spectrochimica Acta A, 61(7), 1647-1652 (2005).
13). Paul Rulis, Jun Chen, Lizhi Ouyang and **W.Y. Ching**, Xiaotao Su, S.H. Garofalini, "Electronic structure and bonding of the intergranular glassy films (IGF) in polycrystalline Si_3N_4: Ab-initio studies and classical MD simulations", Phys. Rev. B71, 235317-1-10 (2005).
14). Jun Chen, L. Ouyang, and **W.Y. Ching**, "Molecular dynamic simulation of Y doped Σ=37 grain boundary in α-Al_2O_3", Acta Materialia, 53 [15], 4111-4120 (2005)
15). **W.Y. Ching**, Lizhi Ouyang , Paul Rulis and I. Tanaka, "Prediction of the x-ray absorption near-edge edge spectra of the new high-density phase of SiO_2", Phys. Stat. Sol. (b): Rapid Research Letters, 242 (11), R94-R96 (2005).
16). Y.-N. Xu, P. Rulis and **W.Y. Ching,** "Electronic structure and bonding in a new quaternary $Y_3Si_5N_9O$", Phys. Rev. B72, 113101-04 (2005).
17). J. Chen, P. Rulis, L. Ouyang, A. Misra, and **W.Y. Ching**, "Complex nonlinear deformation of a nanometer intergranular glassy films in silicon nitride ceramics", Phys. Rev. Lett. 95, 256103-07 (2005).
18).J. Buban, K. Matsunaga, J. Chen, N. Shibata, **W.Y. Ching**, T. Yamamoto, Y. Ikuhara, "Grain Boundary Strengthening in Alumina by Rare Earth Impurities", Science, 311, 212-215 (2006).
19). **W.Y Ching** and Paul Rulis, "Ab-initio calculation of the electronic and spectroscopic properties of spinel γ-Sn_3N_4", Phys. Rev. B73, 045202-1-9 (2006).
20). **W.Y. Ching**, Paul Rulis, Yong-Nian Xu and L. Ouyang, "The electronic structure and spectroscopic properties of 3C, 2H, 4H, 6H, 15R, 21R polymorphs of SiC", Materials Science and Engineering A, 422 C1-2, 147-156 (2006).
21). A. Zerr, R. Riedel, T. Sikine, T. Lowther, **W.Y. Ching**, and I. Tanaka, "Recent Advances in New Nitrides", Advanced Materials (accepted and in press).
22). **W. Y. Ching**, Jun Chen, Paul Rulis, Lizhi Ouyang, and Anil Misra, "*Ab initio* Modeling of Clean and Y-doped Grain Boundaries in Alumina and Intergranular Glassy Films (IGF) in β-Si_3N_4", J. Materials Science (in press, 2006).
23). Jun Chen, Paul Rulis, Lizhi Ouyang, S. Satpathy, and **W.Y. Ching**,, "Vacancy enhanced ferromagnetism in Fe-doped rutile TiO_2", submitted to Phys. Rev. Lett.
24).J.B. MacNaughton, A. Mowes, J.S. Lee, S.D. Wetting, H.-B. Kraatz, L. Ouyang, **W.Y. Ching** and E.Z. Kurmaev, "Dependence of the DNA Electronic Structure on Environmental and Structural Variations", J. Phys. Chem. 110(32), 15742-15748 (2006).
25). Paul Rulis and **W.Y Ching**, "Comparative studies of the Si-K, Si-L, Ge-K, Ge-L and N-K edges in the XANES/ ELNES spectral calculations of four spinel nitrides: γ-Si_3N_4 , γ-Ge_3N_4, γ-$SiGe_2N_4$, γ-$GeSi_2N_4$", submitted to J. Phys. Condensed Matter.

Metallic Interfaces and Dislocations

Douglas L. Medlin, John C. Hamilton, Emmanuelle A. Marquis
dlmedli@sandia.gov, jchamil@sandia.gov, emarqui@sandia.gov
Sandia National Laboratories, Livermore, CA 94551

Program Scope

Our program seeks to establish the basic principles that govern the structure and behavior of internal interfaces. We concentrate on metallic interfaces, including both grain boundaries and heterophase interfaces, with a central goal of determining how the incompatibilities and discontinuities that arise at such interfaces are accommodated and the implications of these relaxations on the behavior and properties of the interface. To address such questions, we combine detailed experimental observations using atomic resolution microscopies with comprehensive theory and modeling, encompassing electronic structure, atomistic, and continuum simulations. We see a crucial challenge in exploring what controls the *three-dimensional* evolution of interfaces. Thus, we are applying new imaging techniques, such as atom probe tomography, and developing new theoretical approaches to provide fundamental insights into this important class of problems.

Recent Progress

One key to determining the mechanisms that control the three-dimensional structural evolution of interfaces is to establish the function of interfacial line defects. Such defects play important roles in defining the step structure and accommodating angular deviations from low energy boundary orientations. Interfacial defects are also important in accommodating *coherency strains* at boundaries [1]. We have recently explored in detail the step and dislocation character and dissociation mechanisms of line defects at such a boundary [2]. An example, from an asymmetrical 90°<110> grain boundary in gold, is shown in Figure 1. Here, the line defects required to maintain coherency across the {111}/{112} terrace have dissociated into two components. From the measured Burgers vectors, we have shown that this dissociation is favored by elastic energy criteria and can occur readily because one of the components (indicated as $b_{3/1}$) is glissile--a result that is borne out by atomistic simulations. The defects we have discovered are in many ways analogous to those that occur at epitaxial or transformation interfaces between different crystallographic phases, and serve a dual function in accommodating both the interfacial coherency strain and controlling the three dimensional boundary configuration.

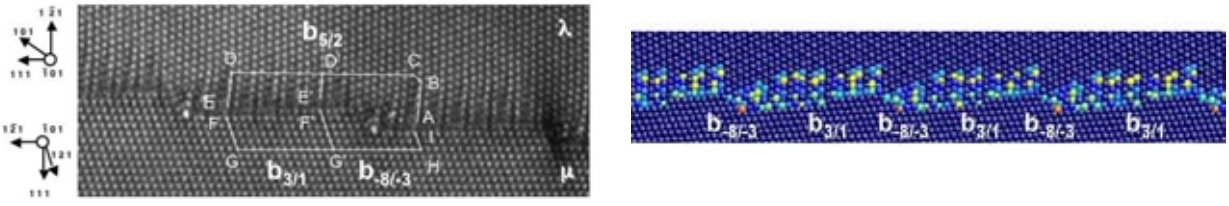

Fig. 1. *HRTEM image and atomistic simulation of a 90° <110> tilt boundary in Au. The atomic steps possess dislocation content that accommodates coherency strains across the {111}/{112} interface. The* $\mathbf{b}_{i/j}$ *notation indicates the {242}/{111} step heights. Because the coherency strain controls the step spacing, the boundary inclination is coupled to the strain relief mechanism.*

Interfacial defects can also interact between closely spaced boundaries, an issue that is particularly important in nanocrystalline materials. Our work has shown previously how the balance of elastic and interfacial energies controls the structure of finite-length boundary facets, producing a structure with localized strain fields at the junctions [3]. We have now demonstrated how such junctions interact with dislocations, focusing on {111}/{112} junctions in nanometer-scale twins in Au. For instance, a 1/3<111> interfacial dislocation, which has a Burgers vector magnitude twice that of the junction dislocation, can react with the junction, reversing the sign of its displacement and reducing the overall strain energy of the system. Importantly, junction interactions also can drive the *emission* of dislocations from a boundary when the neighboring junctions are sufficiently close. Figure 2 illustrates such a case. Here, a 1/3<111> boundary dislocation has dissociated, creating a fault that links the two junctions. We observe faults as wide as 8 nm in this configuration. This width is surprisingly large compared to the width of a normal dissociated lattice dislocation in gold (1.8 nm). The explanation is that these faults produce an offset of the {111} planes that significantly reduces the strain energy at the boundary junctions. Our calculations show that this reduction in strain energy more than compensates the increase in energy due to stacking fault creation.

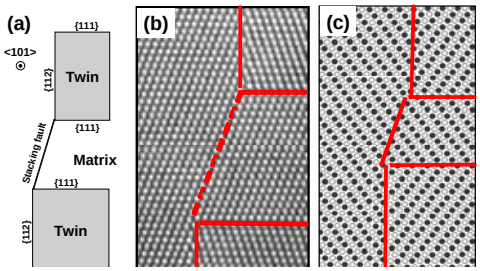

***Fig. 2**. Observation and simulation of extended stacking fault joining two {111}/{112} junctions in Au.*

We are also investigating how size-effects control the three-dimensional morphology of nanoscale precipitates. Size-dependent shape effects at the nanoscale have been observed frequently. For larger objects, the Wulff construction predicts the shape based only on interfacial energies; but as the object size decreases, an increasing contribution due to the edge-energy at the facet junctions is often invoked to explain the size dependent shapes. Rigorous testing of this explanation requires quantitative atomistic calculation of the edge energy. In attempting to calculate this parameter, we discovered and resolved a fundamental ambiguity in the definition of edge-energy related to the uncertainty in the placement of the Gibbs dividing surface at an interface [4]. With this ambiguity resolved, we have conducted the first atomistic calculations of edge energy, focusing on Pd clusters [4]. These results show that, in fact, the edge energies are very small and have essentially no effect on the calculated cluster shape at any scale.

With this insight in hand, we have revisited the origin of the size-dependent shape effects that have been observed in nanoprecipitates of Pb in Al [5,6]. Our work is being done in collaboration with U. Dahmen (LBL-NCEM). We have constructed and relaxed three-dimensional cuboctahedral, tetrakaidecahedral, and octahedral Pb inclusions in a regular fcc Al solid using the embedded atom method (EAM), and computed the precipitate energies as a function of size. These energies and those predicted from an analytical model based solely on strain and interface energy are in excellent agreement for the wide range of inclusion shapes represented. This proves that the energies for Pb precipitates in Al can be explained solely by interfacial and strain energies and that edge energies play an insignificant role, even for the smallest possible precipitates. Building on this result, we have developed a method for constructing strain-free precipitate shapes based on octahedral and tetrahedral "structural units" that correspond to units that maintain strain-free ratios of Al:Pb atoms along their edges. A wide variety of strain-free precipitates with "magic-shapes" can be assembled from these structural units, and this magic-shape effect explains the observed size dependence of the precipitates.

Finally, we have started to explore the relationships between composition and nanoscale precipitate structure and morphology. So that we can decouple the effects of composition and strain, we have initiated this work in Al-Ag alloys, a prototypical phase separating system with

very low misfit (<1%) between the Al and Ag rich phases. It is known that this system forms intermediate metastable precipitates (Guinier Preston zones); however, the exact structure of the GP zones and, in particular, the existence of temperature-dependent phases (ordered at low T and disordered at high T), is still a matter of debate. Significantly, recent x-ray scattering and STEM measurements have indicated that in the initial stages of decomposition, the precipitates form with a very surprising morphology consisting of a silver-rich shell surrounding an Al-rich inner core [7]. At present, no thermodynamic explanation for this interesting morphology has been developed and, from the existing qualitative observations, it has not been possible to assess details, such as the local Ag concentration, or sharpness of the interface, which are critical to developing a model to explain the morphological observations. Our measurements using atom probe microscopy are beginning to address these questions. We have found that the composition of the GP zones is time dependent despite their well defined shape. This time dependence resolves the long standing debate over how the exact composition of the GP zones results from different aging conditions used by various researchers. The slow time dependence is remarkable, however, given the short diffusion lengths involved, and may reflect effects resulting from vacancy-solute interactions.

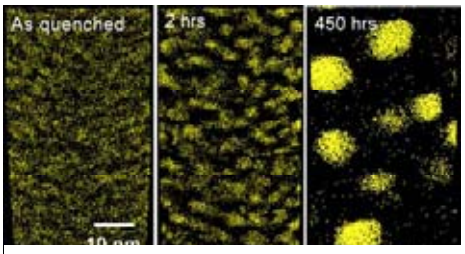

Fig. 3. *Three-dimensional evolution of silver-rich clusters in an Al-Ag alloy measured using Atom Probe tomography.*

Future Plans

A focus area in our planned work will be to explore how grain boundaries transition between a faceted and defaceted state. Such transitions are important because they are coupled with other abrupt changes in boundary properties and behavior[8]. In our previous work [9], we developed a detailed theoretical understanding of the prototypical defaceting transition observed first in the aluminum $\Sigma=3$ system by Hsieh and Balluffi [10]. To rigorously test this theory and to develop a more robust understanding of the faceting/defaceting transition, we plan to quantify experimentally how the facets first evolve out of the fluctuations of the defaceted interface and, conversely, how the facets initially decay with increasing temperature. We plan *in situ* TEM observations on specially prepared thin-film bicrystals. Also, because the transition times are predicted to occur over nanosecond time-scales, we have initiated a collaboration with G. Campbell and N. Browning to use LLNL's newly developed Dynamic Transmission Electron Microscope (DTEM) [11], which is now attaining the requisite temporal and spatial resolutions. Besides temperature, changes in interfacial segregation can also drive such faceting/defaceting transitions. We plan to take advantage of our capabilities in atom probe tomography to explore the microscopic details of such compositionally induced transitions. A model material for these experiments is the copper/bismuth system. We have already successfully targeted and extracted faceted boundaries in this system and are initiating atom probe studies to explore the connections between the three-dimensional compositional distribution and the boundary structure.

Even the structure of flat interfaces is often more complex than would be anticipated from the simple operation of joining two single-crystal surfaces. Our past work has shown that some heterophase interfaces can reconstruct into a non-bulk-like arrangement, consisting of a dense, three-dimensional network of interwoven dislocations [12]. This network accommodates large misfit strains. Importantly, the dislocation junctions, which consist of monolayer long *threading* segments, play a critical role in optimizing the local atomic density. We have suggested qualitative explanations for why this reconstruction occurs at some heterophase interfaces (e.g. Ag(111)/Ru(0001)) but not at others (e.g. Cu(111)/Ru(0001)) and now plan to explore this question in greater detail. We will employ simple model potentials that can be

varied in a systematic way to determine the phase diagram for heterophase reconstructions at hexagonal surfaces as a function of the potential parameters.

Finally, we plan continued work to unravel how interfacial and elastic strain energies interplay to control the three-dimensional morphology and chemistry of clusters and precipitates in metallic alloys. Even when strain does not play a significant role, as we have shown in the Al-Ag system, the development of precipitate composition and morphology can be complex. For example, we observe that the composition within the Ag-rich precipitates evolves surprisingly slowly as they grow in size. To solve this mystery, we will compare our experimental data with theories of concentration dependent diffusivities caused by vacancy-solute interactions. As this question is resolved, we plan further studies to vary systematically the precipitate strain through a series of alloying additions.

References

[1] D.L. Medlin, D. Cohen, R.C. Pond, *Phil. Mag. Lett.* **83**(4) 223 (2003).

[2] R.C. Pond, D.L. Medlin, A. Serra, *Philosophical Magazine* 86 (29-31) 4667-4684 (2006).

[3] E.A. Marquis, J.C. Hamilton, D.L. Medlin, and F. Léonard *Phys. Rev. Lett.* **93**, 156101 (2004).

[4] J.C. Hamilton, *Phys. Rev.* B **73**, 125447 (2006).

[5] U. Dahmen, S.Q. Xiao, S. Paciornik, E. Johnson, A. Johansen, *Phys. Rev. Lett.* **78**, 471 (1997).

[6] E. Johnson, A. Johansen, U. Dahmen, S. Chen and T. Fujii, *Mat. Sci. and Eng*. **A304-306**, 187 (2001).

[7] R. Erni, H. Heinrich, G. Kostorz, *Phil. Mag. Lett.* **83**, 5999 (2003).

[8] S.B. Lee, Mat. Lett. **57**, 3779 (2003).

[9] I. Daruka, J.C. Hamilton, *Phys. Rev. Lett.* 92 (24) Art. No. 246105 (2004).

[10] T.E. Hsieh, R.W. Balluffi, *Acta Metall.* 37, 2133 (1989).

[11]T. Lagrange et al., Applied Physics Lett. 89(4) art no. 044105 (2006).

[12] W.L. Ling, J. de la Figuera, N.C. Bartelt, R.Q. Hwang, A.K. Schmid, G.E. Thayer, J.C. Hamilton, *Phys. Rev. Lett.* 92 (11) Art. No. 116102 (2004).

DOE Sponsored Publications in 2004 - 2006

Atomistic and Lattice Model of a Grain Boundary Defaceting Phase Transition, I. Daruka, J.C. Hamilton, Physical Review Letters 92 (24) Art. No. 246105 (2004).

Strain Relief through Heterophase Interface Reconstruction: Ag(111)/Ru(0001), W.L. Ling, J. de la Figuera, N.C. Bartelt, R.Q. Hwang, A.K. Schmid, G.E. Thayer, J.C. Hamilton, Physical Review Letters 92 (11) Art. No. 116102 (2004).

Finite-Size Effects on the Structure of Grain Boundaries, E.A. Marquis, J.C. Hamilton, D.L. Medlin, and François Léonard, *Physical Review Letters* **93**, 156101 (2004).

Structural Duality of 1/3<111> Twin Boundary Disconnections, E.A. Marquis and D.L. Medlin, *Philosophical Magazine Letters 85(8)* 387-394 (2005).

Edge energies: Atomistic calculations of a continuum quantity, J.C. Hamilton, Physical Review B 73 (12): Art. No. 125447 (2006).

A Study of the Accommodation of Coherency Strain by Defects at a Grain Boundary in Gold, R.C. Pond, D.L. Medlin, A. Serra, *Philosophical Magazine* 86 (29-31) 4667-4684 (2006). Invited article for special issue commemorating the 50th anniversary of imaging dislocations by electron microscopy.

Computational Investigations of Crystal-Melt Interfaces in Metals and Alloys

Mark Asta[1] and Jeffrey J. Hoyt[2]
mdasta@ucdavis.edu, jjhoyt@sandia.gov
[1]Dept. of Chem. Eng. & Mat. Sci., University of California at Davis, Davis CA 95616
[2]Sandia National Laboratories, Albuquerque, NM 87185

Program Scope

This project focuses on development and application of atomic-scale computational methods for predictive modeling of hetero-phase interfaces in metals and alloys. Accurate knowledge of the magnitudes and crystalline anisotropies of interface structure, free energies, mobilities and segregation coefficients are critical to increasing predictive capabilities in the modeling of microstructural evolution accompanying phase transformations in materials processing, and to understanding nanoscale effects on phase transformations. Despite the fundamental importance of hetero-phase interfaces, direct experimental measurements of their properties remains elusive in many cases. This is particularly true of crystal-melt interfaces, which form the primary focus of this project. Simulations of crystal-melt interfaces are undertaken as a framework for increasing predictive capabilities in multi-scale modeling of solidification microstructures for alloys processed from the melt. The development and application of first-principles-based computational methods in studies of solid-solid interfaces are also pursued, to exploit opportunities for collaborations with experimentalists investigating interfacial structure and composition through applications of state-of-the-art electron and atom-probe microscropies. In the development of predictive atomic and multi-scale computational methods for alloys, this project is well aligned with the DOE-BES long-term goal that seeks to "demonstrate progress in … modeling … new materials and structures, including metals (and) alloys, … – particularly at the nanoscale – for energy-related applications" (see URL: http://www.sc.doe.gov/bes/BES_PAR_Performance_Measures.pdf).

Recent Progress

Over the past five years, this project has focused primarily on atomic-scale modeling of the thermodynamic and kinetic properties of solid-liquid hetero-phase interfaces. Our efforts in this area have included the development of the so-called capillary-fluctuation method [1-3] for computing anisotropic crystal-melt interfacial free energies and mobilities from the static and dynamic spectra characterizing interface-height fluctuations in equilibrium molecular-dynamics simulations. This method was initially applied in studies of fcc crystal-melt interfaces, and more recently we have pursued applications to a broader range of systems with both bcc and hcp crystal structures [4-8]. These results have been used to elucidate the strong correlation between crystal-melt interface properties and crystal structure in elemental metal systems [4-8]. We also have made substantial progress extending previously developed molecular-dynamics methods to studies of crystal-melt interface properties in faceted systems and alloys. This work includes progress towards elucidating the factors governing composition dependencies of solid-liquid interfacial free energies and associated

anisotropies in binary alloys [9], and the first molecular-dynamics-based calculation of step mobilities at faceted crystal-melt interfaces.

Research over the past two years has also involved collaborations with two Northwestern DOE-BES-supported projects devoted to the design of precipitate-strengthened, creep-resistant Al alloys. Our own efforts related to these projects have focused on the development of first-principles lattice-model-based methods for quantitative calculations of thermodynamic properties in multicomponent, multiphase materials, as a critical step in the modeling of heterophase solid-solid interfaces in commercially relevant Al-based materials. This work included the development of a theoretical explanation for the surprising experimental finding, based on atom-probe microscopy, of pronounced solute segregation at a coherent precipitate/matrix interface [10,11]. Specifically, it was found that the driving force for Mg segregation to coherent Al/Al_3Sc interfaces is primarily electronic in origin.

Finally, the expertise of the PIs in the thermodynamics of stressed solids and the properties of crystalline surfaces have been utilized in theoretical studies elucidating the origin of size effects on phase transformations in nanometer-scale confined geometries, specifically melting/freezing in nanopores [12] and atomic ordering in alloy nanoparticles [13].

Future Plans

Future work will include continuing efforts aimed at the development and application of atomistic simulation methods to investigate fundamental properties of faceted crystal-melt interfaces, focusing specifically on the excess free energies and kinetic mobilities of steps. The properties of steps at solid-liquid interfaces are critical factors governing the formation of defects and morphologies in a variety of crystal-growth processing ranging from liquid phase epitaxy to solution growth. Compared to the case of crystal-vapor interfaces, steps at solid-liquid boundaries are far less studied experimentally. As a consequence, little quantitative data is available concerning the microscopic factors influencing the magnitudes of step free energies, step interactions, or mobilities. Our preliminary simulation results in the modeling of crystal-melt interfaces in Si, vicinal to the faceted (111) orientation, establish that steps in this model system have a structure that is highly diffuse on length scales of several nanometers. This structural feature stands in contrast to the situation at crystal-vapor interfaces, where steps are generally atomically sharp. The diffuse nature of step structure can have important consequences for the magnitude and anisotropy of step mobilities and step interactions, particularly at the nanoscale. Future work will explore the generality of these results by extending simulations to alloys where the degree of undercooling below the interface roughening temperature can be controlled. Through systematic studies of step structure, thermodynamic and kinetic properties as functions of composition and temperature, our aim will be to elucidate the microscopic factors governing step structure and properties at faceted crystal-melt interfaces in alloys.

Future efforts will also be devoted to extending computational investigations in the study of interface wetting and coalescence phenomena. A primary motivation for this work is provided by phenomena associated with the late stages of solidification, where two merging grains will experience a repulsive force inhibiting coalescence if the grain

boundary free energy is greater than twice the solid-liquid interfacial free energy, i.e., if the liquid prefers to wet the grain boundary. This phenomenon can have important consequences on the properties of alloys in casting and welding, as the presence of a thin intergranular liquid film can lead to stress concentration and cracking. Future work will aim to elucidate the coupling between alloy chemistry, temperature, and interface orientation in governing the equilibrium wetting behavior of grain boundaries in alloys as functions of temperature and composition.

These future efforts related to grain-boundary coalescence and wetting will be a component of a larger effort, proposed under the BES Computational Materials Science Network (CMSN) program, entitled "Dynamics and Cohesion of Materials Interfaces and Confined Phases Under Stress". This work will address challenging new methodological developments required to understand at a fundamental level the physics governing complex interface-dominated processes associated with the breakdown of crystal cohesion and failure of stressed polycrystalline materials. It will include a focused effort aimed at application of state-of-the-art ab-initio molecular dynamics methods in the study of finite-temperature interfacial phenomena. Such methods are particularly powerful in their application to studies of materials with complex chemical bonding, and provide a framework for extending the interface simulation methods to a broader range of materials systems relevant for diverse energy-related applications.

References

(1) J.J. Hoyt, M. Asta and A. Karma, Phys. Rev. Lett. **86**, 5530-5533 (2001).
(2) M. Asta, J. J. Hoyt and A. Karma, Phys. Rev. B **66,** 100101(R) (2002)
(3) J.J. Hoyt, M. Asta and A. Karma, Mat. Sci. Engin. R **41**, 121-163 (2003).
(4) D. Y. Sun, M. Asta, J. J. Hoyt, M. I. Mendelev and D. J. Srolovitz, Phys. Rev. B **69**, 020102(R) (2004).
(5) D. Y. Sun, M. Asta and J. J. Hoyt, Phys. Rev. B **69**, 174103 (2004).
(6) D. Y. Sun, M. I. Mendelev, C. A. Becker, K. Kudin, Tomorr Haxhimali, M. Asta, J. J. Hoyt, A. Karma and D. J. Srolovitz, Phys. Rev. B **73**, 024116 (2006).
(7) J. J. Hoyt, M. Asta, and D. Y. Sun, Phil. Mag. **86**, 3651-3664 (2006).
(8) Z. G. Xia, D. Y. Sun, M. Asta and J. J. Hoyt, Phys. Rev. B (submitted).
(9) C. A. Becker, M. Asta, J. J. Hoyt and S. M. Foiles, J. Chem. Phys. **124**, 164708 (2006).
(10) E. A. Marquis, D. N. Seidman, M. Asta, C. Woodward and V. Ozolins, Phys. Rev. Lett. **91**, 036101 (2003).
(11) E.A. Marquis, M. Asta, D. N. Seidman, and C. Woodward, Acta Mater. **54**, 119-130 (2006).
(12) J. J. Hoyt, Phys. Rev. Lett. **96**, 045702 (2006).
(13) Bo Yang, M. Asta, O. N. Mryasov, T. Klemmer and R. W. Chantrell, Scripta Mater. **53**, 417-422 (2005).
(14) T. Haxhimali, A. Karma, F. Gonzales and M. Rappaz, Nature Mat. **5**, 660-664 (2006).

DOE Sponsored Publications in Fiscal Years 2005-2006

Crystal-Melt Interfaces and Solidification Morphologies in Metals and Alloys, J. J. Hoyt, M. Asta, T. Haxhimali, A. Karma, R. E. Napolitano, R. Trivedi, B. B. Laird and J. R. Morris, *MRS Bulletin* **2004**, *29*, 935-939.

Partitioning of Impurities in Multi-Phase TiAl Alloys, R. Benedek, A. van de Walle, S. S. A. Gerstl, M. Asta, D. N. Seidman, and C. Woodward, Phys. Rev. B **2005**, *71*, 094201.

First-Principles Calculation of Structural Energetics of Al-TM (TM=Ti, Zr, Hf) Intermetallics, G. Ghosh and M. Asta, Acta Mater. **2005**, *53*, 3225-3252.

Monte-Carlo-Simulation Study of A1-$L1_0$ Ordering Transitions in FePt Nanoparticles, Bo Yang, M. Asta, O. N. Mryasov, T. Klemmer and R. W. Chantrell, Scripta Mater. **2005**, *53*, 417-422.

Composition Evolution of Nanoscale Al_3Sc Precipitates in an Al-Mg-Sc Alloy, E. A. Marquis, M. Asta, D. N. Seidman and C. Woodward, Acta Mater. **2006**, *54*, 119-130.

Crystal-Melt Interfacial Free Energies in HCP Metals: A Molecular Dynamics Study of Mg, D. Y. Sun, M. I. Mendelev, C. A. Becker, K. Kudin, Tomorr Haxhimali, M. Asta, J. J. Hoyt, A. Karma and D. J. Srolovitz, Phys. Rev. B **2006**, *73*, 024116.

Effect of Stress on Melting and Freezing in Nanopores, J. J. Hoyt, Phys. Rev. Lett. **2006**, 96, 045702.

Ginzburg-Landau Theory of Crystalline Anisotropy for BCC-Liquid Interfaces, Kuo-An Wu, A. Karma, J. J. Hoyt and M. Asta, Phys. Rev. B **2006**, *73*, 094101.

Equilibrium Adsorption at Crystal-Melt Interfaces in Lennard-Jones Alloys from Monte-Carlo Simulations, C. A. Becker, M. Asta, J. J. Hoyt and S. M. Foiles, J. Chem. Phys. **2006**, *124*, 164708.

Molecular Dynamics Simulations of the Crystal-Melt Interfacial Free Energy and Mobility in Mo and V, J. J. Hoyt, M. Asta and D. Y. Sun, Phil. Mag. **2006**,*86*, 3651-3664.

Stability and Elastic Properties of $L1_2$-$(Al,Cu)_3(Ti,Zr)$ Phases: Ab Initio Calculations and Experiments, G. Ghosh, S. Vaynman, M. Asta and M. E. Fine, Intermetallics **2006**, (on line).

Molecular Dynamics Calculations of the Crystal-Melt Interfacial Mobility for Hexagonal-Close-Packed Mg, Z. G. Xia, D. Y. Sun, M. Asta and J. J. Hoyt, Phys. Rev. B **2006**, submitted.

Session V

Nanostructured Materials

Microstructural Origins of the Dielectric Behavior of Ferroelectric Thin Films

Susanne Stemmer
stemmer@mrl.ucsb.edu
Materials Department, University of California, Santa Barbara, CA 93106-5050

Program Scope

Ferroelectric thin films show drastically different properties from what is anticipated from the bulk materials properties. The objective of the project is a comprehensive, experimental research program aimed at an atomic level understanding of the strongly modified properties of ferroelectric thin films. We address the role of point defects, extended defects, film stresses and interfaces in determining dielectric properties, ferroelectric and structural phase transitions of ferroelectric thin films. The project focuses on interfaces and materials with known atomic arrangements and microstructures. These are obtained by controlled thin film growth experiments and by utilizing the unique capabilities of scanning transmission electron microscopy techniques, in particular high-angle annular dark-field (HAADF) imaging, as well as other advanced structural characterization techniques. Towards this goal, we will establish a quantitative understanding of HAADF image contrast in these materials systems to analyze defects in films and at interfaces. Results from atomic resolution characterization are compared with macroscopic measurements of the dielectric and ferroelectric properties as a function of temperature to establish the fundamental limits that interfaces, stresses and defects impose on the properties. The knowledge gained in this study impact fundamental understanding of ferroelectric materials and the role of interfaces in determining their properties.

Recent Progress

Our recent efforts have focused on (*i*) an understanding of the origins of the pronounced thickness dependence of the apparent permittivity ("dielectric dead layer") that is typically observed in ferroelectric thin films and (ii) a quantitative understanding of HAADF images of interfaces. Towards the first goal, epitaxial $SrTiO_3$ thin films were developed on epitaxial metal (Pt) electrodes to serve as a model metal/ferroelectric heterostructures [1,2]. Epitaxial $PbTiO_3$/$SrTiO_3$ interfaces were studied by HAADF for a fundamental understanding of image contrast [3].

(a) Quantifying HAADF Image Contrast: Consequences for Heterointerfaces

Experimental HAADF images were obtained from a model system consisting of an epitaxial perovskite $PbTiO_3$ film grown on a $SrTiO_3$ single crystal (Fig. 1). This sample allowed for the study of the intensities of a wide range of atomic numbers. The main objective was to quantify the influence of TEM foil thickness on the image contrast, but the effects of the annular detector inner angle and the probe forming lens focus were also studied. Sample thicknesses ranging from ~ 10 nm to more than 400 nm were investigated. The image contrast was relatively insensitive to changes in inner angle [3]. The main impact of sample thickness was a rapid increase in a background intensity that contributed equally to the intensities of the atomic columns and the channels between them (Fig. 2) [3]. The background intensity and its increase with thickness reflected the average atomic number of the crystal.

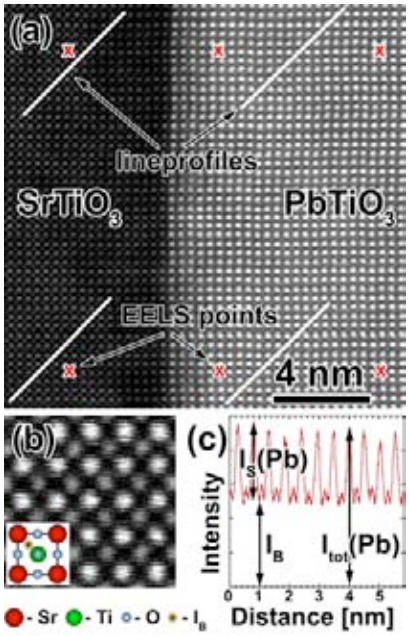

Figure 1: (a) HAADF image of the $PbTiO_3/SrTiO_3$ interface along $\langle 100 \rangle$ showing the positions where the low-loss EELS spectra (crosses) and the intensity line profiles were acquired. The intensity line profiles (thick lines) were measured along $\langle 110 \rangle$. (b) HAADF image of $SrTiO_3$ showing the position of the atom columns along $\langle 100 \rangle$. (c) Intensity line profile across $PbTiO_3$, where I_B denotes the intensity of background, $I_{tot}(Pb)$ the intensity of the Pb column position and $I_s(Pb)$ the intensity of the Pb column after subtraction of the background I_B [3].

Image simulations did not reproduce the large background intensity, indicating that some of the largest contributions to HAADF image intensities are not yet understood. After subtraction of the background, calculated (elastic scattering only) and experimental image contrast showed qualitatively similar behavior as a function of sample thickness (Fig. 2) [3]. For analysis of heterointerfaces in terms of atom column occupancy, very thin TEM samples are required to minimize the contribution of the background that cannot (yet) be calculated or experimentally extracted at interfaces [3].

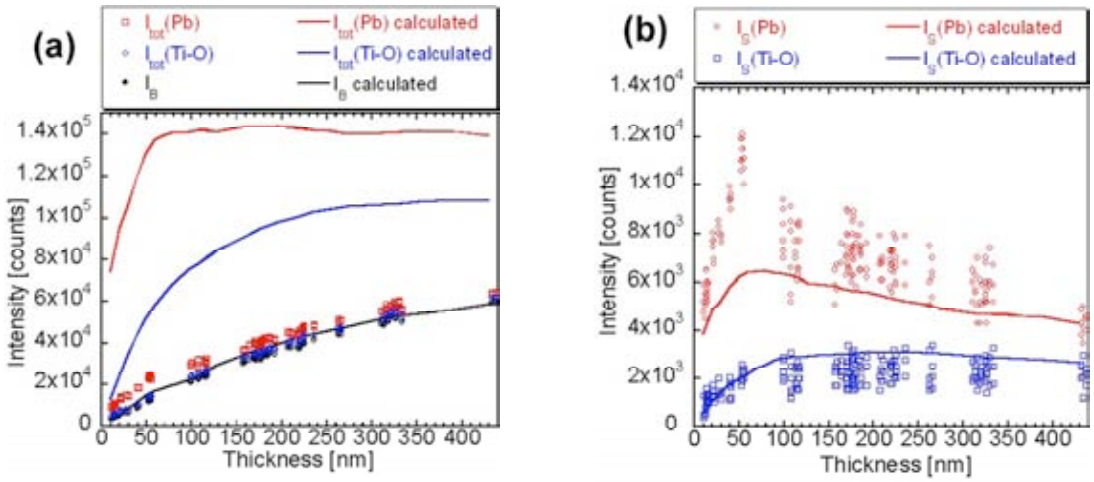

Figure 2: (a) Comparison of experimental and simulated $PbTiO_3$ column and background intensities as a function of sample thickness, scaled so that the calculated values for I_B at the largest thickness corresponded to the experimental value. (b) Comparison of experimental and simulated $PbTiO_3$ atom column intensities after subtraction of the background intensity as a function of sample thickness, scaled so that the calculated values of $I_S(\mathrm{Pb})$ at the largest thickness corresponded to the experimental value [3].

(b) Dielectric Characterization

Dielectric measurements showed that film microstructures had a pronounced influence on the dielectric dead layer capacitance density. (111) oriented $SrTiO_3$ films had a lower interfacial capacitance density than predominantly (110) $SrTiO_3$ films. In addition to differences in the

texture, the (111) films showed (i) greater roughness at the electrode interfaces than (110) films, (ii) different film stress [compressive versus tensile in (110) [4]], (iii) a larger "bulk" permittivity due to the proximity to a ferroelectric phase transformation and (iv) a higher extended defect density near the bottom electrode interface (Fig. 3). The temperature dependence of the interfacial capacitance density was weak compared to that of a typical (incipient) ferroelectric, and nearly independent of the microstructure. We developed a method to analyze the dielectric dead layer thickness and permittivity. The dead layer thickness was extremely small (< 2 nm) and its permittivity was 1-2 orders of magnitude lower than that of the bulk of the film. Thus the dielectric dead layer was unlikely to be directly associated with a defective nucleation layer seen in the TEM images (Fig. 3) that extended significantly into the film. Given its small permittivity, thickness and weak temperature dependence, the results point to origins of dielectric dead layer located very near the electrode/$SrTiO_3$ interface, such as interfacial defect states, roughness, finite screening or depletion layers (the presence of distinct contamination layers of more than a monolayer thickness were ruled out by atomic resolution TEM [5]). The results showed, however, that the magnitude of the contributions of these near-interface effects could be influenced by the films' microstructure, either directly, or indirectly via the films' polarizability.

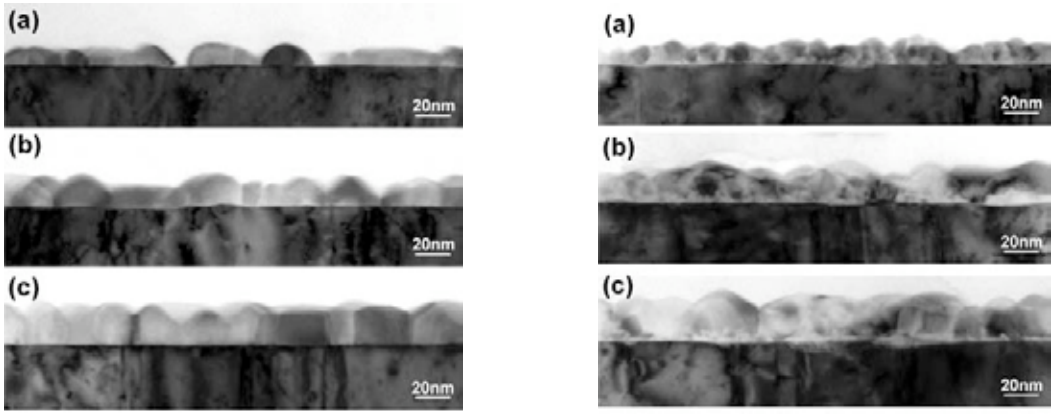

Figure 3: Cross-section TEM images of (110) oriented epitaxial $SrTiO_3$ on epitaxial Pt electrodes (left) and of (111) oriented epitaxial $SrTiO_3$ on epitaxial Pt electrodes after (a) 10 min, (b) 20 min and (c) 30 min of growth. Note the highly defective nucleation layer for the (111) oriented film. All films show twinning.

(c) Interface Atomic Structures

To further investigate the origins of atomic scale dielectric dead layers, atomic resolution HAADF was used to investigate the interface atomic structure of epitaxial, (111) oriented $SrTiO_3$ films on epitaxial Pt electrodes grown on (0001) sapphire. The cube-on-cube orientation relationship of $SrTiO_3$ on Pt was promoted by the use of a Ti adhesion layer underneath the Pt electrode. While a Ti-rich Pt surface was observed before $SrTiO_3$ growth, HAADF images showed an atomically abrupt $SrTiO_3$/Pt interface with no interfacial layers. The $SrTiO_3$ films contained two twin variants that were related by a $180°$ rotation about the $\langle 111 \rangle$ surface normal. HAADF images showed two different interface atomic arrangements for the two twins (Fig. 4). Furthermore, the dielectric dead layers could not be explained with the presence of a chemically distinct interface phase at the bottom electrode interface [5].

Future Plans

We will perform further systematic investigations of the image contrast in experimental HAADF, with the ultimate goal to determine, in combination with image simulations, the sensitivity with which impurity atoms and defects in films and at interfaces can be detected by HAADF. Future studies on the origins of dielectric dead layers in clean metal/perovskite thin

film interface systems grown in-situ. We will HAADF in combination with EELS to relate interfacial defect states to the properties of dielectric deadlayers. Another goal are fundamental investigations of the stability of ferroelectric polarization in ultrathin films with metal electrodes and the influence of interface atomic structure on the transport properties across them.

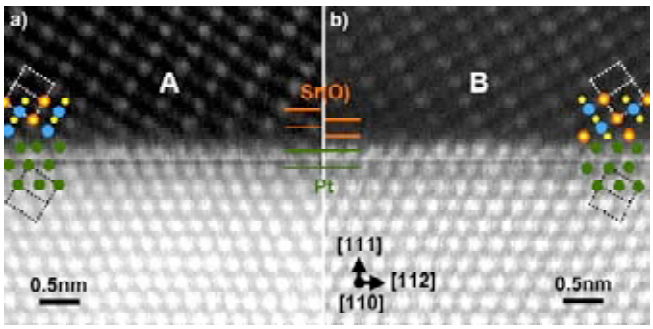

Figure 4: HAADF/STEM images of the interface between $SrTiO_3$ and Pt for (a) twin variant A and (b) twin variant B recorded along the $\langle 110 \rangle$. Red and green horizontal lines mark the position of Sr-O (111) layers and Pt (111) planes, respectively. The overlay shows the average atom column positions (see legend in Fig. 1) determined from intensity line scans across several locations in the images. The oxygen-only columns were not visible and their positions were inferred from the cation positions [5].

References

1. S. Schmidt, J. W. Lu, S. P. Keane, L. D. Bregante, D. O. Klenov, and S. Stemmer, J. Amer. Ceram. Soc. **88,** 789 (2005).
2. S. Schmidt, Y.-W. Ok, D. O. Klenov, J. W. Lu, S. P. Keane, and S. Stemmer, J. Mater. Res. **20,** 2261 (2005).
3. D. O. Klenov and S. Stemmer, Ultrmicroscopy **106,** 889 (2006).
4. S. P. Keane, S. Schmidt, J. W. Lu, and S. Stemmer, J. Appl. Phys. **99,** 033521 (2006).
5. S. Schmidt, D. O. Klenov, S. P. Keane, J. W. Lu, T. E. Mates, and S. Stemmer, Appl. Phys. Lett. **88** (2006).

DOE Sponsored Publications in 2004 – 2006

D. O. Klenov, T. R. Taylor, S. Stemmer, *$SrTiO_3$ films on platinized (0001) Al_2O_3: characterization of texture and nonstoichiometry accommodation*, J. Mater. Res. 19, 1473-1482 (2004).

S. Schmidt, J. W. Lu, S. P. Keane, L. D. Bregante, D. O. Klenov, S. Stemmer, *Microstructure and dielectric properties of textured $SrTiO_3$ thin films* (Invited Feature Article), Journal of The American Ceramic Society 88, 789-801(2005).

S. Schmidt, Y.-W. Ok, D. O. Klenov, J.W. Lu, S. P. Keane, S. Stemmer, *Microstructure of epitaxial $SrTiO_3$/Pt/Ti/sapphire heterostructures*, J. Mater. Res. 20, 2261-2265 (2005).

J. W. Lu, S. Schmidt, Y.-W. Ok, S. P. Keane, S. Stemmer, *Contributions to the dielectric losses of textured $SrTiO_3$ thin films with Pt electrodes*, J. Appl. Phys. 98, 054101 (2005).

S. P. Keane, S. Schmidt, J. W. Lu, A. E. Romanov, S. Stemmer, *Phase transitions in textured $SrTiO_3$ thin films on epitaxial Pt electrodes*, J. Appl. Phys. 99, 033521 (2006).

S. Schmidt, D. O. Klenov, S. P. Keane, J. W. Lu, T. E. Mates, S. Stemmer, *Atomic Structure of (111) $SrTiO_3$/Pt Interfaces*, Appl. Phys. Lett. 88, 131914 (2006).

D. O. Klenov, S. Stemmer, *Limitations in through-focus depth sectioning in non-aberration corrected high-angle annular dark-field imaging*, Jap. J. Appl. Phys. 45, L602 - L604 (2006).

D. O. Klenov, S. Stemmer, *Contributions to the Contrast in Experimental High-Angle Annular Dark-Field Images*, Ultramicroscopy 106, 889-901 (2006).

Nanoscale Imaging of Electrostatic and Magnetic Fields

Martha R. McCartney and David J. Smith
molly.mccartney@asu.edu, david.smith@asu.edu
Department of Physics, Arizona State University, Tempe, AZ 85287

Program Scope

Nanoscale electromagnetic fields are essential for the function and operation of many nanostructured objects and devices. Important examples include elemental and compound semiconductor p-n junctions and non-volatile magnetic storage media. Theory and modeling can be used to estimate field strengths but direct measurements are preferable for smaller dimensions, especially to understand and control the effects of local inhomogeneities and two-dimensional dopant diffusion on macroscopic properties.

Our research program focuses on the observation and quantification of electrostatic potential distributions in and around complex heterojunctions, and the micromagnetic structure of ferromagnetic thin films and small particles. The primary characterization method is the technique of off-axis electron holography, which provides access to the change in phase of the electron wave after it has passed through the specimen region of interest.[1] These phase changes can be directly related to the electromagnetic fields of the object. Electron holography has recently experienced a major upsurge of interest and activity because of the ready availability of electron microscopes equipped with field-emission-gun (FEG) electron sources, and the realization that the technique provides access to much useful information at a level that is otherwise inaccessible. Coupled with recent developments in digital recording and data processing, electron holography can be used to extract quantitative details about electrostatic and magnetic fields at the nanoscale, which can then lead to a better theoretical understanding of their effects.

Recent Progress

Wedge polishing and focused-ion-beam milling have been used to prepare one-dimensional Si p-n junctions and Si p-channel MOSFET samples for electron holography examination. Uniform thickness profiles were obtained, and no significant charging was observed. Sample thickness effects were also investigated: the minimum thickness for reliable results was ~ 160 nm, whereas measured phase changes were smaller than expected below this thickness.

The two-dimensional electrostatic potential distribution associated with 90-nm Si p-MOSFETs were quantified using off-axis electron holography. The results for two p-MOSFETs with different offset spacer oxide widths were compared in relation to the separation of the extension junctions and the source/drain (S/D) junctions. Quantitative measurements of the junction position indicated that the S/D regions encroached under

the gate on each side by 8nm. (See Fig 1) This information concerning the lateral diffusion of dopant is unattainable by any other means.

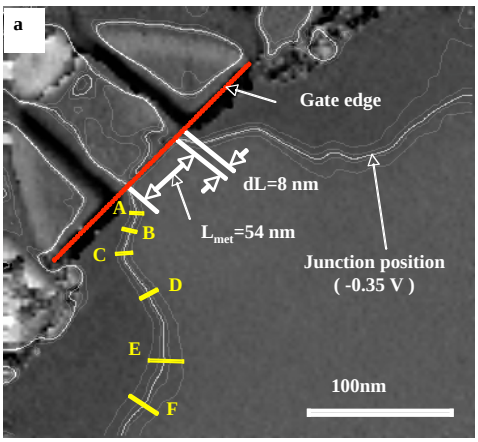

Fig. 1. Voltage map of Si pMOSFET indicating position of pn junction. The S/D extension extend under the gate by 8nm reducing the effective gate length.

Electron holography and Lorentz microscopy were used to study domain wall nucleation, motion and annihilation in nanopatterned Co elements. The native (or 'virgin') states of these elements showed centered and off-centered vortices in most cases, with precise details determined by the element dimensions. Remanent states and magnetization reversal involved single or multiple domains, while the occurrence of single or double vortex states during switching caused significant increases in the average switching field values.

Electron holographic studies of an AlAs/GaAs structure, using samples prepared by wedge polishing have resulted in the determination of the inelastic mean free path for inelastic interaction for both AlAs and GaAs. These parameters will allow determination of the thickness of future device samples where the sample preparation required would give ambiguous thickness. The mean inner potentials for AlAs and GaAs were also determined. The value obtained for GaAs agrees with previously measured data.[2] With knowledge of the thickness and mean inner potential for these materials, we will be able to separate the electrostatic doping effects of devices from the material effects in devices made of the alloys of these materials.

A similar project to measure the material parameters of GeSi/Ge/Si samples has been initiated. The samples, with varying concentrations in the alloy layers are being analyzed to determine whether there is a linear relationship between the Ge concentration of the alloy and the mean inner potential. Initial work on doped heterojunction bipolar trasistor (HBT) structures has been inconclusive. The HBT sample had been prepared by focussed ion beam (FIB) milling using a Ga ion beam. Further studies involving additionalent sample preparation steps will be used to determine if Ga implantation or subsurface damage can be moderated.

A new specimen biasing holder has been tested and calibrated. Initial tests were directed towards identifying reliable method(s) for providing contacts and biasing across nanoscale heterojunctions. Steps are being taken to minimize parasitic voltage drops across the areas of interest.

Electron-beam lithography and lift-off processes were evaluated and then used to fabricate a wide range of ferromagnetic elements with different shapes and sizes, including rectangles with different lengths and aspect ratios, as well as rings and slotted rings with varying inner and outer diameters. Slotted rings were found to have the best properties for use as magnetic random access memory (MRAM): bimodal, reproducible, small switching fields, negligible interactions between closely spaced elements. (See Fig. 2.)

The students working on this project have been trained in advanced materials preparation and characterization techniques. They have interacted directly with leading scientists from other academic institutions and industrial companies, and they have each attended national conferences for direct exposure to latest developments in their areas of scientific research.

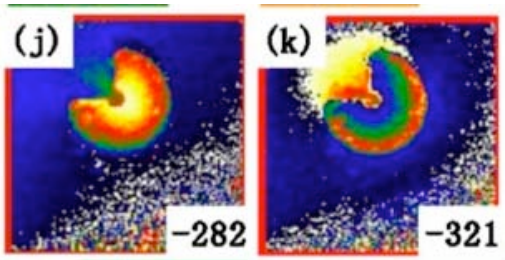

Fig. 2. False colored phase image of slotted ring of 10nm thick cobalt showing complete magnetization reversal after change in applied field of 40 Oe. Ring diameter: 400nm. Change in direction of magnetization is indicated by reversal in the order of color, red/green -> inside to outside.

Future Activities

One major focus of our future research will emphasize the electrostatic potential developed across undoped and doped heterojunctions. Direct measurements using electron holography are essential for characterizing nanoscale devices, since theoretical modeling and simulations are no longer able to account properly for lateral dopant diffusion in highly doped materials with steep concentration profiles. We will examine Si/Ge/Si heterostructures with and without B doping in order to gain a better understanding of dopant diffusion and band-bending effects. The new specimen biasing holder will be used for evaluating the biasing behavior of nanoscale devices.

The second focus of our future research will relate to the micromagnetic behavior of exchange-biased spin-valve samples and thin ferromagnetic (FM) layers exchange-coupled to antiferromagnetic (AFM) thin films. We plan to probe the nature of the coupling between the layers, in particular to examine how magnetization reversal at the nanoscale is altered for nanopatterned elements of different shapes and sizes, and to study the effects of polycrystallinity, defect structure and grain size on this behavior. Careful annealing experiments will enable the impact of interdiffusion across the FM/AFM interfaces to be determined.

References

[1] D.J. Smith, W.J. de Ruijter, J.K. Weiss and M.R. McCartney (1999) Quantitative Electron Holography, In: E. Völkl, L.F. Allard, and D.C. Joy (eds.) Introduction to Electron Holography. Kluwer Academic, New York. pp. 107-124..

[2] M. Gajdardziska-Josifovska, M. R. McCartney, W. J. DeRuijter, Smith, D. J., Weiss, J. K., Zuo, J. M., “Accurate measurements of mean inner potential of Crystal wedges using digital electron holograms” Ultramicroscopy, **50** 285-299 (1993).

Recent Publications

M.-G. Han, J. Li, B. Xie, P. Fejes, J. Conner, B. Taylor, **M.R. McCartney**, "Sample Preparation for Precise and Quantitative Electron Holography Analysis of the Electrostatic Potential in Semiconductor Devices", in: Proc. Microscopy and Microanalysis 2005, pp. 586-587CD

Myung-Geun Han, Jing Li, Qianghua Xie, Peter Fejes, James Conner, Bill Taylor, and **Martha R. McCartney**, "Sample preparation for precise and quantitative electron holographic analysis of semiconductor devices", Microscopy and Microanalysis, **12**, 295-301 (2006).

Myung-Geun Han, **M. R. McCartney**, Peter Fejes, Qianghua Xie, Sandeep Bagchi, Bill Taylor, and James Conner, "Quantitative analysis of 2D electrostatic potential distributions in 90nm Si p-MOSFETs using off-axis electron holography", Superlattices and Microstructures, submitted for publication

N. Agarwal, H. Wang, **D.J. Smith**, and **M.R. McCartney**. "Remanent states and magnetization reversal for nanopatterned Co elements using Lorentz microscopy and off-axis electron holography", IEEE Trans. Mag. **42,** October 2006.

Suk Chung, David J. Smith and M. R. McCartney, " Determination of the inelastic mean free path and mean inner potential for GaAs and AlAs using off-axis electron holography", Ultramicroscopy, submitted.

N. Agarwal, **David J. Smith** and M. R. McCartney, "Switching behavior of Co magnetic nanoelements: double pac-man shape", Appl. Phys. Lett., submitted.

Quantitative Electron Nanocrystallography

Jian-Min Zuo
jianzuo@uiuc.edu
Dept. of Materials Science and Engineering and Materials Research Laboratory,
University of Illinois, Urbana-Champaign, IL 61801

Program Scope

The properties of materials ultimately depend on their local atomic structure, understanding structure-property relationships in nanomaterials thus depends critically on further progress in nanostructure characterization. This program is to develop electron crystallographic techniques for scanning nanoarea electron diffraction and diffraction based 3-D, atomic resolution, tomography, and apply the techniques to the structural determination of individual nanostructures and complex crystals. The proposed research takes advantages of the spatial resolution offered by a nanometer-sized coherent electron probe and the quantitative diffraction information obtained from the high angular resolution achieved with a parallel illumination. The current focus is on 1) the atomic structure of single- and multi-wall carbon and boron nitride nanotubes and 2) ab initio phase retrieval algorithm for image reconstruction. The electron diffraction techniques developed here are general, applicable to a broad range of nanomaterials and can be implemented in many existing electron microscopy facilities across the country. Broad impact is expected from the contribution of this valuable new characterization tool to the nation's science and technology programs. Specific impact toward nanotube structure optimization is also expected from the elucidation of nanotube structures and understanding of their growth mechanisms.

Recent Progress:

Various forms of nanotubes are building blocks for nanoscience and nanotechnology and have attracted considerable interest recently. However, their structure can be highly complex and their growth mechanism is poorly understood. In case of a carbon double wall nanotube (DWNT), the tube consists of two concentric tubes, the structure is incommensurate if the outer and inner tubes have different chiral angles. The combination multiplies further for multi-wall nanotubes (MWNT). The interaction between inner and outer tubes determines a variety of properties in both DWNTs and MWNTs[1,2]. While there are several techniques for characterizing single wall carbon nanotubes[3, 4, 5], MWNT structure determination requires a penetrating probe, which has been done only in few cases of DWNT using electron diffraction [6]. As the result, our knowledge of MWNT structures is very limited.

Using the Nanoarea Electron Diffraction (NED) technique that we developed under the previous DOE support, we carried a systematic structure determination for 30 DWNTs. By recording electron diffraction patterns from individual DWNTs using this technique and using equatorial oscillations to measure the diameters of inner and outer walls and the ratios of layer line distances to measure chiral angles, we show that most

carbon nanotubes are chiral with preference for the chiral angles from 18° to 28°. About 1/3 of the tubes are metallic. From the chiral vectors of the 18 DWNTs determined unambiguously, we are able to measure the spacing between two tubes precisely and predict the electronic structure of each tube.

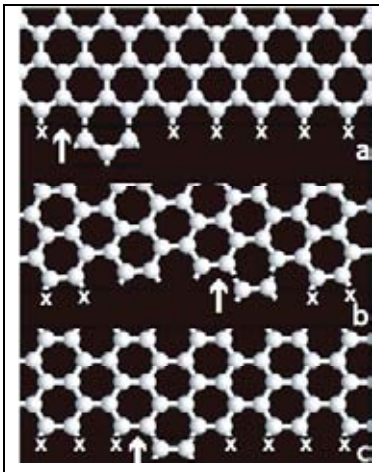

Fig. 1. Hexagon growth of (left) zigzag, (middle) chiral (α=25º) and (right) armchair carbon nanotubes with horizontal tube direction. The X marks the carbon-metal bond at the nanotube and catalyst interface. The stepped tube-metal interface of a chiral tube requires few bond breakings and provides favored attachment sites as shown by the arrow.

To explain the preferred chiral growth in CVD carbon nanotubes, we proposed a kinetic growth model. In the classical growth theory the interface process controlled growth rate is proportional to $|\Delta G|\exp[-q/kT]/kT$, where q is the interfacial energy barrier and $|\Delta G|$ is the driving force. The energy barrier q includes a bond-breaking term for carbon-metal bonds at the nanotube and catalyst interface. For a pure zigzag or armchair tube, all bonds have to be broken in order to grow an additional layer, while for a chiral tube, only a few bonds need to be broken (see Fig. 1). Thus, carbon nanotubes grow by preferential attachment to steps that come with a chiral tube, and the growth is very much like the Frank's growth model for real crystals where steps formed by dislocations flow by preferential attachment.

In a separate study, we elucidated a new nanotube structural form that resembles a double helix in multiwall boron nitride nanotubes (MW-BNNT). Diffraction patterns recorded from small sections of the nanotube lack the 2mm symmetry. The lack of symmetry is also evidenced in bright- and dark-field electron images, which reveal regular zigzag dark and bright spots on the sidewalls of the nanotubes. The repeating distance between the bright, or dark, spots is related to the chiral angle of the nanotube. In a detailed paper published in Acta Cryst. A, we show that all experimental evidence supports the structure model of two helices; one is polygonal in cross section and highly crystalline and the other is circular and less ordered. It is further suggested that the double-helix structure is a result of stronger wall–wall interactions associated with the ionic bonding in boron nitride. The significance of this work is two-fold. One is the new double-helix structural form in nanotubes. The double helix structure is formed as the result of the competition between ordered layer structure and the strain associated tubular structure. The second significance is the scanning electron diffraction technique and the demonstrated structural sensitivity, which has a lot of future potentials that deserves further development.

Future Plans:

A still unresolved problem in nanotube research is the correlation of nanotube properties to tube structure and tube defects. While there are a number of works based on

scanning probe microscopy on structure-property relationships in single wall carbon nanotubes, structure characterization of other forms of nanotubes (including double and multiwall nanotubes and tube bundles) requires electron diffraction and electron microscopy. To facilitate structure determination and property measurement of carbon nanotubes, we designed and fabricated an array of carbon nanotube (CNT) field effect transistors (FETs) with slits etched through the substrate (see Fig. 2). The carbon nanotubes are grown by CVD and self-assembled across the electrodes. The combination of the device structure and slit allows us not only to measure electrical current through a CNT, but also to investigate its structure by TEM. The device structure provides a powerful tool for investigating the structure and property relationship in carbon nanotubes and nanostructure in general. While nanotubes have been proposed for a range of applications, the self-assembly process of nanotube growth often produces a mixture of nanotubes of different structural forms and defects, we expect that the combination of structure characterization with property measurements will lead to significant breakthrough in our understanding of nanotube properties.

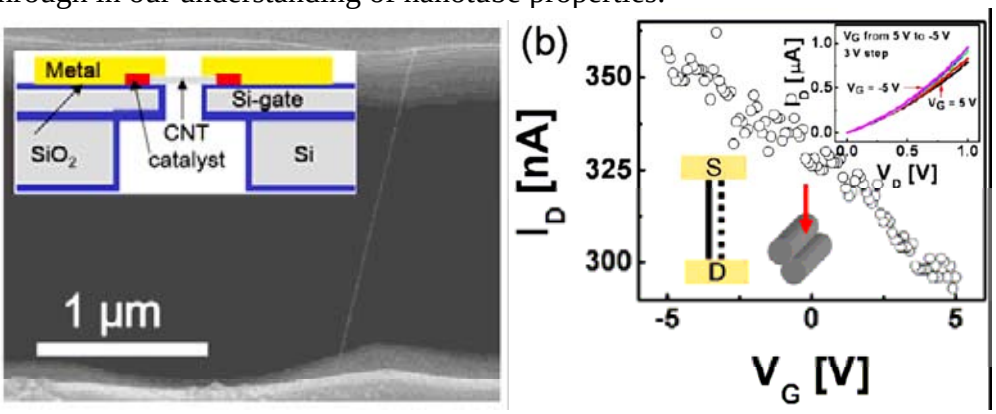

Fig. 2 (Left) A SEM image of a carbon nanotube field effect transistor device with an etched window for TEM characterization. The design is shown in inset. (Right) Measured source drain current as a function of gate voltage. The device is designed for in-situ TEM observation.

Our work shows that the average structure of individual single and double wall carbon nanotubes can be determined from a single diffraction pattern. For nanotube bundles and multiwall nanotubes, structure determination is still a challenge. The bundles are difficult because it contains multiple tubes and tubes of very small diameter. The difficult of multiwall nanotubes comes from its large diameter. One possibility is to use higher layer lines for structure determination. The relationship between the layer lines and tube structure is based on high order Bessel functions.

Our work shows that the recorded electron diffraction patterns from individual carbon nanotubes are exceptionally high and not all structural information are extracted from diffraction. In the near future, we plan to carry out quantitative analysis of nanotube diffraction patterns. Specifically, we will address the following issues: 1) the circularity of single and double wall carbon nanotubes, 2) structure of carbon nanotube junctions and defects and 3) thermal vibrations. Nanotube defects will be studied using diffractive imaging and phase retrieval technique. Issues 1) and 3) will be studied by quantitative analysis.

Reference:

1 J. Cumings and A. Zettl, Science 289, 602 (2000)
2 R. Saito, R. Matsuo, T. Kimura, G. Dresselhaus, &M.S. Dresselhaus, Chem. Phys. Lett., 348, 187-193 (2001)
3 A. Jorio, R. Saito, J. H. Hafner, C. M. Lieber, M. Hunter, T. McClure, G. Dresselhaus, & M. S. Dresselhaus, Phys. Rev. Lett. 86, 1118-1121 (2001); Bachilo, S.M., Strano, M.S., Kittrell, C., Hauge, R.H., Smalley, R.E. & Weisman, R.B., Science 298, 2361-2366 (2002)
4 Gao, M., Zuo, J.M., Twesten, R.D., Petrov, I., Nagahara, L.A. & Zhang, R., Appl. Phys. Lett. 82, 2703-2705 (2003)
5 Qin, L.-C., Iijima, S., Kataura, H., Maniwa, Y., Suzuki, S. & Achiba, Y., *Chem. Phys. Lett.* **268**, 101-106 (1997)
6 M. Kociak, K. Hirahara, K., Suenaga, & S. Iijima, Euro. Phys. J. B, 32, 457 (2003)

DOE Sponsored Publications in 2004-2006

1. J. Tao and J.M. Zuo, Nanoscale Phase Competition during Charge Ordering in Intrinsically Strained $La_{0.33}Ca_{0.67}MnO_3$, Phys. Rev. B (Rapid Comm.), 69, 180404 (2004)
2. J.M. Zuo, M.Gao, J.Tao, B.Q. Li, R. Twesten and I. Petrov, Coherent Nanoarea Electron Diffraction, Microscopy Research Techniques, Invited, 64, 347-355 (2004)
3. A.C. Aktas, J.M. Zuo, J.F. Stubbins, C. Tang and Y. Bando, “Chirality Distribution in Boron Nitride Nanotubes”, *Appl. Phys. Lett.*, 86, 133110, (2005)
4. J. Tao, D. Niebieskikwiat, M.B. Salamon, and J.M. Zuo, “Lamellar phase separation and dynamic competition in $La_{0.23}Ca_{0.77}MnO_3$”, Phys. Rev. Lett. 94, 147206, (2005)
5. T. Kim, J.M. Zuo, E.A. Olsen and I. Petrov, " Imaging suspended carbon nanotubes in field-effect transistors configured with microfabricated slits for transmission electron microscopy", Appl. Phys. Lett. 87, 173108 (2005)
6. A.C. Aktas, J.M. Zuo, J.F. Stubbins, C. Tang and Y. Bando, "Double-helix structure in multiwall boron nitride nanotubes", Acta Cryst. A, 61, 533-541 (2005)
7. M. Gao, J. M. Zuo, R. Zhang, L. A. Nagahara, " Structure determinations of double-wall carbon nanotubes grown by catalytic chemical vapor deposition", Journal of Materials Science, in print, (2006)

Toward the Development of Cluster-Based Materials

Kit H. Bowen
kbowen@jhu.edu
Depts. of Chemistry and Materials Science, Johns Hopkins University, Baltimore, MD 21218

Program Scope

The large surface-to-volume ratios, unique geometric structures, and low dimensionalities of clusters lead to properties that are very different from those of the same substance in bulk form. Clusters containing a few to several thousand atoms and/or molecules constitute an ideal class of nano- and sub-nano-structures, since their size and composition can be controlled one atom or molecule at a time. Because of the unique characteristics of clusters, there exists the potential of synthesizing new (cluster-assembled) materials with highly tailored optical, magnetic, and/or chemical properties, if clusters, instead of atoms and molecules can serve as their building blocks.[1-3] This program provides experimental results which make fundamental, underpinning contributions to the development of cluster-based materials. Specific topics we have studied (or are studying) include the non-metal-to-metallic transition in divalent metal clusters, the search for (and discovery of) theoretically-predicted, ionically-bonded cluster-assembled "molecules" and other Magic Clusters, the interaction of transition metal atoms and clusters with organic molecular templates, the synthesis and characterization of Zintl phase clusters, the magnetic properties of semiconductor clusters, the molecular properties of electronic materials, the magnetic properties of silicon-encapsulated rare earth metal atom cages, and the magnetic and electronic properties of gold/silica and gold/iron clusters. In carrying out this program, we utilize mass spectrometry, anion photoelectron spectroscopy, reactivity studies, and through a collaboration, magnetic deflection experiments. Computational support is provided by synergistic partnerships with several theoretical collaborators.

Recent Progress

The Transition to Metallic Behavior in the Finite Size Regime A collection of metal atoms does not necessarily exhibit metallic behavior. Thus, the nonmetallic-to-metallic transition in the finite size regime is a fundamental problem in sub-nanoscale materials science. We approached this topic through the study of homogeneous metal clusters, each of which is composed of atoms from divalent (or usually divalent) metals. Our first study was on magnesium cluster anions. By following the closing HOMO-LUMO gap as a function of cluster size, we found that gap closure, and thus the onset of metallic behavior, occurred with clusters containing 18 magnesium atoms. We also found strong but unexpected adherence to the jellium-like, electronic shell model, both through gap "re-openings" and through magic numbers in their mass spectra. We then extended our studies beyond magnesium to clusters of zinc, calcium, and manganese. While their electronic behaviors differed in several ways from magnesium, zinc and calcium also showed HOMO-LUMO gap closures at around 18 atoms per cluster as well as shell model effects. Manganese offered several surprises, including the discovery of half-metallicity in clusters. Theoretical support was provided by J. Jellinek at Argonne National Laboratory.

The Basic Units of Cluster-Assembled Materials Cluster-assembled "molecules" can act as the basic units of cluster-assembled materials. Theoretical calculations by Khanna and Jena had predicted KAl_{13} to be an ionically bonded, cluster-assembled "diatomic-like molecule", i.e.,

$K^+Al_{13}^-$. The Al_{13}^- cluster anion is unusually stable, having both electronic and geometric sources of high stability. Since the electron affinities of Al_{13} and Cl are the same, Khanna and Jena reasoned that perhaps icosahedral Al_{13}^- could replace Cl^- in an ionic molecule such as KCl , i.e., K^+Cl^-, to form KAl_{13}, i.e., $K^+Al_{13}^-$. Extensive calculations supported this hypothesis, raising the exciting possibility that it might be possible to make macroscopic, extended lattices consisting of cations and intact Al_{13}^- anions. We conducted both mass spectral and anion photoelectron spectroscopic studies on KAl_n^- cluster anions. While some of our studies focused on electron affinity trends as qualitative indicators of ionic bonding in KAl_{13}, quantitative comparisons between our photoelectron spectrum of KAl_{13}^- and its calculated photodetachment transitions [provided by Khanna and Pederson (NRL)] proved decisive in showing that KAl_{13} is indeed a salt and the prototype of a basic building block for cluster assembled materials.

Interactions of Transition Metal Clusters with Organic Molecules The small clusters of several transition metals are known to exhibit higher magnetic moments per atom than the same metal in its macroscopic state. If these clusters were to be used for information storage and processing, it would be important to know how their magnetic moments are affected by interaction with a substrate. Given that molecular organic materials are among the likely substrate candidates, this is one of our reasons for studying the interactions of transition metal atoms and clusters with organic molecules as models for such substrates. Another reason is the possibility that extended sandwich structures of transition metal clusters and organic molecules might be viable components of cluster-assembled materials. For these reasons, we studied the structures and stabilities of transition metal cluster/organic complexes as well as modifications to the magnetic moments of metal clusters due to their interaction with molecular organic templates. While much of this information is revealed via mass spectral patterns and photoelectron spectral similarities, we extract magnetic information by comparing our measured photodetachment transitions for a given cluster anion with calculated photodetachment transition energies between that cluster anion and its various terminal neutral electronic states along with the spin multiplicities of each of those states. A match serves to confirm the predicted multiplicities of the various electronic states. From multiplicities, spin magnetic moments are computed from the fact that the spin magnetic moment in units of Bohr magnetons (μ_B) is equal to the multiplicity minus one, i.e., 2S. This synergetic approach allows us to determine how different molecular organic environments modify the magnetic moments of small transition metal clusters. We have applied this approach to a variety of systems, including $Co_n(benzene)_m^-$, $Ni_n(benzene)_m^-$, $Ti_n(benzene)_m^-$, $Fe_n(benzene)_m^-$, $Co_n(pyridine)_m^-$ and $Co_n(coronene)_m^-$. Our results showed that the magnetic moments of small transition metal clusters are highly sensitive to their immediate environments. Theoretical support was provided by Jena and Khanna.

Clusters of Zintl Phase Species Zintl ions are a family of multiply-charged polyatomic anions which readily form compounds with alkali cations in solids and "melts" [Zintl phases]. The similarity between Zintl ions and Al_{13}^- and potentially between Zintl phases and species such as $K^+Al_{13}^-$ suggests that further studies of Zintl species, which are already known to exist in the bulk, may aid in developing cluster-assembled materials. Zintl phases are typically formed between highly electropositive metals, such as alkali metals, and mildly electronegative atoms, generally those of the post-transition elements, i.e., the heavier members of Groups 13, 14, 15 and sometimes 16. Among the simpler examples of Zintl phases are the 1:1 MTt compounds, formed between M = Na, K, Rb, and Cs and Tt (tetrel) = Si, Ge, Sn, and Pb. These compounds have been shown to contain tetrahedra, Tt_4, and they are typically described as $(M^+)_4Tt_4^{4-}$, depicting the interaction of four alkali cations with the multiply-charged polyatomic anions known as Zintl anions. A famous example is the Zintl phase, $(Na^+)_4Sn_4^{-4}$, which is composed of four sodium cations and the tetrahedral Zintl ion, Sn_4^{-4}. The anion, Sn^- is isoelectronic with P, and Sn_4^{-4} is thus isoelectronic with P_4, which itself has a tetrahedral structure. While it is

generally assumed that ionic bonding dominates, the bonding in Zintl phases can be complicated, and there is thought to be a substantial degree of covalent character present as well. We have measured the photoelectron spectra of $[Na_nSn_4]^-$, where n = 1-4. In the spectrum of $[Na_4Sn_4]^-$, one sees a decrease in the electron affinity relative to the other members of this series and a large energy splitting between the lowest EBE and the next highest EBE peaks. This is symptomatic of a large HOMO-LUMO gap and thus of enhanced stability. It also means that Na_4Sn_4, despite its composition, is not metallic. The trend in electron affinities together with the large HOMO-LUMO gap in the photoelectron spectrum of $[Na_4Sn_4]^-$ resembles the situation in the spectrum of $[KAl_{13}]^-$, suggesting that $[Na_4Sn_4]^-$ is the anion of the largely ionically-bonded Zintl species, Na_4Sn_4, where multi-charged Sn_4^{4-} is stabilized by four sodium cations, each one located at a face of the Sn_4^{4-} tetrahedron, viz., $(Na^+)_4Sn_4^{4-}$. Khanna has provided theoretical support.

Magnetic Semiconductor Clusters Here, we studied three systems and/or topics. These were (1) magnetic bistability in Mn_2O^-, (2) isomers and isomags in Mn_5O and Mn_6O, and (3) chromium-doped silicon cluster anions. In a synergetic study involving our photoelectron spectra and calculations by Khanna, his calculations found that the ground state of the Mn_2O^- anion has two nearly degenerate isomers, one of which is ferromagnetic (11 μ_B), while the other is antiferromagnetic (1 μ_B). Comparison between our measured photoelectron spectrum and his predicted photodetachment transitions for each of the anionic isomers revealed the presence of both isomers in our anion beam, supporting his prediction that these magnetically dissimilar isomers are nearly degenerate. In another collaborative study with Khanna, we measured the photoelectron spectra of Mn_5O^- and Mn_6O^-. His calculations had predicted the presence not only of isomers in each case but also of their isomags, where the latter term refers to isomers that differ only in their local magnetic moment distributions. By comparing our measured spectra with his predicted photodetachment transition energies and with his calculated density of states for the anion, together we concluded that the isomers/isomags predicted by his calculations are also seen in our photoelectron spectra. In a theoretical study on $CrSi_n$ clusters, Khanna, Rao, and Jena[9] found the magnetic moment of the chromium atom inside a twelve atom silicon cage to be quenched. This was an extraordinary prediction given that chromium has the highest magnetic moment among the first row transition metal atoms. Our measurement of the photodetachment transition energy of $CrSi_{12}^-$ agreed with their predicted value, supporting their findings.

Molecular Properties of Electronic Materials We have also explored the molecular properties of several electronic materials. For example, there is a need in the microelectronics industry to replace SiO_2, which is a low-k gate dielectric, with a high-k gate dielectric material. While ZrO_2 would appear to be a good candidate, the ZrO_2/Si interface is unstable with respect to silicide formation. HfO_2/Si interfaces, on the other hand, are stable in this regard. The difference between these materials, which have otherwise very similar properties, traces back to subtle differences in their electronic structures. To explore those differences, we measured the anion photoelectron spectra of ZrO_2^- and HfO_2^-, finding their electron affinities to be significantly different (1.64 and 2.14 eV for ZrO_2 and HfO_2, respectively) and providing a foothold from which to explain their observed differences as materials. M. Gutowski, then at PNNL, provided theoretical support.

Future Plans

We have begun an extensive effort aimed at studying silicon-encapsulated rare earth atom cages. This work builds on the propensity of silicon to encapsulate metal atoms and on the potential of the electronic structure of the rare earths to provide large magnetic moments and stability simultaneously. These magnetic semiconductor clusters straddle the worlds of traditional silicon-based electronics and the emerging field of spintronics. While part of this

project utilizes photoelectron spectroscopy, part of it also utilizes magnetic deflection. The latter experiments are conducted in collaboration with M. Knickelbein at Argonne National Laboratory. Thus far, we have made two trips there to work on this topic with him. We will also continue our work on the interaction of transition metal clusters with model organic molecular templates, exploring how the anomalously large magnetic moments of several small transition metal clusters may be affected by prospective support surfaces, such as organic films. Again, we are already proceeding with this research. We are also planning to study several promising magic clusters, each of which has potential for serving as a component of a cluster-assembled material. Candidates include theoretically-predicted clusters, such as $Fe_{12}Zn$. Another topic that we plan to study involves small gold/silica and gold/iron clusters. In the former cases, we plan to measure how the HOMO-LUMO (optical) gap depends on cluster size and composition, while in the latter cases, we are interested in determining their magnetic properties.

References

(1) P. Jena, S. Khanna & B. Rao, *Cluster and Nanostructure Interfaces*, (World Scientific, Singapore, 2000)
(2) A. W. Castleman and K. H. Bowen, J. Phys. Chem. **1996**, 100, 12911-12944.
(3) K. Sattler, *Cluster Assembled Materials*, (Trans Tech Publications, 1996).

DOE Sponsored Publications in 2005-2006

Photoelectron Spectroscopy of Chromium-Doped Silicon Cluster Anions, W.-J. Zheng, J. M. Nilles, D. Radisic, and K. H. Bowen, J. Chem. Phys. **2005**, 122, 071101/1-4.

Photoelectron Spectroscopy of Titanium-Benzene Cluster Anions, W.-J. Zheng, J. M. Nilles, O. C. Thomas, and K. H. Bowen, Chem. Phys. Lett. **2005**, 401, 266-270.

Photoelectron Spectroscopy of Nickel-Benzene Cluster Anions, W.-J. Zheng, J. M. Nilles, O. C. Thomas, and K. H. Bowen, J. Chem. Phys. **2005**, 122, 044306/1-5.

Electronic Structure Differences in ZrO_2 vs. HfO_2, W.-J. Zheng, K. H. Bowen, J. Li, I. Dabkowska, and M. Gutowski, J. Phys. Chem. A **2005,** 109, 11521-11525.

The Role of Water in Electron-Initiated Processes and Radical Chemistry: Issues and Scientific Advances, B. C. Garrett, K. H. Bowen et al., Chem. Rev. **2005**, 105, 355-389.

Structure and Stability of $Co_n(pyridine)_m^-$ Clusters: Absence of Metal Inserted Structures, B. D. Edmonds, A. K. Kandalam, S. N. Khanna, X. Li, A. Grubisic, I. Khanna, and K. H. Bowen, J. Chem. Phys. **2006**, 124, 074316/1-6.

The Ionic KAl_{13} Molecule: A Stepping Stone to Cluster-Assembled Materials, W.-J. Zheng, O. C. Thomas, T. P. Lippa, S.-J. Xu, and K. H. Bowen, J. Chem. Phys. **2006** 124, 144304/1-5.

Mn_n^- Clusters: Size-Induced Transition to Half-Metallicity, J. Jellinek, P. H. Acioli, J. Garcia-Rodeja, W.-J. Zheng, O. C. Thomas, and K. H. Bowen, Phys. Rev. B **2006** (in press).

Session VI

New Directions in Probing Local Phenomena

Martensitic Transformation Kinetics in Ti Films Studied using Single-Shot Dynamic Transmission Electron Microscopy

Geoffrey H. Campbell, Thomas LaGrange, Nigel D. Browning, Wayne E, King
ghcampbell@llnl.gov, lagrange2@llnl.gov, browning20@llnl.gov, weking@llnl.gov
Material Science and Technology Division, Chemistry and Materials Science Directorate,
Lawrence Livermore National Laboratory, Livermore, CA 94550

Program Scope

Much of the transmission electron microscopy (TEM) community is typically focused on improving the spatial resolution of static images, however a complementary effort has been underway to improve the temporal resolution during *in-situ* experiments.[1] This approach has recently caught the attention of the international research community, and efforts to develop the next-generation time-resolved electron microscopes are underway.[2,3] The development of the dynamic transmission electron microscope (DTEM) at Lawrence Livermore National Laboratory is motivated by the potential scientific applications of a technique that has both high temporal and spatial resolution. With nanoscale resolution, the transient events and salient microstructural features in rapid materials processes can be captured. One such process is the martensitic phase transformation, where we have applied the DTEM's capabilities in the study of martensitic nucleation and growth kinetics in nanocrystalline and coarse-grained titanium foils.

Our attention is focused on generating single-shot images and diffraction patterns capturing material processes with resolutions in the nanometer and nanosecond regimes.[3] By "single-shot" we mean that there are sufficient electrons in a single nanosecond pulse to form an image, which is unlike stroboscopic experiments[2] that accumulate the signal over a number of pulses. The single-shot approach is essential for studying most dynamic material phenomena, such as the phase transformations, which are dissipative and hence irreversible.

The DTEM consists of a JEOL 2000FX transmission electron microscope modified to allow access for two laser pulses. One laser pulse drives the photocathode (which replaces the standard thermionic cathode) to produce the nanosecond electron probe pulse. The other laser pulse strikes the sample, initiating the process to be studied, such as heating the sample via laser absorption above the martensitic start temperature. Both selected-area diffraction and real-space imaging (with better than 20 nm resolution as shown in Figure 1) are available.[4] This approach has allowed us to study nucleation and growth kinetics in Ti foils, as a function of initial grain size and temperature, in spatial and temporal regimes difficult to access with any other technique.

Recent Progress

We have quantitatively tracked the rapid martensitic-type phase transformation in pure Ti films, namely the hexagonal close packed (HCP) α to body centered cubic (BCC) β transition, using single-shot selected area diffraction (SAD) to distinguish the two phases. The transformation has been tracked through a series of SAD patterns collected using different delays between the pump laser heating pulse and the electron probe pulse. An example of a pump/probe SAD experiment is given in Figure 2, in which 40 nm thick films of nanocrystalline Ti were rapidly heated (10^8 K/s) above the transition temperature (1155 K) with 1064 nm, 12 ns laser pulses (20-10μJ in 0.075 mm^2 spot). The transformation initiates at ~100ns after the 17 μJ pump pulse

(which corresponds to a temperature of 1625 K estimated by laser absorption models). At 250 ns after the pump laser pulse interacts with the specimen, the HCP, α phase (the stable room temperature phase) was partially transformed into the BCC, β phase, indicated by the appearance of the diffuse rings. The pattern acquired at the 500 ns delay is strikingly different from the ground state pattern; the diffuse ring is more intense and additional spots are apparent. The amount of BCC phase contributing to the electron diffraction can be extracted by taking the difference between the ground-state pattern and time-delayed pattern (See Figure 3). To determine the intensities of SAD rings, the respective difference SAD pattern is rotationally averaged, the radial intensity with reciprocal lattice spacing is plotted, and the integrated intensities of the reflections are calculated from Gaussian fits of the peaks.

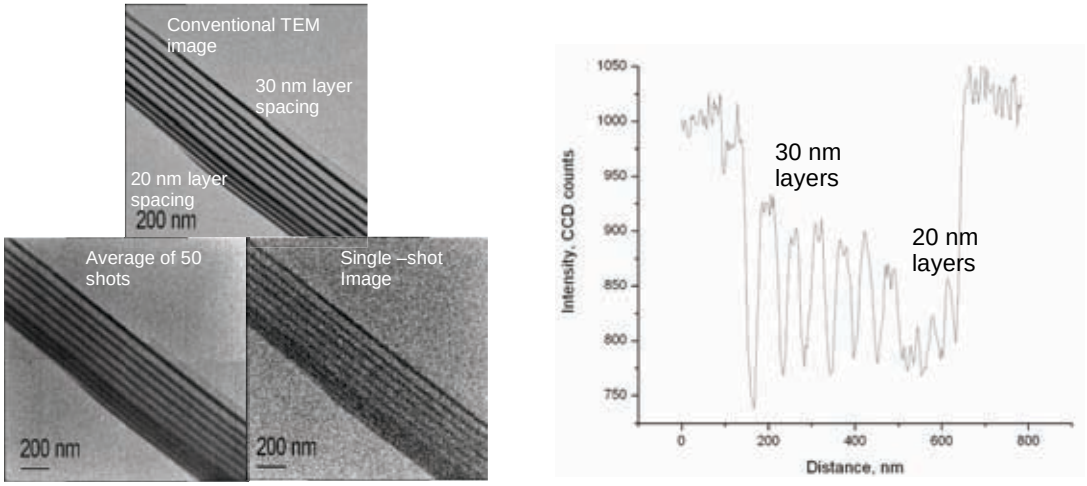

A) **B)**

Figure 1. A) Composite figure of three images of a cross section of an Au/C multilayer foil. The image at top is a conventional TEM image. The image on the lower left is an average of 50 DTEM pulses. The image on lower right is a single-shot image of the same area. **B)** Graph shows the pixel intensity as a function of distance across the multilayers for the single-shot image in Figure 1 A).

We have also studied the nucleation and growth kinetics as a function of temperature and initial grain size. In nanocrystalline Ti films, the transformation proceeds rapidly at temperatures near melt, i.e. at ~1900 K, the transformation was complete at <30 ns, which is too fast to study the evolution with a 30ns electron probe pulse. At temperatures near the β transition temperature, ~ 1200 K, the complete transformation to β-phase was not observed even after 5μs. It is probable that the film cooled below the transition temperature at these long times and is thus unable to completely transform. The incubation times for nucleation are strongly dependent on grain size, i.e. vastly different between nanocrystalline and coarse-grained bulk Ti materials. The nanocrystalline Ti films have incubation times of ~100 ns, while materials with 100 μm grain sizes have incubation times on the order of 500 ns. This difference is most likely due to the lower number of nucleation sites and higher barrier energies in the coarse-grained bulk materials.

Another observable difference between the nanocrystalline and coarse-grained Ti was in the repeatability of the transformation. After one laser shot, the microstructure of the nanocrystalline material changed dramatically, and after repeated shots to the same region, the film ceased to transform to the β-phase, indicating possible oxygen (α stabilizing) incorporation. In coarse-grained materials, only one BCC variant was formed during the laser heating, and the

microstructure reverted to the initial HCP crystal orientation and grain sizes upon cooling. The transformation characteristics were repeatable with continued shots to the same region with no observable change in incubation times or transformation rates. It is not completely understood why only one crystallographic variant forms and why the transformation is crystallographically reversible. Future experiments using time-resolved bright-field imaging to study the grain size dependence on nucleation processes and martensite/parent interface dynamics are required.

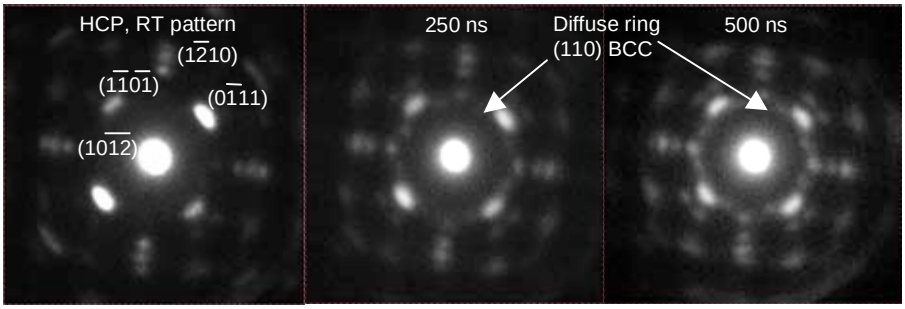

Figure 2. Diffraction pattern montage showing the evolution in the α→β phase transformation with different pump/probe delays.

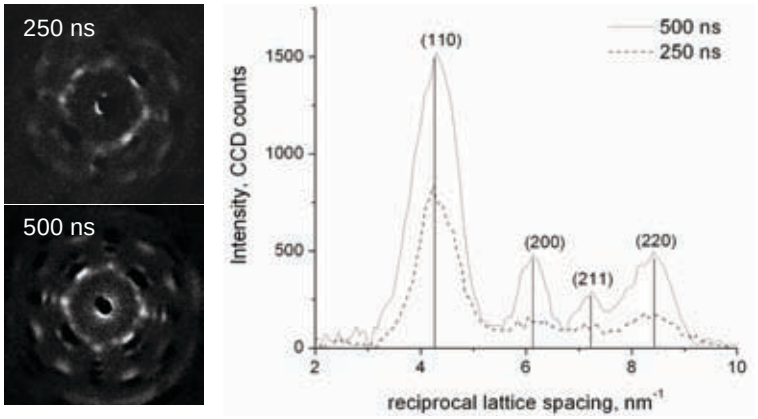

Figure 3. Upper left: difference diffraction pattern for the 250 ns delay. Lower left: difference diffraction pattern for 500 ns delay. Right image: radial intensity distribution generated from the rotational average of the difference patterns on the left.

Future Plans

From a series of electron SAD data collected at different pump laser delays and energies, we will attempt to assemble an isothermal phase diagram for the nanocrystalline Ti films. However, there are certain aspects of Ti materials that hinder quantitative analysis in the DTEM which must be consider: (1) Ti is very reactive; it must be confirmed through ex-situ chemical analysis that Ti does not react and form other compounds during laser heating, (2) there are difficulties in tracking the transformation at temperatures near melt; high intensity background resulting from thermal diffuse scattering and low signals limit the structural refinements; secondly, transformation rates can be faster than the time resolution of the instrument, (3) the experiments are not truly isothermal and rely on the fact that lateral heat diffusion is slower than the transformation; this is a problem at lower temperature near the α-β transition, where transformation rates are slow and the film may cool significantly before completion. We will use laser absorption and heat diffusion models to calculate the temperature as a function of laser

energy and time. These calculations will be used to determine the temperature regime corresponding to a near isothermal hold. Computer coupling of phase diagrams and thermochemistry (CALPHAD) simulations will be generated to compare with the experimental isothermal diagram. In combination with thermal modeling, they will be used to asses the validity of experimental data and give a phenomenological basis for understanding these transformations on the nanosecond timescales.

With planned instrument upgrades and enhanced capabilities, the ability to collect high quality pulsed images will be possible. These new capabilities will be used to study phase front interface propagation and elucidate the interfacial defect dynamics. Given the spatial and time resolution limitations, we intend to study the nature of martensitic nucleation events with hopes to answer some of the most intriguing questions about these transformations, such as how the phase front dynamics and relaxation-accommodation mechanisms, i.e. dislocation nucleation in parent and daughter phases, influence the nucleation events ahead of the transformation front.

This work performed under the auspices of the U.S. Department of Energy by University of California, Lawrence Livermore National Laboratory under Contract W-7405-Eng-48.

References

1. H. Dömer and O. Bostanjoglo, *Rev. Sci. Instr.* **2003,** 74, 4369-4372.
2. H. Zewail, *Phil. Trans. R. Soc. London, Series a-Math. Phys. and Eng. Sci.* **2005,** 363, 315-329.
3. W. E. King, et al., *J. Appl. Phys.* **2005**, 97**,** 111101.
4. T. LaGrange, et al., *Appl. Phys. Let.* **2006**, 89, 044105.

BES Sponsored Publications in 2005-2006

- W. E. King, G. H. Campbell, A. Frank, B. Reed, J. Schmerge, B. J. Siwick, B. C. Stuart, and P. M. Weber, "Ultrafast electron microscopy in materials science, biology, and chemistry," *J. Appl. Phys.* **97**, 111101 (2005).
- H. Kleinschmidt, A. Ziegler, G.H. Campbell, J.D. Colvin, O. Bostanjoglo, "Phase transformation analysis in titanium at nanosecond time resolution," *J. Appl. Phys.* **98**, 054313 (2005).
- *The HCP to BCC Phase Transformation in Ti Characterized by Nanosecond Electron Microscopy*, G.H. Campbell, T.B. LaGrange, W.E. King, J.D. Colvin, A. Ziegler, N.D. Browning, H. Kleinschmidt, and O. Bostanjoglo, in *Proceedings of the Solid-Solid Phase Transformations in Inorganic Materials 2005*, Vol. 2, edited by J.M. Howe, D.E. Laughlin, J.K. Lee, U. Dahmen, and W.A. Soffa (TMS, Warrendale, PA, 2005) p. 443 - 448.
- *In-situ Studies of the Martensitic Transformation in Ti Thin Films using the Dynamic Transmission Electron Microscope (DTEM)*, T. LaGrange, G.H. Campbell, J.D. Colvin, W.E. King, N.D. Browning, M.R. Armstrong, B.W. Reed, J.S. Kim, and B.C. Stuart, in *In-Situ* Electron Microscopy of Materials, eds. P.J. Ferreira, I.M. Robertson, G. Dehm, and H. Saka (*Mat. Res. Soc. Symp. Proc. Vol. 907E*) p. 0907-MM05-02.1-6.
- *Nanosecond Time Resolved Electron Diffraction Studies of the α to β Transition in Pure Ti Thin Films using the Dynamic Transmission Electron Microscope (DTEM)*, T. LaGrange, G.H. Campbell, J.D. Colvin, B. Reed and W.E. King, *J. Mat. Sci.*, **41** (2006), pp. 4440–4444.
- *Single Shot Dynamic Transmission Electron Microscopy for Materials Science*, T. LaGrange, M.A. Armstrong, K.R. Boyden, C.G. Brown, N.D. Browning, G.H. Campbell, J.D. Colvin, W.J. DeHope, A.M. Frank, D.J. Gibson, F.V. Hartemann, J.S. Kim, W.E. King, B.J. Pyke, B.W. Reed, M.D. Shirk, R.M. Shuttlesworth, B.C. Stuart, and B.R. Torralva, *Appl. Phys. Let.*, **89**, 044105 (2006).
- *Practical Considerations for High Spatial and Temporal Resolution Dynamic Transmission Electron Microscopy*, M.R. Armstrong, K. Boyden, N.D. Browning, G.H. Campbell, J.D. Colvin, W.J. DeHope, A.M. Fran, D.J. Gibson, F. Hartemann, J.S. Kim, W.E. King, T.B. LaGrange, B.J. Pyke, B.W. Reed, R.M. Shuttlesworth, B.C. Stuart, and B.R. Torralva, *Ultramicrscopy* in press.

Ultrafast Dynamics at Nano-Interfaces

Chong-Yu Ruan
ruan@pa.msu.edu
Department of Physics and Astronomy, Michigan State University, MI 48824

Program Scope

The correlation between the material structures and the size-dependent properties is a fundamental problem in nanoscience. Nano-particles and interfaces exhibit physical, chemical, and biological properties that are absent in their bulk counterparts. New regimes of reactions and functions have been explored by modifying nanoscaled materials atom-by-atom [1]. But to detail the mechanisms, characterization of the steady-state structures is often insufficient. This is because the pathways of reaction are often determined or influenced by the inhomogeneity from a large surface-volume ratio pertaining to nanostructures and the nonstochastic nature of transient interactions [2]. Hence, their elucidation requires characterizations at the atomic scale in both space and time (i.e. $\leq 10^{-12}$ sec, and $\leq$0.01 Å); and at nanoineterfaces molecular sensitivity is necessary. Through the development of ultrafast electron diffraction [3,4,5] and spectroscopy techniques, we are poised to elucidate some important mechanisms pertaining to the nanometer scales. In the scope of this program, via femtosecond laser excitations, we prepare the materials far from equilibrium. By isolating structure, energy, and dynamics, we are able to repetitively investigate photophysical and photochemical processes in a pump-and-probe setup. To study carrier-lattice couplings and phonon scatterings at nanointerfaces, we prepare atomic, molecular, and material multilayers. Launching selectively heated electron gases in confined boundary, we determine and discern dynamics and interactions by following the nonequilibrium vibronic couplings and averaged atomic arrangements following electronic de-excitations at the relevant time scales. To accentuate the structurally correlated transformations from bulk to the molecular length scale, we size-select and deposit nanoparticles (Au, Ag) on well characterized interfaces. Energy is varied and selectively infused into isolated particles by resonance femtosecond excitation. Since we are able to reach isolations in both space and time, the intrinsic properties of temperature driven transformations of nanostructures and phases can be examined at calibrated levels on the energy landscape [6]. This program falls within the National Nanoscience Inititiative to 'develop novel experimental characterization tools to drive the nanoscale revolution'. The underlying physics and chemistry that will be concluded from these studies are relevant to the DOE missions in the areas of molecular electronics and sensing, renewable energy research, and catalysis.

Recent Progress

Although this program started recently, we have some early successes to report.

In the studies of nanoparticles and interfacial dynamics, the Au nanoparticles (2-20nm) were isolated on a silicon substrate (>95%) and their distribution, morphology and

atomic structures were characterized using SEM and small angle diffraction methods. A molecular linker layer was employed to facilitate the anchoring mechanism of nanoparticles on silicon substrate. Pattern identification in the full diffraction images was used successfully to isolate nanoparticle signals from diffraction patterns of the substrate and linker molecule for particle coverage as low as 5%, and for particles as small as 2nm. It should be possible to detect even smaller particles with a higher coverage. With a proximity coupled photoelectron source [5], the transient structural dynamics of 20nm Au nanoparticles molecularly linked to a silicon substrate were examined at ~ 1ps resolution. The phase transformations of linker molecules as well as Au particles were established using laser excitation, but occurred in very different regimes in time and energy. This is in contrast to the recent studies of the dynamical transformation of supported Au nanoparticle using a synchrotron radiation X-ray source. That setup investigates ~100nm particles with a time-resolution of ~100 ps defined by the bunch duration of the X-ray pulses [7]. There was also no report of molecular signals in the diffraction pattern. In comparison, we are able to resolve many fine details in both structure and dynamics as outlined below.

A novel charging dynamics of the linker molecules was identified. Aided by our density functional theory calculation, the observed structurally correlated molecular charging process appeared to satisfy a hopping mechanism that was controlled initially by Coulomb blockade resulting in an induction period of ~ 10 ps before further charge transfer was allowed. A rapid dynamical reversal of structures was established in as short as 1.5 ps when additional charges were added and reached a steady state. These processes were found to be completely reversible on the nanosecond time scale. The melting of nanoscale Au particles was found to be distinct from that of the bulk process. With a high excitation fluence, phase transformation was induced but exhibited a nonreciprocal characteristics between the melting and recrystallization processes. There was no apparent lattice expansion preceding the melting, but instead a softening of the lattice gradually led to the collapse of the long-range order. The process completed in an ultrafast time scale. The recrystallization process was very different. It proceeded by building a long-range order from the melt in tens of picoseconds. The new structure could be characterized with a larger lattice constant, but smaller than the prediction based on the Lindemann criterion [8]. With a lower excitation fluence below the melting threshold, the lattice expanded upon heating with no induction period. The transient structures of Au nanoparticles are being investigated with Radial Distribution Function method and compared with atomic modellings. Because the dynamics are nonuniform along different lattice planes, it is thus possible to identify the soft-phonon mode that leads to the melting. We are also investigating the order parameters that describe the recrystallization process.

Concerning the nanoacoustic phenomena, graphite multilayers were investigated under different driven conditions. Coherent wave-like dynamics as well as energy dependent driven processes were studied that reflect the carrier-lattice interactions at the nanometer scale. Our theoretical effort focussed on elucidating the different behaviors in the bulk as well as multilayer structures. The modeling was based on a two-temperatures model [9] and a hyperbolic heat transfer theory [10] – the charge carriers and lattice were

treated as two subsystems with independent temperature descriptions. These predictions were compared with our experimental findings. In the fs-ps regime, the 'thermal' prediction based on the two-temperature model, which treated only one unified temperature for the lattice, was found to be insufficient. In fact, our diffraction experiments determined two types of temperature – one, defined locally as the 'vibrational' energy, can be estimated from the loss of Bragg peak intensity due to fluctuation in different lattice planes; and the other one, defined globally for the probed slab as the 'strained' energy, could be determined by the overall expansion or contraction of the lattices. Both of them were not in thermal equilibrium conditions in the short time. We are investigating different scenarios that could account for such behaviors.

Future Plans

It will be particularly instructive to lay out a 'phase-diagram' for size-selected melting and pre-melting phenomena of Au and Ag nanoparticles in the range between 5nm to 100 nm. In this regime, the metallic phase is largely preserved, and the size-dependent effects can be evaluated based on similar force field but considering different topography and surface chemistry. Combining real-time structural determination and spectroscopic investigation, the structure-function correlations are to be defined in such a phase diagram. New challenges will lie in further investigation of 1-5 nm ultrafine particles and cluster system. Molecular scale phenomena should emerge in this regime as the metallic attributes no longer dominate their functions. Metal-to-semiconductor transition, loss of nobility in chemical reactivity, and even catalytic reactions will take place depending on the chemical environments and the specific structural formations involved. Atomic scale imaging techniques (STEM, STM) and further development of sample preparations (such as cluster depositions on well characterized substrate surfaces) need to be deployed. Collaboration with theorists to conduct first principle quantum chemical calculations to address the finer details of the dynamics is deemed necessary. Furthermore, in order to accommodate the scarcity of sample in the ultrasmall scale, it will become imperative to develop a next generation diffraction/spectroscopy system with bunched high-density electron pulses to boost the sensitivity. Ultimately we hope to be able to reach combined spatiotemporal resolutions and sensitivity to resolve in real time the 'local' structural motif, chemistry, and the transient dynamics during nanoscale catalytic reactions.

In nanoacoustics studies, emphasis will aim at elucidating the confinement effects. Although the mechanism for carrier-phonon interaction and transport of heat in continuous media has been extensively studied by optical pump-probe techniques, it is still relatively unclear the effects of interfaces and the restrictions imposed by the nanoboundaries – particularly for the study of vibrational energy couplings between media. These 'nuances' are unavoidable in the nanometer scale, and will have important contributions towards understanding the conduction and the dissipation from molecular and nanoscale devices. The nature of vibronic couplings on the nanoscale is to be elucidated via simultaneous structure and spectroscopy determinations. The current two-temperature model will be expanded to include the nanoscaled confinement effects. Wave-like behaviors will be considered in the framework including energy oscillations

between the electronic and atomic subsystems – pertaining to the nanoconfinement. The long-range 'temperature' and local 'temperature' as defined from our experiments will be separately treated theoretically in describing the energetic profile. The conclusions of this study may provide the basis for engineering a novel transient high temperature interface for novel reactions, for thermal energy concentration using coherent scattering of phonons in nanostructured materials, and for fabricating efficient thermal dissipator by matching the thermal impedance on the nanometer scale.

References

(1) H. Hakkinen, S. Abbet, A. Sanchez, U. Heix & U. Landman, *Angew. Chemie* **2003**, 42, 1297-1300.
(2) G. Ertl, *Adv. Catal.* **2000,** 45, 1-69.
(3) R. Srinivasan, V.A. Lobastov, C.-Y. Ruan & A. H. Zewail, *Helv. Chim. Acta* **2003**, 86, 1761-1799.
(4) C.-Y. Ruan, V. Franco, V.A. Lobastov, S. Chen & A.H. Zewail, *Proc. Natl. Acad. Sci. U.S.A.* **2004**, 101, 1123-1128.
(5) C.-Y. Ruan, Y. Murooka, R.K. Raman, R. Murdick & M.A. Khasawneh, *Microsc Microanal (Supp 2)*, **2006**, 150-151.
(6) C.-Y. Ruan, V.A. Lobastov, V. Franco, S. Chen & A.H. Zewail, *Science* **2004**, 304, 80-84.
(7) A. Plech, S. Gresillon, G. von Plessen, K. Scheidt & G. Naylor, *Chem. Phys.* **2004**, 299, 183-191.
(8) F. Lindemann, Z. Phys. **1910**, 11, 609.
(9) S.I. Anisimov, B.L. Kapeliovich, T.L. Perelman, Sov. Phys. JETP **1974**, 39, 375-377.
(10) D.E. Glass, M.N. Ozisik, D.S. McRae & B. Vick, *Numerical Heat Transfer* **1985**, 8, 497-504.

DOE Sponsored Publications in 2004-2006

In preparation.

Automated nanocrystallography

John C. H. Spence and H. He*
Dept of Physics, ASU. Tempe, 85287-1504
*NCEM, Lawrence Berkeley Lab, Berkeley, Ca.

Program Scope

The host of new microcrystalline structures being designed and synthesised for new applications in nanoscience has created an urgent need for new methods to rapidly solve these structure at the atomic level. While powder X-ray methods may work well in some cases (if the number of atoms per unit cell is small, and large quantities are available), new methods are needed which can rapidly solve individual nanocrystals. The aim of this project is therefore to automate methods for finding the positions of atoms in individual nanocrystals, using the electron micro-diffraction mode of an electron microscope [1]. In addition, we are interested in other uses of the microdiffraction mode, such as strain mapping by CBED, and diffractive imaging. Solving crystal structures by electron diffraction has been re-vitalised lately by the development of the TEM precession mode [2], and by new iterative phasing algorithms such as the charge-flipping method. We have also been able to apply these algorithms to other fields, such as the solution of powder diffraction patterns, where we find they have advantages over conventional methods, and to the inversion to 3D images of soft X-ray diffraction patterns from porous foam materials.

This project is based on the recently installed Zeiss Libra 200 kV field emission TEM-STEM Omega instrument at NCEM (LBNL). The symmetrical deflection coils for precession came with the STEM. The Libra is fitted with an Omega imaging filter (and monochromator), which provides elastically filtered diffraction patterns from which most of the background due to inelastic scattering has been removed. A film cassette allows use of Image Plates for recording weak diffuse scattering, while a 2K x2K CCD camera provides conventional data collection of elastically filtered nanodiffraction patterns. Libra's Koehler mode design when working with a small illumination aperture provides an approximately 50nm diameter beam with parallel-beam illumination, which is very useful for diffraction from single nanoparticles. All TEM functions are accessible with the scripting language (Digital Micrograph). Alternatively one can also use Zeiss's own macro language within WinTEM for controlling all TEM hardware. A complete API function interface provides the best solution for controlling all TEM functions from any third party software using essentially any programming language. Because of the in-column Omega filter the instrument is superbly well suited to the quantitative convergent-beam method (QCBED). In summary , this

new instrument at NCEM is ideally suited to the collection and quantification of the highest quality diffraction data. While it is often suggested that electron diffraction data is not accurately quantifiable, the following applications demostrate the power of quantitative electron microdiffraction in its application to modern materials science problems. It provides the ideal tool for nanostructural materials characterisation, because the modern field emission electron microscope, in microdiffraction mode, produces the largest signal from the smallest volume of matter in all of modern science. (The field-emission source is brighter than a synchrotron, and the elastic scattering cross section very large). It is therefore ideal for the study of individual nanostructures.

Recent progress.

1. Our first project [3] involved setting up the QCBED mode on the Libra and testing it by application of strain mapping around the gate of a single 65nm node CMOS transistor from an Intel computer chip. The speed of modern computers is controlled by the intentional introduction of strain around the gate, which strongly affects the mobility of charge-carriers. However, as the semiconductor road map points out, "no methods currently exist for the quantification of this strain-field in real devices". We believe we have developed such a method based on QCBED. Our method is based on the realisation that the important strains in such a device run normal to the thinning direction of a TEM sample, and hence are unaffected by thinning. By reading the central disk of [340] CBED patterns taken from 10nm areas near the gate oxide of a thinned FET (beam lying in plane of gate-oxide, normal to [001] and between SiGe source and drain), we were able to fit the positions of the higher-order Laue zone lines to calculations. From this we can deduce map the lattice parameter changes due to uniaxial strain, chiefly along [1-10], parrallel to the gate oxide, and so produce a strain map.

2. In a second application of QCBED, we have demonstrated that the chemical bonds in noncentrosymmetric crystals can be "imaged" using QCBED data combined with X-ray data [4]. In this work, intensity measurements of CBED patterns from AlN crystals were compared with multiple scattering calculations, allowing the low-order bonding structure factors to be refined. Because all multiple scattering effects are included and a probe size of about 10 nm is used, extinction errors are elliminated, and structure-factor phases can be measured accurately (unlike the X-ray method). We make use of the fact that electron scattering factors rise rapidly at low angles for ions (unlike X-ray scattering factors). Our results are compared with ab-initio electronic structure calculations. They show the charge deficit around Al ions, the surplus around N, and the covalent bonding distribution along the interatom vector. This work resulted in the development of a new refinement metric for the popular program "VALRAY", which has not been

modified to include measurements of phase for non-centrosymmetric crystals, whose bonding densities could not previously be accurately measured, since they depend on phases which cannot be measured accurately by X-ray diffraction.

3. Our third project over the last three years has been the development of new methods for solving the structure of nanocrystals. We have developed experimental tests for the absence of multiple scattering which do not require a knowledge of the atomic structure [1]. We have developed the "Blank disk" method of CBED, in which single-scattering CBED patterns, which blank disks (but obtained from very small areas) are used to measure structure factors [5], and we have developed a method in which only the central pixel is selected from each CBED disk, to provide a "small-area" selected area pattern. These methods have been applied to long-chain paraffins, tetracontane and paralene data collected at liquid helium temperature. The method has the great advantage that the central disk may be included within the dynamic range of the detector, so that absolute intensities may be recorded, while the regions analysed are so small as to be perfectly crystalline and not bent. We have also started the process of automating diffraction data collection in three dimensions on the Libra [6]. We have developed a STEM mode for selecting the nanocrystal of interest,in which the probe can be quickly defocussed for diffraction-data collection. By returning to dark-field image mode, the sample may be returned to the optic axis after tilting for each diffraction pattern. After tests using MgO smoke cubes, trials are now under way with nanocrystals of Bi2S3 in collaboration with M. Scheele and D. Talapin at the Molecular Foudary at LBL who have synthesised these nanostructures for possible use as molecular labels.

Future plans.

1. We are most excited about the possibility of collecting a full three-dimensional microdiffraction data set from a single particle of Bi2S3 of sufficiently high quality to allow the phase problem to be solved. (We will do this using the Ozlanyi-Suto charge flipping method, which we have developed also for solving powder X-ray patterns [7]). Nanoparticles are ideal for structure solution by TEM, since their small thickness minimized multiple scattering artifacts. We hope within a year to be able to collect a full data set, phase it, and present to the TEM user a charge-density map showing all the atom positions in 3D within the nanocrystal. Some human intervention will probably be needed to assist with bringing the particle back onto the axis during tilting (assited by cross-correlation). We also wish to experiment with a tilt-rotate holder, since this allows a single reciprocal lattice vector to be aligned along the major tilt axis, so that data collection is then reduced to a one-dimensional search about this major axis.

2. Work continues on diffractive imaging, in which diffuse elastic scattering from small particles is phased and inverted into a sub-Angstrom resolution image

of the particle. Our current work is based on using a periodic substrate of graphite as a thin substrate for small particles. We have also used the diffractive imaging method recently with soft X-rays to image the internal labyrinthine structure of an aerogel foam, which is not possible by other methods [8]. This is relevant to oil and water diffusion in rocks, and modellling of the strength of foam materials.

References

[1] See J. Spence in "Electron Crystallography" T. Weirich Ed. Nato Science Series Vol 211 (2006), Erice Electron Crystallography School, for a review. Also "Electron Microdiffraction" by J. Spence and J. Zuo (1992) Plenum.

[2] Vincent R. and Midgely, P. *Ultramic* **53** (1994) 271.

[3] "Direct measurement of nanoscale strain in a 65nm node locally strained silicon device by energy-filtered convergent beam diffraction". P. Zhang, J. Spence. et al. Applied Phys Letts. 2006. In press.

[4] Phase measurement for accurate mapping of chemical bonds. M. Spackman, B.Jiang, T. Groy, H. He, A.Whitten, J..Spence. Phys Rev Letts. 95, 085502**.** '05

[5] Low-dose, low temperature CBED analysis of Aromatic Hydrocarbons. J. Wu and J.C.H.Spence. Micros. and Microan. 9, p.428. (2003).

[6] H. He, J. Spence. Proc 16th Int Congress on Microscopy. Sapporo.Japan.'06.

[7] Ab initio phasing of X-ray powder diffraction patterns by charge flipping". J.Wu, J.Spence, M. O'Keeffe, K. Leinenweber. Nature Materials.5, 647 '06.

[8] Three-dimensional ceramic nanofoam lattice structure determination using coherent X-ray diffractive imaging: deformation mechansisms. A. Barty, J.Spence, et al . Nature Materials. Sept 06 Submitted.

Publications supported by DOE FG03-02ER45596 in last 2 years.

354 "Analysis of nanoscale stress in strained silicon materials and microelectronic devices by energy-filtered CBED. P. Zhang, A. Istratov, H. He, C. Nelson, J. Ager, E. Stach, J. Spence, C. Kiselowski, E. Weber. J. Electrochemical Soc. (2006). In press

342 A Simple constraint for phase retrieval. H. He. J.Opt. Soc. Am, 23, 550. ('06)

338 Evidence against a charge-density wave on Bi (111) . T.K. Kim, H. He, J. Spence, et al Phys Rev. B 72, 085440. (2005).

333 Imaging dislocation cores - the way forward. J.C.H.Spence et al Phil. Mag. 86, 4781 (2006). Special issue for 50 years since first observation of dislocations by TEM.

323 EELS near-edge structure in the Laves-phase compounds TiCr2 and TiCo2. J.Sun, B.Jaing and D.J.Smith. Phys Rev B69, p. 214107 (2004)

319 Phase measurement for accurate mapping of chemical bonds. M. Spackman, B.Jiang, T. Groy, H. He, A.E.Whitten, J.Spence. Phys Rev Letts. 95, 085502**.** (2005)

316. Ab initio calculation of the phase stability, mechanical properties and electronic structure of ZrCr2 Laves phases. J,Sun, B.Jiang Phil Mag 84, 3133 (2004)

309 Extinction-free electron diffraction refinement of bonding in SrTiO3. J. Friis, B.Jiang, J. Spence, K. Marthinsen, R. Holmstad. Acta Cryst A59. p.402 (2004)

295 "Valence charge density distribution and chemical bonding in MgB2". B. Jiang, N. Jiang and J.C.H.Spence. Phys Rev B (2006) submitted**.**

Single Atom and Molecule Manipulation and Its Application to Nanoscience and Technology

Saw-Wai Hla, hla@ohio.edu, www.phy.ohiou.edu/~hla
Ohio University, Physics & Astronomy Department, OH-45701.

Program Scope

The needs to develop even smaller devices with higher functionalities continue to dominate research in large sector of nanoscience. If the current miniaturization trends were to continue, the scale of devices will soon reach to that of single atoms and molecules. It is therefore vital to investigate properties of single atoms/molecules to develop novel device architectures with useful functionalities. Investigating and developing of prototype devices at single atom/molecule level require specialized instrumentation and techniques. The scanning tunneling microscope (STM) manipulation in combination with tunneling spectroscopy measurements offer a *unique* opportunity to probe properties of single atoms/molecules on surfaces at an atomic limit. Using STM tip as an analytical or engineering tool, artificial atomic-scale structures can be constructed, novel quantum phenomena can be probed, and physical, electronic and mechanical properties of single atoms/molecules can be studied at the atomic level[1-5]. STM is not only an instrument used to '*see*' individual atoms by means of imaging, but also a tool used to '*touch*' and '*take*' atoms and molecules or to '*hear*' their vibrating sound by manipulations[5]. In this respect, STM can be considered as the '*eyes*', '*hands*' and '*ears*' of the scientists connecting our macroscopic world to the exciting atomic and nanoscopic world. In our research projects, we combine single atom/molecule manipulation schemes with a variety of tunneling spectroscopy measurements to investigate the physical properties specific to the type of atoms on molecules on metallic surfaces. The innovative experiments in this project are tailored to address several critical issues covering both fundamental understanding, and development of novel atoms/molecules based nano-devices. Our focus research areas include molecular spintronics, nanobiotechnology, and the atomistic interactions on surfaces.

Recent Progress

Molecular Switches

We have recently demonstrated single molecule switches in two different areas: Nanobiotechnology and molecular spintronics. The former concerns with the making of a four-step molecular switch using spinach molecules and the latter is a manipulation of the Kondo effect.

For the first type of switch, we use Chlorophyll-a produced from spinach. Chlorophyll-a is responsible for the green color in plant leaves, and it is a central molecule in photosynthesis: An important biological process that converts sun light into chemical energy. In this work, individual chlorophyll-a molecules adsorbed on a Au(111) surface are manipulated by injecting tunneling electrons from a STM-tip at 4.6 K. The molecules can be switched into four different conformations in a controlled step-by-step manner with atomic-scale precision (Fig. 1). The energy barrier for the switching process was determined by means of I-V tunneling spectroscopy. The rotation of $\sigma_{C\text{-}C}$ bond within the phytyl chain of the molecule at two different locations causes such conformation changes. By means of statistical analyses we show that the energy transfer of a single tunneling electron into the molecule initiates all the switching events. This achievement not only opens a novel route to study conformations of larger biological molecules but also demonstrates possible usage of a plant molecule in the development of environment-friendly nanoscale devices or even possibly in the green energy generation. **(*Read media news at **).**

The second type of molecular switch is related to the Kondo effect. The interaction between a magnetic impurity and electrons from a nonmagnetic metal surface can give rise to a resonance near the Fermi level, known as the Kondo effect[6]. We investigate the Kondo effect generated from the spin-electron interactions between the cobalt atom of a CoTBrPP molecule, and free electrons from a Cu(111) substrate at 4.6 K. TBrPP-Co anchors on the Cu(111) surface in two molecular conformations: saddle and planar

(Fig. 2). In the saddle, the central part of molecule is bent thereby lifting the cobalt atom away from the surface. In planar, the porphyrin unit is lying flat on the surface providing a stronger molecule-substrate interaction. The two conformations of isolated molecules are switched by applying +2.2 V voltage pulses from a STM-tip. Tunneling spectroscopy data reveal that switching from the saddle to the planar enhances spin-electron coupling, and increases the Kondo temperature from 130 to 170 K. This result demonstrates that Kondo temperature can be manipulated just by changing molecular conformation without altering chemical composition of the molecule. The Kondo effect in molecules currently is a hot pursuit research area because of its potential applications in molecular spintronics, and this single molecule switch may be useful to develop molecular memory devices or molecular magnetic switches. **(*Read media news at **).**

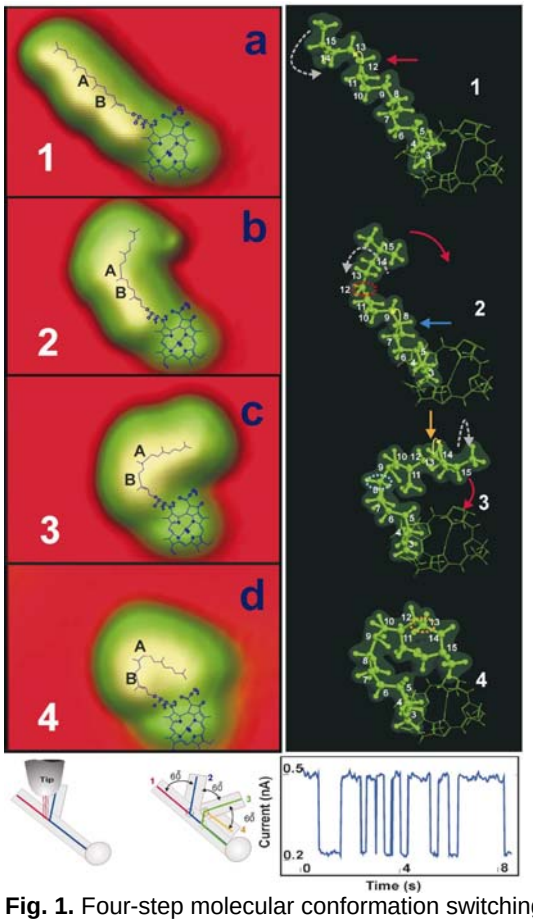

Fig. 1. Four-step molecular conformation switching. STM images (left) and calculated structures (right).

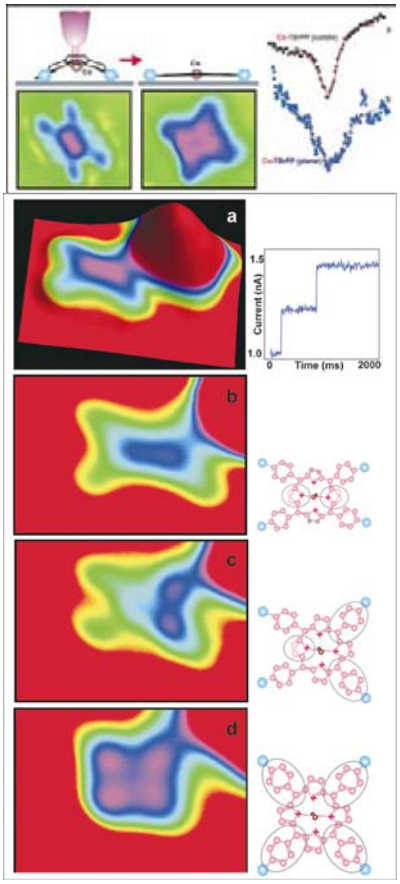

Fig. 2. Single molecule Kondo switch. Switching from saddle (top-left) to planar conformation (top-center) increases associated Kondo temperature (top-right). A sequence of STM images showing two-step switching process to change from the saddle (b) to planar (d).

Atom-Molecule Hybrid Device

We have also demonstrated a novel manipulation scheme for a controlled transport of weakly adsorbed sexiphenyls on a Ag(111) surface at 6 K. Sexiphenyl is composed of six benzene rings (π-rings) connected to form as a chain. Using STM manipulation and density functional theory calculation, we show that the π-rings of sexiphenyl are alternately twisted on the Ag(111) surface. Furthermore, from the lateral manipulation geometry, the torsional angle of a single sexiphenyl has been determined for the first time. During STM manipulation, sexiphenyl occasionally travels much further across the surface than the STM-tip travel distance but its movement path is not straight. We find that the molecule is sensitive to the local electronic structural environment and non-uniform electronic structures can deflect the molecule from the straight trajectory. In order to control the trajectory and the molecule movement, an innovative

experimental scheme is developed (Fig. 3): A uniform background electronic structure environment is first created by building a linear electron resonator using individual silver atoms extracted from the native Ag(111) surface with the STM-tip. Inside this electron resonator, a sexiphenyl molecule can be manipulated to propagate in an atomically straight path and hence, it operates as a nano device to transport the molecules. This work represents the first single molecule transport inside an artificial atomic scale structure, and it opens up innovative ways to tailor experiments in artificial local environments within a few tens of nanometer range.

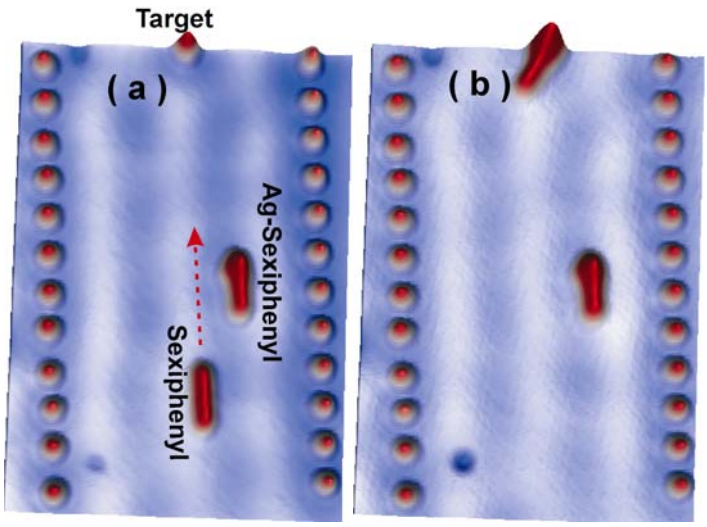

Fig. 3. A sexiphenyl molecule is shot towards a target using STM-tip (a). After traveling across the surface, the molecule hits the target atom, thereby proving its atomically straight trajectory (b).

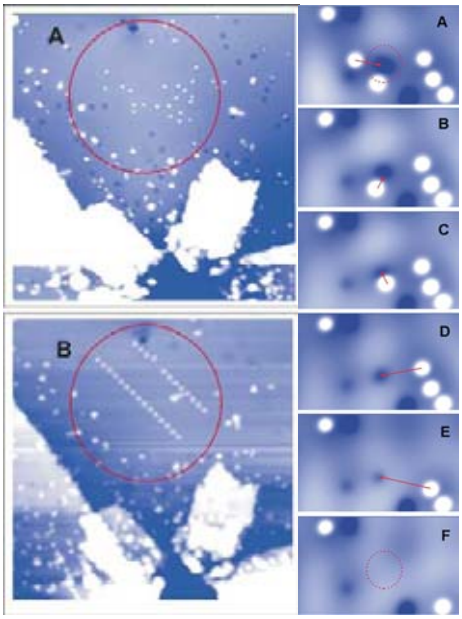

Fig. 4. Single atoms extracted by means of a controlled tip-crash are used for atomistic construction (left). A sequence of STM images showing atom-by-atom filling of a vacancy on Ag(111) surface. After the filling, the area has the same contrast as the surrounding area.

Atom Extraction and Atom Manipulation

The tip crashing into the substrate in STM applications is an unwanted event that can alter the tip-shape and destroy the surface area under investigation. We have systematically investigated the tip-crash mechanisms and developed an in-situ tip preparation technique to form an atomically sharp and chemically identified tip-apex (Fig. 4). We have also shown extraction of single atoms using this technique. The chemical identity of the extracted atoms is verified by filling them into a surface vacancy on a one atom-at-a-time basis (Fig. 4). After filling the vacancy, the area is not distinguishable from the surrounding area confirming that the extracted atoms are indeed the native atoms. This scheme sets an example for a novel application of STM manipulation. Fig. 5 displays various atomistic structures constructed by using single atoms extracted from the native surface. **(*Read media news at **).**

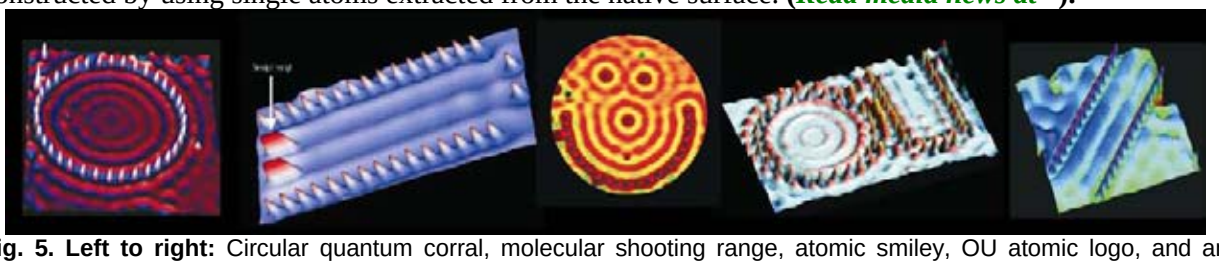

Fig. 5. Left to right: Circular quantum corral, molecular shooting range, atomic smiley, OU atomic logo, and an atomic fence. The atomic smiley and OU logo are used for the nanoscience outreach.

Future Plan

Following the achievement of four-step molecular switch, we will continue to investigate the mechanical and electronic properties of single chlorophyll-a molecules as well as other plant molecules on metallic surfaces. In case of molecular Kondo effect, we will extend our investigation to two-dimensional molecular clusters to explore influence of spin-lattice in the Kondo effect. We are also planning to perform single molecule experiments to get a deeper understanding on the coupling of molecular spin and free electrons from the substrate. For the atom manipulation part, we are exploring manipulation on three-dimensional surfaces and the effect of tip-cluster interactions.

References

[1] D.M. Eigler, E.K. Schweizer, ***Nature 344***, 524-527 (1990).
[2] H.J. Lee, W. Ho, ***Science 286***, 1719-1722, (1999).
[3] H.C. Manoharan, C.P. Lutz, D.M. Eigler, ***Nature 403***, 512-515 (2000).
[4] S.-W. Hla, L. Bartels, G. Meyer, K.-H. Rieder, ***Phys. Rev. Lett. 85***, 2777-2780 (2000)
[5] S.-W. Hla, ***J. Vac. Sci. Tech. B 23***, 1351-1360 (2005).
[6] Kondo, J. ***Prog. Theor. Phys.*** **32**, 37-49 (1964).

DoE Sponsored Publications in 2004 – 2006 (only published papers are listed.)

1*****. V. Iancu, & S.-W. Hla, "Realizing of a Four-Step Molecular Switch in Scanning Tunneling Microscope Manipulation of Single Chlorophyll-a Molecules", ***PNAS*** **103**, 13718-13721 (2006).

2. K.-F. Braun, V. Iancu, N. Pertaya, K.-H. Rieder, & S.-W. Hla, "Decompositional, Incommensurate Growth of Ferrocene Molecules on a Au(111) Substrate", ***Phys. Rev. Lett.*** **96**, 246102 (2006).

3*. G. Newkome, P. Wang, C.N. Moorefield, T.J. Cho, P. Mohapatra, S. Li, S.-H Hwang, O. Lukoyanova, L. Echegoyen, J.A. Palagallo, V. Iancu, & S.-W. Hla, "Nanoassembly of a Fractal Polymer: A Molecular "Sierpinski Hexagonal Gasket ' ***Science*** **312**, 1782-1785 (2006).

4*. V. Iancu, A. Deshpande, & S.-W. Hla, "Manipulating Kondo Temperature via Single Molecule Switching", ***Nano Lett.*** **6**, 820-823 (2006).

5. K.-F. Braun, & S.-W. Hla, "Probing the Conformation of Physisorbed Molecules at the Atomic-Scale using STM Manipulation***", Nano Lett.*** **5**, 73-76 (2005).

6. S.-W. Hla, "STM Single Atom/Molecule Manipulation and Its Application to Nanoscience and Technology ", ***J. Vac. Sci. Technol. B*** **23**, 1351-1360 (2005). [Invited review article].

7*****. S.-W. Hla, K.-F. Braun, V. Iancu, A. Deshpande, "Single Atom Extraction by Scanning Tunneling Microscope Tip-Crash and Nanoscale Surface Engineering", ***Nano Lett.*** **4**, 1997-2001 (2004).

8. S.-W. Hla, A. Prodan, H.J.P. van Midden, "Atomistic Stress Fluctuation at Surfaces and Edges of Epitaxially Grown Silver Nanorods", ***Nano Lett.*** **4**, 1221-1224 (2004).

9. S.-W. Hla, K.-F. Braun, B. Wassermann, K.-H. Rieder, "Controlled Low-Temperature Molecular Manipulation of Sexiphenyl Molecules on Ag(111) using Scanning Tunneling Microscopy", ***Phys. Rev. Lett.*** **93**, 208302 (2004).

****Media news: www.phy.ohiou.edu/~hla/HotResearch.html***

INTERFACE INDUCED PHENOMENA AT GRAIN BOUNDARIES AND INTERFACES

Dawn A. Bonnell
The University of Pennsylvania

Program Scope

The dramatic increase in the variety of materials from which nanotubes, wires and dots can be made suggests opportunities for complex functional devices. Exploiting these materials in nanoelectronics, molecular electronics, integrated sensors, etc requires that interface properties be understood and controlled. In an effort to relate the atomic structure at model interfaces to local properties two classes of interfaces are being examined: atomically ideal oxide grain boundaries and nanosized metal/semiconductor interfaces. New techniques for measuring local properties based on scanning probes are developed. These are combined with transport measurements, high resolution transmission electron microscopy and first principles calculations to relate electron-lattice interactions to properties.

Recent Progress

$SrTiO_3$, often regarded as a model system for perovskites, possesses unique properties that have attracted extensive research over the past decades. At low temperatures, it undergoes an antiferrodistortive phase transition at 105K, a soft phonon anomaly and possible phase transition at around 37K, as well as superconductivity below 1K with certain levels of donor doping. Few studies of the effects of boundaries in $SrTiO_3$ have been done in this temperature range despite the broad interest in interface mediated transport in this class of materials

We have used temperature dependent Scanning Impedance Microscopy, STM, Scanning Surface Potential Microscopy, along with transport measurements to characterize interface properties. These have been related to electron occupation at the grain boundary unit cell structure by comparison with high resolution Z-contrast TEM and first principles calculations based on the VASP code. We have discovered an anomaly in GB resistance and capacitance, which suggests ferroelectric-type ordering induced by the oxide interface.

Atomically abrupt interfaces with 2 ideal atomic structures were compared. Bicrystal samples containing [001] symmetric tilt GB's of either 24^o or 36.8^o ($\Sigma 5$) misorientation joined by diffusion bonding were used. These boundaries consist of well ordered structural units consisting of Sr and Ti columns along the dislocation core and no second phase or impurity segregation was detected.

Figure 1 shows the intersection of the 24o boundary with the (100) surface. The surface contains unit cell height steps which are often reconstructed. The interface potential at the surface can be imaged directly. Note that issues regarding screening need to be considered to quantify such measurements, which essentially requires that they be done in UHV. See ref [1] and [2].

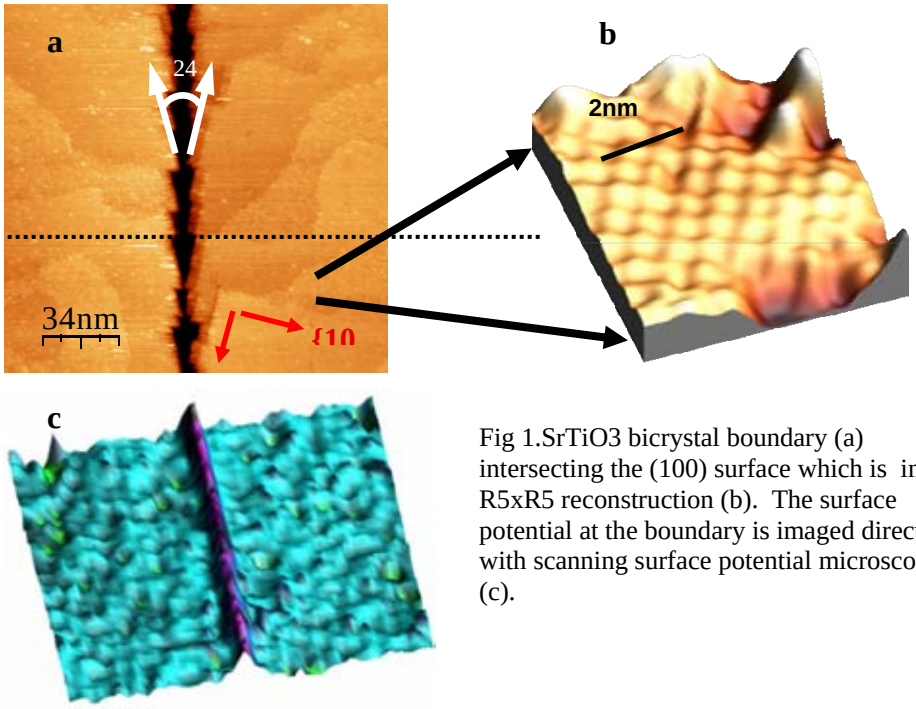

Fig 1.SrTiO3 bicrystal boundary (a) intersecting the (100) surface which is in a R5xR5 reconstruction (b). The surface potential at the boundary is imaged directly with scanning surface potential microscopy (c).

The 100 fold decrease in GB resistance is a clear indication that the interface charge is compensated by alignment of dipoles. In fact, Fig. 2(right) implies the classic positive temperature coefficient of resistance response. These observations can be explained as follows. There is a cubic to tetragonal phase transition that occurs at 105K for pure crystals but is a function of composition. Above the structural phase transition the temperature dependence is due to the temperature dependence of the dielectric constant. At the transition either the local field or the local strain alters the energy landscape such that dipole alignment occurs. Standard transport models were used to extract interface charge, which scaled with the size of the interface unit cell, i.e. ~1 electron trapped at each structural unit.

Fig 2. Temperature and bias dependent transport show a resistance anomaly at low temperatures. The signature for this behavior was also observed in temperature dependent SIM, STM, and SSPM (KFM) which all agreed quantitatively.

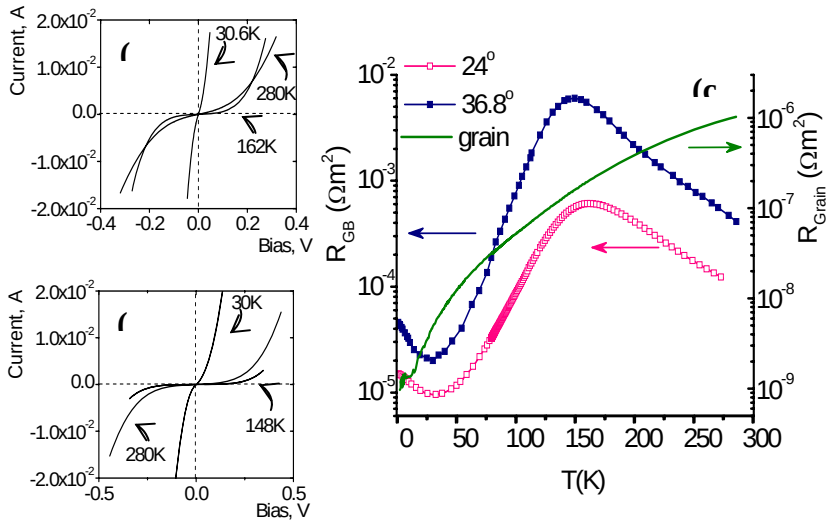

The results of the calculations of fully relaxed structures are superimposed on the experimentally determined structure in Fig. 3. The generalized structure of $SrTiO_3$ [001] tilt boundaries consists of pentagonal defect units containing two cation columns. The pentagons are formed on both the SrO and TiO_2 sublattices. The 36.8 ^{o} GB (Fig. 3) is seen to contain only these defect units. The 24^{o} GB contains an additional heavily distorted unit cell-like structural unit between the pentagons (not shown) to accommodate the different tilt angle. The calculations show that fully occupied cation columns in the units produce low energy structures. The GB energy can be further reduced by removing an oxygen column from the pentagonal unit containing two Ti-O columns. This structure also yields the best match to the experimentally observed boundary and agrees well with the interface charge determined from transport measurements: one electron per boundary repeat unit and suggests that the charge originates from the oxygen deficient pentagonal unit containing two Ti-O columns

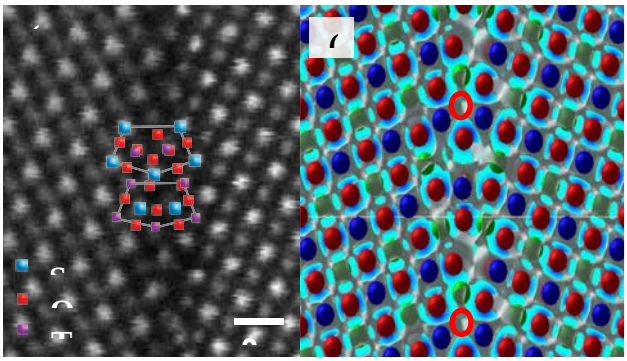

Fig. 3. High resolution z-contrast image (left) with calculated structure. The associated charge density map (right) is shown.

We have discovered an anomaly in GB resistance and capacitance, which suggests ferroelectric-type ordering induced by the oxide interface. While ferroelectricity has been observed in $SrTiO_3$ under extreme conditions, (large fields [3], large stresses [4], or constrained in a thin film [5]) the GB effect is surprising

Future Plans

These results illustrate how local measurements of properties yield quantitative information about the behavior of interfaces. In addition, while not detailed here, the development of Scanning Impedance Microscopy and Nano Impedance Spectroscopy add frequency dependence to localized measurements which yield new characterization of interface properties.

Future work is focusing on applying this strategy to metal nanoparticle/semiconductor interfaces in order to elucidate the origin of size dependent interface properties measured earlier.[6] [7] Mono dispersed metal particles of various sizes are deposited on atomically smooth surfaces and properties of the interface extracted from tunneling spectroscopy measurements. With SIM we will add the frequency dependence to probe interface trap states and interface potential.

DoE Supported Publications

Low-Temperature Resistance Anomaly at SrTiO/sub 3/ Grain Boundaries: Evidence for an Interface-Induced Phase Transition R. Shao, M.F. Chisholm, G. Duscher, D.A. Bonnell *Physical Review Letters*. **95** (2005) 197601/1-4

Local Phenomena in Oxides by Advanced SPM S.V. Kalinin, R. Shao, D.A. Bonnell *Journal of the American Ceramic Society*. **88** (2005) 1077-1098

Probing Electrical Transport Across Oxide Interfaces by Noncontact Atomic Force Microscopy R. Shao and D.A. Bonnell *Appl. Phys. Lett.* **85** (2004) 4968-70

Scanning Probes of Nonlinear Properties in Complex Materials R. Shao and D.A. Bonnell *Japanese J. of Appl. Phys.* **43** (2004) 4471-4476

Local Electronic Transport at Grain Boundaries in Nb-doped $SrTiO_3$ S. Kalinin. D. Bonnell *Phys. Rev. B* **70** (2004) 235304

Low Temperature Study of Nonlinear Transport Across Oxide Grain Boundaries R. Shao, J. Vavro, D. Bonnell *Appl. Phys. Lett*. **85** (2004) 561-3

References

[1] S. Kalinin, D.A. Bonnell *Nanoletters* **4** (2004)555

[2] R. Shao, J. Vavro, D. Bonnell *Appl. Phys. Lett*. **85** (2004) 561-3

[3] J. Hemberger, P. Lunkenheimer, R. Viana, R. Böhmer, and A. Loidl, Phys Rev. **B 52**, 13159 (1995).

[4] H. Uwe, and T. Sakudo, Phys. Rev. B **13**, 271 (1976).

[5] O. Tikhomirov, H. Jiang, and J. Levy, Phys. Rev. Lett. **89**, 147601(2002).

[6] D.Carroll, M. Wagner, M. Rühle, D.Bonnell *Phys. Rev. B* **55** (1997) 9792-99.

[7] D. A. Bonnell, Y. Liang, M. Wagner, D. Carroll, M. Rühle, *Acta Met* **46** (1998) 2263-2270.

Atomistic Mechanisms in Interface Science-Direct Imaging and Theoretical Modeling

Stephen J. Pennycook, Matthew Chisholm, Maria Varela
Postdocs: Klaus van Benthem, Mark P. Oxley, Jing Tao
pennycooksj@ornl.gov, chisholmmf@ornl.gov, mvarela@ornl.gov
Materials Science and Technology Division, Oak Ridge National Laboratory, Oak Ridge, TN 37831

Program Scope

The properties of a vast range of materials and devices are determined by interfaces, whose structures are typically completely different from those of the bulk, making them natural sites for the segregation of impurities or dopants. The key goal of this program is to identify the atomistic mechanism at interfaces that control the macroscopic properties. Success in this field would facilitate the enormous potential of interfacial engineering for bringing new materials properties. In the last few years, our ability to determine interface atomic and electronic structure directly from experiment has advanced faster than at any time in history through the successful correction of electron microscope aberrations. We use the aberration-corrected scanning transmission electron microscope (STEM) to probe interface structure, atomic positions, species and electronic structure. Through density functional theory we relate observed structures to properties, and make predictions for improvements. We aim to solve key interface science issues in structural ceramics, complex alloys and a range of complex oxide materials and device structures.

Recent Progress

Structural Ceramics: Si_3N_4. It is well understood that grain growth is controlled by the type of cations used as additives for the liquid-phase sintering process. Figure 1 shows a direct image of the rare earth atoms which are located at specific sites on the prismatic plane of the β-Si_3N_4 lattice. In conjunction with first-principles calculations, the toughening mechanism can be understood [Shibata *et al.*, 2004].

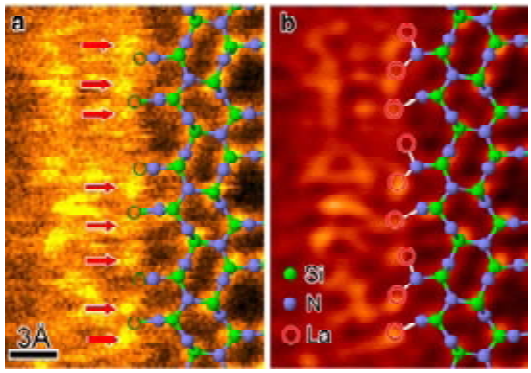

Figure 1. Z-contrast image of the interface with a superimposed projection view of the β-Si_3N_4 lattice. Red arrows point to La atoms, seen slightly displaced from the Si sites (green circles) (b) Pixon reconstructed image with calculated La positions shown as red circles.

Structural Alloys: Bi in Cu. Another longstanding issue solved by the application of Z-contrast STEM and first-principles theory is the embrittlement of Cu by Bi, a classic example of the phenomenon [Duscher *et al.*, 2004]. The grain boundary configuration is little affected by the presence of Bi, which simply substitutes for Cu on a specific atomic site in the boundary. The calculated charge density difference revealed that Bi induces a slight reduction in the directionality of bonding between Cu atoms. In addition, the

calculations show an enhanced electron density at the Cu sites that surround the Bi impurity. Therefore electrons further fill the usually half-filled s-bands of Cu, reducing the bond strength between the Cu atoms that surround the Bi impurity, explaining the embrittlement.

Complex Alloys: Quasicrystals. In contrast to diffraction studies that give accurate average structures, Z-contrast STEM has shown the local atomic structure, revealing details of the cluster packing and atomic decoration that explain the perfect quasicrystalline order in the Al-Co-Ni decagonal phase. The 2 nm clusters show reduced symmetry at their center, which are also sites of an enhanced thermal vibration anomaly. Total energy calculations revealed that the phase is thermodynamically stable [Abe *et al.*, 2004].

Complex Alloys: Cr_2Hf. Z-contrast imaging revealed that the synchroshear dislocation core in the C14 variant of Cr_2Hf contained 'extra' Cr columns [Chisholm *et al.*, 2005]. During dislocation motion the Cr atoms must move into and out of these columns, which hinders their motion and contributes to the brittleness of this material at low temperatures.

Complex Oxides: Grain Boundaries in High Temperature Superconductors. In $YBa_2Cu_3O_{7-\delta}$ (YBCO), a single grain boundary can result in orders of magnitude reduced critical current. Theoretical calculations reveal the oxygen vacancy formation energy to be reduced in the high stress region near the dislocation core, causing non-stoichiometry and hole depletion. Doping with Ca has been shown to alleviate the problem, and the assumed mechanism was that Ca substitutes on the Y site, as it is known to do in bulk material, and introduces compensating holes. Theoretical calculations reveal the effect to be quite different. In the enormous strain fields surrounding grain boundary dislocation cores, Ca takes whichever cation site lowers the local strain, Cu in the tensile side of the core, Bi in the compressed side of the core. The reduced strains restore the O vacancy formation energy to near bulk values, and the hole concentration is restored, thanks to this cooperative doping effect [Klie *et al.*, 2005].

Complex Oxides: Manganites. The first direct images of electronic stripes in a complex oxide were obtained in a $Bi_xCa_{1-x}MnO_3$ (BCMO) manganite along the pseudocubic projection with x = 0.37 which has an ordering temperature above room temperature. The ratio of the intensity of the L_3 peak to the L_2 peak, the $L_{2,3}$ ratio, correlates with the 3d-band occupation, i.e., the formal oxidation state, and showed a stripe geometry perfectly consistent with the macroscopically averaged periodicity observed in electron diffraction. Density functional calculations are able to reproduce the observed diffraction pattern, showing that the electronic striping is structural in origin [Varela et al., 2005].

Future Plans

Structural Ceramics: The studies described above will be extended to other dopants and the local electronic structure investigated by EELS. Density functional calculations should lead to a fundamental understanding of how the atomic-level structure of the interface controls grain growth and mechanical properties.

Complex Alloys: Quasicrystals. Not only the atomic structure of quasicrystals has been a longstanding issue, but also the origin of their peculiar electronic structure, which from bulk studies appears to show a pseudogap at the Fermi level. We plan spatially-resolved

investigations using the transition metal $L_{2,3}$ ratios to see if the local electronic valence of the elements in the center and edge of the 2 nm clusters is actually different.

Complex Oxides: Grain Boundaries. Due to the 100% spin polarization in their conduction band, manganites are very appealing materials to be integrated in devices such as sensors or magnetoresistive reading heads for hard drives. However, the switching fields needed are too high, of the order of Teslas in bulk materials. Grain boundaries represent the key to successful applications of these materials because they show low field magnetoresistance. However, the phenomena underlying this behavior are far from understood, and we will study ferromagnetic epitaxial $La_{0.67}Ca_{0.33}MnO_3$ films grown on $SrTiO_3$ bicrystals with misorientation angles of 12º, 24º and 36º, performing the same detailed compositional and electronic structure analysis as described for the YBCO grain boundaries. We will also examine bicrystals of ZrO_2, both pristine and doped, available from Prof. Y. Ikuhara's Group at the University of Tokyo. These materials are of interest for their superplastic deformation properties and are also fast ion conductors of major interest for fuel cell and sensor applications. The special sites at the boundary are clearly responsible for both the dopant segregation and the fast ion conduction. We will again combine experiment with first-principles theory to establish the nature of these sites, the role of nonstoichiometry, the diffusion path, and the effect of impurity segregation on creep behavior.

DOE-sponsored journal publications 2004-2006

Abe, E., Y. F. Yan and S. J. Pennycook, "Quasicrystals as cluster aggregates," *Nature Mat.*, **3**, 759-767 (2004).

Baik, H. S., M. Kim, G. S. Park, S. A. Song, M. Varela, A. Franceschetti, S. T. Pantelides and S. J. Pennycook, "Interface structure and non-stoichiometry in HfO_2 dielectrics," *Appl. Phys. Lett.*, **85**, 672-674 (2004).

Becher, P. F., G. S. Painter, N. Shibata, R. L. Satet, M. J. Hoffmann and S. J. Pennycook, "Influence of additives on anisotropic grain growth in silicon nitride ceramics," *Mat. Sci. and Eng. A*, **422**, 85-91 (2006).

Cantoni, C., D. K. Christen, E. D. Specht, M. Varela, J. R. Thompson, A. Goyal, C. Thieme, Y. Xu and S. J. Pennycook, "Characterization of suitable buffer layers on Cu and Cu-alloy metal substrates for the development of coated conductors," *Supercond. Sci. Technol.*, **17**, S341-S344 (2004).

Chambers, S. A., J. R. Williams, M. A. Henderson, A. G. Joly, M. Varela and S. J. Pennycook, "Structure, band offsets and photochemistry at epitaxial alpha-Cr_2O_3/alpha-Fe_2O_3 heterojunctions," *Surf. Sci.*, **587**, L197-L207 (2005).

Cui, H. T., X. J. Yang, M. L. Simpson, D. H. Lowndes and M. Varela, "Initial growth of vertically aligned carbon nanofibers," *Appl. Phys. Lett.*, **84**, 4077-4079 (2004).

Duscher, G., M. F. Chisholm, U. Alber and M. Ruhle, "Bismuth-induced embrittlement of copper grain boundaries," *Nature Materials*, **3**, 621-626 (2004).

Frey, N.A., S. Srinath, H. Srikanth, M. Varela, S. J. Pennycook, G. X. Miao and A. Gupta, "Magnetic anisotropy in epitaxial CrO_2 and CrO_2/Cr_2O_3 bilayer thin films," *Physical Review B.* **74**, 024420 (2006).

Gapud, A. A., D. Kumar, S. K. Viswanathan, C. Cantoni, M. Varela, J. Abiade, S. J. Pennycook and D. K. Christen, "Enhancement of flux pinning in $YBa_2Cu_3O_{7-\delta}$ thin films embedded with epitaxially grown Y_2O_3 nanostructures using a multi-layering process," *Supercond. Sci. Technol.*, **18**, 1502-1505 (2005).

Goyal, A., S. Kang, K. J. Leonard, P. M. Martin, A. A. Gapud, M. Varela, M. Paranthaman, A. O. Ijaduola, E. D. Specht, J. R. Thompson, D. K. Christen, S. J. Pennycook and F. A. List, "Irradiation-free, columnar defects comprised of self-assembled nanodots and nanorods resulting in strongly enhanced flux-pinning in $YBa_2Cu_3O_{7-\delta}$ films," *Supercond. Sci. Technol.*, **18**, 1533-1538 (2005).

Griffin, K. A., M. Varela, S. J. Pennycook, A. B. Pakhomov and K. M. Krishnan, "Atomic-scale studies of cobalt distribution in Co-TiO_2 anatase thin films: Processing, microstructure, and the origin of ferromagnetism," *J. Appl. Phys.*, **99,** 08M114 (2006).

Kim, D. H., H. M. Christen, M. Varela, H. N. Lee and D. H. Lowndes, "Effect of strain on structure and charge order transitions in epitaxial $Bi_{0.4}Ca_{0.6}MnO_3$ films on perovskite (001) and (011) substrates," *Appl. Phys. Lett.*, **88** (2006).

Kisa, M., L. Li, J. Yang, T. K. Minton, W. G. Stratton, P. Voyles, X. D. Chen, K. van Benthem and S. J. Permycook, "Homogeneous silica formed by the oxidation of Si(100) in hyperthermal atomic oxygen," *Journal of Spacecraft and Rockets*, **43**, 431-435 (2006).

Klie, R. F., J. P. Buban, M. Varela, A. Franceschetti, C. Jooss, Y. Zhu, N. D. Browning, S. T. Pantelides and S. J. Pennycook, "Enhanced current transport at grain boundaries in high-Tc superconductors," *Nature*, **435**, 475-478 (2005).

Miao, G. X., P. LeClair, A.Gupta, G. Xiao, M. Varela and S. J. Pennycook, "Magnetic tunnel junctions based on CrO_2/SnO_2 epitaxial bilayers," *App. Phys. Lett.* **89**, 022511 1-3 (2006).

Pena, V., Z. Sefrioui, D. Arias, C. Leon, J. Santamaria, M. Varela, S. J. Pennycook, M. Garcia-Hernandez and J. L. Martinez, "Strain induced phase separation in $La_{0.67}Ca_{0.33}MnO_3$ultra thin films," *J. Phys. Chem. Solids*, **67**, 472-475 (2006).

Pena, V., Z. Sefrioui, D. Arias, C. Leon, J. Santamaria, M. Varela, S. J. Pennycook and J. L. Martinez, "Coupling of superconductors through a half-metallic ferromagnet: Evidence for a long-range proximity effect," *Phys. Rev. B*, **69,** 224502 (2004).

Pennycook, S. J., M. Varela, C. J. D. Hetherington and A. I. Kirkland, "Materials advances through aberration-corrected electron microscopy," *MRS Bulletin*, **31**, 36-43 (2006).

Prabhumirashi, P., V. P. Dravid, A. R. Lupini, M. F. Chisholm and S. J. Pennycook, "Atomic-scale manipulation of potential barriers at $SrTiO_3$ grain boundaries," *Appl. Phys. Lett.*, **87** (2005).

Shao, R., M. F. Chisholm, G. Duscher and D. A. Bonnell, "Low-temperature resistance anomaly at $SrTiO_3$ grain boundaries: Evidence for an interface-induced phase transition," *Phys. Rev. Lett.*, **95,** 197601 (2005).

Sefrioui, Z., V. Cros, A. Barthelemy, V. Pena, C. Leon, J. Santamaria, M. Varela and S. J. Pennycook, "Tunnel magnetoresistance in $La_{0.7}Ca_{0.3}MnO_3/PrBa_2Cu_3O_7/La_{0.7}Ca_{0.3}MnO_3$," *Appl. Phys. Lett.*, **88,** 022512 (2006).

Shibata, N., G. S. Painter, R. L. Satet, M. J. Hoffmann, S. J. Pennycook and P. F. Becher, "Rare-earth adsorption at intergranular interfaces in silicon nitride ceramics: Subnanometer observations and theory," *Phys. Rev. B*, **72,** 140101 (2005).

Shibata, N., S. J. Pennycook, T. R. Gosnell, G. S. Painter, W. A. Shelton and P. F. Becher, "Observation of rare-earth segregation in silicon nitride ceramics at subnanometre dimensions," *Nature*, **428**, 730-733 (2004).

van Benthem, K., C. Elsasser and M. Ruhle, "Bonding of thin Pd films on (100)$SrTiO_3$ substrates: Ab initio density functional theory investigations," *Phys. Rev. B*, **72** 125435 (2005).

Varela, M., S. D. Findlay, A. R. Lupini, H. M. Christen, A. Y. Borisevich, N. Dellby, O. L. Krivanek, P. D. Nellist, M. P. Oxley, L. J. Allen and S. J. Pennycook, "Spectroscopic imaging of single atoms within a bulk solid," *Phys. Rev. Lett.*, **92,** 095502 (2004).

Varela, M., A. R. Lupini, K. van Benthem, A. Borisevich, M. F. Chisholm, N. Shibata, E. Abe and S. J. Pennycook, "Materials Characterization in the Aberration-Corrected Scanning Transmission Electron Microscope," p. 539-569 in, *Annu. Rev. Mater. Res*, Annual Reviews, v. 35 (2005).

Varela, M., T.J. Pennycook, W. Tian, D.G. Mandrus, S.J. Pennycook, V. Pena, Z. Sefrioui, J. Santamaria. "Atomic scale characterization of complex oxide interfaces". *J. Mat. Sci*. **41**, 4389 (2006).

Yan, W. F., B. Chen, S. M. Mahurin, V. Schwartz, D. R. Mullins, A. R. Lupini, S. J. Pennycook, S. Dai and S. H. Overbury, "Preparation and comparison of supported gold nanocatalysts on anatase, brookite, rutile, and P25 polymorphs of TiO_2 for catalytic oxidation of CO," *J. Phys. Chem. B*, **109**, 10676-10685 (2005).

Yan, Y. F., M. M. Al-Jassim, M. F. Chisholm, L. A. Boatner, S. J. Pennycook and M. Oxley, "[1-100]/(1102) twin boundaries in wurtzite ZnO and group-III-nitrides," *Phys. Rev. B*, **71**, 0413091 (2005).

Zeng, C. G., P. R. C. Kent, M. Varela, M. Eisenbach, G. M. Stocks, M. Torija, J. A. Shen and H. H. Weitering, "Epitaxial stabilization of ferromagnetism in the nanophase of FeGe," *Phys. Rev. Lett.*, **96** 127201 (2006).

Research Summaries

Imaging Molecules and Active Sites for Oxide-Supported Nanocatalysts

Arthur P. Baddorf, Sefa Dag, Sergei V. Kalinin, Vincent Meunier, David R. Mullins, Steven H. Overbury and Jing Zhou
baddorfap@ornl.gov, dags@ornl.gov, sergei2@ornl.gov, meunierv@ornl.gov, mullinsdr@ornl.gov, overburysh@ornl.gov, zhouj1@ornl.gov
Oak Ridge National Laboratory, Oak Ridge, TN 37831-6030

Program Scope

The promise of nanoscale materials science is universally recognized in the realm of catalysis, a trillion dollar industry whose underpinnings have been built on chemical reactants too small to see. With rapid transformations in imaging capabilities and modeling power, we now have the potential to observe individual molecules on single clusters of a supported catalyst. This program applies the sensitivity of scanning tunneling microscopy to individual molecules and electronic orbitals with high-performance computation to provide a picture of the active sites and energetics of supported metal catalyst particles on oxide surfaces. The goal of this project is to accelerate progress in catalysis by developing our fundamental understanding of molecular reactivity in the presence of an interface, using real space, local imaging. Key issues are: (1) the spatial distribution of reactive electronic orbitals as modified by the substrate, (2) the strength of molecular bonds, (3) identification of the molecular environment, and (4) control and selectivity of reaction pathways. These can be explored for individual molecules and catalyst clusters, bypassing the averaging of ensemble measurements.

Recent Progress

Metal particles dispersed on oxides are of great importance in heterogeneous catalysis, and for this reason, supported transition metals on single crystal oxide surfaces have been studied extensively as model systems for practical oxide-supported catalysts.[1-4] The catalytic properties of supported nanoparticles can be altered by their size and structures[5-8] as well as their interactions with the oxide support[9-11]. Although much has been learned about the physical and structural properties of metal nanoparticles supported on oxides[1, 3, 4], our understanding of their catalytic function is still rudimentary. Still unresolved are the role of the substrate, diffusion and mobility of the molecules on the surface, molecular transfer between oxide support and metal particles, and the specific sites for molecular adsorption and reaction. To obtain a molecular-scale understanding of the catalytic reactivity of oxide-supported particles, it is important to use experimental tools that provide in situ observations of reactants, catalysts and products and to employ accurate theoretical methods to model and interpret the findings.

Adsorption and reaction of molecules at oxide-supported catalyst clusters are being directly imaged and modeled on surfaces with exceedingly well-characterized structural and chemical properties and in controlled ultrahigh vacuum environments. Scanning tunneling microscopy (STM) using an Omicron variable temperature microscope has been used to obtain atomic scale images. Computational modeling for theoretical interpretation is treated by using first-principles calculations based on Density Functional Theory coded at NCCS (National Center for Computational Sciences). These

tools are complemented with a variety of electron spectroscopies, electron diffraction, and thermal desorption to characterize the environment and reactivity of the systems.

Our initial focus has been on oxidation reactions at Pd particles on single crystal TiO_2, a model system of broad interest to the catalytic community. The first step was to produce atomically ideal TiO_2 surfaces, with result shown in the STM image in Fig. 1a. The few defects observed in this image can be assigned to oxygen vacancies. Absorption of benzene at room temperature produced no molecular images in STM, although spectroscopy proves the molecule does bond to the surface. First principles calculations revealed benzene has a high mobility along the surface rows, which precludes imaging above 50 K. At 40 K, STM images revealed that low coverages of benzene adsorb in rows (Fig. 1b). Although the barrier calculated to cross the bridging oxygen rows was 0.8 eV and much too high for benzene to thermally hop, we did observe tip induced hopping, shown in Fig. 1c. Only for a complete monolayer of benzene at 20 K did STM images resolve individual molecules (Fig. 1d). However, coupled with theory, these images show that benzene binds weakly with TiO_2(110) with an adsorption energy of 670 meV. The molecule lies flat with the aromatic ring parallel to the surface on top of the Ti rows. High mobility along the bridging oxide rows requires low temperatures for imaging. Benzene bonds between the oxygen rows, between two five-fold coordinated Ti atoms. At monolayer coverage, calculations show that benzene rings alternate in azimuthal orientation to form chains between the bridging oxygen rows (Fig. 2).

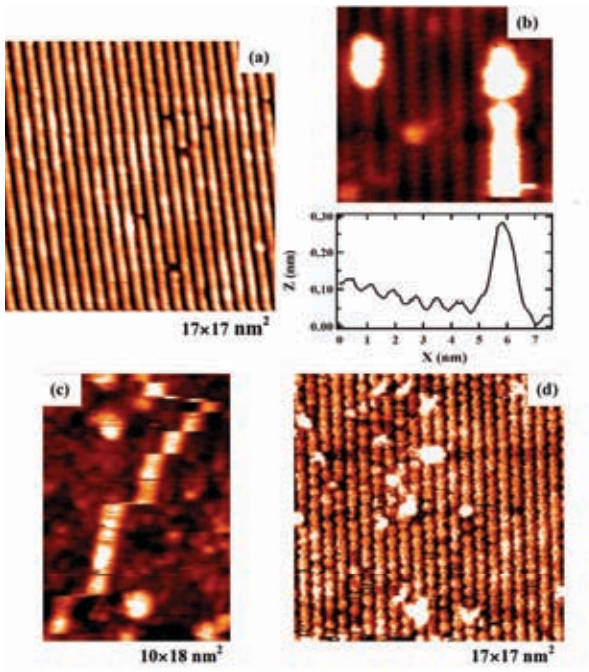

FIG. 1. STM images: (a) a clean TiO_2(110) surface, (b) after a low benzene dose of 0.1 L at 40 K, (c) 0.1 L at 30 K and (d) after a high benzene dose at 20 K. A line profile over one of the benzene chains is also shown in (b).

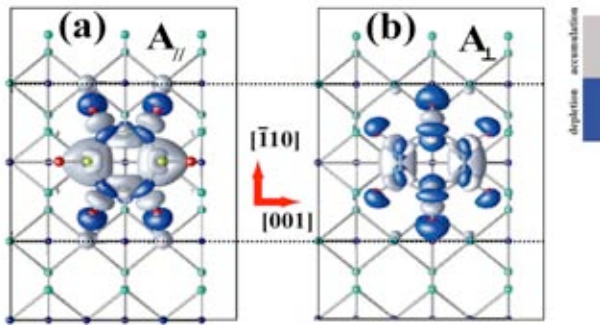

Fig. 2 First principles calculations of the charge density transfer for the two bonding configurations observed for benzene on TiO_2.

No benzene dissociation was observed on titania, even at elevated temperatures. In contrast, the presence of Pd nanoparticles on the TiO_2(110) surface leads to the decomposition of benzene into atomic H and C atoms at elevated temperatures, governed by a multistep process. The STM image in Fig. 3 shows the distribution of

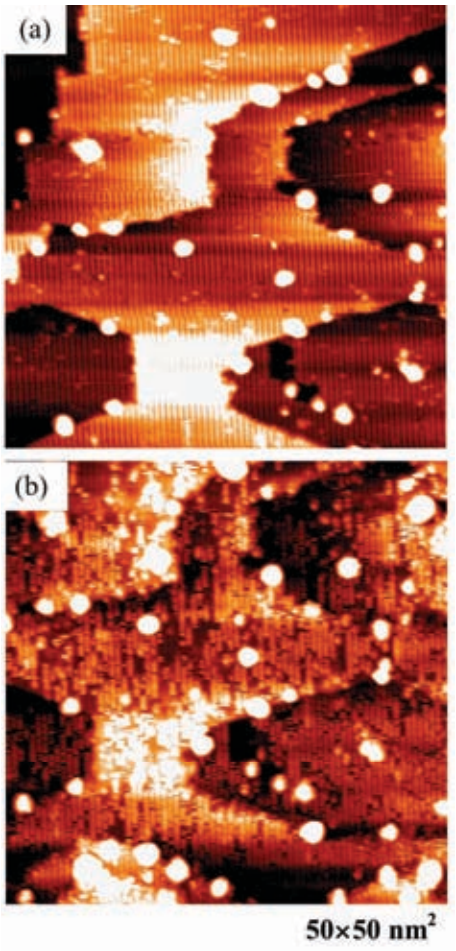

Fig. 3 STM images of 0.2 ML coverage of Pd deposited at 295 K on TiO_2(110): (a) before benzene dose at 40 K and (b) after a 0.7 L benzene dose at 40 K.

Pd particles deposited by MBE at room temperature. The particles are fairly uniform in size, with diameter of 2-3 nm and height of 0.6-0.7 nm, and prefer a location at TiO_2 step edges. The lower panel shows the same area of the surface after benzene adsorption at 40 K. Again rows of benzene are observed, which here extend completely to the Pd particles. Despite the close proximity, reaction products are observed only at higher temperatures.

We next examined other molecules which interact more strongly with the TiO_2 than benzene. Fig. 4 shows atomically resolved images of phenol (top) and formic acid (bottom) on TiO_2. The stronger bonding of these molecules allows imaging at 300 K. The phenol appears to bridge two oxygen rows of the substrate. Calculations are being performed to determine the configuration, which may involve dimerization.

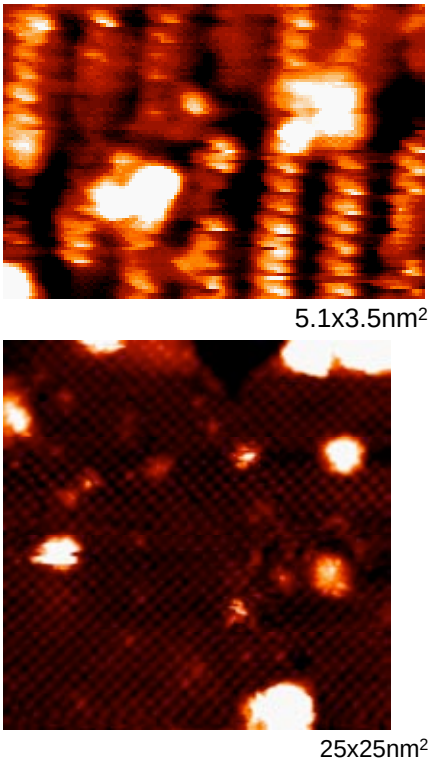

Fig. 4 STM images of (a) isolated phenol molecules on TiO_2 observed spanning the bridging oxygen rows and (b) an array of formate covering both titania and Pd particles.

Formic acid adsorption leads to formate molecules by loss of a proton. As seen from STM, the majority of formate species bond in a bi-dentate adsorption configuration with oxygen atoms bridge-bonded between two five-fold coordinated Ti atoms and formed a regular p(2x1) pattern with a distance of 6 Å between the neighbouring molecules along the [001] direction. One fascinating aspect of STM images of formate was our ability to resolve molecules on Pd particles (Fig 4b). The reaction of formate after heating in the presence of Pd particles produces a reaction intermediate that appears quite differently in tunneling. The identity of this intermediate is still under investigation.

Future Directions

Clearly there are many possible directions for real space imaging of catalytically interesting systems. One avenue we would like to pursue is heterogeneous catalysis supported by cerium oxide. Ceria is more readily reduced than titania and is a more practical catalyst support (in automotive exhaust systems for example). Ceria is not conductive, however, and is therefore more difficult to study with electron tunneling and spectroscopy. Freund, et al., have recently shown that CeO_2 can be epitaxially grown on Ru.[12] Our initial foray, shown in Fig. 5 shows that flat terraces can be produced of greater size than those previously published and atomic resolution achieved. We are now beginning studies of metal deposition and molecular adsorption on CeO_2.

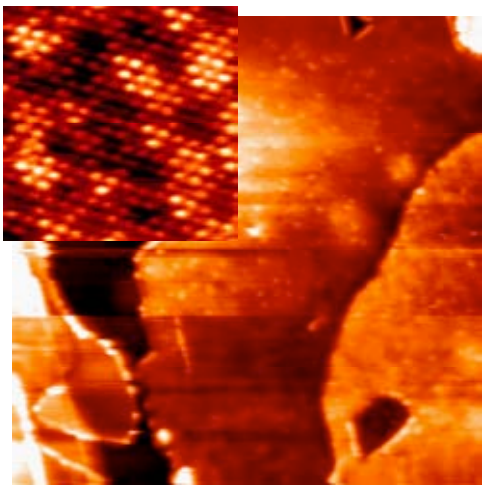

Fig. 5 CeO2 thin film grown on Ru(0001) by MBE. Large, flat, terraces are observed. The inset shows atomic resolution.

References

[1]C. T. Campbell, Surf. Sci. Rep. **27**, 1 (1997).
[2]J. Libuda and H. J. Freund, Surf. Sci. Rep. **57**, 157 (2005).
[3]D. W. Goodman, Chem. Rev. **95**, 523 (1995).
[4]P. A. Cox, *Transition metal oxides-An introduction to their electronic structures*, (Clarendon: Oxford, 1992).
[5]M. Valden, X. Lai, and D. W. Goodman, Science **281**, 1647 (1998).
[6]M. Aizawa, S. Lee, and S. L. Anderson, J. Chem. Phys. **117**, 5001 (2002).
[8]C. Becker and C. R. Henry, Surf. Sci. **352**, 457 (1996).
[9]S. K. Shaikhutdinov, R. Meyer, M. Naschitzki, M. Baumer, and H. J. Freund, Catal. Lett. **86**, 211 (2003).
[10]D. R. Mullins, L. Kundakovic, and S. H. Overbury, J. Catal. **195**, 169 (2000).
[11]D. R. Mullins and K. Zhang, J. of Phys. Chem. B **105**, 1374 (2001).
[12]D. R. Mullins, M. D. Robbins, and J. Zhou, J. Surf. Sci. **600**, 1547 (2006).
[13]J.-L. Lu, H.-J. Gao, S. Shaikhutdinov, and H.-J. Freund, Surf. Sci. in press.

DOE Sponsored Publications in 2002-2004

Surface defects on TiO_2(110): from atomic and electronic structure to catalytic activity, K. T. Park, M. Pan, S. V. Kalinin, V. Meunier, A. P. Baddorf, and E. W. Plummer, in *Nanoporous and Nanostructured Materials for Catalysis, Sensor, and Gas Separation Applications*, ed. S. W. Lu, H. Hahn, J. Weissmuller, and J. L. Gole (Mater. Res. Soc. Symp. Proc. Vol. 876E, Warrendale, PA) R 4.6 2005.

Adsorption, Desorption, and Dissociation of Benzene on TiO_2(110) and Pd/TiO_2(110): Experimental Characterization and First-Principles Calculations, J. Zhou, S. Dag, S. D. Senanayake, B. C. Hathorn, S. V. Kalinin, V. Meunier, D. R. Mullins. S. H. Overbury, and A. P. Baddorf, Phys. Rev. B **74**, 1 (2006).

Surface Reconstructions of TiO2(110) Driven by Sub-Oxides, K. T. Park, M. H. Pan, V. Meunier, and E. W. Plummer, Phys. Rev. Lett. **96**, 226105 (2006).

Experimental and Theoretical Studies of Alloyed Semiconductor Surfaces

Jessica E. Bickel[*], Normand A. Modine[+], Chris A. Pearson[^], Anton VanDerVen[*], Joanna Mirecki-Millunchick[*]
jebickel@umich.edu, namodin@sandia.gov, avdv@umich.edu, joannamm@umich.edu
[*]Department of Materials Science and Engineering, University of Michigan, Ann Arbor, MI 48105
[+]Sandia National Laboratories, Albuquerque, NM 87185
[^] Department of Computer Science, Engineering Science and Physics, University of Michigan-Flint, Flint, MI 48502

Program Scope

The atomic surface structure of compound semiconductors plays an important role in the growth of thin films and devices made of these alloys, influencing the compositional uniformity and the morphology of the grown material. It also influences ordering and surface segregation of individual atoms [1]. It is important to understand the surface structure in order to control the growth of electronic and optoelectronic devices made of III-V semiconductors where planar and compositionally abrupt interfaces are required to obtain optimal device properties. A great deal of work has been aimed at understanding binary compound semiconductors such as GaAs [2], InAs [3], and GaSb [4], however, less is known about the surface structure of ternary alloys such as InGaAs and GaAsSb.

This program is a combined effort of experimental and theoretical work to examine and understand the structure of semiconductor alloy surfaces of InGaAs and GaAsSb. Experimentally, we have been examining the formation of GaAsSb alloy surfaces, specifically to understand the incorporation of Sb in the growing film. Theoretically, we have performed density functional theory (DFT) calculations to explain some of the recent experimental findings of the InGaAs alloy surfaces, specifically to establish the details of the atomic surface structure. In both aspects of the work, we ultimately wish to understand growth mechanisms such as surface segregation in these strained alloy layers.

Our short-term goals work toward this long-term understanding. In the GaAsSb portion of the program, a hitherto unreported surface reconstruction on Sb-capped GaAs has been seen, which we are now studying in order to understand the growth mechanism of this surface with respect to both GaAs and GaSb. In the InGaAs portion of the program, alloys of InGaAs have been shown to have a mixed surface reconstruction of (4x3) and (nx4) [5, 6] with a debate over what is the actual structure of the (4x3) reconstruction. Our first goal is to determine the correct model of the (4x3) reconstruction using DFT and simulated STM. Our second goal is to understand the presence of a zigzag-α2(2x4) seen in low In content alloys rather than the stochastic α2(2x4) generally seen in binary alloys.

Recent Progress

<u>Sb Incorporation in GaAs</u>

Thin layers of GaSb and Sb were grown on GaAs(001) surfaces, resulting in the observation of a hitherto unreported intermediate-height surface reconstruction. This intermediate reconstruction appears in both GaSb/GaAs and Sb/GaAs films of thickness of up to a few monolayers (MLs) and is shown in Figure 1. Both the lower level and upper level reconstructions are α2(2x4) with a lattice parameter of ~0.57Å which is between that of GaAs and GaSb. The intermediate reconstruction has a row spacing corresponding to a x3 reconstruction which is consistent with the fact that bulk GaSb has a (4x3) surface reconstruction that has been described by Barvosa-Carter [5]. Reflection High Energy Electron Diffraction (RHEED) studies of fractional monolayer coverages of Sb/GaAs show that for thicknesses less the 0.8 ML, the film exhibits a x3 reconstruction upon cooling. For these thin x3 reconstruction films, the STM images look highly disordered with only partially discernable rows. At thicknesses greater than 0.8 ML a 2x4 reconstruction is observed in the RHEED. The STM of these films, however, exhibit the mixed (nx3)-α2(2x4) surface seen in Figure 1. These observations suggests that the Sb first incorporates into the surface in a x3 reconstruction, then transitions quickly to a x4 reconstruction, presumably due to strain. Based upon these data, we have developed an atomistic growth model for incorporation of Sb onto a GaAs surface.

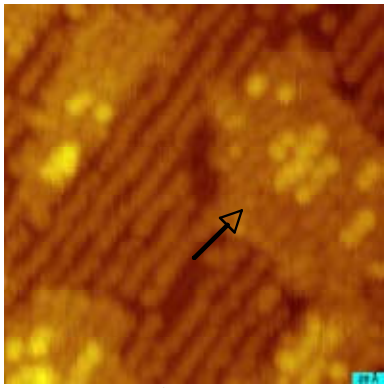

Figure 1: 500Å STM image of 1ML Sb/GaAs(001). The arrow points to the intermediate reconstruction

<u>InGaAs Surface Structures</u>

This portion of the program utilizes DFT to explain recent experimental work on InGaAs which shows that, under most growth conditions, a disordered (4x3) reconstruction dominates the surface. Under some conditions mixed surfaces are seen where mostly (4x3) surfaces contain domains of α2(2x4), β2(2x4), and c(4x4) reconstructions [6, 7]. DFT and simulated STM are used to examine the (4x3) reconstruction and explain the occurrence of the zigzag variant of the α2(2x4) reconstruction in this alloy system.

An example of the observed structure of an InGaAs (001) surface is displayed in Figure 2, which shows an STM image of a 20 monolayer (ML) thick film of $In_{0.27}Ga_{0.73}As$ /GaAs (lattice mismatch = 1.9%) deposited at T= 475°C. The surface reconstruction consists primarily of a disordered (4x3) surface reconstruction, with small domains of α2(2x4) structures. It is interesting to point out that these α2(2x4) domains have a configuration where the dimer location alternates positions in the unit cell at a rate of 80%. Binary surfaces, on the other had, have a stochastic configuration of the dimers.

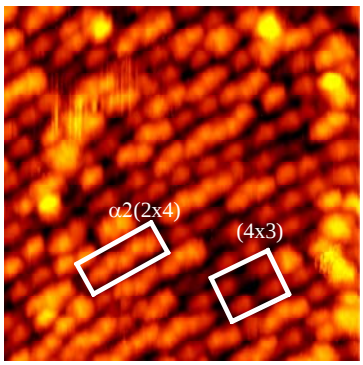

Figure 2: STM of $In_{0.27}Ga_{0.73}As$ taken at -2.3V, 100pA

In order to examine the relative stability of the alternating configuration, DFT calculations were performed using the Vienna *Ab Initio* Simulation

Package (VASP) [8] with both a straight-row α2(2x4) and a zigzag α2(2x4) reconstruction. In general, these calculations show that the zigzag configuration is slightly more stable than the straight-row configuration and slightly stabilized under tensile strain. However, these effects are smaller than the temperature effects which act to randomize the system which explains the stochastic α2(2x4) generally seen in binary III-As systems. On the other hand, specific alloying effects have a much larger impact on the stabilization of the zigzag structure. For a Ga slab with In in 2 or 4 of the surface cation sites, the zigzag was found to be over 100meV more stable than the straight-row configuration which is much larger than the energy added by the temperature effects. Increasing the In concentration of the surface further, however, decreases the stability of the zigzag configuration.

Experimentalists have suggested two different models to account for the (4x3) reconstruction seen in the InGaAs system, the Mirecki-Millunchick (MM) model [6] and the Jones (SSJ) model [7], which is a variation of a model originally proposed by Sauvage-Simkin [9]. There are a few important differences between these models. The MM model has heterodimers (cation-anion pairs) on the surface as well as cation and anion homodimers, whereas the SSJ model only has anion homodimers. We used DFT to calculate the surface energies and simulate STM images using the method described by Tersoff and Hamann [10]. Figure 3 shows simulated filled state (left) and empty state (right) STM images of both models. Comparison of the simulated images to the experimental data (see for example the (4x3) reconstruction marked in Figure 2), suggests that the MM model is more accurate. However, this model has a considerably higher surface energy than the α2(2x4), which has the same stoichiometry, suggesting that it is not stable under any growth conditions. Similarly, the SSJ model has a slightly higher surface energy than known reconstructions with the same stoichiometry.

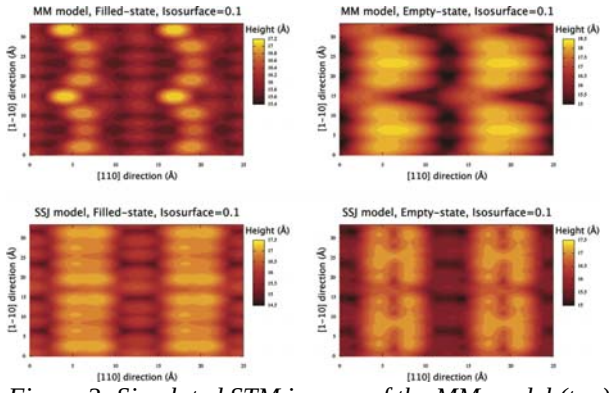

Figure 3: Simulated STM images of the MM model (top) and SSJ model (right) at +1V (right) and -1V (left)

Future Work

These results indicate that several different experiments and calculations still need to take place to fully understand the detailed atomic structure and growth mechanisms of alloy surfaces. In the GaAsSb work, we will utilize DFT to verify that our atomistic mechanism for Sb incorporation is indeed correct. Furthermore, we will grow thicker samples to determine the experimental conditions for which the reconstruction transitions back to the bulk-like x3 reconstruction. We will also use DFT to simulate both the (4x3) and α2(2x4) surface reconstructions to determine the relative energies of the reconstructions and the role of strain and alloying effects play in the stabilization of the x4 reconstruction.

In the InGaAs work, we will continue to search for a plausible model for the reconstruction observed on that surface. We will also plot the relative energies of all surface reconstructions relaxed using VASP to create a surface phase diagram of the InGaAs alloys at different lattice parameters. By comparing the resulting phase diagrams we determine the role of strain on the surface reconstruction of this ternary alloy. We also wish to better understand the influence of temperature on the zigzag-α2(2x4) reconstruction. To this point, it has been assumed that temperature effects equal to k_BT acted to randomize the dimer placement within the α2(2x4) reconstruction. Utilizing kinetic Monte Carlo code (kmc) we will simulate the temperature effects on variations of surface dimer coverage and surface percentage of In to note the effect all three variables have on each other and map out a surface reconstruction map based on these three variables.

References

(1) S. Froyen, A. Zunger, Phys. Rev. B 53 (1996) 4570.
(2) V. Bresslerhill, M. Wassermeier, K. Pond, R. Maboudian, G.A.D. Briggs, P.M. Petroff, W.H. Weinberg, J. Vac. Sci. Technol. B 10 (1992) 1881.
(3) W. Barvosa-Carter, R.S. Ross, C. Ratsch, F. Grosse, J.H.G. Owen, J.J. Zinck, Surf. Sci. 499 (2002) L129.
(4) A.S. Bracker, M.J. Yang, B.R. Bennett, J.C. Culbertson, W.J. Moore, J. Cryst. Growth 220 (2000) 1492.
(5) W. Barvosa-Carter, A.S. Bracker, J.C. Culbertson, B.Z. Nosho, B.V. Shanabrook, L.J. Whitman, Phys. Rev. Lett. 84 (2000) 4649.
(6) J. Mirecki-Millunchick, A. Riposan, B.J. Dall, C. Pearson, B.G. Orr, Surf. Sci. 550 (2004) 1.
(7) P.A. Bone, J.M. Ripalda, G.R. Bell, T.S. Jones, Surf. Sci. 600 (2006) 973.
(8) G. Kresse, J. Hafner, Phys. Rev. B 47 (1993) 558. G. Kresse, J. Haafner, Phys. Rev. B 49 (1994) 14251. G. Kresse, J. Furthmüller, Comput. Mat. Sci. 6 (1996) 15. G. Kresse, J. Furthmüller, Phys. Rev. B 54 (1996) 11169.
(9) M. Sauvage-Simkin, Y. Garreau, R. Pinchaux, A. Cavanna, M.B. Véron, N. Jedrecy, J.P. Landesman, J. Nagle, Appl. Surf. Sci. 104/105 (1998) 16177.
(10) J. Tersoff, D.R. Hamann, Phys. Rev. B 31 (1985) 805.

DOE Sponsored Publications in 2005-2006

Ab Initio Simulations of Compound Semiconductor Alloys, J.E. Bickel, N.A. Modine, J. Mirecki-Millunchick, Internal Sandia Publication for NECIS program, July, 2006.

Surface Growth Model for thin layers of Sb and GaSb on GaAs(001), J.E. Bickel, C.A. Pearson, J. Mirecki-Millunchick, manuscript in preparation

Ab Initio determined alloying effects on the surface reconstruction of InGaAs, J.E. Bickel, N.A. Modine, J. Mirecki-Millunchick, manuscript in preparation

Epitaxial multifunctional oxide heterostructures

Venkat Chandrasekhar[1] and Chang-Beom Eom[2]
v-chandrasekhar@northwestern.edu, eom@engr.wisc.edu
[1]Department of Physics and Astronomy, Northwestern University
[2]Department of Materials Science and Engineering, University of Wisconsin, Madison

Program Scope

Strongly-correlated perovskite oxides have attracted a tremendous amount of interest due to the wide range of physical properties they can exhibit.[1–6] These properties include ferromagnetism, antiferromagnetism, ferroelectricity, piezoelectricity and superconductivity. One of the more intriguing aspects of some of these perovskites is the possibility of the coexistence of two or more properties (such as ferromagnetism and superconductivity) in a single material, opening up the possibility of making devices that creatively utilize this multifunctionality. In spite of decades of intensive study and a greatly improved understanding of the underlying physics, however, many fundamental properties of perovskite structures are still not understood. The most famous example is perhaps the case of high temperature superconductivity in the cuprates, which still defies explanation almost two decades after its discovery.

There has been renewed interest in complex oxides in the last few years, particularly after recent advances in the ability to make *epitaxial* perovskite multilayers, where each layer is lattice-matched to the previous one but may exhibit a different functionality. For example, it is possible to grow the high-temperature superconductor YBCO on top of a layer of ferromagnetic $La_{1-x}Sr_xMnO_3$ (LSMO) or $La_{1-x}Ca_xMnO_3$ (LCMO).[7–13] One can also think of fabricating magnetic tunnel junctions with the ferromagnetic elements as well as the insulator being lattice-matched perovskites, resulting in devices with atomically smooth interfaces.[4,14,15] Indeed, it is also possible to make alternating multilayers of such materials where each layer is only a few atoms thick, creating in essence new materials with new functionalities, opening up a range of new device possibilities.

It is thought that understanding the role of intrinsic inhomegeneities in the perovskites may be central to understanding their unusual properties. For example, in the manganites (e.g., LSMO), the metal-insulator transition (MIT) is determined by the interplay between metallic ferromagnetic regions and non-magnetic insulating regions that are also thought to play a role in the colossal magnetoresistance (CMR) that these materials exhibit. Similarly, the presence of the anomalous pseudogap in high-temperature superconductors has been attributed to the presence of a stripe phase that coexists with the superconducting phase on a microscopic level. Epitaxial multifunctional perovskites represent an even newer class of materials where the properties of the material are deliberately made to vary on the nanometer scale. The investigation of such inhomegeneities requires tools that can probe the physical properties of materials on the submicrometer and even nanometer length scales. Scanning probe microscopy, including scanning tunneling microscopy (STM), atomic force microscopy (AFM), magnetic force microscopy (MFM) and electrostatic force microscopy (EFM) and its variations have been used to probe the perovskites, but much work remains to be done to further our understanding of these interesting materials.

Future Plans

It is proposed to use scanning probe techniques to investigate the properties of epitaxial perovskite

structures as a function of temperature and magnetic field. Three different types of epitaxial perovskite structures will be investigated. The first type will be manganites, where the interest will be to correlate the intrinsic magnetic structure with electrical transport properties as a function of temperature, magnetic field and the biaxial strain induced by epitaxial growth on different substrates. This is particularly relevant to the growth of epitaxial magnetic devices such as magnetic tunnel junctions. The second set of structures will be epitaxial multilayers consisting of high-temperature superconductors (HTSC) (in particular, YBCO) and perovskite manganites. There is tremendous interest in the interplay between superconductivity and ferromagnetism, two phenomena that are normally considered to be antagonistic, since the presence of ferromagnetism is typically expected to destroy superconductivity. However, there have been reports of the coexistence of superconductivity and ferromagnetism in a single material, for example, in the ruthenocuprates, naturally layered materials where one layer can order magnetically while another layer can undergo a superconducting transition. Epitaxial superlattices of HTSC and manganites may have properties similar to the ruthenocuprates, but properties that might be tailored by atomic engineering. Devices made from such superlattices may prove useful in making high resolution magnetic sensors. The final set of structures are those that incorporate both ferromagnetism and ferro- or piezoelectric properties, the so called multiferroics. Such structures allow one to control the ferromagnetic properties by an electric field or the ferroelectric properties by a magnetic field, and again may form the basis of a new class of devices.

The structures will be grown in Chang-Beom Eom's group at the University of Wisconsin. Eom's group has extensive experience in growing a wide variety of epitaxial magnetic oxides, and indeed has already grown many of the structures that will be investigated here. The primary tool that we will use to probe the properties of these structures is a variable temperature scanning probe microscope developed at Northwestern. This instrument can be attached to a number of cryogenic inserts allowing operation to temperatures down to the millikelvin regime in magnetic fields of up to 14 T, although for the studies proposed here, a cryogenic insert that is capable of going down to 4.2 K in a cryostat with a two-axis magnet will probably be sufficient. This instrument is capable of performing atomic force microscopy (AFM), magnetic force microscopy (MFM) and electrostatic force microscopy (EFM); we anticipate that we will mostly use the AFM and MFM modes to investigate the magnetic properties as a function of magnetic field and temperature, with EFM investigations of the multiferroics later in the project. A unique feature of this instrument is the ability to perform electrical transport measurements simultaneously with AFM, MFM or EFM. This ability will let us correlate directly the magnetic and transport properties of the samples. Finally, as part of this project, a collaboration will be initiated with Professor Anjan Gupta of the Indian Institute of Technology, Kanpur. Professor Gupta's group is active in the area of scanning tunneling microscopy (STM) of perovskites, and we hope to apply this technique to the epitaxial structures discussed above.

References

[1] M.B. Salamon and M. Jaime, 'The physics of manganites: Structure and transport,' Rev. Mod. Phys. **73**, 583 (2001).

[2] M. Fiebig, 'Revival of the magnetoelectric effect,' J. Phys. D: Appl. Phys. **38**, R123 (2005).

[3] J.Z. Sun and A. Gupta, 'Spin-dependent transport and low-field magnetoresistance in doped manganites,' Annu. Rev. Mater. Sci. **28**, 45 (1998).

[4] M. Zeise, 'Colossal magnetoresistance, half-metallicity and spin electronics,' Phil. Trans. R. Soc. Lond. A **358**, 137 (2000).

[5] C.H. Ahn, J.-M. Triscone and J. Mannhart, 'Electric field effect in correlated oxide systems,' Nature **424**, 1015 (2003).

[6] C.H. Ahn, K.M. Rabe and J.-M. Triscone, 'Ferroelectricity at the Nanoscale: Local Polarization in Oxide Thin Films and Heterostructures,' Science **303**, 488 (2003).

[7] N.-C. Yeh, R.P. Vasquez, C.C. Fu, A.V. Samoilov, Y. Li and K. Vakili, 'Nonequilibrium superconductivity under spin-polarized quasiparticle currents in perovskite ferromagnet-insulator-superconductor heterostructures,' Phys. Rev. B **60**, 10522 (1999).

[8] P.A. Kraus, A. Bhattacharya and A.M. Goldman, 'Magnetic-field scaling of the conductance of epitaxial cuprate-manganite bilayers,' Phys. Rev. B **64**, 220505 (2001).

[9] V.A. Khokhlov, A. Yu. Prokhorov, V.F. Drobotko, G.G. Levchenko, P.N. Mikheenko, R. Chakalov and C. Muirhead, 'Temperature dependence of the critical current of YBCO-STO-LCMO heterostructures,' Low Temperature Physics **29**, 113 (2003).

[10] S. Soltan, J. Albrecht and H.-U. Habermeier, 'Ferromagnetic/superconducting bilayer structure: A model system for spin diffusion length estimation,' Phys. Rev. B **70**, 144517 (2004).

[11] P. Przyslupski, I. Komissarov, W. Paszkowicz, P. Dluzewski, R. Minikayev and M. Sawicki, 'Structure and magnetic characterization of $La_{0.67}Sr_{0.33}MnO_3/YBa_2Cu_3O_7$ superlattices,' J. Appl. Phys. **95**, 2906 (2004).

[12] V. Pĕna, Z Sefrioui, D. Arias, C. Leon, J. Santamaria, M. Varela, S.J. Pennycook and J.L. Martinez, 'Coupling of superconductors through a half-metallic ferromagnet: evidence for a long-range proximity effect,' Phys. Rev. B **69**, 224502 (2004).

[13] Z. Sefrioui, M. Varela, V. Pĕna, D. Arias, C. León, J. Santamaría, J.E. Villegas, J.L. Martínez, W. Saldarriaga and P. Prieto, 'Superconductivity depression in ultrathin $YBa_2Cu_3O_{7-\delta}$ layers in $La_{0.7}Ca_{0.3}MnO_3/YBa_2Cu_3O_{7-\delta}$ superlattices,' Appl. Phys. Lett. **81**, 4568 (2002).

[14] Yu Lu, X.W. Li, G.Q. Gong, G. Xiao, A. Gupta, P. Lecoeur, J. Z. Sun, Y.Y. Wang and V.P. Dravid, 'Large magnetotunneling effect at low magnetic fields in micrometer-scale epitaxial $La_{0.67}Sr_{0.33}MnO_3$ tunnel junctions,' Phys. Rev. B **54**, R8357 (1996).

[15] K.R. Nikolaev, A. Yu. Dobin, I.N. Krivorotov, W.K. Cooley, A. Bhattacharya, A.L. Kobrinskii, L.I. Glazman, R. R. Wentzovitch, E. D. Dahlberg and A.M. Goldman, 'Oscillatory Exchange Coupling and Positive Magnetoresistance in Epitaxial Oxide Heterostructures,' Phys. Rev. Lett. **85**, 3728 (2000).

Fundamental Investigations of Candidate Ferromagnetic Oxide Semiconductors

Scott A. Chambers, Timothy C. Droubay, Tiffany C. Kaspar, Chongmin Wang, Steven M. Heald, V. Shutthanandan, David E. McCready
Pacific Northwest National Laboratory, Richland, WA 99352
sa.chambers@pnl.gov

Program Scope

The maturation of semiconductor spintronics requires the discovery and utilization of ferromagnetic semiconductors that exhibit spin polarization in the majority carrier band at and above room temperature. Intrinsic remanent magnetization would allow spin polarized currents to be propagated in such materials without the need for a continuous magnetic field. However, the discovery and understanding of such materials is proving to be a grand challenge in solid-state science. Indeed, one of the 125 critical unanswered scientific questions posed in Science in 2005 asks, "*Is it possible to create magnetic semiconductors that work at room temperature*?" The goals of this program are to use state-of-the-art epitaxial film growth methods (MBE, PLD and MOCVD), in conjunction with definitive materials characterization plus magnetic and magnetoelectronic transport measurements, to prepare very well-defined materials and elucidate critical structure-function relationships based on atomic scale properties. Of particular importance are various atom-specific x-ray absorption spectroscopies, carried out at the Advanced Photon Source and the Advanced Light Source. X-ray absorption near-edge spectroscopy (XANES) and extended x-ray absorption fine structure (EXAFS) at the dopant K-edge have generated invaluable information on the dopant charge state and bonding site within the host lattice in a volume-average fashion. These spectroscopies allow us to probe the dopant with exquisite sensitivity, and nicely complement high-resolution XRD and TEM. Since the magnetic character of these materials is strongly influenced by the dopant, which is typically present at the 1-10 at. % level, the importance of these measurements in elucidating defensible structure-function relationships cannot be overstated.

Recent Progress

We have focussed on three host oxides -- TiO_2 anatase, ZnO and α-Fe_2O_3. The first two are nonmagnetic, wide gap semiconductors (E_g = 3.2 and 3.4 eV) that we have doped with Co and Cr. Co and Cr substitute for the host cation with formal charge states of +2 and +3, respectively, leading to maximum expected spin moments of 1 and 3 μ_B per dopant for the low- and high-spin states of Co(II) and Cr(III), respectively. α-Fe_2O_3 is a canted antiferromagnet in the bulk, but is also a wide bandgap semiconductor (E_g = 2.1 eV) that we have doped with Ti. Ti(IV), a d^0 cation, substitutes for Fe(III), a d^5 cation, leading to a localized reduction in moment. In the antiferromagnetic corundum-like structure of α-Fe_2O_3, the spin orientations in adjacent cation layers are antiparallel. That is, along the *c* axis, the spin orientation and layer structure can be represented schematically as ($M^{\uparrow}$-$M^{\uparrow}$-O_3-$M^{\downarrow}$-$M^{\downarrow}$-O_3…), where M-M represents a buckled cation layer. If a d^0 dopant locates preferentially in a buckled cation layer of one particular spin orientation (either $M^{\downarrow}$-$M^{\downarrow}$ or $M^{\uparrow}$-$M^{\uparrow}$), then its presence will reduce the total spin in that

layer. Thus, the total spin (summed over both kinds of layers) will be nonzero, and should increase with dopant concentration. If on the other hand a d^0 dopant is randomly distributed in cation layers of both spin orientations, a dilute system with essentially zero net spin is expected to form. Moreover, Ti(IV) should be a donor in α-Fe_2O_3.

In the case of MBE-grown Co:TiO_2 and Cr:TiO_2 anatase, we found that the room temperature (RT) saturation moment scaled inversely with the crystallographic quality of the films. In our early film growth work on these systems, we used MBE growth conditions that resulted in quasi-epitaxial growth of oriented films. Cr-doped films typically exhibited significant roughening compared to undoped films. Additionally, inclusion of the Co dopant typically resulted in segregation of a Co-rich $Co_xTi_{1-x}O_2$ phase (x larger than expected based on fluxes) embedded as nanoparticles within a continuous epitaxial $Co_xTi_{1-x}O_2$ film phase (x smaller than expected based on fluxes). Nevertheless, the materials consistently exhibited RT ferromagnetism (RTFM), although the magnetic properties did not scale with dopant and carrier concentrations in any way expected for a magnetic semiconductor. However, as we optimized growth to get crystallographically superior material, the ferromagnetism essentially disappeared. The saturation moment was found to scale inversely with mosaic spread. Our results strongly suggest that defects created at small-angle grain boundaries between crystallites of slightly different orientation activate ferromagnetism. This unanticipated result established that charge compensating O vacancies, introduced when Co(II) or Cr(III) substitutes for Ti(IV) in an otherwise structurally perfect lattice, are not effective at aligning the dopant spins.

In contrast, Co-doped ZnO grown by MOCVD and PLD appears to exhibit *bona vide* carrier mediated ferromagnetic exchange interaction. As-grown films were highly resistive and paramagnetic. However, post-growth *n*-type doping by vacuum annealing or Zn indiffusion resulted in the simultaneous onset of conductivity and RTFM, although the carrier concentrations achievable by this means were limited to a small fraction of the Co dopant concentration.. Significantly, the moment per Co was also a small fraction of the value expected for Co(II). Nevertheless, controlled experiments in which Zn-diffused films were annealed in air to draw to the surface and oxidize interstitial Zn revealed a direct kinetic correlation between interstitial Zn concentration, conductivity and saturation moment. In fact, ferromagnetic exchange coupling between Co spins depends on both itinerant electrons and shallow bound electrons from interstitial Zn donors. This work constitutes the first definitive demonstration of a direct coupling between donor electrons and RTFM in a magnetically doped oxide.

Finally, Ti:α-Fe_2O_3 also exhibits RTFM, but not as much as expected if Ti preferentially replaces Fe in one particular magnetic sublattice. Displacement in exclusively one magnetic sublattice results in a structure not unlike that of ilmenite ($FeTiO_3$), in which one of the two cation sublattice bilayer types is occupied entirely by Ti and the other by Fe. The magnetic hysteresis loops exhibited a dual-lobe structure which is best interpreted as two microstructurally distinct regions. The dual lobes suggest the presence of two magnetic phases, one of high coercivity and one of low coercivity. Our data suggest that the loop originates with the ilmenite-like phase, some of which contains anti-phase boundaries. The low-coercivity portion results from coherent rotation with magnetic field while the high-coercivity portion is caused by grain boundary domain wall pinning. Our combined magnetic and structural results suggest that a minority (~1/8) of Ti forms a ferromagnetically ordered ilmenite-like phase and the remainder is

randomly distributed throughout the lattice. The resistivity drops with increasing Ti concentration, but not to values expected if all Ti donor electrons are itinerant. This result suggests some degree of carrier localization, and indeed, photoemission shows that localization on Fe sites is detectible at higher Ti concentrations. Ti thus acts as either a deep donor or the source of hopping conductivity through electron localization on Fe sites, and as a magnetic 'undopant'. In the latter role, Ti substitutes for Fe somewhat preferentially in one magnetic sublattice, producing a net spin. Carriers are also generated by the Ti dopants, but the saturation magnetization is independent of carrier concentration. Thus, we conclude that the ferromagnetism in Ti:α-Fe_2O_3 is an intrinsic result of Ti(IV) substituting for Fe(III) in a partially non-random way, and is not coupled to the presence of carriers, which originate with Ti donors.

Future Work

Our future thrusts include expanding and refining our understanding of some of the above systems, and investigating new ones. Increasing the carrier concentration in *n*-type Co-doped ZnO by Al doping, along with determining the effect of higher carrier concentration on exchange coupling of Co spins, is an immediate goal. We also want to grow and understand (Mn,N):ZnO. This system shows promise as a *p*-type high-T_c DMS, although there is considerable controversy in the literature about its true character. In order to gain a deeper understanding of this material, we are developing a novel preparation method for it and for (Co,Al):ZnO. We are collaborating with Professor Daniel Gamelin of the University of Washington to fashion nanoparticles of these materials, grown by direct chemical methods in the Gamelin lab, into PLD targets. At issue is whether or not compositional uniformity on the nanoscale in the target results in superior epitaxial film properties. We also intend to collaborate with Professor Marija Gajdardziska-Josifovska of the University of Wisconsin at Milwaukee to do HRTEM and EELS on MBE-grown Ti-doped α-Fe_2O_3, in order to probe the relationship between nano- and mesoscale structure and magnetic/electronic properties. Finally, we plan to initiate work on epitaxial Cr- and Co-doped $SrTiO_3$ with the goal of determining the relationship between dopant charge and structural environment and magnetic/ magnetoelectronic properties in these materials.

DOE Sponsored Publications in 2004-2006

S.A. Chambers, T. Droubay, T.C. Kasper, M. Gutowski, M. van Schilfgaarde, "Accurate Valence Band Maximum Determination for $SrTiO_3$(001)", Surf. Sci. **554**, 81 (2004).

S.A. Chambers, T. Droubay, T.C. Kasper, M. Gutowski, "Experimental Determination of the Valence Band Maximum for $SrTiO_3$, TiO_2 Anatase, and SrO and the Associated Band Offsets with Si(001)", J. Vac. Sci. Technol. **B 22**, 2205 (2004).

A.C. Tuan, J.D. Bryan, A.B. Pakhomov, V. Shutthanandan, S. Thevuthasan, D.E. McCready, D. Gaspar, M. Engelhard, J.W. Rogers, Jr., K. Krishnan, D.R. Gamelin, S.A. Chambers, "Epitaxial Growth and Properties of Co-doped ZnO on α-Al_2O_3 Single Crystal Substrates", Phys. Rev. **B 70**, 054424 (2004).

T. Droubay, S.M. Heald, V. Shutthanandan, S. Thevuthasan, S.A. Chambers, "Cr-doped TiO_2 Anatase – A Ferromagnetic Insulator", J. Appl. Phys. **97**, 046103 (2005).

J. Osterwalder, T. Droubay, T. Kaspar, J. Williams, S.A. Chambers, "Growth of Cr-doped TiO_2 Films in the Rutile and Anatase Structure by Oxygen-Plasma Assisted Molecular Beam Epitaxy", Thin Solid Films **484**, 289 (2005).

T.C. Kaspar, T. Droubay, C.M. Wang, S.M. Heald, A.S. Lea, S.A. Chambers, "Co-doped Anatase TiO_2 Heteroepitaxy on Si(001)", J. Appl. Phys. **97**, 073511 (2005).

J.E. Jaffe, T.C. Droubay, S.A. Chambers, "Oxygen Vacancies and Ferromagnetism in $Co_xTi_{1-x}O_{2-x-y}$", J. Appl. Phys. **97**, 073908 (2005).

S.M. Heald, S.A. Chambers, T. Droubay, "XAFS Study of Epitaxial $Co_xTi_{1-x}O_{2-x}$ Anatase", Phys. Script. **T115**, 597 (2005).

Scott A. Chambers, Timothy C. Droubay and Tiffany C. Kaspar, "Epitaxial Growth and Properties of Magnetically Doped TiO_2" (invited book chapter), Ch. 7 in *Thin Films and Heterostructures for Oxide Electronics*, ed. Satish Ogale, Kluwer Academic Publishers (2005).

T. C. Kaspar, S. M. Heald, C. M. Wang, J. D. Bryan, T. Droubay, V. Shutthanandan, S. Thevuthasan, D. E. McCready, A. J. Kellock, D. R. Gamelin, S. A. Chambers , "Negligible Magnetism in $Cr_xTi_{1-x}O_2$ Anatase with Excellent Structural Quality: Contrast with High-T_c Ferromagnetism in Structurally Defective $Cr_xTi_{1-x}O_2$", Phys. Rev. Lett. **95**, 217203 (2005).

T.C. Kaspar, T. Droubay, V. Shutthanandan, S.M. Heald, C.M. Wang, D.E. McCready, S. Thevuthasan, J.D. Bryan, D.R. Gamelin, A.J. Kellock, M.F. Toney, X. Hong, C.H. Ahn, S.A. Chambers, "Ferromagnetism and Structure in Epitaxial Cr-doped Anatase TiO_2", Phys. Rev. **B 73**, 155327 (2006).

T.C. Kaspar, T. Droubay, D.E. McCready, S.M. Heald, C.M. Wang, A.S. Lea, V. Shutthanandan, S.A. Chambers, "Magnetic Properties of Epitaxial Co-doped Anatase TiO_2 Thin Films with Excellent Structural Quality", J. Vac. Sci. Technol. **B24**, 2012 (2006).

K.R. Kittilstved, D.A. Schwartz, A.C. Tuan, S.M. Heald, S.A. Chambers, D.R. Gamelin, "Direct Kinetic Correlation of Carriers and Ferromagnetism in Co^{2+}:ZnO", Phys. Rev. Lett. **97**, 037203 (2006).

Scott A. Chambers, "Ferromagnetism in Thin-Film Oxide and Nitride Semiconductors and Dielectrics" (invited review), Surf. Sci. Rep. **61**, 345 (2006).

Scott A. Chambers, William K. Liu, Kevin Kittilstved, Daniel R. Gamelin, "Growth, Electronic and Magnetic Properties of Doped ZnO Epitaxial and Nanocrystalline Films", App. Phys. A: Mat. Sci. & Proc., in press (2006).

Scott A. Chambers, "Electron Mediated Ferromagnetism in Oxide Semiconductors?" (invited review), Materials Today, in press (2006).

T.C. Droubay, K.M. Rosso, S.M. Heald, D.E. McCready, C.M. Wang, S.A. Chambers, "Structure, Magnetism and Conductivity in Epitaxial Ti-doped α-Fe_2O_3 Hematite", Phys. Rev. B, submitted (2006).

FILTERED ELECTRON BACKSCATTER DIFFRACTION

Andrew Deal[1], Tejpal Hooghan, and Alwyn Eades[2]
[1]deal@research.ge.com, [2]jae5@lehigh.edu
Department of Materials Science and Engineering, Lehigh University

Program Scope

The Electron Backscatter Diffraction (EBSD) analytical technique is invaluable for determining the crystallography of bulk alloys, thin films, and nanoparticles [1-4]. Presently, the highest demonstrated EBSD resolution is on the order of 10 nm. As the EBSD technique continues to develop, debate over its ultimate limitations exists, since our physical picture of EBSD is incomplete. Our current understanding is that most diffracted electrons come from a small portion of the interaction volume and, consequently, have energies close to the incident beam energy. Specifically, only electrons of energy within 10% of the incident beam energy have been considered as major contributors to EBSD patterns, a range stemming from Monte Carlo simulations [5]. Contributing electrons that experience a significant energy loss due to inelastic collisions are generally thought to be small in number and compose the diffuse background of EBSD patterns. In this article, we present our initial efforts to both advance EBSD capabilities and experimentally investigate the physics of the technique using an energy filter with a resolution of 10 eV, over a large atomic number range. We verify that low-loss electrons are the major contributors to EBSD patterns, but that there is still a diffraction contribution from electrons with only 80% of the incident beam energy. The bands in filtered EBSD patterns have contrast that is more than twice the contrast of their unfiltered counterparts which may lead to improvements in automated indexing speed with future development of the filter.

Recent Progress

STAIB Instruments Inc. developed the energy filter we used in this work, shown in Figure 1. Two electrostatic lenses (L1, L2) collimate the backscattered electrons so that they approach a fine, planar, wire grid (G) at normal incidence. The electrons maintain their spatial distribution as they approach the grid, and a voltage applied to the grid induces a filtering action. Electrons with energies below the grid potential energy, the cutoff energy, are repelled; consequently, they are eliminated from the EBSD pattern. Electrons with energies above the cutoff pass through the filtering grid, and they are reaccelerated by a third electrostatic lens (L3) towards a phosphor screen (S). The EBSD pattern on the screen is digitally captured by a cooled, low-noise CCD camera.

The cutoff energy of the filter is tunable from 0 keV to 20keV with better than 10eV resolution, enabling a precise investigation of contributing electron energies. Moreover, the lens settings scale automatically with cutoff energy, so that focusing at a single cutoff energy ensured the EBSD pattern was filtered with a sharp energy cutoff through the entire energy range of the filter.

We examined {001} single crystals of Si, Fe, and Ir using the energy filter to cover a range of atomic numbers. The filter resided on a FEI DB 235 dual-beam FIB, with a thermal FEG SEM column. (The ion column was not used in these experiments.) We mounted the crystals on a 70^{o} pre-tilted specimen holder, and we aligned the pattern

center with the axis of the energy filter to ensure proper filtering. Using a 15keV beam, we digitally recorded a series of EBSD patterns for each crystal, varying the filter cutoff energy from 0 to 15 keV over 48 increments.

One of the first observations we made when analyzing the recorded EBSD patterns was that there is significantly higher contrast in the filtered EBSD patterns. Figure 2 demonstrates this qualitatively: images a-c are unfiltered Si, Fe, and Ir patterns, while images d-f are filtered Si, Fe, and Ir patterns using a 14keV cutoff energy. We obtained more quantitative contrast data by focusing on the strongest Kikuchi band for each material and calculating the contrast at each cutoff energy (Figure 3). The data show that, by filtering, the band contrast for Si, Fe, and Ir can be increased by a factor of 2.8, 2.2, and 2.1, respectively. It is also evident that, for a given cutoff energy, the increase in band contrast for the Si is greater than that for the Fe, which is more than that for the Ir. Thus, the enhancement of the contrast, resulting from the energy filtering, seems to decrease monotonically with increase of atomic number. Our observation of the enhanced contrast is consistent with the current belief that low-loss electrons are the major contributors to EBSD patterns. Since the widths of Kikuchi bands increase as the energy of the diffracting electrons decreases, the low-loss, high-energy electrons will produce an EBSD pattern with narrow Kikuchi bands. However, high-loss, low-energy electrons that diffract will produce a pattern with wider bands. The weaker contribution of these high-loss electrons will smear the strong pattern of the low-loss electrons. Moreover, high-loss electrons have a greater possibility of scattering diffusely, since the scattering cross-section increases with decreasing energy. These electrons will contribute to the overall diffuse background signal inherent in unfiltered EBSD patterns. We believe that energy filtering enhances the contrast of the patterns simply by removing the background signal generated by scattered and diffracted high-loss electrons.

These results lead to several conclusions about the diffraction contribution of electrons in EBSD patterns. First, electrons having 90% of the incident beam energy are major contributors to the EBSD patterns, although there is a clear dependence on the scattering ability of the material. Si, with its lesser scattering ability, has the greatest contribution at 90%, whereas Ir has the weakest pattern. Second, at least for Si and Fe, electrons with 80% of the beam energy still diffract and contribute to the pattern. This is an important point to consider when measuring lattice constants from EBSD patterns. Third, the diffraction contrast is lower at 80% of the incident beam energy than at 90%, which means that the lower energy electrons contribute more to the diffuse background than to the EBSD pattern.

We were able to obtain information about the energy distribution of electrons from the data we collected. By summing the pixel intensities in each image, we calculated the backscatter yield as a function of the cutoff energy for each material, as shown in Figure 4. The intensity for each material stays relatively constant for about half of the cutoff energy range, drops rapidly at higher cutoff energies, and finally levels out to zero as the cutoff energy approaches incident beam energy. The relatively constant initial intensity indicates that the signal from high-loss backscattered electrons to an EBSD pattern is minimal. The steepest drop occurs for Ir, followed by Fe, and then Si, which has the shallowest approach. This is consistent with scattering strength of the materials, which increases with atomic number.

Future Plans

We have shown that energy filtered EBSD leads to enhanced band contrast. This increased contrast may prove useful for automated EBSD analysis by possibly eliminating the need for a background subtraction step and improving the ability to detect Kikuchi bands. Both would likely increase the speed of automated indexing routines. Additionally, we have demonstrated that there is a diffraction contribution from electrons well below the incident beam energy. While this contribution is small, it serves to blur the Kikuchi bands and may hinder the ability to accurately determine the lattice parameters of a material. Filtering the EBSD patterns eliminates this problem. Our experiments have also verified that the major contributors to the EBSD patterns are electrons within 5% of the incident beam energy. Finally, we recognize that another possible benefit of energy filtering EBSD pattern is an increase in spatial resolution. Low-loss electrons obtained with a high cutoff energy must emanate from a region of the sample that is very close the beam impact point. It seems plausible that filtered patterns could therefore be used to obtain crystallographic information from grains smaller than would be possible with unfiltered patterns, and we intend to explore this possibility.

References:

[1] D.J. Prior et al., *American Mineralogist.* 84 (1999) 1741-1759.

[2] F.J. Humphreys, *Journal of Materials Science.* 36 (2001) 3833-3854.

[3] K.Z. Baba-Kishi, *Journal of Materials Science.* 37 (2002) 1715-1746.

[4] D. Dingley, *Journal of Microscopy.* 213 (2004) 214-224.

[5] S.X. Ren, E.A. Kenik, K.B. Alexander, and A. Goyal. *Microscopy and Microanalysis* 4 (1998) 15-22.

Figures:

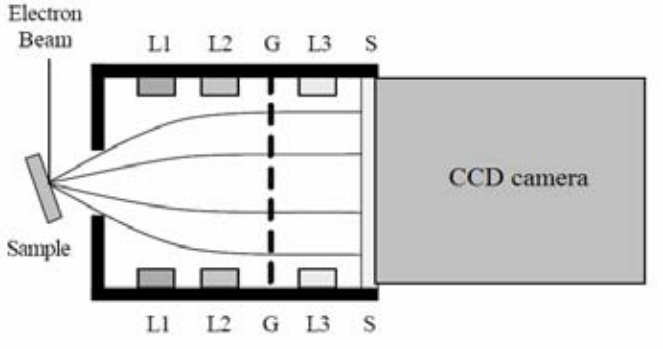

Figure 1 – Schematic diagram of the energy filter. L1, L2 are collimating lenses, G is the filtering grid, L3 is an accelerating lens, and S is the phosphor screen.

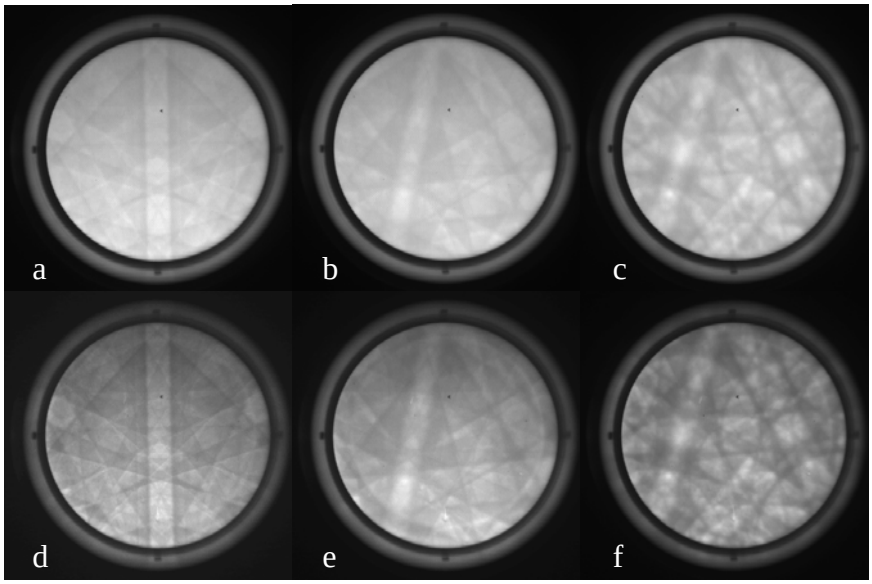

Figure 2 – Energy filter results for a 15keV incident beam. (a-c) Unfiltered Si, Fe, and Ir EBSD patterns, respectively. (d-f) Filtered EBSD patterns with a 14.5 keV cutoff for Si, Fe, and Ir.

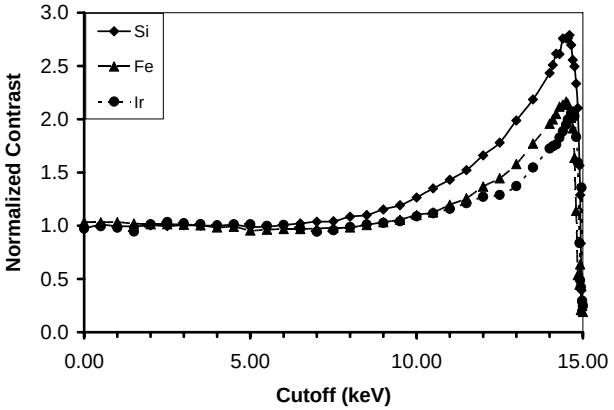

Figure 3 – Experimental contrast vs. cutoff energy. The contrast is normalized by its unfiltered value for comparison.

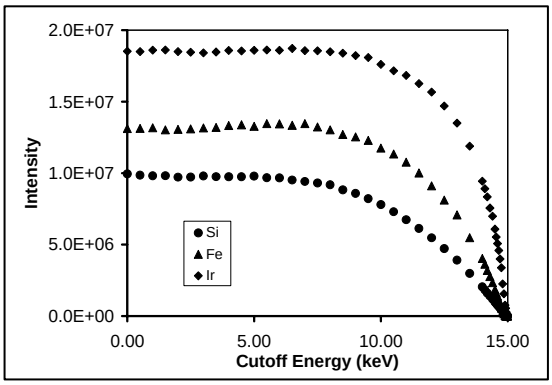

Figure 10 – Total image intensity vs. filter cutoff energy

Recent Publications:

1. EBSD geometry in the SEM: simulation and representation, A. Deal, X. Tao, and A. Eades. *Surface and Interface Analysis*. 37 (2005) 1017-1020.
2. Errors, artifacts, and improvements in EBSD processing and mapping, X. Tao, and A. Eades, *Microscopy and Microanalysis*, 11 (2005), 79-87.
3. Measurement and mapping of small changes of crystal orientation by electron backscattering diffraction, X. Tao, and A. Eades, *Microscopy and Microanalysis*, 11 (2005), 341-53.

In-Situ Synchrotron X-Ray Studies of Interfacial Reactions

Jeffrey A. Eastman[1], Dillon D. Fong[1], Paul H. Fuoss[1], Fan Jiang[1], G. Brian Stephenson[1,2], Stephen K. Streiffer[2], Carol Thompson[3], Ruey-Ven Wang[1,2], and Guang-Wen Zhou[1]
jeastman@anl.gov, fong@anl.gov, fuoss@anl.gov, fjiang@anl.gov, stephenson@anl.gov, streiffer@anl.gov, cthompson@niu.edu, rvwang@anl.gov, gzhou@anl.gov
[1]Materials Science Division, Argonne National Laboratory, Argonne, IL 60439
[2]Center for Nanoscale Materials, Argonne National Laboratory, Argonne, IL 60439
[3]Physics Department, Northern Illinois University, DeKalb, IL 60115

Program Scope

A broad spectrum of scientific and technological needs that are critical to the mission of Basic Energy Sciences require understanding of atomic-scale processes at interfaces under elevated temperature and non-vacuum reaction conditions, where many structural and chemical probes can not operate. Discovery research is required in these areas utilizing a probe that is tailored to the environment, rather than compromising environmental conditions to allow use of traditional methods. In-situ x-ray scattering techniques are particularly well-suited for providing the needed information, and are being used in our programs to address central issues relevant to the following areas:

Oxide Thin Film Synthesis – Our studies are providing a detailed understanding of complex oxide thin film growth processes, particularly focused on metalorganic chemical vapor deposition (MOCVD) of $PbTiO_3$ and $Pb(Zr_x,Ti_{1-x})O_3$ (PZT) thin films. Insight is being provided into the effects of nanoscale size, strain, and chemistry (sample and environment) on the growth behavior and ferroelectric properties of these films.

Early-stage Oxidation – We address major unresolved issues associated with the oxidation behavior of metals and alloys, emphasizing early-stage behavior, during which oxide nano-islands nucleate and grow. These studies bridge the current information gap between UHV surface science studies and investigations of bulk oxidation behavior. Our ability to perform these measurements under quasi-equilibrium conditions allows for the separation of thermodynamic and kinetic effects. The current emphasis of our program is on understanding the oxidation behavior of Cu and Pd alloys.

Catalysis of redox reactions – In-situ x-ray scattering and fluorescence techniques are being employed to provide needed information on structure-chemistry-property relations for catalysts under reaction conditions, eliminating the “pressure gap” that is universally acknowledged to be one of the primary experimental challenges for the community. Our recent initial efforts in this area are focused on understanding structure-property relations during oxidation of methanol catalyzed by oxide-supported Cu and Pd single crystal alloy films and nano-islands.

Recent Progress

We have developed two unique facilities at the Advanced Photon Source (APS), one for in-situ MOCVD oxide growth [1], and a second system for processing and properties studies of materials, including metals and alloys, in controlled gas composition (*e.g.*, oxygen partial pressure) and temperature [2]. Recent accomplishments using these facilities relate to determining the effects of environment on the behavior of ferroelectric $PbTiO_3$ films, as well as the early-stage oxidation and catalytic behavior of copper single crystal films, as briefly described in the following:

Environmental Control of Ferroelectricity in Coherently-Strained $PbTiO_3$ Films

Compensation of the depolarization field by free charge at interfaces is a determining factor for the ferroelectric phase transition and for domain structures in ferroelectric thin films. Our studies of coherently-strained films of $PbTiO_3$ on (001) $SrTiO_3$ have shown that ferroelectricity persists in films

as thin as three unit cells [3]. As temperature is lowered from the ferroelectric transition temperature, we observe a sequence of domain structures [4], controlled by changes in charge compensation at interfaces [5]. The stability of monodomain polarization in ultrathin films has been explained by ionic adsorption on the surface [6]. These results indicate that, by modifying interface chemistry, we may be able to control ferroelectric domain structure and manipulate ferroelectricity.

We recently investigated the behavior of $PbTiO_3$ thin films, coherently grown on insulating (001) $SrTiO_3$ or conducting (001) $SrRuO_3/SrTiO_3$, that were then equilibrated under different gas environments chosen to manipulate surface chemistry. Utilizing synchrotron x-ray surface scattering, we monitored the evolution of ferroelectric polarization and domain structure in real time as the oxygen partial pressure of the ambient was varied. The sign of the polarization was determined to be reversible by changing between reducing and oxidizing conditions. Different surface structures were also found to form in response to different gas environments.

Early-Stage Oxidation Behavior of Cu (001)

A serious drawback to typical previous studies of oxygen-induced surface structures and metal and alloy oxidation is that they were done under conditions where there was no dynamic interaction between the surface and the gas phase. We have recently performed in-situ synchrotron x-ray studies of the Cu (001) surface as functions of the oxygen partial pressure (pO_2) and temperature. Initial exposure of clean Cu (001) to low pO_2 results in a disordered adsorbate structure, with oxygen residing in 4-fold hollow sites. Larger pO_2 produces large *c*(2×2)-O domains and is concurrent with a small in-plane surface contraction and a large out-of-plane surface expansion. We also observe that the often-reported $\left(2\sqrt{2}\times\sqrt{2}\right)R45°$ reconstruction [7] is stable only at lower temperatures (below ~ 150 °C) [8]. Above a critical pO_2, Cu_2O nano-islands nucleate and grow. Interestingly, we find that the equilibrium Cu/Cu_2O phase boundary for these nano-islands occurs at orders-of-magnitude larger pO_2 than predicted by bulk thermodynamics [9], indicating that size plays an important role in determining oxidation thermodynamics.

Catalysis of Methanol Oxidation over Cu (001)

Copper-based catalysts are used in a number of important chemical processes including methanol production, methanol reforming to produce hydrogen, and the partial oxidation of methanol to synthesize formaldehyde. Oxygen on Cu surfaces is known to increase activity for methanol decomposition [10], but the effects of nanoscale Cu_2O islands or oxygen-induced surface structures on catalytic properties are not understood, primarily because of the scarcity of atomic-scale structural and chemical information obtained under typical reaction conditions. We are employing in-situ x-ray techniques to characterize methanol oxidation on Cu (001). Our quartz-walled deposition system at the APS allows controlled mixtures of oxygen, methanol vapor, and other gases to be flowed under a wide range of pressures. Reaction products are monitored with a quadrupole mass spectrometer at reaction temperatures from 25 to 1000 °C. We have determined the effects of methanol vapor on the stability of the *c*(2×2)-O surface structure and on the Cu/Cu_2O T-pO_2 phase diagram, providing insight into the important structural features responsible for catalytic activity [11].

Future Plans

We are continuing to explore the synthesis, processing, and properties of oxides and oxidized metal and alloy surfaces, making use of the unique capabilities available through the use of in-situ synchrotron x-ray techniques.

In the area of ferroelectric thin film growth and properties, to date we have primarily studied the phase transition in $PbTiO_3$ films maintained in an oxidizing environment and with a PbO surface termination. We are now in a position to vary the surface chemistry to understand the mechanism of charge compensation. For these experiments, $PbTiO_3$ films will be grown in-situ by MOCVD to

achieve desired surface terminations and film thicknesses and to avoid surface contamination. Our previous results give us confidence that we will be able to study the interaction of the vapor environment with the polarization structure using real-time x-ray techniques. To determine the nature of the interface compensation, we will measure the interface and film domain structures (through modeling of reconstruction and crystal truncation rod intensities) as we vary temperature, oxygen partial pressure, PbO vs. TiO_2 surface termination, $PbTiO_3$ film thickness, and use substrates with different electrical properties (*e.g*. insulating $SrTiO_3$, conducting $SrRuO_3$ layers on $SrTiO_3$, and semiconducting Nb-doped $SrTiO_3$). Through these studies we will determine whether the compensating species at the surface are better described as adsorbed ions, or as point defects in the crystal (e.g. oxygen vacancies). We will also determine how the film domain structure and polarization orientation respond to the vapor environment, how the surface structure and polarization orientation interact, and whether the compensating species differ for PbO and TiO_2 terminated surfaces.

Related to our interests in early-stage oxidation and catalytic behavior of metal alloys, we are continuing to determine the links between oxide nucleation/growth and surface structure in model binary systems, including Cu-Ni, Cu-Pd, and Pd-Fe alloys. Through choice of pO_2 we can control whether both or only the less noble component in the alloy oxidizes. By monitoring total x-ray reflection fluorescence (TXRF) signals in combination with diffraction measurements we can determine the interplay between surface segregation and oxidation behavior. One goal is to determine the effects on oxidation behavior of adsorbate-induced segregation behavior, where adsorbates alter the surface energetics such that the previously unfavored element in an A-B alloy can become thermodynamically preferred at the surface. Since this can strongly affect the subsequent processes of oxide nucleation and growth, understanding adsorbate-induced segregation is a necessary step in the course of alloy oxidation studies. In the case of Cu-Ni alloys, it is known that Gibbsian segregation of Cu is favored when samples are annealed under vacuum conditions, but that annealing in a CO environment instead causes Ni surface segregation [12]. As for Cu-Pd, a popular bimetallic catalyst for a variety of reactions including CO oxidation, O and CO have been shown to have opposite effects on the Pd segregation behavior [13]. Studies of Cu-Pd alloy oxidation behavior are thus also directly relevant to better under the catalytic behavior of this alloy. Studies of Pd-Fe alloys will provide an understanding of the additional complexity induced by a composition- and temperature-dependent order-disorder transition in the alloy. Understanding the effects of structure and morphology of Pd-Fe alloys under oxidizing conditions is also of importance for understanding the behavior of this potentially important catalytic system [14].

References

1) G.B. Stephenson, J.A. Eastman, O. Auciello, A. Munkholm, C. Thompson, P.H. Fuoss, P. Fini, S.P. DenBaars, J.S. Speck, *MRS Bulletin*, **24**, 21(1999).
2) P.H. Fuoss, J.A. Eastman, L.E. Rehn, P. Baldo, G.-W. Zhou, D.D. Fong, L. Thompson, *APS Science 2004*, Argonne National Laboratory Report ANL-05/04, 119(2005).
3) D. D. Fong, G. B. Stephenson, S. K. Streiffer, J. A. Eastman, O. Auciello, P. H. Fuoss, and C. Thompson, *Science*, *304*, 1650(2004).
4) S.K. Streiffer, J.A. Eastman, D.D. Fong, Carol Thompson, A. Munkholm, M.V. Ramana Murty, O. Auciello, G.-R. Bai, and G.B. Stephenson, *Phys. Rev. Lett.* **89**, 067601 (2002).
5) G. B Stephenson, K.R. Elder, *J. Appl. Phys*., **100**, 051601 (2006).
6) D. D. Fong, A. M. Kolpak, J. A. Eastman, S. K. Streiffer, P. H. Fuoss, G. B. Stephenson , C. Thompson, D. M. Kim, K. J. Choi, C. B. Eom, I. Grinberg, A. M. Rappe, *Phys. Rev. Lett.* **96**, 127601 (2006).
7) M. Wuttig, R. Franchy, and H. Ibach, *Surf. Sci*., **213**, 103 (1989); I.K. Robinson, E. Vlieg, and S. Ferrer, *Phys. Rev. B*, **42**, 6954 (1990).

8) P.H. Fuoss, D.D. Fong, J.A. Eastman, G.-W. Zhou, P.M. Baldo, L.J. Thompson, L.E. Rehn, "In-Situ Synchrotron X-Ray Observations of Oxygen-Stabilized Equilibrium Surface Structures on Cu (001)," submitted to *Phys. Rev. Lett.* (2006).
9) J.A. Eastman, P.H. Fuoss, L.E. Rehn, P.M. Baldo, G.-W. Zhou, D.D. Fong, and L.J. Thompson, *Appl. Phys. Lett*. 87, 051914, (2005).
10) I.E. Wachs and R.J. Madix, *J. Catal*., **53**, 208 (1978); B.A. Sexton, A.E. Hughes, and N.R. Avery, *Surf. Sci.*, **155**, 366 (1985).
11) J.A. Eastman, D.D. Fong, P.H. Fuoss, P.M. Baldo, L.J. Thompson, G.-W. Zhou, "In-Situ Synchrotron X-Ray Studies of Structure-Property Relationships During Methanol Oxidation on Cu (001)," in preparation.
12) J. Nerlov and I. Chorkendorff, *Catal. Lett.*, **54**, 171 (1998).
13) J.S. Bradley, E.W. Hill, B. Chaudret, and A. Duteil, *Langmuir*, **11**, 693 (1994).
14) T. Schalow, B. Brandt, D.E. Starr, M. Laurin, S. Schauermann, S.K. Shaikhutdinov, J. Libuda, and H.-J. Freund, *Catalysis Letters*, 107, no. 3-4, 189-196 (2006).

DOE Sponsored Publications in 2004-2006

Dillon D. Fong, G. Brian Stephenson, Stephen K. Streiffer, Jeffrey A. Eastman, Orlando Auciello, Paul H. Fuoss, Carol Thompson, "Ferroelectricity in Ultrathin Perovskite Films," *Science*, **304**, 1650-1653 (2004).

D.D. Fong, Carol Thompson, S.K. Streiffer, J.A. Eastman, O. Auciello, P.H. Fuoss, G.B. Stephenson, "*In situ* synchrotron X-ray studies of $PbTiO_3$ thin films," *Ann. Phys. (Leipzig)* **13**, no. 1-2, 27-30 (2004).

D.D. Fong, J.A. Eastman, G.B. Stephenson, P.H. Fuoss, S.K. Streiffer, Carol Thompson, and O. Auciello, "*In Situ* Synchrotron X-ray Studies of Ferroelectric Thin Films," *Journal of Synchrotron Radiation*, **12**, pp. 163-167 (2005).

D.D. Fong, C. Cionca, Y. Yacoby, G.B. Stephenson, J.A. Eastman, P.H. Fuoss, S.K. Streiffer, C. Thompson, R. Pindak, E.A. Stern, D.A. Walkko, R. Clarke, "Direct Structural Determination in Ultrathin Ferroelectric Films by Analysis of Synchrotron X-Ray Scattering Measurements," *Phys. Rev. B*, **71**, 144112 (2005).

P.H. Fuoss, J.A. Eastman, L.E. Rehn, P.M. Baldo, G.-W. Zhou, D.D. Fong, L.J. Thompson, "A Controlled-Atmosphere System for In-Situ Materials Processing at the APS," APS Science 2004, ANL-05/04, pp. 119-120 (2005).

J.A. Eastman, P.H. Fuoss, L.E. Rehn, P.M. Baldo, G.-W. Zhou, D.D. Fong, and L.J. Thompson, "Early-Stage Suppression of Cu (001) Oxidation," *Appl. Phys. Lett*. **87**, 051914, (2005).

P.H. Fuoss, R.-V. Wang, J.A. Eastman, D.D. Fong, G.B. Stephenson, S.K. Streiffer, Carol Thompson, F. Jiang, G.-W. Zhou, L.E. Rehn, P.M. Baldo, L.J. Thompson, "In-Situ X-Ray Analysis of Materials Growth and Processing," *J. Taiwan Vac. Tech. Soc.*, **18** (2005).

G. B. Stephenson, S. K. Streiffer, D. D. Fong, M. V. Ramana Murty, O. Auciello, P. H. Fuoss, J. A. Eastman, A. Munkholm, C. Thompson, "In-Situ Synchrotron X-Ray Studies of Processing and Physics of Ferroelectric Thin Films," Chapter 8 in Polar Oxides - Properties, Characterization and Imaging, VCH Wiley Pub. (2005).

D. D. Fong, A. M. Kolpak, J. A. Eastman, S. K. Streiffer, P. H. Fuoss, G. B. Stephenson , C. Thompson, D. M. Kim, K. J. Choi, C. B. Eom, I. Grinberg, A. M. Rappe, "Stabilization of Monodomain Polarization in Ultrathin $PbTiO_3$ Films," *Phys. Rev. Lett.*, **96**, 127601, (2006).

G.-W. Zhou, L. Wang, R.C. Birtcher, P.M. Baldo, J.E. Pearson, J.C. Yang, J.A. Eastman, "Cu_2O island shape transition during Cu-Au alloy oxidation," *Phys. Rev. Lett.*, **96**, 226108 (2006).

New Magnetic Behavior of Nanostructures

Zheng Gai and Jian Shen
gaiz@ornl.gov, shenj@ornl.gov

Materials Science and Technology Division & Center for Nanophase Materials Science Division, Oak Ridge National Laboratory, Oak Ridge, TN 37830

Program Scope

The primary goal of this program is to investigate the consequences of spatial confinement on spin structure, and spin dynamics. New properties that emerge at the nanoscale have at least three origins. First, as the surface to volume ratio increases, material properties are increasingly dominated by surface and interface effects. Secondly, spatial confinement results in new quantum phenomena. The oscillatory exchange coupling [1], GMR, spin tunneling[2], and exchange bias[3-5] manifest in magnetic multilayers are linked with one or both of these factors. Finally, spatial confinement will enhance correlation effects. Surface and interface effects modify moment sizes, exchange interactions, anisotropy energies, and modes of electron transport. These changes affect the spin structure (moment size and order, non-collinear magnetism), spin dynamics (spin wave dispersion and lifetime, switching modes and times, moment stability at finite temperature and phase transitions, quantum tunneling), and spin transport (disorder and spin-flip scattering, channeling, quantum conductance, spin current-driven changes in moments). The richness of magnetism in nanostructured materials arises from the interplay between all of these effects. Uncovering and exploiting these interrelationships in different classes of materials requires a concerted research effort involving novel synthesis, advanced characterization, and innovative theory and modeling. Success will result in increased scientific understanding, new classes of nanostructured materials, new physical phenomena, and new technological opportunities.

Recent Progress

To cleanly and systematically study the magnetic and transport properties of nanostructures, well controlled growth is an essential first step. For example, the magnetic behavior of nanodot assemblies depends on the strength of interactions and anisotropy, which are controlled by dot-dot spacing and the electronic structure of the substrates. It would be ideal to simultaneously achieve tunable uniformity in size, spatial distribution, chemical composition, and crystallographic orientation. Recently we have been successful in two generic approaches to synthesize magnetic nanostructures: buffer layer assisted growth (BLAG) [6] and Volmer-Weber (VW) growth on various substrates [7]. To gain an additional tuning parameter for the dot system, we have extended our growth to fabricate 3D dot assemblies, i.e., multilayer dots [8].

The BLAG technique is applicable to growing nanodots on many types of substrates. Moreover, by either changing the dosage of magnetic elements or the thickness of the inert gas buffer layer, there is a big advantage in terms of the ease of tuning the average spacing and the size of the nanodots [6] (Fig.1). While a broad size distribution is a common problem

in VW growth, our recent work showed that one could achieve remarkable size uniformity in VW systems by optimizing epitaxial strain mediated long-range interaction between the dots [7]. The average spacing between the magnetic dots can be tuned conveniently by controlling the nominal thickness of the deposited materials, and the chemical composition can be easily controlled by adjusting the relative deposition rate of element sources, which gives us an additional handle for tuning the magnetic behavior of the dots (Fig.2).

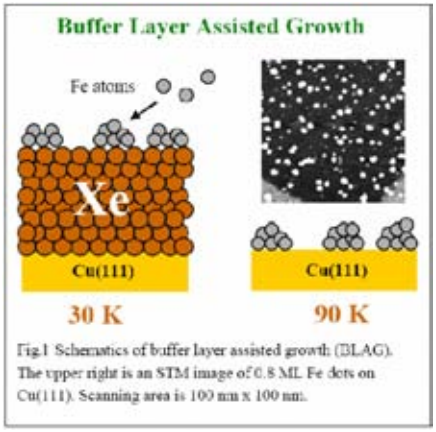

Fig.1 Schematics of buffer layer assisted growth (BLAG). The upper right is an STM image of 0.8 ML Fe dots on Cu(111). Scanning area is 100 nm x 100 nm.

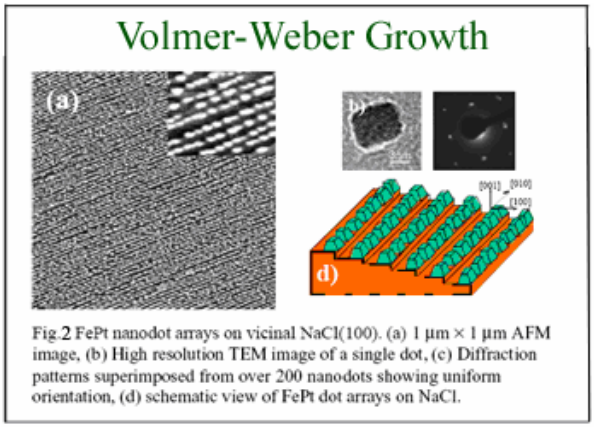

Fig.2 FePt nanodot arrays on vicinal NaCl(100). (a) 1 μm × 1 μm AFM image, (b) High resolution TEM image of a single dot, (c) Diffraction patterns superimposed from over 200 nanodots showing uniform orientation, (d) schematic view of FePt dot arrays on NaCl.

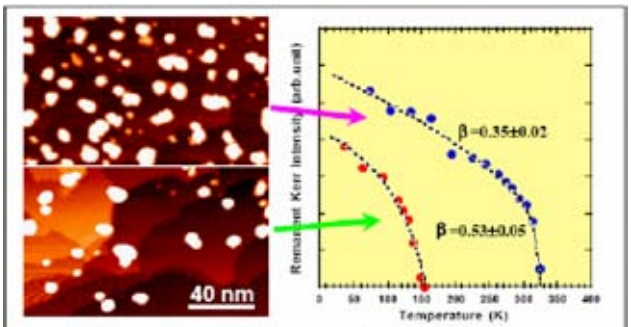

Fig.3 Morphology of two Fe/Cu(111) nanodots assemblies with the same average size but different density. The denser dot assembly exhibits a considerably higher Curie temperature

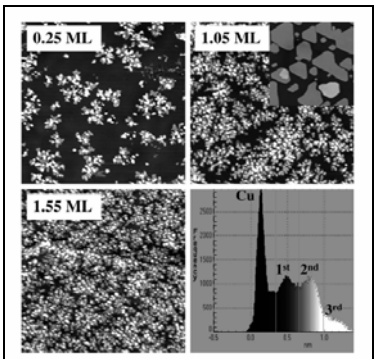

FIG. 4 100 nm × 100 nm STM images of LT-grown Fe/Cu(111) films. The inset in the 1.05 ML image is the morphology of a RT grown Fe/Cu(111) film with the same thickness and the same scanning area. The histogram of the LT-grown 1.05 ML image is shown in the lower right. The labels of Cu, 1st, 2nd, and 3rd correspond to the terraces of bare Cu, and the 1st, 2nd, and 3rd layer of Fe, respectively.

Collective ferromagnetic behavior in the two-dimensional (2D) Fe dot assemblies on single crystal Cu(111) surfaces that originates from an indirect exchange interaction via the surface state of the Cu(111) substrate were observed [6]. The ferromagnetic ordering temperature appears to be strongly dependent on the average spacing between the dots. As shown in Fig. 3, for relatively dense nanodot assemblies, the exchange interaction is strong enough to allow the ferromagnetic order to persist above room temperature. Stacking these 2D Fe nanodot assemblies with Cu spacer layers allows for the formation of multilayer Fe nanodots. With an increasing number of Fe dot layers, one would expect a 2D to three-dimensional (3D) crossover. Interestingly, we found an unusual 2D to 3D crossover exists in the Fe nanodot multilayers, which displays a striking ferromagnetic to spin-glass-like transition [9]. The topmost layer of the Fe dots remains ferromagnetic throughout the phase transition, creating an interesting scenario where live surface ferromagnetism prevails despite all layers underneath becoming spin-glass-like.

For another nanostructure, an Fe fractal structure on Cu(111) grown at a low temperature (Fig.4), we recently reported an unusual interface magnetism featuring a frozen low-spin state in a thickness-driven low spin (LS) to high spin (HS) magnetic phase transition [9]. Combined information from thickness-dependent layer distributions and SMOKE signals indicates that a ferromagnetic LS interface layer stays live during and after the phase transition. This peculiar interface magnetism does not exist in room temperature (RT) 300 K grown Fe/Cu(111) films after a similar LS to HS phase transition. We speculate that the live LS interface in the LT Fe films originates from a frozen face centered cubic (fcc) Fe layer that survives a thickness-driven fcc to body centered cubic (bcc) structural transition.

Future Plans

We have been successful in finding the unusual magnetic behaviors by combining STM and AFM study of the nanostructures with magnetic measurement like MOKE and SQUID. But SPM is much more than morphology measurement. SPM is a powerful tool to study the interplay between structural, electronic, and magnetic properties on the nanometer scale. STS can reveal the electronic structure of the sample along with the morphology, while Spin Polarized –STM (SP-STM) can image the magnetic domains with ultimate resolution even down to the atomic scale. In our future plans, we will fulfill the promise of SPM to answer the questions of why those unusual magnetic behaviors exist. As an example, for the Fe nanodot assemblies, which the surface state of the substrate mediate the indirect exchange interaction, STS would be a good candidate for monitoring how the surface state changes with the dots spacing and anisotropy, and finally help us to understand how it influences the magnetic properties. Although a single nanometer-scale dot is a uniformly magnetized single domain, a nanodot assembly could have magnetic domains because of the quasi long-range order, as we showed earlier. SP-STM can be used to study the relationship between the collective domain structures of the magnetic dots assemblies and the statistical behavior of the independent dot domains with the ultimate resolution. The combination of SP-STM and STS would be unique in giving information on how the electronic structures and magnetic domain structures are related.

References

1. M.D. Stiles, *J. Magn. Magn. Mater.* 200, 322-337 (1999).
2. P.M. Levy, and S. Zhang, *Current Opinion in Solid State and Materials Science* 4, 223-229 (1999).
3. J. Nogues, and I.K. Schuller, *J. Magn. Magn. Mater.* 192, 203-232 (1999).
4. T.C. Schulthess, and W.H. Butler, *J. Appl. Phys.* 85, 5510-5515 (1999).
5. M. Kiwi, *J. Magn. Magn. Mater.* 234, 584-595 (2001).
6. J. P. Pierce, M. A. Torija, Z. Gai, J. Shi, T. C. Schulthess, G. A. Farnan, J. F. Wendelken, E. W. Plummer, and J. Shen, *Phys. Rev. Lett.* 92, 237201 (2004).

7. Z. Gai, B. Wu, J. P. Pierce, G. A. Farnan, D. J. Shu, M. Wang, Z. Zhang, and J. Shen, *Phys. Rev. Lett.* 89, 235502 (2002); Z. Gai, G. A. Farnan, J. P. Pierce, and J. Shen, *Appl. Phys. Lett.* 81, 742 (2002); Z. Gai, J.Y. Howe, J.D. Guo, D.A. Blom, E.W. Plummer, and J. Shen, *Appl. Phys. Lett.* 86, 023107 (2005).
8. M. A. Torija, A. P. Li, X. C. Guan, E. W. Plummer, and J. Shen, *Phys. Rev. Lett.* 95, 257203 (2005).
9. M.A. Torija, Z. Gai, N. Myoung, E.W. Plummer, and J. Shen, *Phys. Rev. Lett.* 95, 027201 (2005).

DOE Sponsored Publications in 2004-2005

1. "Influence of different substrates on phase separation in La1-x-yPryCaxMnO3 thin films", D. Gillaspie, J.X. Ma, H.Y. Zhai, T.Z. Ward, H.M. Christen, E.W. Plummer, and J. Shen, *J. Appl. Phys.* 99, 08S901 (2006).
2. "Effects of ferromagnetic nanowires on singlet and triplet exciton fractions in fluorescent and phosphorescent organic semiconductors", B. Hu, Y. Wu, Z.T. Zhang, S. Dai, and J. Shen, *Appl. Phys. Lett.* 88, 022114 (2006).
3. "Visualization of localized holes in manganite thin films with atomic resolution", J.X. Ma, D.T. Gillaspie, E.W. Plummer, and J. Shen, *Phys. Rev. Lett.* 95, 237210 (2005).
4. ""Live" Surface Ferromagnetism in Fe Nanodots/Cu Multilayers on Cu(111)", M. A. Torija, A. P. Li, X. C. Guan, E. W. Plummer, and J. Shen, *Phys. Rev. Lett.* 95, 257203 (2005).
5. "Magnetism in MnxGe1-x semiconductors mediated by impurity band carriers", A.P. Li, J.F. Wendelken, J. Shen, L.C. Feldman, J.R. Thompson, and H.H. Weitering, *Phys. Rev. B* 72, 195205 (2005).
6. "Frozen low-spin interface in ultrathin Fe films on Cu(111)", M.A. Torija, Z. Gai, N. Myoung, E.W. Plummer, and J. Shen, *Phys. Rev. Lett.* 95, 027201 (2005).
7. "Self-Assembled two-dimensional alloy FePt nanodot arrays with mono-dispersion and orientation", Z. Gai, J.Y. Howe, J.D. Guo, D.A. Blom, E.W. Plummer, and J. Shen, *Appl. Phys. Lett.* 86, 023107 (2005).
8. "Morphologically templated growth of aligned spinel CoFe2O4 nanorods", Z.T. Zhang, A.J. Rondinone, J.X. Ma, J. Shen, and S. Dai, *Adv. Mater.* 17, 1415 (2005).
9. "Ferromagnetic percolation in MnxGe1-x dilute magnetic semiconductor", A.P. Li, J. Shen, J.R. Thompson, and H.H. Weitering, *Appl. Phys. Lett.* 86, 152507 (2005).
10. "Ferromagnetic Stability in Fe Nanodot Assemblies on Cu(111) Induced by Indirect Coupling Through the Substrate," J. P. Pierce, M. A. Torija, Z. Gai, J. Shi, T. C. Schulthess, G. A. Farnan, J. F. Wendelken, E. W. Plummer, and J. Shen, *Phys. Rev. Lett.* 92, 237201 (2004).
11. "Growth and magnetism of metallic thin films and multilayers by pulsed-laser deposition", J. Shen, Z. Gai, and J. Kirschner, *Surf. Sci. Rep.* 52, 163 (2004).

Microscopic Subsurface Characterization of Layered Magnetic Materials using Low Temperature Magnetic Resonance Force Microscopy

P. Chris Hammel
Department of Physics, Ohio State University, Columbus, OH 43210
hammel@mps.ohio-state.edu

Program Scope

New magnetic materials and devices with unprecedented capabilities and levels of performance are now being created by tailoring the structure and composition of multi-component materials at the nanometer scale. Some of the most important examples are systems incorporating and exploiting magnetism and ferromagnetic materials. The field of spin electronics offers a new generation of devices based on the interaction of the electronic spin with these materials. The present revolution in information processing is based on manipulation of electronic charge. Spin electronics envisions exploiting the spin degree of freedom of the electron either in concert with its charge, or by itself. This could offer significant new advantages including nonvolatile memory, increased speed and reduced power consumption relative to charge-based electronics and information processing. Spin based electronics offers the possibility of new capabilities extending from high density non-volatile solid state memory to spin-transistors to spin-based quantum computation and communication.

Major obstacles that must be overcome to achieve the vision of spin electronics include understanding and extending spin lifetimes, detecting spin magnetization in nanoscale structures and improved understanding of and control over spin transport across interfaces within these composite devices. It will be essential to have characterization and imaging tools with spatial resolution finer than device dimensions, sensitivity sufficient to detect very weak magnetic moments, and, very importantly, selective sensitivity to the *deeply buried interfaces* whose characteristics play a crucial role in determining the properties of these materials in order to address these challenges.

MRFM detection of Ferromagnetic Resonance (FMRFM) and Nuclear Magnetic Resonance (NMRFM) provides the basis for very high resolution imaging and studies of subsurface features of submicron layered magnetic constituents of spin-based electronics.

Magnetic Resonance Force Microscopy (MRFM) is a novel scanned probe technique based on mechanical detection of magnetic resonance. At the heart of the technique is the compliant force sensing micromechanical element, typically a single crystalline cantilever, outfitted with a micromagnetic probe tip. This micromagnet generates a nonuniform magnetic field $\mathbf{H}_{\rm tip}$ the gradient of which $\nabla\mathbf{H}_{\rm tip}$ couples the cantilever to the magnetic moment $\mathbf{m}$ of the sample with the resulting force of probe-sample interaction given by

$$\mathbf{F} = (\mathbf{m}\cdot\nabla)\mathbf{H}_{\rm tip}.$$

This force displaces the compliant cantilever generating the measured signal. The MRFM mechanism of probe-sample coupling is much more effective than the inductive coupling mechanism between the magnetic moments under investigation and the detector coil used in conventional magnetic resonance experiment. MRFM sensitivity is further improved by application of standard *rf*/microwave magnetic resonance techniques to manipulate the sample magnetic moment $\mathbf{m}$ at the natural resonant frequency ω_c of the force sensing cantilever. As a result the response of the cantilever to an oscillating force of probe sample interaction F is amplified by the dynamic magnification (quality) factor Q of the cantilever which can be as high as 10^5. The excellent sensitivity of the MRFM has enabled detection of single electronic spin magnetic resonance [1, 2].

The generality of MRFM is a key strength: in principle, it is applicable to any signal detectable in a conventional magnetic resonance experiment (in contrast to many single spin detection techniques). MRFM detection has been demonstrated for Electron Spin Resonance (ESR), Nuclear Magnetic Resonance (NMR) and Ferromagnetic Resonance (FMR). The ultimate limit on MRFM sensitivity is imposed by the spontaneous ther-

mally induced cantilever oscillations stemming from the contact of the cantilever with the surrounding thermal bath at temperature T, so the best MRFM sensitivity is achieved at low-temperatures; all the experiments presented here have been conducted at $T = 4$ K.

Recent Progress

The goal of imaging in ferromagnets will be founded on detailed experimental and theoretical understanding of spatially localized ferromagnetic resonance. This is more complicated than magnetic resonance imaging in paramagnets where the magnetic resonance frequency is an entirely local function of applied magnetic field. In a ferromagnet strong interactions and dipolar fields cause the local resonance frequency to depend on the magnetic configuration of other regions of the material. In order to better understand imaging mechanisms in a ferromagnet we have performed local studies of both continuous and patterned ferromagnetic films as we report here.

Our FMRFM investigation of 5 nm thick, continuous permalloy film employed a high coercivity Sm_2Co_{17} micromagnetic probe. Its high coercivity allows us to reverse the applied field $\mathbf{H}_{\rm ext}$ relative to the micromagnetic tip magnetization $\mathbf{M}$. The strength of the FMRFM force signal is measured for both relative orientations of $\mathbf{H}_{\rm ext}$ relative to $\mathbf{M}$ (parallel and anti-parallel) at a variety of vertical probe-film separations as shown in Fig. 1.

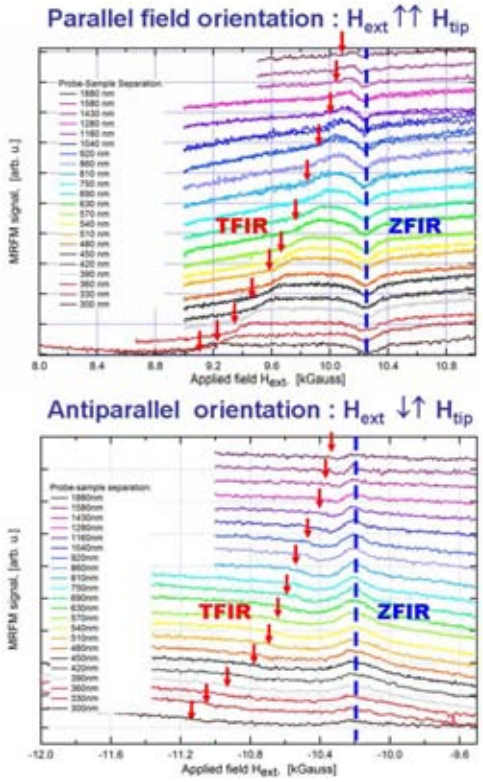

Figure 1: FMRFM spectra obtained at multiple probe-sample separations and two orientations of $\mathbf{H}_{\rm ext}$. The data exhibits two distinctive features: Zero Field Resonance (ZFIR) and Tip Field Influenced Resonance (TFIR).

We see two features. One is independent on the probe-sample separation and is attributed to FMR mode of the majority of sample which laterally remote from the tip and is designated a Zero Tip Field Resonance (ZTFR). In contrast, the second feature shifts strongly as the probe approaches the sample, and its offset relative to the ZTFR is determined by the strength of $H_{\rm tip}$ which increases as the tip approaches the sample surface. This is the FMR signal confined to the area directly below the probe magnet where the total magnetic field seen by the magnetic moments in the sample is altered by $H_{\rm tip}$. We designate this mode as Tip Field Influenced Resonance (TFIR).

The existence of a local mode in a ferromagnetic sample is somewhat unexpected because the magnetic moments in ferromagnetic material are usually assumed to be strongly coupled via exchange interaction and therefore FMR conditions are defined by the properties of the entire sample. We find that the strongly nonuniform field of the micromagnetic tip enables *local* study of ferromagnetic materials where the FMR is defined by the local parameter values.

To further investigate this possibility we have conducted FMRFM experiments on 50 nm thick permalloy dots, 1.5 μm diameter spaced 1.8 μm apart shown in Fig. 2(upper panel). The resulting FMRFM spectrum acquired with a probe magnet located directly over the center of one of the dots is shown in the lower panel. The spectrum shows several resonant features with the positive-going FMR peak located at $H_{\rm ext} \approx 12.38$ kOe again due to dots a significant lateral distance from the micromagnetic probe where $H_{\rm tip}$ is negligible. The negative peaks are from the dots in the immediate vicinity of the micromagnetic probe and are shifted $H_{\rm tip}$. The negative peak at $H_{\rm ext} \approx 11.96$ kOe is the signal originating from a dot located directly below the probe magnet which experiences the strongest probe magnet field $H_{\rm tip}$. In fact, the offset of ≈ 420 Oe of this peak from the resonant peak of the remote dots is in good agreement with the expected strength of the probe magnetic

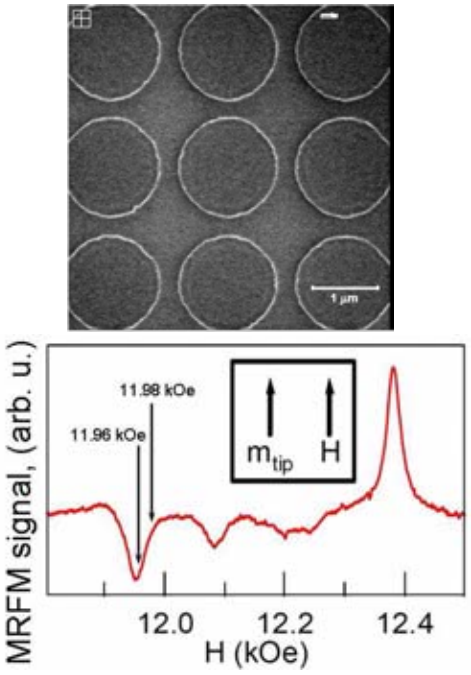

Figure 2: An SEM micrograph of a permalloy dot array used in the experiment (upper panel). FMRFM spectrum obtained with the probe magnet positioned over the center of a dot (lower panel). The positive peak at $H_{\rm ext} \approx 12.38$ kOe is attributed to the signal originating from the remote dots where the probe magnet field is negligible.

field at the probe-sample separation used. Scanning experiments performed at two values of $H_{\rm ext}$ as shown in Fig. 2(lower panel) generate the 2D FMRFM image shown in Fig. 3.

Numerical modeling of local FMR in thin ferromagnetic samples

The interpretation of the acquired image involves a convolution of the gradient of the probe magnet and the FMR signals from the multiple permalloy dots influenced by the field of the probe magnet. We have simulated the FMRFM response of such a system numerically employing a linearization of the Landau-Lifshitz-Gilbert (LLG) equation describing spin dynamics in a magnetic field. The result of micromagnetic modeling is shown in Figs. 3 and 4. To make the problem computationally tractable, we limit it to a sample of a finite size which is modeled as a collection of point dipoles interacting via the dipolar and exchange interactions. The FMR modes of this system have been calculated for

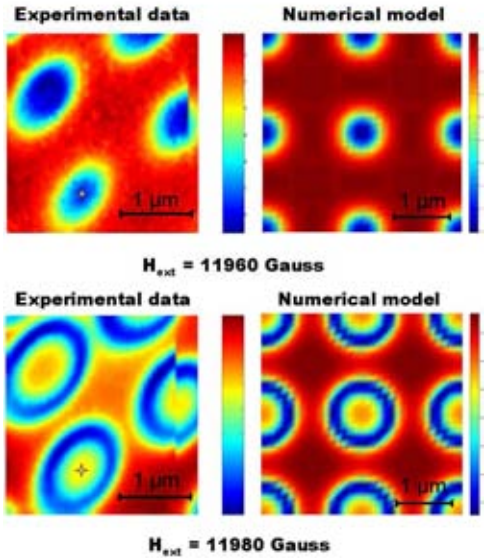

Figure 3: 2D FMR MRFM image: experimental data and micromagnetic modeling conducted for conditions similar to those in the experiment.

various external field configurations to simulate the influence of the non uniform field introduced by the probe magnet. In particular, three configurations of external magnetic field have been considered:

- Uniform magnetic field $H_{\rm ext}$
- Uniform magnetic field $H_{\rm ext}$ combined with a superposed field $H_{\rm tip}$ introduced in a region smaller than the size of the sample; $H_{\rm tip}$ is oriented in the same direction as $H_{\rm ext}$
- $H_{\rm tip}$ applied anti-parallel to the uniform field $H_{\rm ext}$

Fig. 4 shows the calculated spatial profile of the radial component of the precessing magnetization for the lowest frequency (fundamental) FMR mode of a permalloy dot 2.0 μm diameter, 5 nm thick saturated in a 1.3 T field oriented perpendicular to the film plane calculated for the various configurations of the external field. The effect of a 1.0 μm diameter spherical probe magnet located 500 nm above the center of the dot is shown for two orientations of $H_{\rm tip}$.

It can be seen that the results of the modeling are in a fairly good agreement with the experimental data and reproduce the general structure of FMRFM image for both values of $H_{\rm ext}$ (see Fig. 3. The asymmetry of the experimental image is due to the asymmetric shape of the micromagnetic probe.

In the case of a uniform external field the simulation predicts the expected bell shaped mode confined

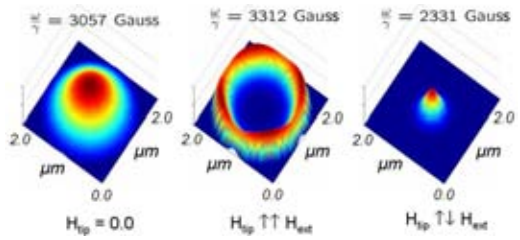

Figure 4: Lateral variation of transverse moment numerically calculated for three configurations of the external field: uniform field only, uniform field with positive tip field perturbation, and uniform field with negative tip field perturbation

only by the sample boundaries. Introducing the tip field parallel to H_{ext} suppresses precessing magnetization at the center of the sample where the total applied field is now higher than on the periphery of the sample. In the case of the opposing tip field the mode is confined to the area where the tip field has been introduced. In this case the field here is lower than at the edge of the sample. Thus, the preliminary numerical simulations of FMR resonance in non uniform applied field confirm the possibility of exciting local FMR modes.

In summary we have observed local FMR modes induced by the strong local magnetic field of the probe magnet. This effect was observed in both a continuous film and a patterned array of dots. Micromagnetic modeling of the resulting FMRFM signal which is good agreement with the experimental data and opens the door for understanding imaging mechanisms in scanned FMR.

MRFM detection of NMR

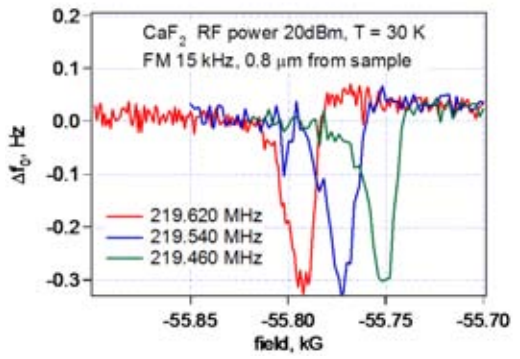

Figure 5: ^{19}F NMR MRFM Signal detected from a CaF_2 sample at $T = 30$ K.

We also have detected Nuclear Magnetic Resonance (NMR) signal using a unique frequency shift detection NMRFM system. The signal was detected from a CaF_2 sample at $T = 30$ K. A Focused Ion Beam (FIB) milled NdFeB particle was used as a probe magnet. Fig. 5 shows the NMRFM signal detected at three different rf frequencies; the shift is as expected from the known gyromagnetic ratio. A preliminary estimate of the system sensitivity is 8×10^5 fully polarized ^{19}F nuclear spins.

Future Plans

In our future effort we will concentrate on the following t directions of FMRFM and NMRFM development:

- Further development of FMRFM sensitivity and data acquisition protocols
- Development of special samples with buried ferromagnetic elements for investigation of ferromagnetic-normal metal interfaces
- Further development of micromagnetic modeling of FMR in nonuniform magnetic fields and the resulting FMRFM signals.
- CaF_2 will be used to develop NMR techniques to enhance sensitivity and enable new capabilities.
- Co based magnetic multilayered structures will be studied using NMRFM

DOE Sponsored Publications 2004-2006

1. P. C. Hammel, "Seeing Single Spins," *Nature* **430**, 300 (2004).
2. T. Mewes, J. Kim, D.V. Pelekhov, G.N. Kakazei, P.E. Wigen, S. Batra, and P.C. Hammel, "Ferromagnetic resonance force microscopy studies of arrays of micron size permalloy dots," *Physical Review B* to appear.

References

[1] D. Rugar, R. Budakian, H. J. Mamin, and B. W. Chui, Nature **430**, 329 (2004).

[2] P. C. Hammel, Nature **430**, 300 (2004).

Atomistic Basis for Surface Nanostructure Formation

Principal Investigators: G. L. Kellogg, P. J. Feibelman, B. S. Swartzentruber, and N. C. Bartelt

Program Scope:

The goal of this program is to establish the scientific principles governing the formation and stability of nanostructures on surfaces. Our current efforts focus on understanding how atomic-scale, kinetic processes control collective phenomena on surfaces such two-dimensional pattern formation, surface smoothing, surface alloying, and 3-d cluster diffusion. Our approach is to combine low energy electron microscope (LEEM) measurements of the time-evolution of nanoscale surface features with scanning tunneling microscope (STM) and theoretical studies of how atoms move and interact on surfaces. From these studies we obtain new insights into the complex physics that takes place during the formation and evolution of surface structures at length scales relevant to the emerging nanotechnologies. The overall program is highly interdisciplinary and draws on expertise from government, industrial and university research labs.

Recent Progress (FY05-06):

- We developed a new experimental technique (with Jim Hannon, IBM, Yorktown Heights and Karsten Pohl, U. New Hampshire), which allows us to obtain three-dimensional maps of surface chemical composition with a lateral resolution of 8 nm. In our **LEEM-IV** analysis, we carry out intensity vs. electron energy (so-called "current-voltage" or simply IV) measurements pixel-by-pixel for an entire LEEM image. We then analyze the reflectivity data using multiple-scattering low energy electron diffraction (LEED) calculations (in analogy with conventional LEED-IV analysis).
- With our new LEEM-IV procedure, we identified the atomic origins of the chemical heterogeneity that develops during the deposition of Pd on Cu(001). Pd is a candidate metal to inhibit the detrimental effects of electromigration in copper interconnects, but little is known about how, and at what temperature, Pd intermixes with Cu. Based on the chemical information provided by LEEM-IV analysis, we showed that the interesting intensity variations observed in LEEM images of Pd/Cu(001) can be explained with a conceptually simple "step-overgrowth" model. Although the model was developed in relation to the specific system of Pd on Cu(001), step overgrowth requires only fast surface diffusion (or equivalently low growth rate) and relatively slow bulk diffusion. This state of affairs is quite common in growth, and the same mechanism should be operative generally.
- The initial stages of Ge and Si growth on *pure* Si(001) are well understood. However, at growth conditions where devices are made, the deposition of Ge leads to the formation of a Ge/Si alloy in the first few atomic layers. It is thus important to determine if the atomic processes active on this alloy surface differ from that on the pure silicon surface. Accordingly, we have used STM to study the initial growth of Ge on the Ge/Si(001)

alloy. We measured the time constant of the evolution of precursor Ge chain-like structures into compact islands as a function of temperature on the Ge/Si(001) surface alloy. We also measured the relative configurational free energy of kinked versus straight segments of the chain-like structures. This energy reflects a second-nearest-neighbor interaction mediated by the alloy substrate. These results, along with those reported last year concerning the formation and migration of adatom pairs, show unequivocally that nucleation and diffusion processes active on the pure silicon surface (and the models used to describe them) are not valid on the Ge/Si alloy.

- Construction of our new combined LEEM-STM instrument is complete. During the past year we made several modifications to the LEEM to accommodate the STM including a new sample manipulator that allows sample transfer from the LEEM to the STM. The STM has been designed, constructed and attached to the LEEM. Preliminary images have been obtained, but there are still vibration issues that need to be resolved to achieve atomic resolution. Once this is accomplished, we will have a unique, surface-imaging microscope capable of viewing objects having dimensions ranging from single atoms to tens of microns.

Future Plans:

- We will measure the effect of subsurface (alloyed) Pd on the mobility of Cu adatoms on Cu(001). A quantitative measure of this effect is important in determining the extent to which Pd/Cu surface alloys can inhibit the detrimental effects of electromigration on Cu interconnects. We will also examine the thermal stability of the surface alloy.
- We will investigate the atomistic processes underlying Ge/Si surface alloying using our entire arsenal of experimental techniques. A main focus will be on determining the critical role of surface steps in the alloying of Ge into Si(001). Our novel **LEEM-IV analysis** will be used to determine the three-dimensional Ge concentration profile in the region around spontaneously formed steps. The combination **LEEM-STM** will be used to identify the atomic structure of the steps and how Ge incorporation occurs in their vicinity. We will also use **scanning tunneling spectroscopy** (STS) to distinguish the atomic species in the surface alloy and the composition of the adsorbed species. We will measure the relative formation free energies of deposited Ge as a function of the underlying alloy composition.
- Following the discovery (Michely group, Aachen, Germany) that a very regular array of Ir islands grows on a single graphene sheet adsorbed on Ir(111), we will study the energetics of this self-organizing system. Using first-principles, Density Functional Theory calculations, we will first investigate the breaking of pi-bonds needed for graphene to bind to the underlying precious metal. Then we will develop an understanding of the potential energy surface that biases the diffusion of Ir adatoms on top of the graphene layer.
- In the longer-term we plan to initiate a theoretical and experimental effort to understand diffusion in “fluid-like” systems. At elevated temperatures and in multicomponent systems many different types of thermal defects can exist simultaneously and have been found to interact in complex ways. Similarly, the nature of diffusing thermal defects in weakly bound systems such as organic thin films is a completely open question. In these situations, the energies of atomic processes cannot be simply extracted from Arrhenius plots. While there exists extensive theoretical formalisms for understanding diffusion in

such complex systems, there has been very little quantitative comparison with experiment. We will attack this problem by measuring the temperature dependence of the evolution of surface morphology on metals at high temperature in sufficient detail to characterize the expected non-Arrhenius behavior. We will then develop the theoretical framework needed to interpret these results in terms of the complex behavior known to occur on such surfaces at the atomic scale. The same procedure will then be applied to organic films (e. g., self-assembled monolayers on Au).

External Interactions

University and Industrial Collaborations with: University of Minnesota, University of Texas at Austin, Princeton University, Ohio State University, North Carolina State University, Cedarville University, IBM, Yorktown Heights, University of New Mexico, University of New Hampshire, Rheinisch Westfische Technische Hochschule (RWTH), Aachen, Germany

Publications (2004-2006):

"Addimer Chain Structures: Metastable Precursors to Island Formation on Ge-Si(001)-(2×n) Alloyed Surface", K. J. Solis, L. R. Williams, B. S. Swartzentruber, and S. M. Han, Surface Sci. (submitted).

"Origins of Nanoscale Heterogeneity in Ultra-thin Films," J. B. Hannon, J. Sun, K. Pohl, and G. L. Kellogg , Phys. Rev. Lett. **96**, 246103 (2006).

"Reversible Shape Transition of Pb Islands on Cu(111)," R. van Gastel, N. C. Bartelt, and G. L. Kellogg, Phys. Rev. Lett. **96** 36106 (2006).

"The Effect of Embedded Pb on Cu Diffusion on Pb/Cu(111) Surface Alloys," M. L. Anderson, N. C. Bartelt, P. J. Feibelman, B. S, Swartzentruber, and G. L. Kellogg, Surface Sci. **600** 1901 (2006).

"Effects of Elastic Anisotropy on the Periodicity and Orientation of Striped Stress Domain Patterns at Solid Surfaces," François Léonard, N. C. Bartelt, and G. L. Kellogg, Phys. Rev. B, **71**, 045416 (2005).

"Surface-Diffusion-Limited Island Decay on Rh(001)", G. L. Kellogg and N. C. Bartelt, Surface Sci. **577**, 151 (2005).

"Oscillatory Interaction between O Impurities and Al adatoms on Al(111) and Its Effect on Nucleation and Growth," C. Polop, H. Hansen, W. Langenkamp, Z. Zhong, C. Busse, U. Linke, M. Kotrla, P. J. Feibelman, and T. Michely, Surf. Sci. **575** 89 (2005).

"Bulk-Surface Vacancy Exchange on Pt(111)", B. Poelsema, J. B. Hannon, N. C. Bartelt, and G. L. Kellogg, Applied Physics Letters **84**, 2551 (2004).

“Relationship Between Domain-Boundary Free Energy and the Temperature Dependence of Stress-Domain Patterns of Pb on Cu(111)”, R. van Gastel, N. C. Bartelt, P. J. Feibelman, F. Leonard, and G. L. Kellogg, Phys. Rev. B **70**, 245413 (2004).

"Thermal Motion and Energetics of Self-Assembled Domain Structures: Pb on Cu(111)," R. van Gastel, R. Plass, N. C. Bartelt, and G. L. Kellogg, Phys. Rev. Lett. **91**, 055503 (2003).

"Vacancy-Mediated and Exchange Diffusion in a Pb/Cu(111) Surface Alloy: Concurrent Diffusion on Two Length Scales", M. L. Anderson, M. J. D'Amato, P. J. Feibelman, and B. S. Swartzentruber, Phys. Rev. Lett. **90**, 126102 (2003).

Alloying at surfaces and interfaces

François Léonard, Roland Stumpf, Sergey Faleev
fleonar@sandia.gov, rrstump@sandia.gov, sfaleev@sandia.gov
Sandia National Laboratories, Livermore, CA 94551

Program Scope

Much effort has been devoted to studying the properties of alloys, motivated by a desire to better understand these industrially relevant materials, but also to explore the basic science that governs alloy stability, processing and microstructure. Traditional theoretical and computational studies of alloys have assumed perfect crystallinity of the material, and have focused on the properties of the bulk. However, real materials are far from this idealized situation, and usually contain a significant density of perturbing elements, such as surfaces, interfaces, and defects like grain boundaries and dislocations. This is especially true for materials that are structured at the nano-scale to enhance their useful properties. These perturbing elements can have a profound influence on the alloy behavior. For example, the alloy composition is often strongly modified at a surface for reasons ranging from differences in the surface energies and atom spacings of the constituents, or interactions with adsorbed species. Surfaces and interfaces are the places where alloying happens, driven by thermodynamics and often constrained by kinetic barriers. Similarly, the long-ranged elastic fields created by dislocations, surfaces, interfaces, and composition variations in misfitting alloys all interact and affect processes such as alloy formation or phase separation.

Our program develops and utilizes theoretical and modeling methods from atom to continuum to study alloying at surfaces and interfaces. Currently the program focuses on four main areas: (i) atomistic mechanisms that govern ultra thin film and surface alloy formation, including self-assembly, (ii) stability, formation and decay of sub-surface alloys on metals, (iii) role of dislocations during alloy phase separation, (iv) development of accurate *ab initio* methods.

Recent Progress

Hydrogen interaction with surface alloys of simple and transition metals

The structure and composition of a surface affect functionality such as the chemical interaction with gaseous species. For example, it has long been known that H_2 and hydrocarbon molecules face significant barriers to chemisorption at, and desorption from, simple metal surfaces. This prevents the use of cheap simple metals as catalysts in H chemistry or as anodes in fuel cells, and also prevents rapid H uptake and release in light hydride materials for H storage applications. The commonly accepted reason for the high barriers is the lack of a partially filled *d*-shell to mitigate the repulsion between surface *s*-*p* and H *s* electrons. An important question is: can doping with *d*-metals lead to surface alloys which speed up the surface chemistry of H-containing molecules? To address these issues, we have studied Ti and Sc on Al surfaces. Others have shown that small amounts of Ti make the formation of $NaAlH_4$

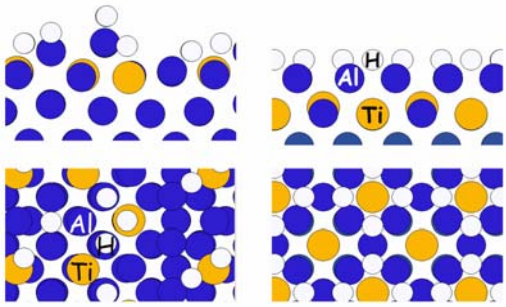

Figure 1: *Left: side and top view of a H stabilized disordered Ti ad-layer on Al(100). The Ti goes partially sub-surface after simulated annealing at 400K. Right: most stable ordered structure of ½ ML of Ti on H covered Al(100).*

reversible and thus useful as a H storage material.

We use first principles global optimization to identify H-stabilized Al-Ti alloy structures at the Al(100) surface (Fig. 1). Ti atoms generally prefer to reside in a ½ ML *sub*-surface substitutional array. This Ti array binds strongly to surface Al atoms, activating them to form strong, almost covalent bonds with adsorbates like H on the surface. Both Ti directly exposed at the surface and Al atoms with Ti neighbors have lower barriers for H_2 dissociation and recombination. This study suggests a new class of near-surface alloys of simple and transition metals with novel catalytic properties, i.e. they combine usually mutually exclusive properties of the constituent metals, like low H binding energies and low H_2 dissociation. We are extending this research into the mechanisms of direct formation of Mg- and Mg-B hydrides.

Self-assembly of surface alloys

Surface alloys can have properties that are difficult to anticipate by simple examination of bulk phase diagrams. For example, Fig. 2 shows a LEEM image of a stripe pattern after Pb was deposited on a Cu(111) surface. The dark regions in the image are a PbCu surface alloy phase while the bright regions are a Pb overlayer phase, with a surface step separating the phases. Our work has indicated that the origin of the patterns is the competition between a short-range attractive interaction due to step energy and a long-range repulsive interaction due to the misfit between the two phases. Detailed analysis of the experiments has also allowed us to extract the basic parameters that describe the interactions, such as the step free energy and the stress difference between the two phases. A puzzling observation has been the orientation of the stripes with respect to the substrate. As Fig. 2 indicates, the stripes are NOT oriented along expected low-energy step directions, but rather are rotated 30 degrees from the close-packed direction. To explain the unexpected stripe orientation, we used anisotropic continuum elasticity to calculate the elastic energy of the stripe phase as a function of its orientation on the surface. Figure 3 shows that the calculated elastic energy has a minimum 30 degrees from the close packed direction, in agreement with experiment. Thus, this provides a striking example that anisotropic elasticity, which is usually discounted as an important effect, can actually determine the orientation of the stripe phase.

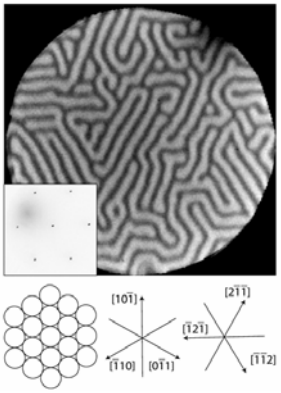

***Figure 2**: LEEM image of PbCu stripe phase. Crystal and stripe orientation are shown below the image.*

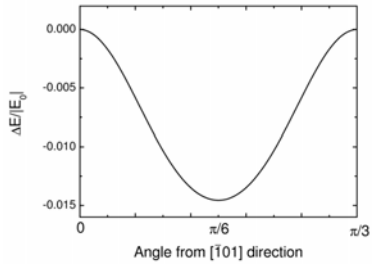

***Figure 3**: Energy of stripe phase as a function of angle on the Cu(111) surface. Energy minimum agrees with that observed in Fig. 2.*

Interaction of layer growth and surface alloying

We apply first principles theory to the study of the growth of Pd on Ru(0001). Our experiment finds a novel growth mechanism in which deposited Pd is not uniformly incorporated along the advancing atomic steps of the growing Pd islands. Instead, Pd mostly attaches to certain sections of the steps, depending on the Pd deposition rate. The active sections create distinctive meandering island shapes. To explain this observation we propose a first principles based model in which the formation of a Pd/Ru surface alloy around the growing Pd islands slows the diffusion and disfavors attachment of deposited Pd atoms. The degree of alloying is higher ahead of slowly advancing steps leading to an instability that selects active and in-active step sections. Density functional theory (DFT) calculations, STM observations, and LEEM measurements of

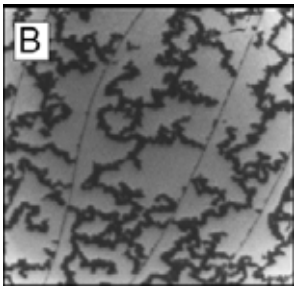

***Figure 4** ½ ML Pd deposited on Ru(0001) at 840K. The Ru step separation is about 2μm*

the growth velocity as a function of deposition flux support this model. Our model suggests conditions under which the meandering island growth mode will occur in other hetero-epitaxy systems and how growth can be tailored by oscillating deposition rates.

Influence of dislocations on phase separation kinetics

Phase separation in alloys has been a problem of long-standing interest due to its technological relevance and the interest in exploring the basic physics of nonequilibrium phenomena. While it is quite clear that dislocations play a crucial role in materials, very little work has addressed the role of dislocations during spinodal decomposition. Our work has been aimed at developing a phase-field model that allows for both mobile dislocations and time-dependent composition evolution, focusing on the coupling between the elastic fields due to dislocations and those due to composition variations. Figure 5 shows snapshots of the composition and dislocation fields at three times after a quench to the spinodal region. As can be seen in the figure, dislocations migrate to interfaces in order to relieve the strain energy between the misfitting alloy elements. The presence of the dislocations at the interfaces influences the rate at which domain growth proceeds. The graph on the right shows the average domain size versus time, for different values of the dislocation mobility. In the absence of dislocations the average domain size grows as $R \sim (\text{time})^{1/3}$. The presence of mobile dislocations modifies this behavior. In fact, we find that there are several new regimes of growth that appear because of the dislocations.

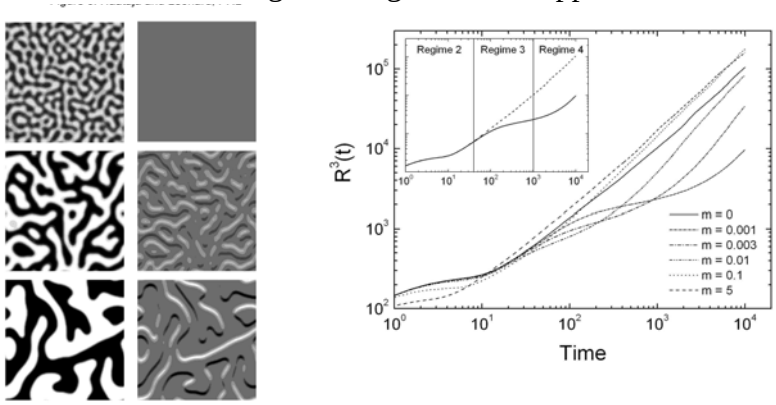

Figure 5*: Composition (left panels) and the horizontal component of the Burger's vector density b_x (right panels) during spinodal decomposition. (white: $b_x > 0$ black: $b_x < 0$). The graph shows the average domain size for different dislocation mobilities. The inset shows three regimes of growth.*

Future Plans

Mechanisms of alloy formation at surfaces

How atoms exchange between bulk and surface can be crucial for a materials properties. In alloys this transport affects the evolution of the surface stoichiometry and is thus critical for the alloy's susceptibility to corrosion or its surface catalytic activity. Bulk-surface mass transport can be inferred from the observation of surface dynamics, e.g. the movement of steps on Pt(111) and NiAl(110). In general, the mechanisms of diffusion in alloys are far more complex and less understood than in single component materials. In the case of NiAl(110) we have started LEEM experiments (K. McCarty) where Al is deposited on NiAl(110), and these indicate complex ways by which the system returns to chemical equilibrium after Al deposition. Our goal is to develop a unified description of the processes active at the NiAl(110) surface. The observation of moving dislocations gives us a unique chance to apply a combination of elasticity theory and atomistic theory to a process that drives alloy formation at the surface and compare our results with experiment. For the first principles work we will have to develop a robust capability to determine the thermodynamic stability of defects at high temperature in a multi-component and low symmetry situation, a challenging global free energy optimization problem.

Self-assembly at solid surfaces
We have made much progress in the quantitative understanding of the *equilibrium* properties of self-assembly in alloys like the Pb/Cu system described above. Given the information we now have on step energies, stress difference between the phases, role of elastic anisotropy and diffusion of surface species, we seek to develop a unified description of several different kinetic transformation processes for these self-assembled phases. For example, by depositing more Pb on the surface, one can transform the stripe phase into a droplet phase. This is an example of a phase transformation between two states with different symmetries, and we seek to understand the mechanisms that govern such a transformation. We thus intend to develop a phase-field model to simulate the time evolution of the patterns, and that will be able to capture many seemingly different observations.

Stability, formation and decay of (sub-)surface alloys on metal surfaces
Sub-surface transition metal alloys are a new class of alloys with special catalytic properties. We want to expand on our discovery of the special properties of the Al-Ti case to more alloys between *s*- and *d*-metals. We will initially focus on alloys with Mg and B, which form reversible hydrides (e.g. $Mg(BH_4)_2$) with high H content. In order to use these for H storage we need to improve the kinetics of H sorption, and catalytic surface alloys could help.

DOE sponsored publications 2004-2006

M. Haataja and F. Léonard, "Influence of mobile dislocations on phase separation in binary alloys", *Phys. Rev. B* **69**, 081201(R) (2004).

D.J. Siegel, M. van Schilfgaarde, J. C. Hamilton, "Understanding the magnetocatalytic effect: magnetism as a driving force for surface segregation", *Phys. Rev. Lett.* **92**, 086101 (2004).

J. B. Hannon, M. Copel, R. Stumpf, M. C. Reuter, R. M. Tromp, "Critical role of surface steps in alloying of Ge on Si(001)", *Phys. Rev. Lett.* **92**, 216104 (2004).

F. Léonard, N. C. Bartelt, G. L. Kellogg, "Effects of elastic anisotropy on the periodicity and orientation of striped stress domain patterns at solid surfaces", *Phys. Rev. B* **71**, 045416 (2004).

R. van Gastel, N. C. Bartelt, P. J. Feibelman, F. Léonard, G. L. Kellogg, "Relationship between domain boundary energy and the temperature dependence of stress-domain patters of Pb on Cu(111)", *Phys. Rev. B* **70**, 245413 (2004).

F. Léonard and M. Haataja, "Alloy destabilization by dislocations", *Appl. Phys. Lett.* **86**, 181909 (2005).

D. J. Siegel, J. C. Hamilton, "Computational study of carbon segregation and diffusion within a nickel grain boundary", *Acta Materialia* **53,** 87 (2005).

M. Haataja, J. Mahon, N. Provatas, F. Léonard, "Scaling of domain size during spinodal decomposition: Dislocation discreteness and mobility effects", *Appl. Phys. Lett.* **87**, 251901 (2005).

P.L. Williams, Y. Mishin, J.C. Hamilton, "An embedded-atom potential for the Cu-Ag system", Mod. Sim. Mat. Sci. Eng. **14,** 817 (2006).

Towards Quantitative Understanding of Strain Induced Nano-scale Self-assembly from Atomic-scale Surface Energetics and Kinetics

Feng Liu (fliu@eng.utah.edu)
Department of Materials Science & Engineering
University of Utah, Salt Lake City, UT 84112

Program Scope

Strain engineered self-assembly in heteroepitaxial growth of thin films has been recognized as an attractive *natural* route for fabrication of nanostructures [1,2]. The nanoscale thin-film structures and morphologies are fundamentally linked to the atomic scale surface/interface energetics and kinetics. However, the atomic scale quantities, especially their dependence on strain, are generally unknown for most systems. This has limited our understanding to a qualitative macroscopic level. The objective of this program is to take a multiscale theoretical and computational approach in an effort to achieve quantitative microscopic understanding of strain induced nanoscale self-assembly. We combine first-principles calculation at the atomic scale with continuum modeling at the nano-scale to make quantitative analysis of nucleation, growth, and stability of quantum dots (QDs, strained islands), focusing on the growth of Ge and SiGe alloy on Si. The approach we develop will also be generally applicable to other systems. Our studies will significantly further our fundamental understanding of QD growth to a quantitative microscopic level and provide useful guidelines for future experimental efforts in strain engineering of QD self-assembly. They have direct technological impact on advancing thin-film based electronic and optoelectronic devices for energy applications, to fulfill the mission of the Department of Energy.

Recent Progress

Extensive experimental and theoretical work has been attempted in the last decade to stimulate, guide, and control the self-assembly processes to improve the uniformity of QDs by manipulating the thermodynamics and kinetics of epitaxial growth. However, our efforts have been hindered by a lack of quantitative information of growth parameters, limiting our understanding to a qualitative macroscopic level. Qualitatively, it is known the formation of QDs, as well as strained islands in general, is driven by relaxation of strain energy at the expense of increase of surface energy, but the quantitative knowledge of these two energy terms, especially their dependence on strain, remains unknown for most systems. Recently, by combining first-principles calculation with continuum modeling, we have made an important breakthrough in performing, for the first time, quantitative theoretical analyses and predictions for growth of Ge and SiGe QDs on Si substrate. These include critical size for Ge and SiGe QD nucleation/formation, stability for self-assembly, and distribution of SiGe alloy concentration in QDs versus in wetting layer [3-5].

One special feature of QDs is that they are usually bound by faceted surfaces of selected orientations [such as (105) facets on Ge hut islands] that are often stabilized by strain. We have carried out extensive first-principles calculations of surface energies and their strain dependence of substrate, wetting layer, and QD surfaces, for the Ge hut on

Si(001) [3,4]. The comparison of the energies between the QD surfaces (facets) and the substrate/film surfaces under strain have allowed us to obtain a much better understanding of the physical origin of QD formation [4]. Using these surface energies as input parameters for continuum modeling, we further obtained quantitative estimates of the "critical" size of nucleation/formation for both pure Ge and SiGe alloy QDs [3], in very good agreement with experiments.

We have also carried out first-principles calculations of surface stress tensors of the QDs and of the wetting layers to assess the stability of QDs for self-assembly. The QD (strained island) formation energy contains generally two major contributions: the strain relaxation energy proportional to QD volume and the cost of surface energy proportional to QD surface area. If only these two terms were present, there would be no stable QD size as the total energy continues to decrease with increasing size [6]. However, the surface stress of the QD is generally different from that of the substrate/film, which gives rise to an additional term of elastic edge relaxation energy. If this edge energy term were large enough, it would introduce a stable island size against coarsening [7]. The significance of such surface stress-induced edge relaxation on QD stability has been a subject of long-standing controversy. Our calculations revealed that for Ge hut on Si(001), this edge term is too small to induce a stable island size [3].

In addition to thermodynamic properties of surface energies and surface stresses, we carried out in parallel quantitative studies of atomic scale kinetic parameters, in particular the surface diffusion energy barriers, to obtain a more complete understanding of QDs. We developed a simple generic method for predicting quantitatively how an external strain will change surface diffusion, by first-principles calculation of adatom induced surface stress along its diffusion pathways on the unstrained surface [8,9]. In a recent work [5], we showed that on a compressive Ge(001) surface, Ge diffuses 10^2-10^3 times faster than Si in the temperature range of 300 to 900 K; while on a tensile surface, the Ge and Si diffusivities are comparable. Consequently, growth of a compressive SiGe film is kinetically different from that of a tensile film, although thermodynamically the two systems have the same strain energy. The diffusion disparity between Si and Ge was shown to be greatly enhanced on the strained Ge islands compared to that on the Ge wetting layer on Si(001), which explained the experimental observation of Si enrichment in the wetting layer relative to that in the islands [5].

Future Plans

We will continue to expand our studies by combining first-principles calculation with continuum modeling to explore the fundamental issues underlying the thermodynamic and kinetic growth of strained films, in particular QDs and quantum wires (QWs), focusing on Ge/Si(001) systems. These include, for example, extension to QDs of difference shapes (Ge domes), SiGe alloy QDs, QD molecules [10], Ge and SiGe QWs, and to the effect of strain on Ehrlich- Schwoebel (ES) step-edge barriers. These studies will involve first-principles calculations with much larger and complex supercells, so the use of DOE-NERSC supercomputers will be critically helpful.

One interesting topic we plan to undertake is on shape transformation of QDs. It is known that Ge QD grows initially in the pyramidal shape of "hut". It will then transform into either an elongated pyramidal shape (as a QW) or a shape of "dome" with steeper side facets. However, it remains unclear how would these two types of shape

transformations compete with each other and which shape transformation has a thermodynamic or kinetic origin. Similar to our study of Ge hut [3], we propose to perform quantitative analysis of the elongated "hut" and dome islands, to compare their relative stability with the hut. These will be done by more extensive first-principles calculations of surface energies and stresses of various Ge facets, such as (113) and (102) on dome, under strain conditions, and by more complex continuum modeling of different island shapes. These studies not only are of great scientific interests in understating strain induced island shape instability, but also have important technological implications in controlling the growth of QDs vs. QWs.

Another subject is to extend our study on a single QD to QD molecules, which has shown an interesting and puzzling kinetic self-limiting growth behavior [10]. In order to shed some new lights on the physical origin underlying the self-limiting growth of QD molecules, we plan to carry out a comprehensive kinetics modeling study by combining three different theoretical approaches of first-principles calculation (FPC), finite element analysis (FEA) and kinetic Monte Carlo (kMC) simulation. The FPCs will be used to determine the Si and Ge diffusion barriers as a function of strain; the FEA will be used to map out the surface strain field at and around the QD molecules; and then the kMC will be used to directly simulate the growth of QD molecules, using the inputs from both FPC and FEA.

We plan also to extend our study of the effect of strain on adatom surface diffusion to adatom diffusion over a surface step, by examining how the ES step-edge barrier would be affected by external strain. Most importantly, we will determine whether the generic model we developed for adatom surface diffusion barrier [8] is applicable to ES barrier. The situation at step edge is much more complex than on surface, because the ES barrier often involves complex atomic-scale processes of concerted motion of multiple atoms. It is interesting as well as useful to know whether the simple linear stress-strain relationship established for adatom jumping on the surface [8,9] is still valid for adatom crossing (ascending or descending) a step. It is expected that strain will have a different effect on different diffusion processes or pathways. This implies that strain may not only change diffusion or step-crossing energy barriers, but even change the diffusion mechanisms and pathways, converting from one scenario of single atom rolling to another of concerted motion of multiple atoms, and vise versa.

References

1. Feng Liu, in "*Handbook of Theoretical and Computational Nanotechnology*", eds. M. Rieth and W. Schommers, **4**, Chapter 10, 577-625(2006).
2. Feng Liu and M.G. Lagally, *Surf. Sci*., **386**, 169 (1997).
3. G.H. Lu and Feng Liu, *Phys. Rev. Lett* **94**, 176103 (2005).
4. G.H. Lu, Martin Cuma, and Feng Liu, *Phys. Rev. B* **72**, 125415 (2005).
5. L. Huang, Feng Liu, G.H. Lu and X.G. Gong, *Phys. Rev. Lett* **96**, 016103 (2006).
6. J. Tersoff and F.K. LeGoues, *Phys. Rev. Lett* **72**, 3570 (1994).
7. V.A. Shchukin *et al*., *Phys. Rev. Lett* **75**, 2968 (1995).
8. D.J. Shu, Feng Liu, and X.G. Gong, *Phys. Rev. B*, **64**, 245410 (2001).
9. L. Huang, Feng Liu, G.H. Lu and X. G. Gong, *Phys. Rev. Lett* **96**, 016103 (2006).
10. J. L. Gray, N. Singh, D. M. Elzey, R. Hull, and J. A. Floro, *Phys. Rev. Lett* **92**, 135504 (2004).

DOE Sponsored Publications in 2005-2006

1. "Modeling and Simulation of Strain-Mediated Nanostructure Formation on Surface", Feng Liu, in "*Handbook of Theoretical and Computational Nanotechnology*", eds. M. Rieth and W. Schommers, **4**, Chapter 10, 577-625(2006) (**Invited chapter**).
2. "Directed Self-assembly of Quantum Dots by Local Chemical Potential control via Strain Engineering on Patterned Substrates", H. Wang, Feng Liu and M. Lagally, in *Nanotechnology*, ed. O. Schmidt (in press). (**Invited chapter**)
3. "Quantitative Prediction of Critical Size for the Formation of Semiconductor Quantum Dots", G.H. Lu and Feng Liu, in "Physics, J. Chinese Phys. Association", **35**, 447 (2006). (**Invited Review**)
4. "Self-organization of semiconductor quantum wires via step-flow growth of strained films", Feng Liu and L. Bai, in Encyclopedia of Nanoscience and Nanotechnology", American Scientific Publisher, (in preparation). (**Invited chapter**)
5. "Computational R&D for Industrial Applications", Feng Liu, News Article of Center for High-Performance Computing, University of Utah, Fall issue, p. 1 (2005). (**Invited review**)
6. "MD simulation of structural and mechanical transformation of single-walled carbon nanotubes under pressure", J. Zang, O. Aldás-Palacios and Feng Liu, *Commun. in Comput. Phys.* (in press) (**Invited Review**).
7. "Pressure-Induced Transition in Magnetoresistance of Single-walled Carbon Nanotubes",J. Z. Cai, L. Lu, H. W. Zhu, C. Zhang, B. Q. Wei, D. H. Wu, and Feng Liu, *Phys. Rev. Le*tt **97**, 026402 (2006).
8. "Surface Mobility Difference between Si and Ge and its Effect on Growth of SiGe Alloy Films and Islands", L. Huang, Feng Liu, G.H. Lu and X. G. Gong, *Phys. Rev. Lett* **96**, 016103 (2006).
9. "Critical Epi-Nucleation on Reconstructed Surfaces and a Model Study of Si(001) Homoepitaxy", R.S. Pala and Feng Liu, *Phys. Rev. Lett* **95**, 136106 (2005).
10. "Nanomechanical Architecture of Strained Bilayer Thin Films: from design principles to experimental fabrication", M. Huang, C. Boone, M. Roberts, D.E. Savage, M. Lagally, N. Shaji, H. Qin, R. Blick, J. A. Nairn and Feng Liu, *Adv. Mater*. **17**, 2860(2005).
11. "Self-organization of Semiconductor Nanocrystals by Selective Surface Faceting", B. Yang, P. Zhang, D.E. Savage, M. Lagally, G.H. Lu, M. Huang, and Feng Liu, *Phys. Rev. B* **72**, 235413 (2005).
12. "Bending of Nanoscale Ultrathin Substrates by Growth of Strained Thin Films and Islands", M.H. Huang, P. Rugheimer, M. Lagally, and Feng Liu, *Phys. Rev. B* **72**, 085450 (2005).
13. "Towards Quantitative Understanding of Formation and Stability of Ge Hut Island on Si(001)", G.H. Lu, M. Huang, and Feng Liu, *Phys. Rev. Lett* **94**, 176103 (2005).
14. "First-principles study of strain stabilization of Ge(105) facet on Si(001)", G.H. Lu, M. Cuma, and Feng Liu, *Phys. Rev. B* **72**, 125415 (2005).
15. "Relative stability of Si surfaces: a first-principles study", G.H. Lu, M. Huang, M. Cuma, and Feng Liu, *Surface Science* **588**, 61 (2005).
16. Pattern Formation on Silicon-on-Insulator", F. Flack, B. Yang, M. Huang, M. Marcus, J. Simmons, O.M.Castellini1, M.A. Eriksson, Feng Liu and M. Lagally, *MRS Proceeding*. Vol. 849, KK1.3.1/JJ1.3.1/U1.3.1 (2005).
17. "Computational Study of Metal Adsorption on TiO_2 (110) Surface", R.S. Pala, T. N. Truong, and Feng Liu, in "Clusters and Nano-Assemblies", World Scientific, eds. P. Jena, S.N. Khanna, and B.K. Rao, 135 (2005).

Atomistic Transport Mechanisms in Revisible Complex Metal Hydrides

PIs: Peter Sutter[1] (psutter@bnl.gov), James Muckerman[2], Y. Chabal[4]
Collaborators: Jason Graetz[3], James Reilly[3], James Wegrzyn[3], Eli Sutter[1]
[1]Center for Functional Nanomaterials, [2]Chemistry Department, [3]Energy Science & Technology Department, Brookhaven National Laboratory, Upton, NY 11978,
[4]Laboratory for Surface Modification, Rutgers University, Piscataway, NJ 08854

Program Scope

Dopants and catalysts have a large, as yet unrealized potential to induce reversibility and to significantly enhance the rates of solid-state hydrogen storage reactions. In sodium alanate ($NaAlH_4$), a complex metal hydride with 7.5 wt. % hydrogen storage capacity, facile hydrogen incorporation and release, as well as substantially increased reaction rates are achieved by doping with titanium, which makes this the only complex hydride with fully reversible hydrogen storage under near-ambient conditions.[1] This fundamental research program aims to identify, quantitatively and at the atomic scale, the effects of Ti-doping on the hydrogen storage reaction for this model system:

$$NaAlH_4 \leftrightarrow 1/3\ Na_3AlH_6 + 2/3\ Al + H_2 \leftrightarrow NaH + Al + 3/2\ H_2.$$

Based on the information obtained on the potentially complex and multifaceted effects of doping in $NaAlH_4$, strategies will be derived for the use of dopants and catalysts to enhance the kinetics and reversibility of other hydrogen storage materials, and more generally, to judiciously modify and tailor hydrogen-solid interactions.

Surface processes in the hydrogen storage reaction in $NaAlH_4$, starting from a depleted phase consisting of NaH and metallic Al, and proceeding via cryolite Na_3AlH_6 to the hydrogen-rich $NaAlH_4$, are considered as the basis for understanding reversible hydrogen storage in the chosen prototype system. Key questions to be addressed via experiments on carefully designed model systems, coupled strongly to theory, include:

- The mechanism of hydrogen dissociation on Al surfaces doped with Ti.
- The identification of the predominant carrier of mass transport, and quantitative measurements of its diffusion kinetics in the presence of different amounts of dopants.
- The detailed reaction mechanisms and their rate-limiting step as NaH and Al react to Na_3AlH_6 and ultimately $NaAlH_4$ in the presence of hydrogen and of dopants such as Ti.

The long-term goal of this project is to develop an atomistic understanding of the interaction of hydrogen with doped metal and alkali-metal surfaces and nanostructures, hence providing a scientific basis for solid-state hydrogen storage in support of the DOE-BES hydrogen fuel initiative.

Recent Progress

A major initial focus has been to investigate the role of Ti dopants in dissociating di-hydrogen (H_2) molecules impinging from the gas phase, a key step in the re-hydrogenation of depleted sodium alanate (fig.1, ❶). The depleted material consists of nanoscale particles of NaH and Al metal. As Al poorly activates molecular hydrogen, and since no catalytic effect of Ti-doping in NaH could be found in model calculations,[2] our working hypothesis is that Ti, localized near the surface of metallic Al, can form active complexes that dissociate H_2 and generate the supply of atomic H or mobile Al-H molecular species (alanes) necessary to crystallize large grains of the hydrogen-rich $NaAlH_4$. Predictive theoretical studies are combined with scanning tunneling microscopy (STM) and infrared (IR)

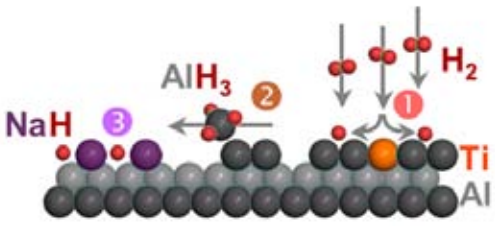

Fig. 1: Elementary reaction steps during the hydrogenation of Al/NaH to $NaAlH_4$. ❶ H_2 dissociation. ❷ Surface mass transport. ❸ Solid-state reaction.

spectroscopy experiments on Al single crystal model surfaces, and with synchrotron x-ray diffraction and fluorescence measurements on the actual storage materials.

In our initial theoretical work, a series of model active sites was constructed by substituting Ti for Al near the Al(001) surface. Based on *ab-initio* density functional theory (DFT), a specific type of Ti:Al complex near Al(001) has been predicted to be highly efficient in dissociating H_2 to atomic-H.[2] The complex consists of two surface Ti atoms replacing Al in third-nearest neighbor sites. Calculations show that H_2 dissociation is spontaneous (barrierless) at these sites. A common feature of this and similar catalytic sites with low computed barriers to H_2 dissociation is an orbital symmetry property that we find responsible for their effectiveness: the highest occupied molecular orbital (HOMO) of the incipient doped-surface/H_2 adduct has a nodal plane perpendicular to the Ti-Ti axis and midway between the two Ti atoms (fig. 2). This nodal symmetry arises from the out-of-surface d_{z2} Ti orbitals having opposite phases such that they overlap with the H_2 σ* orbital. As a result, electron density can be transferred from the surface to the antibonding H_2 orbital to weaken the H-H bond and induce the dissociation of the molecule. Any complexes without this nodal symmetry were found to exhibit large barriers for dissociative H_2 chemisorption.

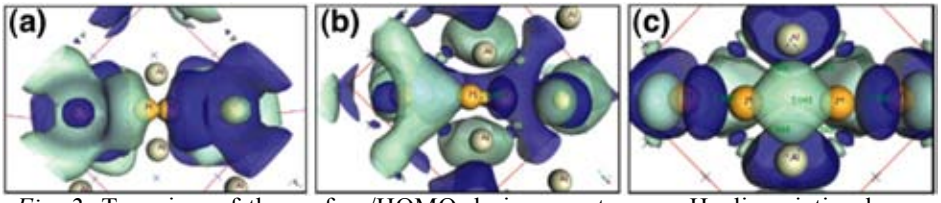

Fig. 2: Top view of the surface/HOMO during spontaneous H_2 dissociation by a Ti:Al complex on Al(001). The HOMO of the Ti-doped surface/H_2 system shows the inclusion of the σ* antibonding molecular orbital character of the incoming hydrogen molecule prior to the dissociation of the H-H bond. The dark and light blue shading indicates different signs of the orbital. The final structure after dissociation has two three-center bonds with atomic hydrogen.

High-resolution STM experiments, coupled with DFT calculations, have been used to study the fundamental thermodynamics of the Ti:Al surface alloy system and to verify the existence of active Ti:Al complexes with the required nodal symmetry on single crystal Al model surfaces. For practical reasons, the experiments have focused on Al(111) surfaces onto which Ti is evaporated to sub-monolayer (ML) coverage. We observe that Ti deposition at room temperature leads to substitution of surface Al, while at elevated temperature Ti is incorporated into sub-surface sites, consistent with DFT results showing that sub-surface Ti is energetically favorable for individual Ti atoms as well as small (2 Ti atom) complexes. At low Ti coverage (few 1/100 ML), a dilute random Ti:Al surface alloy is formed, while Ti clustering is observed at higher coverage. In the dilute Ti:Al surface alloy, most Ti is incorporated as individual atoms (predicted to be inactive in H_2 dissociation), but a significant fraction of the remaining Ti atoms are pairing in a local configuration corresponding to nearest-neighbor Ti on a (111) bulk terminated Al_3Ti alloy, the stable phase of dilute Ti:Al bulk alloys (fig. 3). The resulting Ti-pair:Al complexes exhibit the symmetry and Ti-Ti spacing required for barrierless dissociative chemisorption of H_2. This important finding suggests that under kinetically constrained conditions, where Ti populates surface sites in Al(111), a sizable density of catalytically active sites for H_2 dissociation can be generated spontaneously.[3]

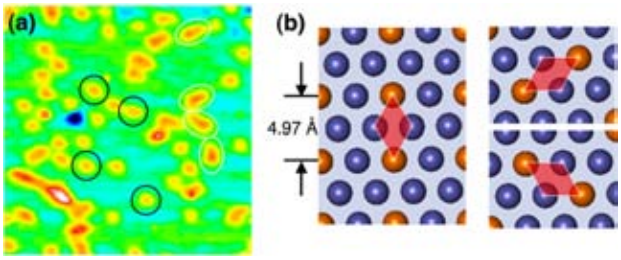

Fig. 3: (a) STM image (10 nm x 10 nm) of Al(111) after 0.04 ML Ti deposition at 300 K. Black circles: individual Ti atoms; White circles: Ti-pairs with 0.5 nm spacing. *(b)* Model of the $Al_3Ti(111)$ surface with nearest-neighbor Ti atoms at 0.5 nm separation.

Additional computational and experimental studies have begun to address the question of how H (and Al) is transported into NaH to ultimately reform hydrogen-rich $NaAlH_4$ (fig. 1, ❷). Previous STM and IR studies have shown the formation of surface alanes (AlH_3 and higher oligomers) during exposure of Al to

atomic-H.[4] This finding points to mobile alanes as a potential primary carrier of mass transport in the hydrogenation reaction to $NaAlH_4$. First-principles molecular dynamics (MD) studies show that atomic-H generated by H_2 dissociation at catalytic Ti:Al sites does not readily recombine at the active sites, is mobile but does not readily migrate to all-Al sites because that process is both endothermic and activated. The likelihood of H being picked up by Al adatoms breaking off from steps and other mechanisms for alane formation is being explored, as is the chemical behavior and mobility of alanes on Al surfaces. The interaction of atomic-H with Al(111) surfaces has been studied by combined microscopy (STM) and spatially averaging spectroscopy (IR) experiments. STM movies during exposure of Al(111) single crystals to atomic H demonstrate a pronounced etching of the Al at surface steps, and the concurrent formation of surface alanes, clearly identified via imaging with functionalized tips.[5] Consistent with this result, IR spectroscopy shows initial Al-H stretch modes due to terminal H adsorbed at Al steps, and a clear evolution from small to larger surface alanes with increasing H coverage.

Based on this initial characterization of the interaction of H with Al surfaces, future STM and IR experiments, complemented by DFT and real-time low-energy electron microscopy (LEEM), can address the identification and quantification of H_2 dissociation at catalytic Ti:Al sites (using the evolution of surface alanes as a fingerprint for H generation), determine the efficiency of Al etching and alane formation in the presence of Ti, and characterize the diffusion of alane molecules on Al and Ti-doped Al surfaces (see below). Preliminary experiments on the interaction of Ti-doped Al with H show a pronounced stabilization of the Al surface by Ti substitution, which can lead to the complete suppression of Al-hydride formation at Ti coverages exceeding ~0.2 ML.

Future Plans

The next phase of work on well-defined model samples will closely link surface microscopy, IR spectroscopy, and theory to address the following key aspects of reversible hydrogen storage in $NaAlH_4$ and, more generally, of the modification of H_2/surface interactions by doping or catalysts: i) Characterization of the detailed atomic pathway and efficiency of Ti-induced H_2 dissociation on Ti-doped Al surfaces (STM, IR); ii) Evolution of surface alanes and their role in mass transport (STM, IR, LEEM); iii) Primary factors affecting the hydrogenation kinetics, and role of Ti (STM, LEEM).

The emphasis of the planned experiments will remain on high-resolution microscopy (STM), coupled with averaging spectroscopy. 'Topographic' STM imaging, as used so far, will be complemented by spectroscopic imaging techniques, such as energy-filtered STM,[6] in an attempt to characterize the complex population of surface species (Al and Ti hydrides, surface alanes) with chemical specificity. In addition to STM and IR spectroscopy, low-energy electron microscopy (LEEM) will be used to map surface mass transport in real time, and to quantify differences in alane and Al diffusion, as well as the modification of surface diffusion kinetics by Ti doping. Building on our initial experiments on the interaction of H/H_2 with Al surfaces, we will attempt to analyze complete steps of the hydrogenation reaction, e.g., use NaH/Al(111) as a model system to study the reaction $6\ NaH + 2\ Al + 3\ H_2 \leftrightarrow 2\ Na_3AlH_6$. Theory will be strongly coupled to the STM and IR studies now underway. The objective will be to suggest experimental models to isolate individual steps in the hydrogenation reaction, and to interpret observed surface structures, dynamic phenomena, and IR signatures.

The transfer of what is being learned about the sodium alanate system to other potential hydrogen storage materials to make them reversible will be another focus of the theoretical effort. A near-term focus, involving also bulk solid-state chemistry experiments, will be to evaluate the possibility of using Ti-catalyzed H_2 dissociation at Al surfaces as a pathway to forming bulk alane (AlH_3), a promising hydrogen storage material with > 10 wt. % gravimetric storage capacity and favorable de-hydrogenation kinetics, which, however, is an irreversible system that lacks an efficient re-hydrogenation process.

References

(1) B. Bogdanovic and M. Schwickardi, *J. Alloys Comp.* **253–254**, 1 (1997).
(2) S. Chaudhuri and J.T. Muckerman, *J. Phys. Chem. B* **109**, 6952 (2005).
(3) E. Muller, P. Zahl, S. Chaudhuri, J.T. Muckerman, and P. Sutter, in preparation.
(4) E.P. Go, K. Thuermer, and J.E. Reutt-Robey, *Surf. Sci.* **437**, 377 (1999).
(5) E.P. Go, K. Thuermer, and J.E. Reutt-Robey, *J. Phys. Chem. B* **104**, 8507 (2000).
(6) P. Sutter, P. Zahl, E. Sutter, and J.E. Bernard, *Phys. Rev. Lett.* **90**, 166101 (2003).

DOE Sponsored Publications Since 2005

Decomposition kinetics of the AlH_3 polymorphs, J. Graetz and J. J. Reilly, *J. Phys. Chem. B* **109**, 22181 (2005).

Structure and thermodynamics of the mixed alkali alanates, J. Graetz, Y. Lee, J. J. Reilly, S. Park and T. Vogt, *Phys. Rev. B* **71**, 184115 (2005).

Characterization of the local titanium environment in doped sodium aluminum hydride using X-ray absorption spectroscopy, J. Graetz, A.Y. Ignatov, T.A. Tyson, J.J. Reilly and J. Johnson, *Mat. Res. Soc. Conf. Proc.* ***837*** (2005).

First-principles study of Ti-catalyzed hydrogen chemisorption on an Al surface: A critical first step for reversible hydrogen storage in $NaAlH_4$, S. Chaudhuri and J.T. Muckerman, *J. Phys. Chem. B* **109**, 6952 (2005).

A Density Functional Theory Study of the Catalytic Role of Ti Atoms in Reversible Hydrogen Storage in the Complex Metal Hydride, $NaAlH_4$, S. Chaudhuri and J.T. Muckerman, *Materials and Technology for Hydrogen Storage and Generation,* ed. G-A. Nazri, C. Ping, R.C. Young, M. Nazri, and J. Wang, *Mat. Res. Soc. Symp. Proc.* **884E**, Warrendale, PA, 2005; GG2.1.

Understanding the role of Ti in reversible hydrogen storage as sodium alanate: A combined experimental and first-principles theoretical approach, S. Chaudhuri, J. Graetz, A. Ignatov, J.T. Reilly and J.T. Muckerman, *J. Am. Chem. Soc.* **128**, 11404 (2006).

First Principles and Atomistic Simulation Studies of Surfaces

C. Z. Wang and K. M. Ho (wangcz@ameslab.gov,kmh@ameslab.gov)
Ames Laboratory, Iowa State University, Ames, IA 50011

Program Scope

We study the geometries and energetics of various surface systems with first-principles density functional and tight-binding calculations. Molecular dynamics simulations are carried out to study the structure and motion of adatoms, ad-dimers, vacancies and steps on surfaces. These studies are carried out in close collaboration with experimental groups at Ames Lab (Tringides and Hupalo) as well as groups outside.

A detailed understanding of surface geometries and kinetic processes is crucial in many areas with high impact on the mission of DOE. It is impossible to describe processes such as film growth, surface catalysis without detailed information of the surface. As electronic devices become smaller, surface effects become important and in the area of nanoscience, surfaces and interfaces are an integral part of the system. Our group has more than 25 years of experience in surface electronic structure and total energy calculations. During that time, the focus of the field has developed from electronic and atomic geometries of perfectly flat crystalline surfaces to more complex problems. One area of interest is the kinetics of film growth [1]. Currently, there is much interest in the formation of nanostructures by manipulation of the thin film deposition process and the stability of such structures after formation [2-7]. Non-equilibrium effects play a big role and factors affecting the kinetics such as the diffusion of adatoms and defects, behavior of steps and kinks and influence of steps on surface kinetics can only be studied effectively through a combination of experimental (using STM, electron diffraction techniques) and a synthesis of theoretical techniques (first principles total energy calculations, molecular dynamics, kinetic Monte Carlo and continuum modeling). Our long-term goal is to develop a synthesis of multilevel theoretical techniques to tackle the problem. Such a program would involve local theoretical groups in Chemistry (Jim Evans and Mark Gordon) as well as other theoretical groups outside Ames Laboratory (e.g. Cristian Ciobanu at Colorado School of Mines, Vivek Shenoy at Brown University, Feng Liu at University of Utah, Zhenyu Zhang at Oak Ridge, Ju Li at Ohio State University and Sidney Yip at MIT, Mei-Yin Chou at Georgia Tech.), especially through the Computational Materials Science Network (CMSN) on the project of "Multiscale Studies of the Formation and Stability of Surface-Based Nanostructures".

Recent Progress:

1. Quantum size effects in diffusion and novel growth morphologies in ultrathin Pb films on Si(111)

The ability to manipulate atoms to form regular nano-structures through the self-assembly is a topic of much current interest. In metallic nano-structures, the quantum size effect has recently been recognized as a strong driving force for self-assembly of certain preferred sizes and geometry of metal islands in the deposition process [3-6,8-10]. Quantum size effects are important in explaining the observed extraordinary efficiency of the system in forming metallic islands of selective heights with flat tops and steep edges on the semiconductor surfaces at high deposition rates and quite low temperatures. This

must involve very fast kinetics that cannot be explained by existing film growth models[11].

Using Pb/Si(111) as a prototype system, we have performed first-principles total energy calculations for the diffusion barrier of Pb adatoms on Pb films with different thicknesses [12]. We found that diffusion of an adatom on the Pb films has very low barriers (less than 60 meV). A bi-layer oscillation in the diffusion barriers due to quantum size effect (QSE) is observed, with lower barriers on the odd-layered, relatively unstable Pb films. The diffusion barrier difference between the odd- and even-layered film is found to be as large as 40 meV.

STM experiments by Hupalo and Tringides observed an unusual growth morphology of Pb islands on Si(111) surface: islands with stable and unstable heights exhibit different growth behavior. The growth of a new layer on unstable islands shows a ring at the island perimeter propagating towards the island center [12]. To our knowledge, this is the first time that an intermediate state before the completion of the island during the growth of Pb islands on Si(111) has been captured experimentally, and this novel ring morphology cannot be explained within the conventional picture by the competition between terrace diffusion vs. interlayer diffusion[13]. Our calculation indicates that this collective growth behavior has a microscopic origin from the quantum size effect on the big difference in diffusion barriers on top of stable and unstable islands. Other factors also contributing to the novel growth morphology include the step barrier at the edge of the islands and attraction or repulsion between Pb adatoms with the island edge. Calculations are underway to obtain accurate values for these quantities. In the long term, our understanding and ability to manipulate these quantities will give us control in manipulating the formation and stability of metal nanostructures on these surfaces.

2. Development of genetic algorithm for surface geometry optimization: Applications to high-indexed Si surfaces

We have adapted the genetic algorithm method we developed for structural optimization of atomic clusters [14,15] for applications in surface geometry optimization. Preliminary tests on the formation of magic clusters on the 7x7 Si(111) surface indicate that the method has advantages over traditional simulated annealing methods also in surface applications. Further applications to search for low energy structures of high-indexed silicon (105), (114) and (337) surfaces have also been successul. The development of this tool allows us to go beyond the traditional way of searching surface structures by intuition to a systematic procedure that can handle much more complicated systems.

Future Plan

1. *Wetting layer dynamics and growth of quantum films in the Pb/Si(111) system*

Experimental observation of the growth Pb films on Si(111) at low temperatures revealed unconventional behavior: Instead of forming three-dimensional (3D) islands of various sizes as commonly observed for nonreactive interfaces, the metal atoms arrange themselves into plateaus or islands of selective heights, with flat tops and steep edges. Fig. 1 shows the STM image of Pb islands on Si(111) of uniform height of about seven layers after deposition of 3 ML at 192 K [4].

The extra stability of metal films with specific thickness has an electronic origin and can be explained by the "quantum size effect" (QSE) due to electron confinement [8,9]. However, further observation of the growth and coarsening process of these 'quantum' islands indicate that, not only are these films structurally unconventional, their kinetic behavior is also fundamentally altered by quantum-size effects and does not obey traditional classical kinetic model predictions. In coarsening experiments, the island decay rate is orders of magnitude faster than expected from the classical Gibbs-Thomson analysis. Quantum size effects impose a strong variation of island free energy on the height of islands, and further guide the selection of islands with preferred heights. The other essential difference is the presence of a dense and dynamic wetting layer surrounding the island greatly shortening communication and mass transport between different islands. For high deposition fluxes, the system is driven sufficiently far-from-equilibrium to create islands with a distribution of heights, including metastable islands with relatively unfavorable heights. As a result, coarsening in these systems is subject to much stronger energetic driving forces than those associated with differences in curvature. These aspects require the development of an entirely new theoretical model to describe the kinetics of the system. We are in the process of formulating such a theory and performing calculations necessary to determine the relevant parameters such as step-edge barrier, adatom-island-edge interaction, step-step interaction, adatom and cooperative diffusion barriers, and structural, energetic and dynamical properties of the wetting layer.

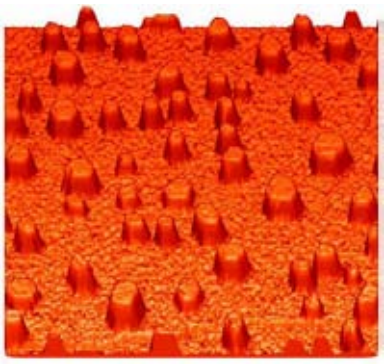

Fig. 1 STM image obtained after deposition of 3 ML of Pb at 192 K on Si(111) showing the uniform height islands with flat tops and steep edges. The scale is 200 x 200 nm^2 [4].

2. Genetic algorithm search for ground state structure of metal overlayers on semiconductor surfaces

Metal overlayers on semiconductor surfaces exhibit a large variety of different geometries and periodicities as a function of both coverage and temperatures. Although there have been numerous experimental and theoretical studies, our understanding of many systems is still quite limited: in the vast majority of systems, there is still no consensus of information as basic as the geometry of the surface because of the large number of plausible models for any given system. Using our recently developed genetic search algorithm and accurate tight-binding potentials, we are able to perform systematic and thorough searches for low energy geometries of several prototype systems. We will present a global picture as a function of various overlayer coverage and examine low energy structural motifs. Such studies will have impact on various surface and interface topics from metallization of semiconductor surfaces to growth of surface nanostructures and vapor-liquid-solid(VLS) growth of semiconductor nanowires.

References

[1] For review, see Z. Y. Zhang and M. G. Lagally, *Science* **276**, 377 (1997); H. Brune, Surf. Sci. Rep. **31**, 121 (1999).

[2] Y. W. Mo, D. E. Savage, B. S. Swartzentruber, M. G. Lagally, *Phys. Rev. Lett.* **65**, 1020 (1990); J. Tersoff, C. Teichert, M. G. Lagally, *Phys. Rev. Lett*. **76**, 1675 (1996).
[3] A. R. Smith, K.-J. Chao, Q. Niu, and C. K. Shih, *Science* **273**, 226 (1996).
[4] K. Budde, E. Abram, V. Yeh, and M. C. Tringides, *Phys. Rev.* B **61**, R10602 (2000); V. Yeh, L. Berbil-Bautista, C. Z. Wang, K. M. Ho, and M. C. Tringides, *Phys. Rev. Lett.* **85**, 5158 (2000).
[5] M. Hupalo, S. Kremmer, V. Yeh, L. Berbil-Bautista, and M. C. Tringides, *Surf. Sci*. **493**, 526 (2001); M. Hupalo and M. C. Tringides, *Phys. Rev.* B **65**, 115406 (2002).
[6] W. B. Jian, W. B. Su, C. S. Chang, and T. T. Tsong, *Phys. Rev. Lett*. **90**, 196603 (2003).
[7] K. Thurmer, E. Williams, J. Reutt-Robey, *Science*, **297** (5589) 2033 (2002).
[8] Z. Zhang, Q. Niu, and C.-K. Shih, *Phys. Rev. Lett*. **80**, 5381(1998)
[9] C. M. Wei, and M. Y. Chou, *Phys. Rev. B* **66**, 233408(2002).
[10] P. Czoschke, H. Hong, L. Basile, and T.-C. Chiang, *Phys. Rev. B* **72**, 035305 (2005).
[11] H. Brune, *Surf. Sci. Rep.* **31**, 121-229(1998).
[12] T. L. Chan, C. Z. Wang, M. Hupalo, M. C. Tringides, and K. M. Ho, *Phys. Rev. Lett*. **96**, 226102, (2006).
[13] J. Tersoff, A. W. Denier van der Gon, and R. M. Tromp, *Phys. Rev. Lett*. **72**, 266 (1994).
[14] D. Deaven and K. M. Ho, *Phys. Rev. Lett*. **75**, 288 (1995).
[15] K. M. Ho, A. Shvartsburg, B. C. Pan, Z. Y. Lu, C. Z. Wang, J. Wacker, J. L. Fye, and M. F. Jarrold, *Nature*, **392**, 582 (1998).

Publications 10/2004-10/2006:

1. *"Impact of Interface Relaxation on Nanoscale corrugation in Pb/Si(111) Islands"*, Z. L. Chan, C. Z. Wang, M. Hupalo, M. C. Tringides, W. C. Lu, and K. M. Ho, *Surf. Sci. Lett*. **600**, L179-L183, (2006).
2. *"Diffusion of Pb Adatom and Ad-dimer on Si(100) From ab initio Studies"* T. L. Chan, Y. Y. Ye, C. Z. Wang, and K. M. Ho, *Surf. Sci. Lett*. **600**, L159-L163, (2006).
3. *"Quantum size effect on the diffusion barriers and growth morphology of Pb/Si(111)"*, T. L. Chan, C. Z. Wang, M. Hupalo, M. C. Tringides, and K. M. Ho, *Phys. Rev. Lett*. **96**, 226102, (2006).
4. *"Magic structures of H-passivated <110>silicon nanowires"* T. L. Chan, C. V. Ciobanu, F.-C. Chuang, N. Lu, C. Z. Wang, and K. M. Ho, *Nanolett*. **6**, 277-281 (2006).
5. *"Global structure optimization of Si magic clusters on the Si(111)7x7 surface"*, F-C. Chuang, B. Liu, C. Z. Wang, T –L. Chan, and K. M. Ho, *Surf. Sci. Lett*. **598**, L339-L346 (2005).
6. *"Diffusion, coalescence and reconstruction of vacancy defects in graphene layers"*, G.-D. Lee, C. Z. Wang, E. Yoon, N.-M. Hwang, D.-Y. Kim, and K. M. Ho, *Phys. Rev. Lett*. **95**, 205501 (2005).
7. *"Model reconstructions for the Si(337) orientation"*, F. C. Chuang, C. V. Ciobanu, C. Z. Wang, and K. M. Ho, *J. Appl. Phys*. **98**, 073507 (2005).
8. *"A first-principles studies of group IV dimmer chains on Si(100)"*, T. L. Chan, C. Z. Wang, Z. Y. Lu, K. M. Ho, *Phys. Rev. B* **72**, 045405 (2005).
9. *"Interface relaxation and electronic corrugation in the Pb/Si(111)-Pb-a-R3xR3"*, M. Hupalo, V. Yeh, T. L. Chan, C. Z. Wang, K. M. Ho, and M. C. Tringides, *Phys. Rev. B* **71**, 193408 (2005).
10. *"Structure of Si(114) determined by global optimization methods"*, F. C. Chuang, C. V. Ciobanu, C. Predescu, C. Z. Wang, and K. M. Ho, *Surf. Sci*. **578**, 183-195 (2005).
11. *"Finding the Reconstructions of Semiconductor Surfaces via a Genetic Algorithm"*, F. C. Chuang, C. V. Ciobanu, V. B. Shenoy, C. Z. Wang, and K. M. Ho, *Surf. Sci. Lett.*, **573**, L375-L381 (2004).

MULTISCALE ATOMISTIC SIMULATION OF METAL-OXYGEN SURFACE INTERACTIONS: METHODOLOGICAL DEVELOPMENT, THEORETICAL INVESTIGATION, AND CORRELATION WITH EXPERIMENT

PI: Judith Yang, Mechanical Engineering and Materials Science, University of Pittsburgh (UPitt), PA, jyang@engr.pitt.edu

Co-PIs: Alan McGaughey, Mechanical Engineering, Carnegie Mellon University (CMU), Pittsburgh, PA, mcgaughey@cmu.edu; Susan Sinnott, Materials Science and Engineering, University of Florida (UF), Gainesville, FL, ssinn@mse.ufl.edu; Simon Phillpot, Materials Science and Engineering, University of Florida, Gainesville, FL, sphil@mse.ufl.edu.

PROGRAM SCOPE

Our long-term vision is the comprehensive and fundamental understanding of a critical gas-surface reaction, nano-oxidation— from the adsorption of oxygen atoms on the metal surface to the coalescence of the bulk oxide—via coordinated multi-scale theoretical and *in situ* experimental efforts. Reaching this goal necessitates close collaborations between theorists and experimentalists. The purpose of this specific DOE program is the development of new theoretical and computational tools that can be used to model nano-oxidation, and the correlation of these predictions with our abundant experimental observations acquired by a unique *in situ* ultra-high vacuum transmission electron microscope (UHV-TEM).

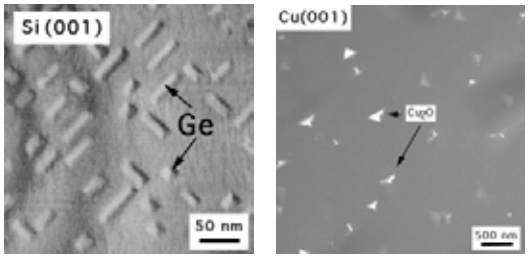

Figure 1: Comparison of Ge on Si heteroepitaxy and Cu_2O nucleation on Cu(001).

The PI has previously shown that heteroepitaxial concepts describe the nucleation and growth to coalescence of Cu_2O islands on Cu(001) surprisingly well (Fig. 1). Models of heteroepitaxial growth, where nucleation rate theory is a standard model used to describe the atomistic processes, have been developed and used successfully to describe metal-on-metal heteroepitaxy. However, these models have not yet been developed to include gas-surface reactions. ***The objective of this program is to further develop heteroepitaxial theories for application to oxidation using a multiscale theoretical approach, and thus allow the direct quantification of the associated experimental observations and lead to a fundamental understanding of nanoscale oxygen gas – metal surface reactions.***

To achieve this goal, we are (i) developing a kinetic Monte Carlo (KMC) approach, called Thin Film oxidation (TFOx), to simulate the atomistics of transport, nucleation and growth of metal oxides during the oxidation process, and (ii) determining realistic input parameters for TFOx through coordinated electronic structure and molecular dynamics. The TFOx development is the primary responsibility of the PI. The electronic-structure calculations and atomic-level simulations are the prime responsibilities of the CMU and UF co-PIs. Figure 2 is a schematic diagram of the synergy and coordination of the multi-scale approach, where molecular dynamics (MD) and electronic structure (ES) calculations will be used to determine the parameters used in TFOx and how TFOx will then be compared to experiments (including both *in situ* UHV-TEM at UPitt and *in situ* X-ray diffraction at Argonne National Lab (ANL, contact: Jeff Eastman) to validate and challenge each method. Our specific goals include gaining fundamental and quantitative insights into the nucleation behavior, morphological evolution of oxide islands during nano-oxidation and coalescence, and provide the surface and interface energies required to

augment the available theoretical treatment of island stability. Each of these aspects has not been demonstrated before for gas-surface reactions and, hence, each represents a potential ground-breaking fundamental science in surfaces and interfaces.

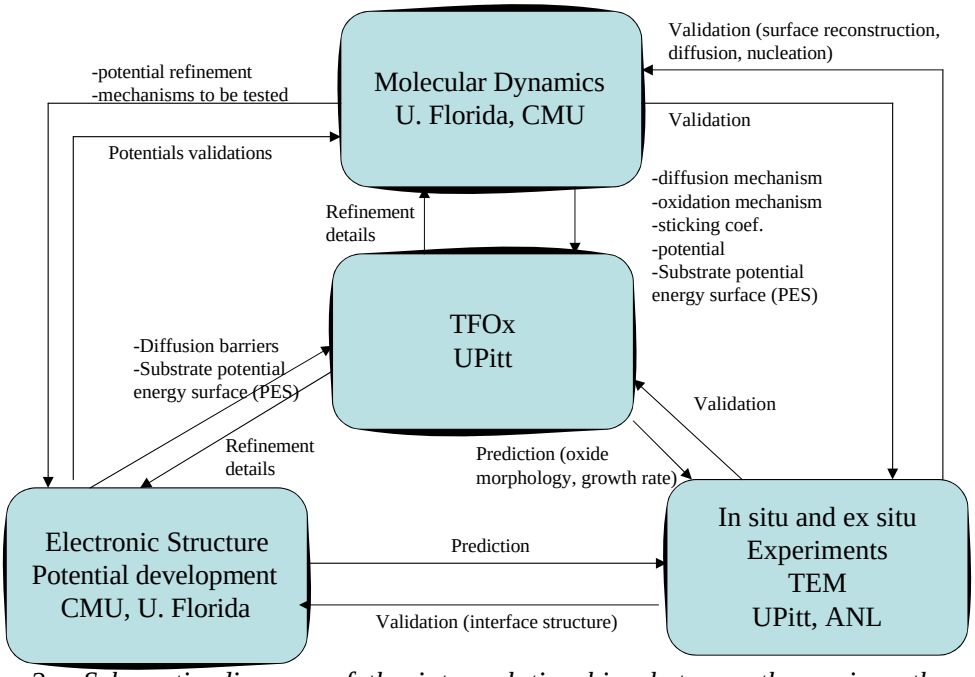

Figure 2: Schematic diagram of the inter-relationships between the various theoretical efforts (Molecular Dynamics, Electronic Structure Calculations, Kinetic Monte Carlo) and in situ and ex situ experiments on oxidation.

RECENT PROGRESS

We have developed a Kinetic Monte Carlo (KMC) code to simulate the complexities of oxygen interactions with a metal surface in 2-D, which is a general and quite versatile KMC program, called Thin Film Oxidation (TFOx), which presently utilizes a user-friendly interface in Visual Basic. TFOx-2D presently simulates the general behavior of irreversible 2-dimensional nucleation and growth of epitaxial islands on a square or rectangular lattice. The TFOx model explicitly considers a very large range of elementary steps, including deposition, adsorption, dissociation of gas molecules (such as O_2), surface diffusion, aggregation, desorption and substrate-mediated indirect interactions between static adatoms. This capability allows for the description of the numerous physical processes involved in nucleation and growth. The large number of possible input parameters used in this program provides a rich environment for the simulation of epitaxial growth or oxidation of thin films. To allow TFOx to be accessible to the rest of the scientific community, a web-site describing TFOx has been developed: www.tfox.org. Through a detailed systematic exploration of affect of various physical parameters, such as sticking probabilities, deposition rate, etc., we have

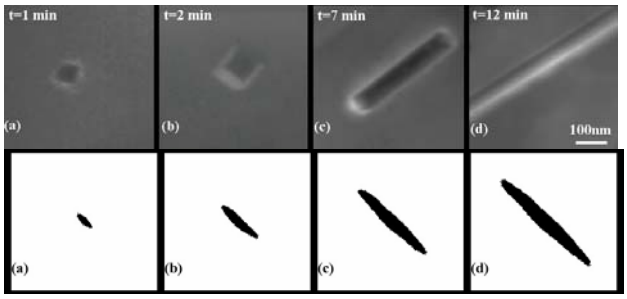

Figure 3. Comparison of nanorod formation observed by in situ UHV-TEM and nanorod growth simulated by TFOx.

already shown that TFOx-2D is capable of displaying a wide variety of thin film oxidation processes, leading to a large number of morphologies, many of which have been observed experimentally. Figure 3 shows one example of nanorod formation in both TFOx simulation and *in situ* UHV-TEM.

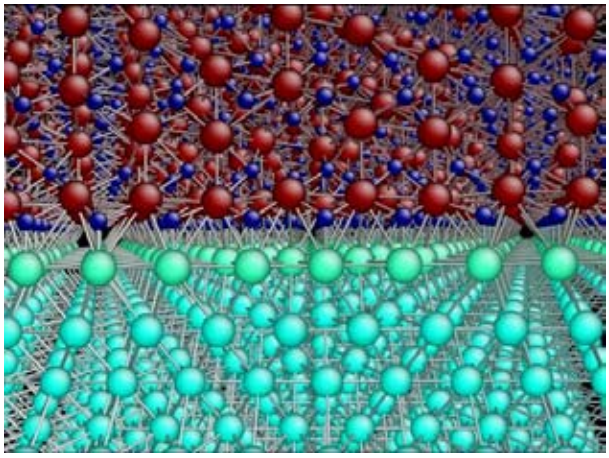

Figure 4: The Al(111)/α Al_2O_3(0001) interface evolved at 300 K. The interface relaxed to an oxygen-terminated oxide phase adjacent to a close packed plane of Al atoms. The colors correspond to charge, with red representing Al in the oxide with a charge near +3, dark blue representing O in the oxide with a charge of near -2. The Al in the base metal near the interface takes on a slight positive charge represented by the slight change in color from the base metal atoms.

To obtain the parameters needed for realistic TFOx simulations (such as sticking coefficients and jump probabilities), atomic-level modeling is needed. To perform molecular dynamics simulations of a metal-oxide system, an interatomic potential that allows for charge transfer is required. Such a potential does not currently exist for Cu-O systems, and we are in the process of parameterizing the Steitz-Mintmire potential (originally developed for Al-O systems) for our system. However, we have successfully implemented a dynamic charge potential into a parallel molecular dynamics program. Simulations of the Al/Al_2O_3 interface (Fig. 4) were conducted using this potential. The starting point was the Streitz-Mintmire potential that was modified through the use of a fourth-order fit to the actual ionization energy of each element and a new fit of the potential to obtain zero charge with zero energy contribution. The changes resulted in a potential that gives a stable, well-ordered interface, as shown in Fig. 4. The charges varied smoothly with realistic values across the interface. We are presently developing parameters for the Cu/Cu_2O system within this potential scheme as well as more accurate ways of modeling the electrostatic interactions. Input for the potential development is from experimental property measurements and from electronic structure calculations of Cu/Cu_2O interfaces. From the molecular dynamics simulations, we will be able to access length and time scales associated with the coordinated movements of oxygen atoms on the copper surface, and better parameterization of TFOx. We will also be able to map the energy surface surrounding different surface geometries, for use as substrate mediated interaction potential parameters in TFOx. Electronic structure calculations will also provide information data for creating surface energy maps.

FUTURE PLANS

Bridging the temporal gap between simulations and experiment is one primary target. Presently, TFOx-2D runs on a PC in Visual Basic and simulates one island growth. As an example of the temporal gap between simulation and experiment, to simulate the island growth to 321nm^2 in 5.79 ns on a 2-D lattice that contains 1000 by 1000 sites with the deposition rate of 0.01 MLs/Loop and sticking coefficient of 0.0002, costs 16 days on a fast PC. For *in situ* experiments, a 3000 nm^2 oxide island forms within 6.5 mins, where the temporal resolution presently is a couple of minutes (defined as the time to take sequential micrographs on the modified JEM200CX). In order to increase the speed of TFOx, we have transformed the Visual Basic code to a C++ program for increased speed as well as for compatibility with supercomputers, such as those available through University of Pittsburgh. We will then continue optimization of the TFOx C++ code for enhanced speed. To reduce the experimental temporal gap, we will take advantage

of new innovations in dynamic TEM (DTEM) that provides nanosecond imaging (contact: Nigel Browning and Geoff Campbell, Lawrence Livermore National Lab), where use of specially developed gas holders will permit the visualization of oxidation, such as oxide island growth, in the microseconds regime.

The next phase for the KMC will be a qualitative leap to TFOx-3D to simulate nucleation and growth in 3-dimensions, i.e. into and above the substrate, and not just laterally on the surface, which virtually all other work using KMC codes of epitaxial growth simulate. A second key component of this DOE program is the determination of real input parameters in TFOx-3D for copper-oxygen systems. This task will be accomplished by performing electronic structure calculations and molecular dynamics simulations of Cu-O systems. The TFOx-3D predictions, utilizing the input parameters obtained via first principles and molecular dynamics will then be directly correlated with *in situ* experiments, including transmission electron microscopy (TEM) and synchrotron X-ray diffraction (XRD), for comprehensive knowledge of nano-oxidation.

Specifically, our future goals include:

- Development of a charge transfer interatomic potential for Cu-O systems.
- Creation of TFOx-3D, an atomistic Monte Carlo simulation program that models island nucleation and growth into and above a substrate, and comparison of the simulation results to experimental observations obtained by *in situ* XRD and TEM
- Determination of the energetic landscape that controls adatom transport, surface reconstructions, nucleation and growth.
- Development of methodologies to determine the realistic input parameters (such as diffusion, sticking coefficients, binding energies, desorption) needed for TFOx-3D from first principles.
- Identification of the critical physical processes and environmental parameters that control nano-island morphologies and coalescence.
- Use of DTEM and *in situ* electron microscopy plus continued development of TFOx in C++ for supercomputers to bridge the temporal gap between theory and experiment.
- Cross-sectional TEM and STEM to gain experimental understanding of interface structure to compare with theoretical determination of interface structure.

Publications:

- G. Zhou and J. C. Yang, "Formation of Quasi One-dimensional Cu_2O Structures by *in situ* Cu(100) oxidation", (2002), Phys. Rev. Let., 89 (10), p.106101-4
- X. Han, R. McAfee and J. C. Yang, "Kinetic Monte Carlo simulations of the dramatic effects of attachment probabilities and potential gradients on island morphology variations under heteroepitaxial growth conditions", Computational Materials Science (2006), (submitted).
- X. Han, R. McAfee and J. C. Yang, "Development of a Versatile Kinetic Monte Carlo Code to Simulate Physical Processes in Thin Film Nucleation and Growth", Multidiscipline Modeling in Materials and Structures (MMMS), Vol.2 No.4 (October 2006).
- A. McGaughey, B. Devine, S.B. Sinnott, S.R. Phillpot, "Adaptation of Dynamic Charge Potentials in Massively Parallel Molecular Dynamics Simulations", Journal of Physics. Condensed Matter (in preparation).
- A. McGaughey, S.R. Phillpot, and S.B. Sinnott, "*Ab Initio* Study of the Cu-Cu_2O Interface", Physical Review B (in preparation).

Conference Proceedings

Xuetian Han, Richard McAfee, and Judith C. Yang, "Kinetic Monte Carlo Model Simulating Nanoscale Oxidation Behavior", JJ9.4 MRS 2004 Fall Boston, Online Proceeding <http://www.mrs.org/members/proceedings/fall2004/jj/JJ9_4.pdf>

Determining the Origins of Electronic States in Semiconductor Nanostructures

Rachel S. Goldman[1] and Harley T. Johnson[2]
rsgold@umich.edu,htj@uiuc.edu
[1]Department of MSE, University of Michigan, Ann Arbor, MI 48109
[2]Department of MIE, University of Illinois at Urbana-Champaign, Urbana, IL 61801

Program Scope

Determining the origins of atom-like electronic states in dimensionally-confined semiconductor structures is a classic problem in materials physics. Although advances in experimental probes and computational power have led to important breakthroughs, several critical fundamental questions regarding the effects of size, interface disorder, and point defects on the electronic states of semiconductor nanostructures remain unanswered. For example, how many atoms are needed in a nanostructure for it to cross over from behaving as an impurity state to a band of states? How do point defects alter the local electronic structure near embedded nanostructures? How does interface disorder contribute to the electronic states of a nanostructure? In this new program, we are investigating these issues with a novel combination of state-of-the-art experiments and theory. Using the probe tip of a scanning tunneling (STM) microscope, we will investigate cross-sections of buried nanostructures in order to count individual atoms and measure their associated electronic states. The experimentally-determined atomic positions will be used as input for real space order(*N*) moments-based tight-binding calculations. The computed local density of states will then be compared to spatially-resolved scanning-tunneling spectroscopy (STS) data. Comparison between XSTM, STS, and tight-binding calculations is expected to elucidate the effects of nanostructure size, shape, strain, and interface disorder on the electronic band structure and confined states. Thus, this project is expected to reveal the origins of the atom-like electronic states in semiconductor nanostructures, as well as test the physical assumptions underlying the experimental and computational techniques.

Future Plans

To achieve our goal of understanding the origins of confined states in dimensionally-confined nanostructures, we will integrate leading-edge experimental and computational methods. We will synthesize tunable arrays of epitaxial semiconductor nanostructures on surfaces patterned with “seeds” and topographical features. Using a combination of plan-view and cross-sectional scanning tunneling microscopy, we will obtain three-dimensional information about structure and electronic states associated with the nanostructures. This information will be input into atomistic computational studies of the electronic properties, using order(N) real-space tight-binding. Local electronic structure computed using this novel method will be compared directly to experimental spectra. Figure 1 shows the direct connection between atomic-resolution XSTM, STS data, and the tight-binding computational approach. Thus, comparison between XSTM, STS, and tight-binding calculations will elucidate the effects of nanostructure size, shape, strain, and interface disorder on the electronic band structure and confined states. Thus, we are exploring the origins of the atom-like electronic states in semiconductor quantum dots, as well as testing the physical assumptions underlying the novel experimental and computational techniques.

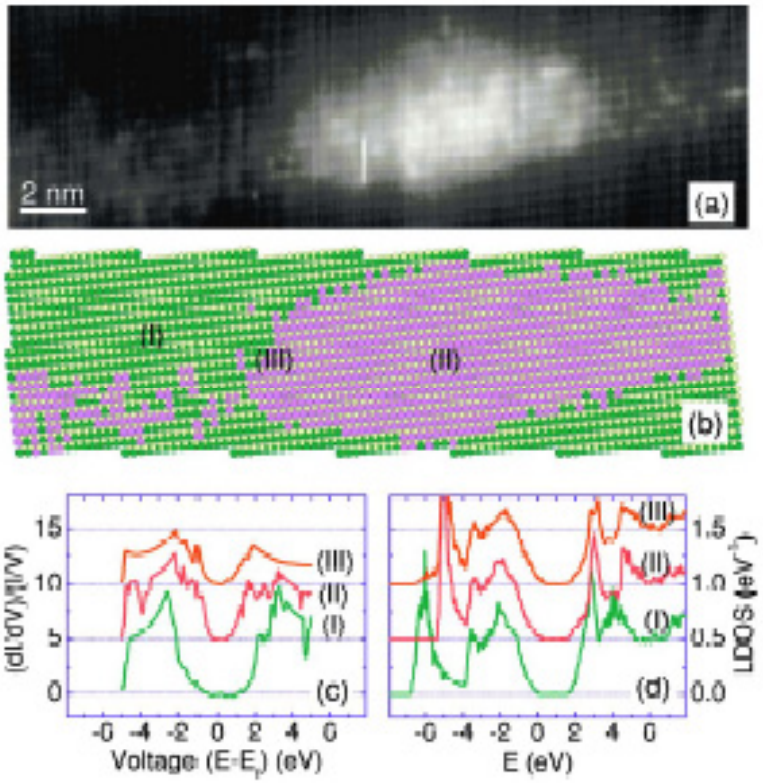

Fig. 1: (a) Atomic resolution scanning tunneling microscope (STM) image of an InAs quantum dot. The bright region is the quantum dot and the dark region is the GaAs buffer at the exposed (110) surface. (b) The atomic structure of the nanostructure recorded from the STM image, using an image reconstruction algorithm. (c) The LDOS of (I) the Ga atom in the buffer; (II) In atom in the nanostructure; and (III) In atom near the interface from the experimental scanning tunneling spectra and (d) local densities of states computed using the moment-based tight-binding method for the same three regions as measured experimentally.

Task 1: Size Effects

Depending on growth conditions and stacking sequences, a variety of nanostructure sizes may be obtained [1]; the apparent diameters of the nanostructures increase monotonically in the growth direction, for example. The effects of these size variations on the confined states in individual and coupled nanostructures are unknown, but will be readily uncovered using our combined experimental and computational approach. We have already begun a comparison of small structures of different sizes [2], to understand the minimum size needed to avoid interface effects that strongly influence the confined states within the nanostructure.

It is straightforward to compute electron states for nanostructures of various sizes, since the tight-binding method can be used to consider any subset of atoms in the overall system in a computationally efficient manner. Empirical potentials, including the valence force field (VFF) method, are being used to accurately relax the atomic positions in larger systems; in the largest systems continuum elasticity can also be used in order to reduce the computational expense associated with relaxing positions for isolated nanostructures. This method will make it possible to relax the atomic positions for structures taken from multi-dot stacks, thus enabling accurate computation of nanostructure size effects on electronic states in realistic systems.

Task 2: Compositional Nonuniformity, Point Defects, and Interface Disorder

We will also examine the role of substitutional point defects on the spectra associated with nanostructures, using a combination of high-resolution XSTM imaging, STS measurements, and tight-binding calculations. We will consider neutral defects including Ga substituting for In (Ga_{In}) or In substituting for Ga (In_{Ga}), as well as charged point defects including group III or V vacancies (V_{In} or V_{Ga}; V_{As}), or dopants (Si_{Ga} or Be_{Ga}). For example, we have presented high resolution XSTM images in the vicinity of a single-period InAs/GaAs nanostructure superlattice. In the darker regions of the image, fringes with a spacing of 5.65 Å, corresponding to the (001) lattice planes of GaAs, are observed. Since

the images were acquired with a positive sample bias voltage (empty state images), the cation sublattice is resolved and the bright spots primarily correspond to In atoms in a GaAs matrix [3,4].

Using the distributions of In_{Ga}, Ga_{In}, V_{Ga}, V_{In}, V_{As}, and Si_{Ga} from atomic-resolution XSTM images, the effects of these defects will be examined computationally. The decay of the electron density of states as a function of distance from point defects will be of particular interest. Because it incorporates an environment dependent self-energy, the tight-binding parameterization used in the computational method is well suited to study this problem. Small clusters of substitutional atoms will also be modeled. This will help to shed light on the important question of how large a cluster of substitutional atoms must be to open a new energy band rather than to simply create a defect state. Preliminary work demonstrates that this question can be readily addressed using the proposed method.

Recent reports have suggested that nanostructures have non-uniform compositions across their widths and heights. For example, both XSTM [5] and diffraction contrast transmission electron microscopy[6] studies have suggested the presence of In-enrichment towards the center of InAs/GaAs structures, with alloy formation towards the edge. To date, the effect of these composition gradients on the confined states in semiconductor nanostructures remains unknown. We have begun to explore these effects in individual (uncoupled) nanostructures using a combination of XSTM and STS, as shown in Fig. 1 (left), which reveals a fairly large InAs/GaAs nanostructure. Figure 2 (right) presents STS spectra acquired from different locations in the nanostructure, in comparison with a region of clean GaAs (in the spacer). The STS data reveal a very small effective bandgap of the nanostructure core, suggesting the presence of bulk-like InAs. Near the edge of the structure, STS data reveal a more substantial effective bandgap, suggesting significant quantization near the edge. Further work is required to explore these effects in individual and coupled nanostructures of various sizes and shapes.

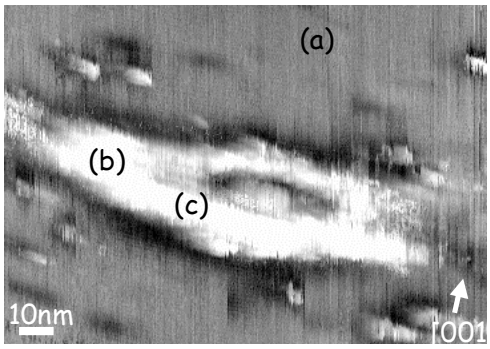

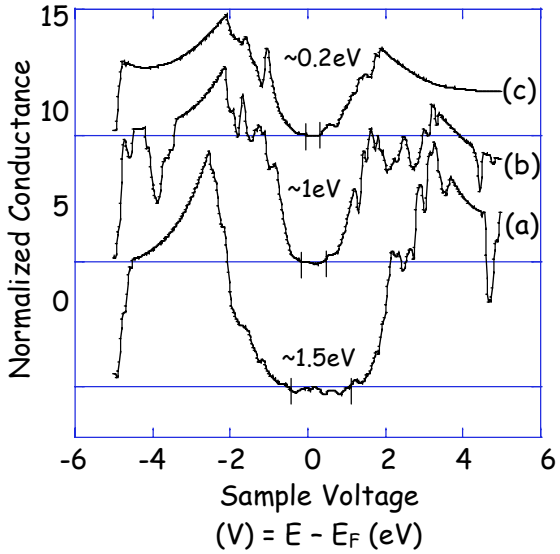

Fig. 2: Spatially resolved STS spectra (right) acquired within the nanostructure (left: b, c) and GaAs spacer (left: a). The sample voltage corresponds to the energy of the state relative to the Fermi level. The valence and conduction band edges are indicated by vertical lines at negative and positive sample voltages, respectively.

The effects of interfacial disorder will also be considered using both idealized geometries and structures observed directly in XSTM images. The key question to be addressed is how typical disorder at interfaces affects the decay of dimensional confinement; spectra computed for different cases will be directly compared to experimental observations.

Task 3: Strain relaxation

Finally, the effects of strain relaxation throughout the nanostructure will be studied both experimentally and computationally. For example, screw components of 60° dislocations are often apparent in stacked nanostructure arrays, especially those with more than 5 superlattice periods [7,8]. Yet, in the literature, models of strain effects on local electronic structure have generally assumed uniform composition and defect-free nanostructures, often with symmetric geometries [9-12]. Recently, Johnson and co-workers studied the effects of localized external strain on nanostructure interactions,

through a comparison of theory [13,14] with NSOM experiments [15-17]. A similar approach will be used here. Realistic representations of compositional variations and defect configurations, along with empirical potentials to relax the atomic positions [12], will be used to directly consider the effects of spatially varying strain on local electronic structure. We expect to observe the effect of nanostructure size on strain relaxation [18]. We will also directly compare the computed signatures for local strain relaxation, defects, and composition variations with the measured experimental spectra.

References

[1] J. Stangl, V. Holy, and G. Bauer, "Structural Properties of Self-Organized Semiconductor Nanostructures", Reviews Of Modern Physics 76, 725 (2004).
[2] J.Q. Lu, H.T. Johnson, V.D. Dasika, and R.S. Goldman, "Moments-Based Tight-Binding Calculations of Local Electronic Structure in Inas/Gaas Quantum Dots for Comparison to Experimental Measurements", Applied Physics Letters 85, 053109 (2006).
[3] J.F. Zheng, J.D. Walker, M.B. Salmeron, and E.R. Weber, "Interface Segregation and Clustering in Strained-Layer Ingaas/Gaas Heterostructures Studied by Scanning Tunneling Microscopy", Physical Review Letters 72, 2414 (1994).
[4] M. Pfister, M.B. Johnson, S.F. Alvarado, H.W.M. Salemink, U. Marti, D. Martin, F. Morier-Genoud, and F.K. Reinhart, "Indium Distribution in Ingaas Quantum Wires Observed with the Scanning Tunneling Microscope", Applied Physics Letters 67, 1459 (1995).
[5] N. Liu, J. Tersoff, O. Baklenov, A.L. Holmes, and C.K. Shih, "Nonuniform Composition Profile in In0.5ga0.5as Alloy Quantum Dots", Physical Review Letters 84, 334 (2000).
[6] A. Lemaitre, G. Patriarche, and F. Glas, "Composition Profiling of Inas/Gaas Quantum Dots", Applied Physics Letters 85, 3717 (2004).
[7] R.S. Goldman, "Nanoprobing of Semiconductor Heterointerfaces: Quantum Dots, Alloys and Diffusion", Journal of Physics D-Applied Physics 37, R163 (2004).
[8] R.S. Goldman, B. Shin, and B. Lita, "Mechanisms of Semiconductor Nanostructure Formation", Physica Status Solidi a-Applied Research 195, 151 (2003).
[9] M. Grundmann, O. Stier, and D. Bimberg, "Inas/Gaas Pyramidal Quantum Dots - Strain Distribution, Optical Phonons, and Electronic-Structure", Physical Review B 52, 11969 (1995).
[10] A. Zunger, "Electronic-Structure Theory of Semiconductor Quantum Dots", Mrs Bulletin 23, 35 (1998).
[11] H.T. Jiang and J. Singh, "Strain Distribution and Electronic Spectra of Inas/Gaas Self-Assembled Dots: An Eight-Band Study", Physical Review B 56, 4696 (1997).
[12] C. Pryor, J. Kim, L.W. Wang, A.J. Williamson, and A. Zunger, "Comparison of Two Methods for Describing the Strain Profiles in Quantum Dots", Journal of Applied Physics 83, 2548 (1998).
[13] H.T. Johnson and R. Bose, "Nanoindentation Effect on the Optical Properties of Self-Assembled Quantum Dots", Journal of the Mechanics and Physics of Solids 51, 2085 (2003).
[14] H.T. Johnson, R. Bose, H.D. Robinson, and B.B. Goldberg, "Simulation Evidence for Lateral Excitation Transfer in a Self-Assembled Quantum-Dot Array", Applied Physics Letters 82, 3382 (2003).
[15] A.M. Mintairov, K. Sun, J.L. Merz, C. Li, A.S. Vlasov, D.A. Vinokurov, O.V. Kovalenkov, V. Tokranov, and S. Oktyabrsky, "Nanoindentation and near-Field Spectroscopy of Single Semiconductor Quantum Dots", Physical Review B 69, (2004).
[16] H.D. Robinson, B.B. Goldberg, and J.L. Merz, "Observation of Excitation Transfer among Neighboring Quantum Dots", Physical Review B 64, (2001).
[17] H.D. Robinson, M.G. Muller, B.B. Goldberg, and J.L. Merz, "Local Optical Spectroscopy of Self-Assembled Quantum Dots Using a near-Field Optical Fiber Probe to Induce a Localized Strain Field", Applied Physics Letters 72, 2081 (1998).
[18] H.T. Johnson, L.B. Freund, C.D. Akyuz, and A. Zaslavsky, "Finite Element Analysis of Strain Effects on Electronic and Transport Properties in Quantum Dots and Wires", Journal of Applied Physics 84, 3714 (1998).

Using Plasmon Peaks in Electron Energy-Loss Spectroscopy to Determine the Physical and Mechanical Properties of Nanoscale Materials

James M. Howe
jh9s@virginia.edu
Department of Materials Science & Engineering, University of Virginia,
Charlottesville, VA 22904-4745

Program Scope

In order to fully utilize the technological advantages of nanostructured materials, it is necessary to characterize their functional properties at the nanoscale. This is a difficult problem, not only due to the small size of the features, but also to the fact that they may be metastable and not accessible in bulk form, as in the case of many strengthening precipitates in metal alloys.

It is well known that one of the primary inelastic scattering processes that occurs as fast electrons travel through a thin specimen in the transmission electron microscope (TEM), is the creation of quantized collective electron excitations, know as volume plasmons, in the specimen [1]. Volume plasmon peaks occur in the low-loss region (0-50 eV energy loss) of electron energy-loss spectra (EELS) from all materials. Since they are associated with the valence/bonding electrons that are responsible for the physical and chemical properties of solids [2,3], this makes them attractive for determining material properties on a local scale. Volume plasmons are longitudinal oscillations that behave as single quasi-particles, with a characteristic angular resonance frequency ω_p and energy E_p. There is a direct correlation between the volume plasmon energy and the properties of materials, because both increase proportional to the valence electron density [4,5], as explained further below. As a result, measurement of the plasmon energy E_p in EELS, can be used to determine a variety of material properties [4-7]. This can be done on a nanoscale in a field-emission gun TEM, where sub-nanometer electron probes are readily obtained.

The main objectives of this research are to: 1) understand the relationships between the volume plasmon peaks in EELS and the mechanical and physical properties of materials on a fundamental level, 2) establish the relationship between the mechanical properties of nanoscale materials and their plasmon energy as a function of material size, so that plasmon measurements in EELS can be used to routinely determine the mechanical properties of nanoscale materials, and 3) apply the technique to a number of model experimental systems and situations in order to understand the accuracy and limitations of the technique.

Recent Progress

During the past year or so, we have developed new insights into the fundamental relationships among the valence electron density, the solid-state physical and mechanical properties of materials, and the volume plasmon energy as measured by EELS. A vast number of materials obey the universal binding energy relation (UBER), which describes the shape of the binding energy curve for materials [8]. In the UBER, the scaled cohesive energy E_{coh}, scaled interatomic separation a, and scaled valence electron density n, can be described by a universal function of the Rydberg type. The volume plasmon energy E_p is related to the valence electron density n as: $E_p \cong [(\hbar\omega_p^f)^2+E_g^2]^{0.5}$, where $\omega_p^f=[ne^2/(\varepsilon_0 m)]^{1/2}$ is the free electron plasma frequency,

e is the electron charge, ε_0 is the permittivity of vacuum, m is the electron mass, and E_g is the bandgap energy. The bulk modulus B_m is directly related to the scaled cohesive energy and equilibrium atomic volume, so that one can derive the following relationships: $B_m \propto E_{coh}/V_{wse} \propto n \propto E_p^2 - E_g^2$, where V_{wse} is the volume of the Wigner-Seitz cell at equilibrium. Due to these relationships, B_m, E_{coh}/V_{wse} and n can be linearized on a log-log scale as a function of E_p^2-E_g^2 (or E_p when E_g=0 or $E_g^2 << E_p^2$), thereby allowing both a measurement of these material properties through measurement of E_p, as well as an understanding of their fundamental origin.

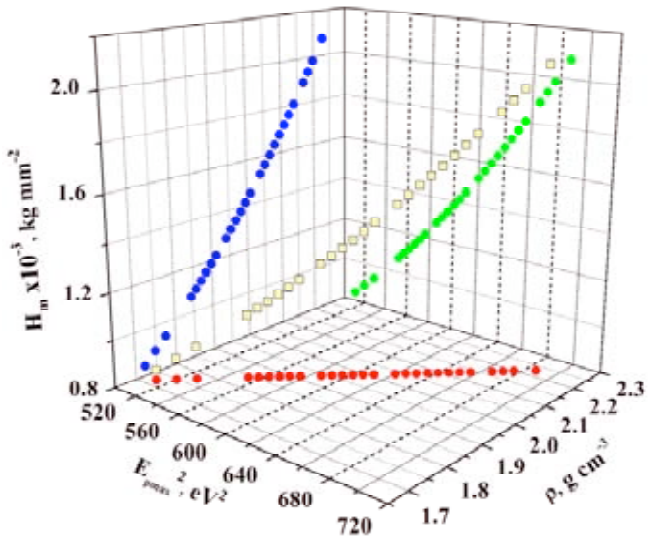

Figure 1. Correlation between Vickers hardness, density and the plasmon peak energy for carbon materials.

Other material properties can be measured using plasmons, provided one has a sufficient correlation between the plasmon energy and property of interest. Recently, we have found that carbon materials, e.g., diamond, graphite, diamond-like carbons, hydrogenated and amorphous carbon films, exhibit strong correlations in density ρ versus E_p (or maximum of the volume plasmon peak), and ρ versus Vickers hardness H_m, from available experimental data and ab-initio DFT calculations. This has allowed us to derive a three-dimensional relationship among these quantities, as shown in Figure 1, that can be used to determine both the hardness and density of this important class of materials based on measurements of their plasmon peak position.

Experimentally, we recently demonstrated the possibility of determining changes in the physical properties of materials with conditions, e.g., temperature, in-situ using EELS, and we applied a plasmon ratio-imaging technique to map multiple physical properties of materials with sub-nanometer lateral resolution, as illustrated in Figure 2. Such techniques present new

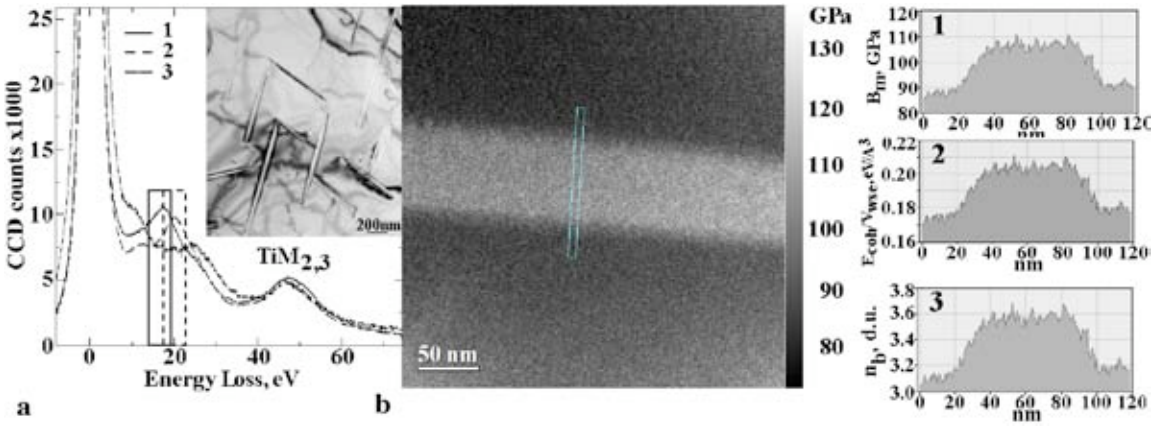

Figure 2. (a) TEM (insert) and EELS of 25-70 nm thick γ-TiH_x precipitates (spectra 2 and 3 are partially oxidized and hydrolyzed γ-TiH_x) in an α-Ti matrix (spectrum 1). (b) B_m map obtained by rescaling the 20 eV/18 eV ratio-image within the 16.5-21.5 eV energy range followed calculation of B_m for each pixel using a correlation function. The rectangular box indicates where the property profiles (inserts 1-3 on right) were taken using a 10-pixel integration window across the γ-TiH_x precipitate and adjacent matrix.

capability for characterizing and understanding material behavior. We also recently demonstrated a new physical phenomenon - electron-beam trapping of a solid metal nanoparticle inside a liquid metal. This phenomenon is analogous to that of optical trapping of solid microparticles in solution, also known as "optical tweezers", which is currently being used to manipulate molecules and inorganic materials in a variety of nanotechnology applications [9,10]. Demonstration of electron-beam trapping was accomplished by partially melting submicron-size Al-Si alloy powder particles in the TEM, and manipulating the solid nanospheres inside the liquid using the electron beam, while observing them in real-time using plasmon spectroscopic imaging. Such “electron tweezers” can potentially be utilized for manipulation and processing of individual nano-objects and fabrication of assembled nano-devices.

Future Plans

So far, our work has concentrated on metals and carbon materials, although we have considered all materials in our initial plasmon-property correlations [5]. The physical basis for the connection between some material properties, such as the bulk modulus and cohesive energy, and the plasmon energy is clear. The fundamental connection for some other important properties, such as the shear modulus, is not so obvious [2]. We have recently begun to apply plasmon spectroscopy to glasses, where the shear and bulk moduli, *G* and *B*, respectively, have been accurately measured and their ratio *G/B* has a major effect on ductility [11]. While we see significant systematic differences in the plasmon energies and ductilities of the glasses we have measured so far, the behavior is not what we expected and suggests that we need additional understanding, both in terms of *G* and the behavior of glasses, which might be considered ideal materials for low-loss EELS due to their non-crystalline structure. We plan continue to pursue these subjects in the future.

We have been somewhat limited in our ability to understand the behavior of plasmons in compound materials, e.g., metal-aluminides or metal-titanates, and elements that do not display simple low-loss spectra, e.g., Au. This situation is partly due to the complexity of the low-loss spectra and difficulty in calculating the spectra from first principles, as well as to the fact that many researchers do not analyze their low-loss spectra when reporting detailed analyses of the near-edge structure during investigations of such alloy series, probably due to their complexity. Unlike the near-edge structure, where atomistic calculations have been widely and successfully employed to explain the features, atomistic calculations are just beginning to be performed to determine low-loss spectra for materials, although with reasonably good success [12]. We do not have the ability to perform such calculations, but we hope to collaborate with researchers who do in the near future and to work toward eventually obtaining this capability. In addition, we plan to contact researchers who have reported systematic investigations of compound materials, to see if we can obtain their low-loss EELS spectra for comparison with our understanding of the variation of plasmons, the valence electron density, and the properties in such materials. We could potentially acquire these spectra ourselves, but it would reduce our task considerably if we can obtain them from others.

We recently acquired a fiber-optic specimen holder for our JEOL 2010F TEM that will allow us to shine light on a specimen while acquiring EELS spectra and/or energy-filtered TEM images. Such experiments have not been tried before and we anticipate that they may allow us to quantify changes in the electronic structure of materials, i.e., the density and/or unfilled density of states, using the low-loss region and the near-edge structures, respectively. This offers very

interesting possibilities in materials analysis. We have installed the optical fiber in the holder and are currently setting up the laser connection. We anticipate being able to perform initial experiments soon, most likely using Si, either in bulk or nanocrystalline form and IR light.

References

[1] R. F. Egerton, *Electron Energy Loss Spectroscopy in the Electron Microscope*, *2nd Ed.*, Plenum Press, NY **1996**, pp. 76-80, 431, 154-16.
[2] J. J. Gilman, *Mat. Res. Innovat.* **1997**, 1, 71.
[3] M. L. Cohen, *Physics Today* **2006**, June, 48.
[4] J. J. Gilman, *Phil. Mag. B* **1993**, 79, 643.
[5] V. P. Oleshko, M. Murayama and J. M. Howe, *Micros. Microanal.* **2002**, 8, 350.
[6] J. M. Howe and V. P. Oleshko, *J. Electron Micros.* **2004**, 53, 339.
[7] L. Laffont, M. Monthioux and V. Serin, *Carbon* **2002**, 40, 767.
[8] J. H. Rose, J. R. Smith, F. Guinea and J. Ferrante, *Phys. Rev. B* **1984**, 29, 2963.
[9] A. Ashkin, J. M. Dziedzic, J. E. Bjorkholm and S. Chu, *Opt. Lett.* **1986**, 11, 288.
[10] K. Avoboda and S. M. Block, *Opt. Lett.*, **1994**, 19, 930.
[11] X. J. Gu, A. G. McDermott, S. J. Poon and G. J. Shiflet, *Appl. Phys. Lett.*, **2006**, 88, 211905.
[12] V. J. Keast, *J. Elec. Spectros. Rel. Phen.*, **2005**, 143, 97.

Selected DOE Sponsored Publications in 2004-2006

Application of Valence Electron Energy-Loss Spectroscopy and Plasmon Energy Mapping for Determining Material Properties at the Nanoscale, J. M. Howe and V. P. Oleshko, *J. Electron Micros.* **2004**, 53, 339.

In Situ EFTEM/PEELS Investigation of the Melting Behavior of Individual Al-Si Alloy Small Particles, V. P. Oleshko and J. M. Howe, in *Micros. Microanal. 2004*, Springer-Verlag, NY **2004**, p. 350.

In-Situ Quantitative Plasmon Spectroscopic Determination and Imaging of Multiple Solid-State Properties at the Nanoscale: a New Capability for Materials Research, V. P. Oleshko and J. M. Howe, in *Electron Microscopy of Molecular and Atom-Scale Mechanical Behavior, Chemistry and Structure*, Mater. Res. Soc., Warrendale, PA **2005**, 839, pp. P2.11.1-6.

"Electron Tweezers" as a Tool for In-Situ Manipulation and Processing of Individual Metal Nanoparticles in a Two-Phase Partially Molten Alloy, V. P. Oleshko and J. M. Howe, in *Micros. Microanal.* **2005**, 11(Suppl. 2), p. 1512.

In-Situ Determination and Imaging of the Physical Properties of Metastable and Equilibrium Precipitates Using Valence Electron Energy-Loss Spectroscopy and Energy-Filtering TEM, V. P. Oleshko and J. M. Howe, in *Proc. Inter. Conf. on Solid-Solid Phase Transformations in Inorganic Materials 2005*, The Min., Met. and Mater. Soc., Warrendale, PA **2005**, p. 455.

In-Situ Determination and Imaging of Physical Properties of Metastable and Equilibrium Precipitates Using Valence Electron Energy-Loss Spectroscopy and Energy-Filtering TEM, V. P. Oleshko and J. M. Howe, *J. Appl. Phys.*, submitted.

An Integrated Computational and Experimental Study of the Dynamics of Grain Boundaries in Impure Systems

Mikhail Mendelev, Shan Liu, and Matthew J. Kramer
mendelev@ameslab.gov, shanliu@ameslab.gov, mjkramer@ameslab.gov
Materials and Engineering Physics, Ames Laboratory, Ames IA 50011
Cai-Zhuang Wang and Kai-Ming Ho
Condensed Matter Physics, Ames Laboratory, Ames IA 50011
wangcz@ameslab.gov, kmh@ameslab.gov

David J Srolovitz
Yeshiva University, NY, NY
srol@yu.edu

Michael K. Miller
millermk@ornl.gov
Materials Science and Technology Division, Oak Ridge National Laboratory, Oak Ridge, TN 37831

Program Scope

A critical feature in the processing and service of most polycrystalline materials is the motion of grain boundaries (GB). The mobility of grain boundaries can vary by several orders of magnitude in two different samples of the same material [1,2]. Intelligent exploitation of this feature holds the potential for unprecedented control of materials properties through material processing. However, much is not understood about the origin(s) of this wide variation in boundary mobility in nominally the same material. Indeed, it is generally understood that impurities can have a profound influence on boundary mobility even at the ppm level [3]. However, while impurities routinely slow boundary migration, there are also examples in which impurities can lead to an increases in boundary migration [4]. The goal of this project is to establish the mechanisms by which impurities modify boundary mobility and develop tools to predict the sign and magnitude of this effect. Both the experiments and simulations will focus on the same alloy systems, the same grain boundaries, and the same material properties. The key feature of this work is the integration of novel computer simulation and experiments.

The development of models to quantitatively predict the GB mobility is severely hampered by the lack of systematic and reliable data on the effects of particular solutes on the migration of different types of grain boundaries. We have chosen pure Al as our model system and select Cu, Ga and Fe as the solutes since their effects on GB migration in Al are significantly different. Computer simulation will entail the development of semi-empirical potentials for the selected solutes in Al and then establish the key parameters necessary for the theoretical treatment of the solute drag effect, i.e., GB mobility in pure Al, heats of solute segregation and GB self- and solute diffusivities. All these parameters will be also determined from experiments on the same system, thus allowing us to validate our computer simulation. We will determine the atomistic mechanism of GB migration from the molecular dynamics (MD) simulation and using this knowledge, we will develop a rigorous analytical model.

Recent Progress

Computer simulation

We have developed new embedded atom method (EAM) potentials for Al, Cu and Fe. In contrast with our previous potential for Al, the new one has a more reasonable value of the surface energy and is in better agreement with X-ray data for liquid Al and Cu. Using this new potential for Al, we conducted MD simulation of GB migration in pure Al in order to obtain M_0 (mobility in a pure system) (Fig. 1). We also performed a MD simulation of Fe diffusion along several GBs in Al. We found that Fe decreases the Al diffusivity. The activation energy for Fe diffusion along the studied GBs is more than a factor of two smaller than that in the bulk. We found that Fe diffuses faster than Al in the <111> Σ7 GB but, slower than Al in the <100> Σ5. Quite importantly, these results indicate that there are some differences in the diffusion mechanisms in these GBs.

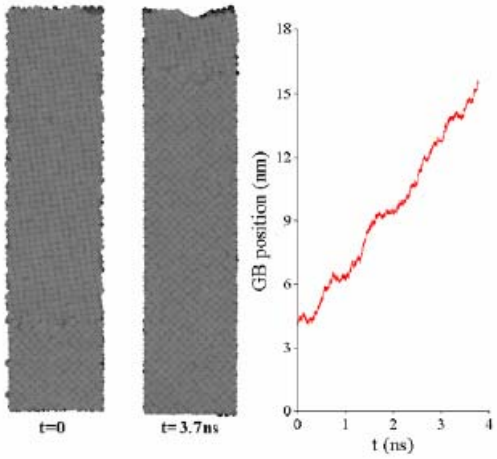

Figure 1. MD simulation of GB migration in pure Al: snapshots of initial and final states and the GB position as function of time.

Experimental study

An experimental study including a preparation of bicrystals containing the <100> ∑5 grain boundary and a measurement of the GB segregation in Al-200ppm (by weight) Cu alloys has been conducted. We started with two half-cylindrical seed crystals with pre-selected orientations that would form the expected GB misorientation. The crystals were cleaned within a glovebox in a NaOH dilute solution to remove any surface oxide layer. The two pieces were annealed in a flowing 80%Ar+20%H_2 atmosphere at 580 ºC to obtain a diffusion bond. The resulting seed piece was subsequently used to grow a bicrystal of Al-200ppm Cu, the orientation of which was checked by backscattered electron channeling patterns (also known as orientation imaging microscopy or OIM). Atom Probe Tomography (APT) specimens were prepared from the GB region in this bicrystal with a FIB miller. However, these test specimens were not successful. Improved specimen preparation procedures designed to reduce the level of gallium implantation coupled with a new laser-pulsed atom probe are expected overcome this problem.

Future Plans

Our future efforts will mainly focus on experimental studies and computer simulations of GB migration in impure Al. **The overall goal of the project is the development of an analytical theory for the solute drag effect, which will be fully parameterized by simulation and validated by both simulation and experiment.** Since it is clear that the GB mobility in the solute-free system, solute diffusivity and solute segregation to GBs are key parameters necessary for predicting the GB mobility in an impure system, complementary investigations to obtain these parameters will be done.

First principles calculations and development of semi-empirical potentials of interatomic interaction

Since it is not realistic to use first principles methods to simulate the GB migration, the first principles calculations will be performed to provide the database which will be used to develop semi-empirical potentials of interatomic interactions and then test these potentials. For our study, we will need a self-consistent set of semi-empirical potentials for all solutes of interest (i.e., Cu, Fe, and Ga) in Al. This means that we cannot take, for example, an Al-Cu potential from one source and the Al-Fe potentials from another source. Unfortunately, there is no such set of self-consistent potentials in the literature and therefore, we will develop them in the framework of this investigation.

Computer simulation and experimental studies of solute segregation

In the computer simulations, the solute segregation will be investigated using two methods. First, we will employ the Monte Carlo simulation technique as it was done previously [5]. This method will allow us to obtain the value of solute segregation as function of temperature. The advantage of this method is that these data can be directly compared with the experimental results (see below). If we find essential disagreement with the experimental data, we will return to the potential development stage. The disadvantage of this Monte Carlo technique is associated with the fact that it can give a detailed picture of the solute segregation only for highly symmetric GBs whether the number of possible segregation sites is limited. However, in our experimental part, we will study the migration of curved GBs, i.e., asymmetric GBs. Moreover, for the development of an analytical model, we need the distribution of the heat of segregation, rather than the segregation itself. Therefore, we will employ a different approach which involves first creating a bicrystal with a GB located near the bottom of the simulation cell. The NVT simulations are then run at 850 K (which is 80 K below the Al melting temperature). Next, a bi-axial strain is applied in order to move the GB to the middle of the simulation cell. Following the removal of the applied strain, the temperature of the system will be step-wise reduced to 0 K under isobaric conditions. It is this 0 K boundary structure which will be used to determine the distribution of the heats of segregation. The obtained distribution of the heats of segregation will be used to calculate the average segregation. First, we will apply this approach to the symmetric GBs which we will also study by the Monte Carlo method and use the Langmuir isotherm as it was done in [6]. Once the methodology is established, it will be used to study solute segregation on non-symmetric GBs as well Cu-Ga and Cu-Fe co-segregations on the Al GBs.

To obtain a bicrystal sample, two methods can be used: in-situ Bridgman growth on a bi-crystal seed or diffusion bonding of the two crystals of known orientation. As discussed in the previous section, we have used Bridgman growth technique to prepare a bi-crystal sample for GB segregation study by atom probe tomography (APT) and we have successfully obtained the <100> $\sum$5 GB.

The experimental study of the solute segregation is particularly challenging and will require the use of multiple, complementary techniques. The atom probe tomography will use the LEAP at the ORNL SHaRE facility. The solute concentration profile in the direction normal to the GB will be determined. Since solute distribution at the GB is essentially limited to a few nanometers, the spatial resolution and sensitivity of a detector of our experimental setup may be technically limiting factors. The LEAP's position-sensitive detector has a detection efficiency of ~50% for all elements so we should be

able to measure Cu concentrations that are less than ~100 appm. To complement the compositional information provided by APT, more detailed crystallography will be obtained using TEM techniques. TEM will provide structural data of the GB and some information of the upper limits of the solute segregation over a larger region than LEAP.

Computer simulation and experimental studies of grain boundary migration

In the computer simulation part, we will first perform a series of molecular dynamic simulations of grain boundary migration in a pure system. We have already established a reliable method for the determination of the mobility of a flat GB in pure systems (see above and [7, 8]) Since in our experimental study, the capillarity will be used as the source of driving force, only the average reduced mobility will be obtained from experiments. In order to compare the simulation predictions with experiments we will also perform MD simulations of the shrinking grains using either halfloop or cylindrical geometry. We will also obtain the flat GB mobility as function of GB inclination. Combination of these two MD simulations will allow us to evaluate the GB stiffness. Note that this important GB characteristic has never obtained from experiments. Next, we will perform MD simulations of GB migration in the presence of solutes. This simulation should be consistent with our experimental studies. Experiments will focus on the cases where the bulk solute concentration is 10-100 ppm. Assuming that the simulation cell cross-section in the GB plane is 40×40 Å, we find that the GB plane contains around 100 atoms. Therefore, on average a GB meets a solute atom only when it moves over about 100 interatomic spacing if the solute concentration is 100 ppm. Hence, we can use the simulation scheme where solute atoms initially sit on a GB and there are no solute atoms in the bulk. This will exclude the problem of reaching the steady-state solute concentration on GB as long as all solute atoms migrate with the GB during MD simulation. The goal of this simulation will be two-fold. First, we will determine the GB velocity as function of the GB solute concentration, temperature and driving force. The corresponding solute bulk concentration will be estimated using our Monte Carlo simulation of the solute segregation. The second goal of this investigation will be to establish how the presence of solutes modifies the mechanism of GB migration.

DOE Sponsored Publications in 2005-2006

Hao Zhang,_ Danxu Du, David J. Srolovitz and Mikhail I. Mendelev, Determination of grain boundary stiffness from molecular dynamics simulation, **Appl. Phys. Lett**., *88*, 121927 (2006)

Hao Zhang, Mikhail I. Mendelev 1, David J. Srolovitz, Mobility of ∑5 tilt grain boundaries: Inclination dependence, **Scripta Materialia** *52* 1193–1198, (2005)

References

1 G. Gottstein and L.S. Shvindlerman, *Grain Boundary Migration in Metals: Thermodynamics,Kinetics, Applications,* Boca Raton, Florida: CRC Press (1999)
2 K. Lücke, G. Masing and P. Nölting, *Z. Metallk.* **47**, 64 (1956)
3 K.T. Aust and J.W. Rutter, *Trans. Metall. Soc. AIME* **215,** 820 (1959)
4 D.A. Molodov, U. Czubayko, et.al., *Phil.Mag. Let.* **72,** 361 (1995)
5 S.M. Foiles, *Phys. Rev. B* **40**, 11502 (1989)
6 M.I. Mendelev, D.J. Srolovitz, G.J. Ackland and S. Han, *J. Mater. Res.* **20**, 208 (2005)
7 H. Zhang, M.I. Mendelev and D.J. Srolovitz, *Acta Materialia* **52**, 2569 (2004)
8 H. Zhang, M.I. Mendelev and D.J. Srolovitz, *Scripta Materialia* **52**, 1193 (2005)

Crystal-melt interfaces and selection at extreme rates

R.E. Napolitano, R. Trivedi, S. Liu, M. Mendelev, M.J. Kramer
Materials & Engineering Physics, Ames Laboratory

Scope

This effort is directed toward gaining an increased understanding of alloy melts and the various dynamics associated with crystallization or other freezing reactions. More specifically, we are interested in the fundamental thermodynamic and kinetic principles that govern the behavior of crystal-melt interfaces and the physical mechanisms that give rise to phase selection, pattern formation, and the wide variety of solidification microstructures that form at extreme rates, both high and low. Development of the requisite theory involves descriptions of the physical interactions that operate at spatial and temporal scales ranging over several orders of magnitude, from the microstructural scale (10^{-6} – 10^{-3}m) down to the atomistic level (10^{-8}-10^{-10}m). Indeed, the thermodynamic and kinetic properties which originate at the atomistic level ultimately govern the dynamics of morphological transitions, and a quantitative understanding of these properties is required for substantive theoretical advancement and the development of predictive capability. The work described here includes three specific area of focus, including (i) fundmental behavior of crystal-melt interfaces, (ii) selection in faceted-nonfaceted eutectics at low growth rates, and (ii) selection in highly driven eut ectics systems. Recent progress and plans for future work are highlighted here.

Recent Progress

Anisotropic interfacial free energy is a critical factor in any predictive theory or computational treatment of the evolution of solidification microstructures, and its quantification is essential to the development of such treatments. In this project, we have used several approaches to quantify the anisotropic behavior of crystal-melt interfaces and to understand its influence on the dynamics of crystalline phases growing from the melt. We have developed a method for experimentally determining the 3-D equilibrium (Wulff) surface by directly measuring the shape of intragranular liquid droplets and have reported results for the Al-Sn system in terms of the relevant cubic harmonics. In addition, we have computed the theoretical shape of coupled crystal-melt interfacial grain boundary grooves as a function of anisotropy, orientation of the solid-liquid interface, and orientation mismatch between the grains. These theoretical groove solution trajectories provide a high sensitivity strategy for the quantification of anisotropy. Measuring groove shapes along portions of the relevant trajectories we have determined interfacial free energy and its anisotropy in transparent organic metal-analogs: $\gamma_0 = 9.28 \pm 0.06$ mJ/m^2 and $\varepsilon_4 = 0.0051 \pm 0.001$ for SCN and $\gamma_0 = 2.78 \pm 0.05$ mJ/m^2 and $\varepsilon_4 = 0.023 \pm 0.012$ for PVA (preliminary).

The crystal-melt interface mobility is a fundamental property indicating the intrinsic resistance to motion of the interface by atomic attachment and detachment mechanisms. The mobility is most often given as a simple kinetic coefficient, μ, which is defined by the relation $V=\mu\Delta T$, where V is the solid-liquid interface (SLI) velocity and $\Delta T=T_m-T$. Using a constant applied external stress to drive the interface, we have established a reliable simulation method for quantifying an interface mobility when the system is far from equilibrium and have compared this method with other simulation methods that use undercooling to drive the interface.

We use periodic boundary conditions in the x and y directions (parallel to the interface) and open surfaces in the z-direction. Thin liquid layers are created in the top and bottom parts of the simulation cell. A constant strain is applied in the x and y directions at $T=T_m$. Since liquid does not support strain, this increased only the free energy of crystal and served as the source of the driving force. During the simulation, the liquid layers grows toward to the center of the simulation cell. Using this method with an embedded atom potential, we have determine the velocity – driving force relationships for pure aluminum, which were found to be linear at all

applied strains. The slope gives the SLI mobility which was found to be 65, 54 and 53 m/(s·GPa) for the <100>, <110> and <111> SLIs, respectively. The kinetic coefficient was calculated from these data by using the Gibbs-Helmholtz equation (using additional simulation data, which are not discussed here). The kinetic coefficient was also determined directly from simulations where ΔT was used as the driving force. The comparison of the kinetic coefficient values obtained by two different techniques demonstrated that the SLI mobility does not depend on the source of the driving force. The experimental value for Al with ~0.5wt% Be is 66 cm/(s·K). This comparison clearly demonstrates the ratability of our simulation.

In an investigation of low-velocity solidification in Al-Si, we have used serial milling and 3D image reconstruction, to investigate the growth mechanisms that lead to rapid lateral propagation of bicrystalline dendritic twin-grains. We have shown the critical role of twinning in the formation of the sideplates, a necessary feature for selection of this diffusive growth morphology. The migration of twin boundaries within the dendritic core enables efficient twin boundary reconfiguration, permitting diffusion-based evolution of sideplate structures, new primary core formation, and the associated selection of primary array spacing. Considering the possible "simple" core structures that would result in the eight-pointed starshape morphology, we classify the cores into three types, according to the connectivity of the individual twins. Using electron backscatter patterns, we have confirmed all three core types, and through the analysis of many such twin structures, we have shown that the twin boundaries are comprised predominantly of segments with {310} and {210} orientations. With direct evidence from high resolution TEM imaging to support our claim, we have proposed a structure for the dendritic core that includes a combination of {310} and {210} symmetric coherent twins and have described an associated twin boundary migration mechanism, at the atomistic level, which would facilitate reconfiguration of the core structure and the sideplate generation required for efficient response to radial supersaturation gradients.

Regarding highly driven eutectic systems, (i.e. high undercooling) the tendency for glass formation in metallic systems has generally been observed to be considerably lower in binary systems than in higher order systems, where the growth of crystalline phases from the homogenous melt may require more substantial chemical rearrangement and, therefore, may be kinetically limited. However, a reasonably strong tendency for glass formation has been reported in the aluminum rare-earth (Al-RE) binary systems. While trends revealed through experimental investigation have given rise to several schools of thought regarding the thermodynamic conditions that may lead to the formation of amorphous phases from the melt, a generally accepted theoretical basis for glass forming tendency in metallic alloys has not been established. Clearly, while any reliable descriptor of glass forming tendency would necessarily include one or more characteristic time scales representing the system kinetics, reliable quantification of relative stability is certainly a prerequisite to meaningful treatment of microstructural dynamics. Unfortunately, detailed thermodynamic descriptions of the Al-RE alloys are generally not well developed, precluding careful investigation of the competition between crystalline and amorphous phases upon cooling from the melt. Accordingly we have investigated the thermodynamic properties of several Al-RE binary systems, coupling solution-based thermodynamic calculations with experimental measurements and first-principles calculations.

In treating the Al-La and Al-Sm binary systems, we have taken a general solution thermodynamics modeling approach to provide a full description of the equilibrium phase diagram, constrained or "metastable" phase boundaries, and the relevant underlying energetics required to properly treat the nonequilibrium phase compositions which may form at high undercoolings. Specifically, we have used a two-state model for the pure component liquid in the sub-melting temperature regime and a three-species association model to describe the solution or mixing properties of the liquid phase. The resulting liquidus boundaries show better agreement with experimental observation than previously reported models. In addition, we model both terminal and intermediate phases as solid solutions and compute the values of T_L, T_0, and T_k, corresponding to the conditions of equal chemical potential, Gibbs free energy, and entropy, respectively. For constant temperature and pressure, the first condition is simply the definition of equilibrium and, thus, defines the liquidus, (T_L,x_L) (and associated solidus) boundaries. With a reasonable description of the undercooled liquid, these boundaries can be computed to very low

temperatures. The second condition yields the locus (T_0,x_0) or the so-called "T-zero" curve, which defines the temperature below which liquid, of composition x_0, can transform to a given solid phase with no chemical partitioning or associated chemical diffusion. Finally, the third condition defines the locus (T_k,x_k), providing a lower (ideal) limit to the glass transition. Comparison with experiment suggests that, as an upper bound to completely partitionless crystallization from the melt, the T_0 temperature may provide a practical limit for the glass formation range.

Experimental studies have been carried out, with appropriate theoretical models, to examine the stability of eutectic microstructure under rapid solidification conditions. Both directional solidification and laser scanning techniques are carried out in the Al-Sm system to obtain low and high growth rates. It is generally observed that regular lamellar eutectic can no longer form beyond certain critical velocity. Above this critical velocity either wavy or banded microstructures form, and in some system the instability of eutectic leads to metallic glass formation. The experimental results show that the regular lamellar eutectic becomes unstable at the growth rate of about 4.0 mm/s. It has been postulated that the instability of eutectic occurs due to the variation in the diffusion coefficient with interface temperature or due to nonequilibrium effects that can become important at high growth rates. We have experimentally measured the variation in the diffusion coefficient with temperature and used the nonequilibrium effects at high growth rates to calculate their effects on lamellar spacing, as shown in the figure. We observe that both these effects are not important at the limit of eutectic instability.

Future Plans

Having established the method for the determination of the solid-interface mobility in a one-component system (i.e. Al), we will continue to investigate interface mobility in a one-component system using molecular dynamics techniques. In particular, we use the applied stress technique to investigate the temperature dependence of the solid-liquid interface mobility. Next, we will choose an interatomic potential for two-component system. In order to avoid some special features of pair potentials (zero Cauchy pressure for lattices with cubic symmetry, zero difference between the unrelaxed vacancy formation and cohesive energies) which are not typical for real metals, we will use an interatomic potential of the embedded atom method (EAM) or Finnis-Sinclair (FS) types. Since we will explore how the solid-liquid interface mobility depends on some microscopic parameters (e.g., atomic radii) and the solution thermodynamics, it will be reasonable to start from a simple model potential containing just few parameters which of them has a clear physical sense. We will try to find such potential for a two-component system with a eutectic phase diagram. If no appropriate potential is available from literature we will have to develop such potential and determine the corresponding phase diagram. Using this interatomic potential we will perform the simulation of the solid-liquid interface migration in two-component system. The goal of this investigation will be to find out how the solid-interface mobility in a two-component system depends on temperature and composition. Special attention will be given to the concentration distribution in the vicinity of the interface as a function of driving force. We will also determine the diffusivities in the liquid phase as a function of temperature and composition. Finally, we will determine the solid-interface free energy as a function of the same parameters. These results will be used for the development of analytical and other computational (i.e. phase-field) models for solid-interface migration and phase selection.

We will continue to investigate the various morphologies that arise from the faceted/nonfaceted coupled growth in Al-Si at low growth rates. In particular, we will examine the mechanisms of twin formation at the dendritic core and the kinetic advantages that twinning presents. We will begin to investigate this faceted twin dendrite formation as a general phenomenon and identify the range of growth conditions under which it may be observed in other materials. Regrading the overall growth mode in Al-Si, we will examine the mechanisms through which "selection" is occurring in the diamond cubic silicon phase, both during fully coupled eutectic growth, primary silicon growth and also under conditions giving rise to mixed–mode growth. Under these conditions, the interaction between the diffusive coupling at the "meso" scale and the kinetic mechanisms at the "micro" and "nano" scales is not well

understood. Our investigation will involve a systematic experimental investigation of the relevant growth kinetics and morphologies, observed over a compositional range spanning both coupled and uncoupled growth. The focus here will be (i) to identify the interfacial mechanisms of growth, such as the role of twinning, (ii) to identify and understand the mechanisms of adjustment and selection, such as branching and crystallographic texture evolution in the Si phase and (iii) to quantify the diffusional coupling through measurement of the relevant solute field in the vicinity of the solid liquid interface. In addition to the experimental effort, we will use numerical and analytical growth models to promote an understanding of the kinetic mechanisms involved in the selection of these solidification structures, particularly with respect to the faceted Si phase.

We will continue to employ laser melting/freezing to achieve high-velocity directional solidification in selected eutectic systems (Al-Cu, Al-Sm, Ag-Sm and Ag-Cu). The stability of eutectic structures at high velocity will be investigated, and the selection of alternate morphologies and nonequilibrium compositions will be examined. Results will be compared with both analytical and computational models for eutectic growth at these high rates (undercoolings). We will also use the techniques of melt-spinning, agas atomization, and electrostatic levitation to access very high undercooling regimes, investigating microstructural selection under highly nonequilibrium conditions, including the glass forming range.

We will employ phase-field methods coupled with our detailed thermodynamic analyses to examine the nonequilibrium chemical partitioning and the associated effects on interface mobility. Results will be compared with embedded atom molecular dynamics simulations, with analytical models for nonequilibrium partitioning at high growth rates, and with our experimental measurements of chemical segregation patterns in rapidly solidified specimens. When appropriate interfacial behavior has been established, phase-field models will be employed to investigate high-velocity eutectic solidification. The limits of analytical theories (e.g. Trivedi, Magnin, and Kurz) will be identified, and morphological selection beyond these limits will be investigated.

DOE-BES Sponsored Publications 2004-2006

- "Phase equilibria and thermodynamic limits for partitionless crystallization in the Al-La binary system", S.H. Zhou and R.E. Napolitano, Acta Materialia (2006), **54**(3), 831-840.
- "Crystal-Melt Interfaces and Solidification Morphologies in Metals and Alloys" J.J. Hoyt, M. Asta, T. Haxhimali, A. Karma, R.E. Napolitano, R. Trivedi, B.B. Laird, and J.R. Morris, *MRS Bull.*, **29**, 935 (2005).
- "Upper Bound Velocity Limit for Free-Jet Melt Spinning", H. Meco and R.E. Napolitano, *Mater. Sci. Forum*, **475-479** 3371 (2004).
- "Developments in Approaches to Determining the Anisotropy of the Solid-Liquid Interfacial Free Energy", J.R. Morris and R.E. Napolitano , *J. Metals*, **56** (4), 42 (2004).
- "Three-Dimensional Crystal-Melt Wulff-Shape and Interfacial Stiffness in the Al-Sn Binary System", R.E. Napolitano and S. Liu, *Phys. Rev. B: Condens. Matter Mater. Phys.*, **70** (21), 214103/1 (2004).
- "The Role of Melt-Pool Behavior in Free-Jet Melt Spinning", R.E. Napolitano and H. Meco, *Metall. Mater. Trans. A*, **35,** 1539 (2004).
- "Faceted Solidification Morphologies in Al-Si Eutectics at Low Growth Rates" , R.E. Napolitano, H. Meco, and C. Jung, *J. Metals*, **56**(4), 16 (2004).

Bulk and Thin Film Alloys for Structural, Electronic and Energy Related Applications

Velimir Radmilovic and Ulrich Dahmen
VRRadmilovic@lbl.gov, UDahmen@lbl.gov
National Center for Electron Microscopy, Materials Sciences Division, LBNL

Program Scope

The objective of this program is a basic understanding of the key features that control the relationship between microstructure and properties in Al-based alloys and to utilize this information to develop materials of interest for energy-related technologies. By applying the fundamental knowledge on phase transformations and interfaces gained from previous BES-supported research, this work utilizes crystallographic and thermodynamic principles to generate microstructures with unusual properties and employs advanced transmission electron microscopy for detailed characterization.

Employing the principle of elastic strain compensation to promote pre-precipitation clustering, we have shown that the dispersion of strengthening precipitates in Al alloys with Si and Ge can be greatly improved. Similar effects of alloying additions to other Al-based alloys have led to the discovery of a core-shell precipitate structure that forms a kinetic barrier to coarsening. Future work will explore the application of these principles of strain-compensated nucleation and kinetic control of coarsening to other alloy systems. This effort will focus on Al-based alloys ranging from bulk materials for energy-efficient transportation technologies to thin film alloys for sensors and actuators.

Recent Progress

An central focus of this program has been the investigation of fundamental aspects of nucleation and coarsening using bulk model alloy systems.

Nucleation: Recent reports on precipitation in ternary Al-Si-Ge alloys showed a greatly enhanced density of nucleation and lower quench sensitivity than either of the binary alloys [1]. Subsequently, this effect was used to enhance dispersion strengthening in Al-Cu-based alloys [2]. Addition of both elements in amounts as small as 0.5at.% each has resulted in the formation of certain intermetallic secondary phases (metastable Al_2Cu known as θ′) at the expense of others (metastable Al_3Cu known as θ′′) [2,3]. This effect was achieved by creating a dense distribution of ultra-fine Si-Ge precipitates as a template for θ’ nucleation. The extremely high number density of these precipitates is only present when both elements, Si and Ge are added. Addition of only a single element, either Si or Ge, results in precipitates that are too coarse to be useful [1]. However, a fundamental understanding of the enhanced density has been lacking.

It has been proposed that misfit compensation during pre-precipitation clustering is the cause of the observed dramatic increase in the precipitate density in this ternary alloy [1]. Since Si and Ge atoms have opposite mismatch with the Al host lattice (Si is 3% smaller, Ge is 2% larger), clusters containing both elements are expected to be much more stable than clusters of either one. The main reason why this hypothesis has not been confirmed directly is that the Si-Ge clusters are extremely difficult to detect by conventional

analytical electron microscopy or x-ray diffraction methods. In this program, atom probe tomography (APT) [4] has been combined with high resolution electron microscopy (HREM) to confirm the existence of such clusters by atomic-resolution observation.

Clusters around ~3 nm in diameter were identified using HREM. The clusters have diffuse boundaries, maintain the same crystal structure as the host lattice and are roughly spherical in shape. This is in contrast to Si-Ge precipitates, which are easily identified by their crystal structure, sharp boundary and internal twinning [5]. In While Si-Ge precipitates are very stable during TEM examination, Si-Ge clusters dissolve when exposed to the electron beam for extended periods. For this reason, the size, distribution and composition of clusters have not been well characterized and there was no unambiguous test of the strain compensation hypothesis.

Atom probe tomography is particularly well suited to this problem because it enables collection of atomic-level statistics from small sample volumes and allows a direct comparison of pre-precipitation clustering in binary and ternary alloys. A random distribution of silicon atoms was found in the binary alloy. In contrast, silicon- and germanium-enriched regions were clearly identified in the ternary alloy. In later stage of aging, the microstructure contained a relatively dense distribution of multiply twinned Si-Ge particles, around 7 nm in diameter, composed of 2/3 Si and 1/3 Ge. These observations support the original hypothesis that in the ternary alloy the strain-compensated clusters transform directly to the Si-Ge precipitates [1], requiring fewer vacancies for the process than either binary alloy. The particles' spherical shape is due to multiple twinning, which is ubiquitous in small precipitates [5,6,7]. The measured Si-rich composition agrees well with previous results obtained by analytical TEM for numerous Si-Ge precipitates [5] and with Calphad calculations of the ternary phase diagram [8].

Coarsening: Addition of Zr together with Sc improves the effectiveness of Sc as an inhibitor of recrystallization [9,]. The addition of Zr reduces the susceptibility of the Al_3Sc precipitates to coarsening. Analysis in bulk material has shown that Zr dissolves in the Al_3Sc phase by replacing Sc, thus forming $Al_3(Sc_{1-x}Zr_x)$. The maximum solubility corresponds to x = 0.5 10. It has therefore been assumed that the precipitates in Al-Sc-Zr alloys are composed of a stoichiometric $Al_3(Sc,Zr)$ phase with a random distribution of Sc and Zr on Sc sublattice sites. Whereas the effect of Sc and Zr on mechanical properties of Al alloys is already well documented [11], relatively little research has been performed on the morphology and phase distribution of precipitates in the ternary alloys. Following our report of a Zr-rich shell around a Sc-rich core [12], a 3-D atom probe study of small precipitates in a Al-Sc-Zr alloy demonstrated a non-homogeneous distribution of Sc and Zr, and confirmed the core-shell structure [13].

The main focus of this part of the program was to study the structure, morphology and chemical composition of Al_3Sc and $Al_3(Sc,Zr)$ precipitates in Al-rich Al-Sc and Al-Sc-Zr alloys. Using dark field imaging and EDX analysis it was clearly shown that the composition is not uniform within the particle. Zr is predominantly found in a thin shell around the particles, while the core contains Al and Sc essentially without Zr. In addition, while under the similar aging condition in the binary Al-Zr alloys the precipitated phase is predominantly Al_3Zr, while in our ternary alloy Zr rich order phase remains metastable cubic.

Future Plans

a) We will explore different Sc-X (X = Zr or other elements) additions to yield the most high temperature stable phase that can be added at the least cost. An exciting possibility, which remains unaddressed by the Al community, is the to use the Sc-Ti and Sc-Ni systems. The addition of Sc-Ti and Sc-Ni intermetallics to Al may be very effective in promoting high temperature strength since bulk Sc-Ti and Sc-Ni intermetallics are known to be very creep resistant. Sc-Ti and Sc-Ni intermetallics are also relatively inexpensive compared to other Sc-X systems. We plan to use our unique microscopy and analytical capabilities to explain the crystallography and composition of pertinent Al-Sc-X phases. These results will be complemented by detailed phase diagram calculations and by precipitation kinetics data. We will determine the effect of Sc and Sc-X additions on the nucleation, growth and coarsening kinetics of other precipitates.

b) We will characterize precipitate-free zones (PFZs) in ternary and quaternary alloys as a function of heat treatment and plan to apply procedures such as a two step heat treatment and alloy additions to reduce the PFZs.

c) As equilibrium solubility is a major obstacle to further improvement of the mechanical properties of Al alloys, we will use non-equilibrium synthesis techniques. Approaches will include co-evaporation, multilayer structures to form in-situ nanocomposites with alternating soft Al and hard Si-Ge phases, or sputter deposition to create either single phase supersaturated solid solutions with relatively coarse intermetallic precipitates (Al-Fe, Al-Ti or Al-Cr-Fe), or completely amorphous structures (Al-Fe). An interesting and relatively unexplored alloy is Al-Mo, which offers several refractory phases that could be used for strength and stability. We will explore the possibility of using a compositionally optimized Al-Mo film as the basic structural building block of NEMS devices, to fabricate 20nm thick cantilevers of various geometries as a proof of principle. We will then perform bulk and nano-scale mechanical testing on the synthesized alloys and characterize them in detail.

References

1. E. Hornbogen, A.K. Mukhopadhyay and E.A. Starke, *Z. Metallk.*, **83** (1992) 577.
2. D. Mitlin, V. Radmilovic, U. Dahmen and J.W. Morris, *Met. Mat. Trans. A*, **32** (2000) 197.
3. D. Mitlin, V. Radmilovic, J.W. Morris and U. Dahmen, *Met. Mat. Trans. A*, **34** (2003) 735.
4. M.M. Miller, Atom probe tomography: Analysis at the atomic level. Plenum, NY.
5. V. Radmilovic, D. Mitlin, B. Dracup, M.K. Miller, U. Dahmen and J.W. Morris, *Mat. Sci. Forum,* **396-402** (2002) 905.
6. V. Radmilovic, D. Mitlin, U. Dahmen and J.W. Morris, *Met. Mat. Trans. A*, **34** (2003) 543.
7. D. Mitlin, V. Radmilovic, J.W. Morris, *Mat. Sci. Eng. A*, **301** (2001) 231.
8. B. Dracup, P.E.A. Turchi, V. Radmilovic, U. Dahmen and J.W. Morris, *Met. Mat. Trans.,* **35** (2004) 2305.
9 V.G. Davidov, et al., *Mat. Sci. and Eng A*, **280** (2000) 30.
10. Y. Harada and D.C. Dunand, *Mat. Sci. and Eng. A*, **329-331** (2002) 686.
11. C.B. Fuller, D.N. Seidman and D.C. Dunand, *Acta Materialia,* **51** (2003) 4803.

12. A. Tolley, V. Radmilovic and U. Dahmen, *Solid-solid phase transformations in Inorganic Materials*, TMS, 2005, pp. 785-790.
13. B. Forbord et al., *Scripta Materialia*, **51** (2004) 333.

DOE Sponsored Publications in 2004-2006

"Metallic NEMS components fabricated from nanocomposite Al-Mo films", Z. Lee, C. Ophus, L.M. Fischer, N. Nelson-Fitzpatrick, K.L. Westra, S. Evoy, V. Radmilovic, U. Dahmen and D. Mitlin , *Nanotechnology* 17 (2006) 3063–3070.

"Strain-compensated nano-clusters in Al-Si-Ge alloys", V. Radmilovic, M.K. Miller, D. Mitlin and U. Dahmen, *Scripta Materialia*, 54 (2006) 1973-1978.

"Manifestations of dynamic strain ageing in 2090 Al-Li alloy", N. Ilic, M.T. Jovanovic, V. Radmilovic, Dj. Drobnjak, *Zeitschrift fur Metallkunde* 96 (2005) 1386-1390.

"Transmission electron microscopy analysis of grain boundary precipitate-free-zones (PFZs) in an AlCuSiGe alloy", A. Tolley, D. Mitlin, V. Radmilovic and U. Dahmen, *Materials Science and Engineering A*, 412 (2005) 204-213.

"Segregation in Al_3(Sc,Zr) precipitates in Al-Sc-Zr alloys", A. Tolley, V. Radmilovic and U. Dahmen, *Scripta Materialia*, 52 (2005) 621-625.

"Bimodal Microstructure and Deformation of Cryomilled Bulk Nanocrystalline Al-7.5Mg Alloy", Z. Lee, D.B. Witkin, V. Radmilovic, E.J. Lavernia and S.R. Nutt, *Materials Science and Engineering A*, 410-411 (2005) 462-467.

"Coarsening kinetics in Al-Sc-Zr alloys", A. Tolley, V. Radmilovic and U. Dahmen, Solid-solid phase transformations in Inorganic materials 2005, Edited by: J.M. Howe, D.E. Laughlin, J.K. Lee, U. Dahmen, and W.A. Soffa, TMS, 2005, pp. 785-790.

"Ultrahard Al-Si thin films", V. Radmilovic, D. Mitlin and U. Dahmen, *Materials Science Forum*, 494 (2005) 13-18.

V. Radmilovic, D. Mitlin, U. Dahmen, Nano-Structured Ultra-Hard Al-Si Films Displaying Elevated Temperature Stability, TMS Annual Meeting, 2005, San Francisco, CA. (Invited talk)

"Core-shell structures in a precipitate-hardened Al-Sc-Zr alloys"V. Radmilovic, , Seventh Yugoslav Materials Research Society Conference, "YUCOMAT 2005", Herceg-Novi, September 12-16, 2005. (Invited plenary lectures).

"In-situ electron microscopy studies of the effect of solute segregation on grain boundary anisotropy and mobility in an Al-Zr alloy", M.L. Taheri, E. Stach, V. Radmilovic, H. Weiland, A.D. Rollett, Symposium on Electron Microscopy of Molecular and Atom-Scale Mechanical Behavior, Chemistry and Structure, Materials Research Society. 2005, pp.187-93. Warrendale, PA, USA.

Patent

D. Mitlin, C. Ophus, S. Evoy, V. Radmilovic and U. Dahmen, "NEMS cantilevers synthesized from atomically-smooth amorphous-nanocrystalline aluminum alloys", patent disclosure submitted, patent pending, (2006).

Ion Beam Irradiation Effects in Pyrochlore and Murataite Ceramics

Rodney C. Ewing, Lumin Wang and Jie Lian
rodewing@umich.edu, lmwang@umich.edu, jlian@umich.edu

Departments of Geological Sciences, Nuclear Engineering & Radiological Sciences and Materials Sciences & Engineering, University of Michigan, Ann Arbor, MI 48109

Program Scope

Radiation effects in materials are of both fundamental and technological importance. The radiation damage-induced, crystalline-to-amorphous (c-a) structural transition has important technological applications because amorphous materials may have increased hardness, are more resistant to corrosion and oxidation, may be used in opto-electronic devices, have high magnetic permeabilities and electrical resistivities, and radiation-induced damage cascades can be used for flux pinning of high T_c superconductors. In the geosciences many geochronological isotopic techniques are affected by radiation damage. Additionally, in materials science, radiation damage often results in order-disorder structural transitions, and thus materials properties can be "tuned" by controlling the degree of structural disordering at the micro- and the nano-scale. Ion beam irradiation or implantation has been widely used for the fabrication of various types of nanostructures. A more fundamental understanding of radiation effects in materials (including the c-a transformation and order-disorder structural transition) is necessary, not only because of the consequences on materials performance, but also because of the potential for developing a basic understanding of the phase stability of crystalline materials.

Recent Progress

During last two years, we have performed systematic ion beam irradiations on the pyrochlore ($A_2B_2O_7$) and murataite ($A_3B_6C_2O_{22-x/2}$, $F\bar{4}3m$) ceramics, and investigated the microstructural evolution as a function of irradiation damage and temperature. Both pyrochlore and murataite-structure types are the derivative of parent fluorite structure but with ordered arrangements of cation and anions. Particularly, pyrochlore structures display diverse chemistry and structural flexibility by accommodating extensive cation and anion substitutions in the crystal structure. The diverse chemistry is coupled to a remarkable variation of properties that are important in numerous technological applications. These include piezoelectricity, ferro- and ferri-magnetism, luminescence and giant magneto-resistance. Pyrochlore compounds exhibit semiconductor behavior or either metallic or ionic conductions, depending on doping, compositions and oxygen partial pressure, and can be used as potential solid electrolyte for the solid oxide fuel cells. The diverse crystal chemistry and structural flexibility provide a great platform for us to investigate how the chemical composition and structural variation (cation substitutions, structural distortion, chemical bonding, etc) affect the radiation response behavior of materials such as the crystalline-to-amorphous and order-disorder structural transitions. Furthermore, we have synthesized murataite polytypes, anion-deficient fluorite-structured oxides, and investigated the effects of different degrees of structural disordering on ion beam-induced amorphization and the order-disorder structural transition.

Systematic ion beam irradiation of pyrochlore compounds $A_2B_2O_7$ (A = La~Lu and Y; B = Ti, Sn, Hf, Zr) indicated that the radiation response behavior of pyrochlore structure-types is

highly composition dependent.[1] Generally, titanate pyrochlores can be amorphized at relatively low doses (e.g., ~0.2 displacements per atom (dpa) at room temperature for $Gd_2Ti_2O_7$), and the critical amorphization temperature is high (~1120 K). However, certain compositions are highly resistant to ion beam-induced amorphization, and Zr-rich compounds, e.g., $Gd_2Zr_2O_7$, retained crystalline state at the dose as high as ~100 dpa. Based on these irradiation data, a strong correlation among subtle changes in crystal structure with changing composition, the energetics of the disordering process, and the temperature above which the material can no longer be amorphized has been discovered for pyrochlore structure-types. As the structure approaches the ideal, ordered pyrochlore structure, radiation-induced amorphization is more easily attained. This is consistent with an increasingly exothermic trend in the enthalpies of formation of pyrochlores from the oxides, that is the greater the thermochemical stability of the pyrochlore structure the more likely it will be amorphized upon radiation damage rather than recover to a disordered fluorite structure. [2,3]

The ionic size of the cations plays a dominant role in determining the radiation response of different pyrochlore compositions. However, the behavior of the pyrochlore also depends on the cation electronic configurations, i.e., the type of bonding, which is closely related to the polyhedral distortion and structural deviation from the ideal fluorite structure. The ion beam irradiation results on stannate pyrochlores emphasize the important effects of the degree of bond covalency on the radiation response behavior of pyrochlore structure.[3] Preliminary ion beam irradiation of the murataite polytypes has indicated a very interesting phenomenon, that is, a decreased susceptibility to ion beam irradiation-induced amorphization for the disordered murataite as compared to murataite superstructure. This result suggests that the amorphization susceptibility for fluorite-related compounds depends, in part, on the initial degree of intrinsic disorder prior to irradiation.[4] This is first experimental report to document the effect of structural disordering on the radiation response of fluorite-related compounds.

Additionally, we have demonstrated the great potential of using ion beam techniques for fabricating novel nanostructure in complex ceramics. Numerous nanostructures including nano-dots and nano-domains, one-dimensional nanowires, and two-dimensional nano-layers, have been created by ion beam techniques in pyrochlore materials. The nanostructures are created via different mechanisms such as radiation damage-induced crystalline-to-amorphous transformation, order-disorder structural transition and phase decomposition processes. The dimensions and morphology of the nanostructure can be controlled at some extent by varying the irradiation conditions, such as the temperature, fluence, deposited energy, and implanted species.

Future Plans

The systematic ion beam irradiations lead to the discovery of highly radiation “resistant” zirconate pyrochlores, and the understanding of the response of the pyrochlore-structured oxides to ion beam damage has been substantially improved. However, there are still important aspects of the process that remain unclear, e.g., the disordering mechanisms (particularly thermodynamic and kinetic issues), damage recovery processes, the correlation of energetics of structural disorder and material parameters. We plan to continue the systematic radiation study of the pyrochlore-structure type in order to fully understand the relation of the radiation response behavior with the irradiation conditions (e.g., energy, dose, ion mass, etc.) and material parameters (e.g., structure and chemical compositions), the damage recovery processes (including thermally-induced recrystallization and ion beam-induced recovery processes). It is of great interest to study the size effects on the structural disordering and amorphization processes

in pyrochlore compositions as the grain size is scaled down to nanometers. Further detailed research will be conducted on murataite-type ceramics, a supercell structure of pyrochlore, particularly to understand the formation of polytypes as a function of composition and synthesis conditions, and the radiation-induced order-disorder structural transition. The effect of intrinsic structural disordering will be further investigated emphasizing the correlation between the long range ordering (the periodic fluorite unit cells) and the radiation susceptibility. The ultimate objective of this research will be to determine the chemical and structural controls on the radiation response of complex ceramics.

Ion beam techniques are a powerful tool for nano-engineering and materials design in a wide range of pyrochlore compounds; however, it is still a challenge to precisely control the morphology, size, and dimension, as well as the density and distribution of the nanostructures. A better understanding of the formation of nanostructure induced by irradiation damage as a function of materials compositions and irradiation conditions is necessary in order to manipulate the microstructure and to explore the properties of these new nanostructures. We plan to study the fundamental nanoscale phenomena and processes in a wide range of pyrochlore compositions by conducting systematic ion beam irradiation/implantation studies of nano-scale chemical and structural evolution. We are particularly interested in determining the relation between material properties and experimental conditions (ion mass, energy, dose rate and temperature) that are required for the formation of these nanostructures. The future research results will be critical in understanding the fundamental nanoscale phenomena and processes that occur in a wide range of pyrochlore compositions and will make it possible to precisely control the morphology, size, and dimension, as well as the density and distribution of the nanostructures. These results will allow us to design or pattern novel nanostructures including 1-D, 2-D and surface nanostructures, and to develop the important technological applications for the pyrochlore structure-type, such as micro- and nano-fuel cells, luminescent compounds and catalysts.

References

(1) R. C. Ewing, W. J. Weber, J. Lian, *J. Appl. Phys.* **2004**, 95, 5949.
(2) J. Lian, J. Chen, L. M. Wang, R. C. Ewing, J. M. Farmer, L. A. Boatner, K. B. Helean, *Phys. Rev. B* **2003**, 68, 134107.
(3) J. Lian, K. B. Helean, B. J. Kennedy, L. M. Wang, A. Navrotsky, R. C. Ewing, *J. Phys. Chem. B* **2006**, 110, 2343.
(4) J. Lian, L. M. Wang, R. C. Ewing, S. V. Yudintsev, and S. V. Stefanovsky, *Journal of Applied Physics* **2005**, 97, 113536.
(5) J. Lian, W. J. Weber, W. Jiang, L. M. Wang, L. A. Boatner, R. C. Ewing, *Nucl. Instrum. Method Phys. Res. B* **2006**, *250, 128-136.*

DOE Sponsored Publications in 2004-2006

Ion beam irradiation of La- and Th-doped $Y_2Ti_2O_7$ titanates, Jie Lian, F. X. Zhang, Lumin Wang, and R. C. Ewing, Journal of Nuclear Materials, **2006**, *in press.*

Irradiation-induced nanostructures in cadmium niobate pyrochlores, W. Jiang, W. J. Weber, J. S. Young, L. A. Boatner, J. Lian, L. M. Wang, R. C. Ewing, Nucl. Instrum. Method Phys. Res. B **2006**, 250, 1*88-191.*

Radiation-induced effects in pyrochlore and nano-scale materials engineering, Jie Lian, Weber, W.J., Jiang, W., Wang, L. M., Boatner, L. A., Ewing, R. C., Nucl. Instrum. Method Phys. Res. B **2006**, *250, 128-136.*

Direct evidence of N aggregation and diffusion in Au^+ irradiated GaN, W. Jiang, Y. Zhang, W. J. Weber, J. Lian and R. C. Ewing Appl. Phys. Lett. **2006**, *89, 021903.*

Patterning Metallic Nanostructures by Ion Beam-induced Dewetting and Rayleigh Instability, Jie Lian, L. M. Wang, X. C. Sun, Q. K. Yu, R. C. Ewing, Nano Letters **2006** *6, 1047-1052.*

Simultaneous Formation of Surface Ripples and Metallic Nanodots Induced by Phase Decomposition and Focused Ion Beam Patterning, Jie Lian, Wei Zhou, L. M. Wang, L. A. Boatner, and Rodney C. Ewing Appl. Phys. Lett. **2006,** *88, 093112.*

Effect of Structure and Thermodynamic Stability on the Response of Lanthanide Stannate Pyrochlores to Ion Beam Irradiation, Jie Lian, K. B. Helean, B. J. Kennedy, L. M. Wang, A. Navrotsky, and R. C. Ewing Journal of Physics Chemistry B **2006**, *110, 2343-2350.*

Microstructural Evolution of Ion Implanted $Gd_2Ti_2O_7$, J. Lian, L. M. Wang, R. C. Ewing and L. A. Boatner Nucl. Instrum. Method Physics B **2006,** *242 448-451.*

Enhanced Recrystallization Rates of Amorphous $SrTiO_3$ under Electron-beam Irradiation, Y. Zhang, J. Lian, C. M. Wang, M. H. Engelhard, R. C. Ewing, and W. J. Weber Physical Review B **2005**, *72, 094112.*

Nanostructures on Ion-cleaved Surface of Cadmium Niobate Pyrochlore, W. L. Jiang, W. J. Weber, C. M. Wang, J. S. Young, L. A. Boatner, J. Lian, L. M. Wang, and R. C. Ewing, Advanced Materials **2005**, *17, 1602-1606.*

Cross-sectional TEM Study of Ion Implanted Lanthanide Titanate Pyrochlore Single Crystals, J. Lian, L. M. Wang, R. C. Ewing and L. A. Boatner Nucl. Instrum. Method Physics B **2005,** *241, 365-371.*

Ion beam-induced Amorphization and Order-disorder Structural Transformation in Murataite Ceramics, J. Lian, L. M. Wang, R. C. Ewing, S. V. Yudintsev, and S. V. Stefanovsky, Journal of Applied Physics **2005**, *97, 113536.*

Nanocrystal Formation and Phase Decomposition in Murataite Ceramics, J. Lian, L. M. Wang, R. C. Ewing, S. V. Yudintsev, S. V. Stefanovsky, Journal of Materials Chemistry **2005**, *15, 709-714.*

Amorphization Resistance of $Gd_2Sn_2O_7$ and $Gd_2Hf_2O_7$ Pyrochlores, Jie Lian, Rodney C Ewing, L. M. Wang, and Katheryn B Helean, Journal of Materials Research **2004**, *19, 1575-1580.*

Pyrochlore ($A_2B_2O_7$): A Nuclear Waste Form for the Immobilization of Plutonium and the "Minor" Actinides, , R. C. Ewing, W. J. Weber, and Jie Lian, *Applied Physics Review* Journal of Applied Physics **2004**, *95, 5949-5971.*

Ion Beam Irradiation in $La_2Zr_2O_7$-$Ce_2Zr_2O_7$ Pyrochlore, Jie Lian, L. M. Wang, R. G. Haire, K. B. Helean, and R. C. Ewing, Nucl. Instrum. Methods Phys. Res. B **2004** *218, 236-243.*

Formation Enthaplies of REE-titanate Pyrochlores, K.B. Helean, S.V. Ushakov, C.E. Brown, A. Navrotsky, Jie Lian, Rodney C. Ewing, J. Matt Farmer and Lynn A. Boatner, Journal of Solid State Chemistry **2004**, *177, 1858-1866.*

Electron Diffraction Determination of Nanoscale Structures

Joel H. Parks, Xiaopeng Xing, Xi Li
parks@rowland.harvard.edu
The Rowland Institute at Harvard, 100 Edwin H. Land Boulevard, Cambridge, MA 02142

Program Scope

The size-dependent evolution of the structures and physical and chemical properties of finite nanoscale aggregates, have been the subjects of continuing basic and applied research interests. The accelerating research into the science and technology of "nanoparticles" has approached a level at which a deeper knowledge of the atomic structure is needed for better understanding of how to manipulate atoms in order to achieve unique properties for nanoscale sizes. The specific goals of this research program are to study the size dependence of cluster structures and relate this understanding to the structure dependence of catalytic activitiy for metal clusters in the size range of 10-100 atoms.

Structure determination is one of the outstanding challenges of cluster science. The development of trapped ion electron diffraction (TIED) [1,2] has enabled the first direct measurements of cluster structure. The TIED technique is based on storing cluster ions in an ion trap to enable the accumulation of *size selected* clusters, collisional relaxation of the vibrational energy and exposure to a high energy electron beam for sufficient time to collect electron diffraction data. Collaborations with theorists have provided an essential contribution to this program because comparisons between the measured diffraction patterns and those calculated for theoretically optimized structures is required in order to fully determine the atomic arrangement. This research program relates to the DOE Materials Science and Engineering Division mission by providing a method for confirming the design of nanosize materials at the atomic level; by providing an experimental tool for characterization of nanoscale phenomena; and by allowing a more complete understanding of nanoscale properties.

Recent Progress

Silver Clusters: local order with fivefold symmetry

The first measurements [3] of mass selected metal clusters by TIED methods investigated the evolution of silver cluster, Ag_n^+, structures over the size range 36 to 55 atoms. This range was chosen to gain a better understanding how cluster structures vary through intermediate sizes to achieve "magic number" structures composed of closed electronic or atomic shells. This size range includes two such closings, an octahedral atomic shell closing at Ag_{38}^+ and an icosahedral atomic shell closing at Ag_{55}^+. These measurements have indicated an evolution from short range order among nearest neighbors having fivefold symmetry to a global order having icosahedral symmetry at n=55. A unique structure is observed at n=38 which exhibits a distortion of fcc symmetry characterized by local order having fivefold symmetry.

Diffraction data was compared with molecular patterns, sM(s), calculated from theoretical structures for cluster sizes n=36-39, 43 and 55. Cluster structures were derived from density functional calculations by the research groups of I. Garzón and K. Michaelian at the Universidad Nacional Autónoma de México. The best fit structure for Ag_{38}^+ is shown in Fig. 1(a) in which experimental data (red) is overlayed with the calculated sM(s) (blue) for the isomer structure

producing the best fit. The data uncertainty (± 1σ) is shown by green shading. The calculated best fit isomer structure exhibits local order having fivefold symmetry concentrated in surface regions as indicated by the groups of atoms (red) shown in Fig. 1(b). This structure shown in Fig. 1(c) includes 4 slightly distorted inner atomic rows of 14 atoms displaying clear evidence of the remnants of fcc symmetry. These inner rows of the best fit structure are observed to correspond to the interior atoms of the truncated octahedral shown on the right in Fig. 1(c) calculated for the n=38 ground state. It is important to point out that only a single isomer structure made a significant contribution to the best fit for Ag_{38}^+ and also for sizes n=36, 39, 43 and 55. This interesting mixture of symmetries arises at the octahedral shell closing at n=38 and probably results from the inherent stability associated with such "magic number" structures. The best fit structure also displays a longer range order with inversion symmetry about planes indicated by the dashed lines in Fig. 1(c).

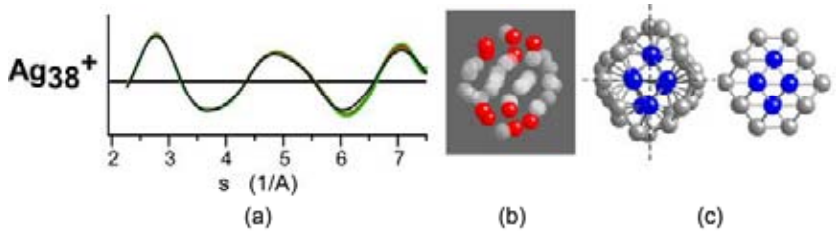

Figure 1

Gold Clusters: evolution from planar to cages to tubelike structures

Recent diffraction measurements [4] have accomplished the first direct structural determination of gold structures, achieved through joint diffraction measurements and density functional calculations of gold cluster anions in the size range 11≤n≤24 by B. Yoon and U. Landman of the Georgia Institute of Technology. Through these investigations we identify specific isomer structures and follow the remarkable structural evolution among different symmetries and forms. Our analysis shows clear evidence of a planar (two dimensional, 2D) to 3D transition [5,6] over the range n=12-14, caged structures [7] for n=16 and 17, culminating in a tetrahedral structure [8] at n=20, and the appearance of a highly symmetric nanotube structure at n=24. This rich array of size-dependent structural motifs is specific to gold clusters, and it is likely to originate from the relativistically enhanced s-d hybridization of gold bonding orbitals [6].

Diffraction data (red curves) for Au_n^- sizes n=16, 24 and best fit molecular diffraction patterns associated with calculated structures (blue curves) are shown in Fig. 2. Experimental data uncertainty (±σ) is shown by green shading. The diffraction pattern for Au_{16}^- is uniquely fit by the cage isomer structure lying 0.08 eV above the 2D ground state. Evidence for this cage structure has recently been observed in photoelectron measurements [7]. The diffraction pattern and calculated structure for Au_{24}^- shown in Fig. 2 present the first evidence for the emergence of an empty single wall tube-like structure. The best fit structure is found to be a highly symmetric ground state isomer. The commonality between the Au_{24} and Au_{16}^- structures is clearly observable in Fig. 2. The diffraction patterns for n=16 and 24 are essentially identical and unique among all the patterns

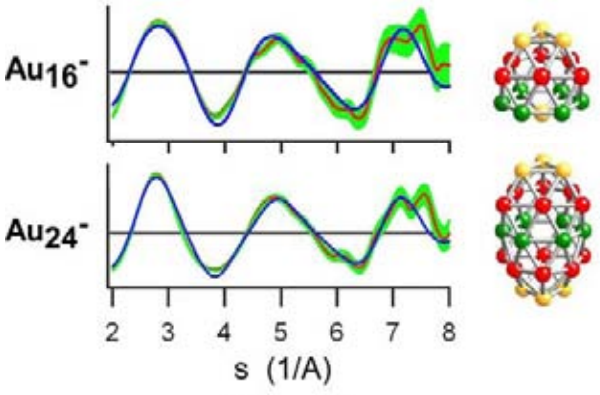

Figure 2

derived from the calculated isomers for these sizes, both exhibiting a triangular second peak, which supports the structural assignments.

Adsorption on gold clusters: dependence on structure

Initial measurements of the reactions of O_2 and H_2O with both gold cluster anions and cations have been performed over the cluster size range $3 \leq n \leq 22$. These measurements have observed a dependence on cluster structure in this size range which was manifest in several different ways. Two examples of O_2 adsorption are shown in Fig. 3. The mass spectra displayed in Fig. 3 were obtained by storing size selected gold clusters in an ion trap, exposing the ions to a partial pressure of O_2, and ejecting the products into a channeltron ion detector to produce the mass spectrum. The adsorption of O_2 on Au_{10}^+ displayed in Fig. 3(a) is interesting in that n=10 is the only size over the range $3 \leq n \leq 22$ which exhibits uptake of O_2 under the exposure conditions of T=150 K, $p_{O2} = 5x10^{-5}$ Torr for a duration of t=1 s. The cluster cation structure at n=20, which does not adsorb O_2, is expected to be similar to the tetrahedral form calculated [8] for n=10 shown in Fig.3(a). Consequently, either the calculated structure for n=10 needs to be reconsidered, or adsorption is not simply occurring at the apex positions.

Figure 3(b) is a remarkable example of structure selectivity. After adsorption of O_2 on Au_{10}^- under the conditions given above, the $Au_{10}O_2^-$ species is selectively ejected and the remaining

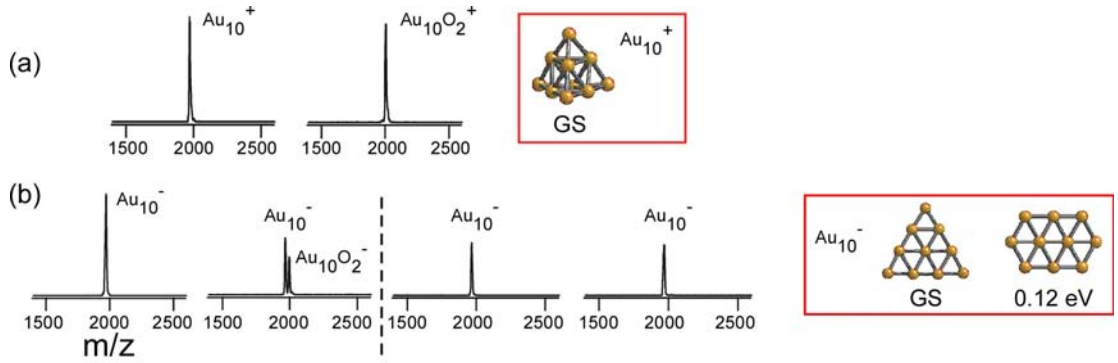

Figure 3

parent ions are exposed again for 10 s under the same temperature and pressure conditions. The complete absence of adsorption indicates that initially two isomers were trapped, only one of which supports O_2 adsorption. Structure calculations for Au_{10}^- identify the two lowest energy, planar isomers shown on the right. Only the higher energy structure is expected to strongly adsorb O_2 having a binding energy, BE=0.74 eV, almost double that of the ground state structure.

Adsorption of H_2O on gold cluster cations only occurs for planar structures [8] with $n \leq 7$ with adsorption strength and saturation number depending strongly on size. Adsorption also exhibits isomer structural variations. For specific sizes, rapid uptake of multiple H_2O molecules is observed immediately after a single water is adsorbed, suggesting the possibility that hydrogen bonding is playing a role in binding additional water molecules.

Future Plans

Metal cluster nanocatalysis offers interesting possibilities to increase catalytic reactivity and perhaps reaction specificity. It is particularly important to be able to identify the relationship, or correlation between structure and reactivity for gas phase clusters. In this case, the utility of

diffraction data and calculations to identify the isomer structure of a gas phase reactant may allow such a correlation to be discerned and related to catalytic processes. The quadrupole ion trap is particularly well suited to measure both the kinetic and steady state adsorption properties of metal clusters over a wide range of temperature and pressure. It is clear from our initial measurements that a broad spectrum of structure related effects are dominating the adsorption of small molecules on gold clusters. How is this sensitivity to structure related to the cluster electronic states? At what size does this structure dependence cease to be a dominating characteristic? Does such a structure-sensitivity extend to reactions, eg. CO_2 generation from the co-adsorption of O_2 and CO?

Studies will continue to investigate the structure dependence of cluster reactivity on gold, silver and aluminum clusters. The adsorption of H_2O, O_2, CO and their co-adsorption will be measured on TIED/DFT determined structures. Theoretical calculations [9] to determine the correlation of adsorption/reactivity with cluster electronic properties are being performed in collaboration with U. Landman.

References

(1) M. Maier-Borst, D. B. Cameron, M. Rokni and J. H. Parks Phys. Rev. A, **1999**, 59, R3162.
(2) S. Krückeberg, D. Schooss, M. Maier-Borst and J.H. Parks, Phys. Rev. Lett. **2000**, 85, 4494.
(3) X. Xing, R. M. Danell, I. L. Garzón, K. Michaelian, M. N. Blom, M. M. Burns, and J. H. Parks, Phys. Rev. B, **2005**, 72, 081405 R.
(4) X. Xing, B. Yoon, U. Landman, J. H. Parks, Phys. Rev. B (accepted for publication).
(5) F. Furche, R. Ahlrichs, P. Weis, C. Jacob, S. Gilb, T. Bierweiler, and M.M. Kappes, J. Chem. Phys. **2002**, 117, 6982.
(6) H. Häkkinen, M. Moseler, and U. Landman, Phys. Rev. Lett. **2002**, 89, 33401.
(7) S. Bulusu, X. Li, L.-S. Wang, and X.C. Zeng, Proc.Nat.Acad.Sci. **2006**, 103, 8326.
(8) J. Li, X. Li, H.-J. Zhai, and L.-S. Wang, Science **2003**, 299, 864.
(9) S. Gilb, P. Weis, F. Furche, R. Ahlrichs, and M. M. Kappes, J. Chem. Phys. **2002**, 116, 4094.
(10) B. Yoon, H. Häkkinen, and U. Landman, J. Phys. Chem. A, **2003**, 107, 4066.

Publications

Size dependent fivefold and icosahedral symmetry in silver clusters, X. Xing, R. M. Danell, I. L. Garzón, K. Michaelian, M. N. Blom, M. M. Burns, and J. H. Parks, Phys. Rev. B 72 (2005) 081405 R.

Gold nanostructural transitions: planar to cage to tubular motifs, X. Xing, B. Yoon, U. Landman, J. H. Parks, Phys. Rev. B (accepted for publication).

The Structures of Ag_{55}^+ and Ag_{55}^-: Trapped Ion Electron Diffraction and Density Functional Theory, D. Schooss, M. N. Blom, J. H. Parks, B. v. Issendorff, H. Haberland, and M. M. Kappes, Nano Lett. 5 (2005) 1972.

Trapped Ion Electron Diffraction: Structural Transitions in Silver and Gold Clusters, J. H. Parks and X. Xing in: The Chemical Physics of Solid Surfaces Volume 12, "Atomic Clusters: from Gas Phase to Deposited", Ed. D. Woodruff, Elsevier (in press).

Electron Microscopy of Materials

Stephen J. Pennycook, Maria Varela, Andrew R. Lupini, Albina Y. Borisevich
Postdocs: Klaus van Benthem, Mark P. Oxley, Jing Tao
pennycooksj@ornl.gov, mvarela@ornl.gov, 9az@ornl.gov, albinab@ornl.gov
Materials Science and Technology Division, Oak Ridge National Laboratory, Oak Ridge, TN 37831

Program Scope

With the successful development of aberration correctors for the electron microscope, its capabilities have advanced faster in the last few years than at any other time since its invention over 70 years ago. Assumptions that have been valid for decades may now be inapplicable, while at the same time entirely new opportunities arise. This program aims to explore and define the limits to resolution in 2 and 3 dimensions, which are no longer limited by geometric aberrations, and to determine the sensitivity and precision for locating single atoms. We use these new tools to investigate topical issues in condensed matter physics, including nanoscale phase separation and charge transfer in complex oxides, 3D atomic and electronic structure in isolated and buried quantum dots, with sensitivity to individual host and dopant atoms, and we plan to explore some in-situ capabilities, specifically, low- and high-temperature imaging and spectroscopy. The experience of the last three years has shown that aberration correction represents a new era in electron microscopy. In the next three years, we will acquire the next generation of aberration correctors, enabling another quantum leap in capability.

Recent Progress

Recent results from our two VG Microscopes' 100 kV HB501UX and 300 kV HB603U scanning transmission electron microscope (STEM) instruments that were retrofitted with Nion aberration correctors have demonstrated enormous gains in both resolution and sensitivity to single atoms, together with other unanticipated benefits:

Sub-Ångstrom resolution: Our aberration-corrected 300 kV (STEM) resolved the Si dumbbell in the ⟨112⟩ projection, the first direct image to show sub-Ångstrom resolution of 0.78 Å, as shown in Fig. 1, with evidence of information transfer to 0.061 nm.

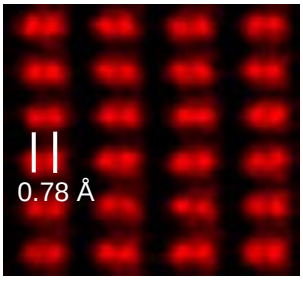

Figure 1. Z-contrast image of Si taken along the ⟨112⟩ zone axis, resolving columns of atoms just 0.78 Å apart [Nellist *et al.*, 2004]. Image recorded with the ORNL 300 kV VG Microscopes HB603U STEM equipped with Nion aberration corrector. The image has been filtered to remove noise and scan distortions.

Imaging of oxygen columns in perovskites: A sub-Ångstrom probe is sufficiently compact to allow oxygen columns to be directly observed in a Z-contrast image of $SrTiO_3$. [Lupini *et al.*, 2005]

Simultaneous, aberration-corrected phase contrast imaging: Historically, STEM phase contrast images were excessively noisy. However, after correction of aberrations, the STEM phase contrast image now has ~100 times greater efficiency, as well as the improved resolution and lack of image delocalization expected for an aberration corrected phase contrast image [Pennycook, 2006].
Single atom imaging: Aberration correction provides a much more localized probe, which greatly increases the visibility of single atoms. Interatomic distances in clusters of high-Z atoms on light supports can be accurately measured and interpreted through density functional calculations [Sohlberg *et al.*, 2004]. Single high–Z atoms can be imaged inside or on the surface of a crystal, even when it is aligned to resolve its lattice. [Wang *et al.*, 2004].
Single atom spectroscopy: The 100 kV STEM demonstrated the first EELS identification of an individual atom embedded within a bulk material [Varela *et al.*, 2004]. The 300 kV STEM has now been equipped with a Gatan Enfina spectrometer and a new objective lens to give higher EELS collection efficiency with a sub-Ångstrom probe.

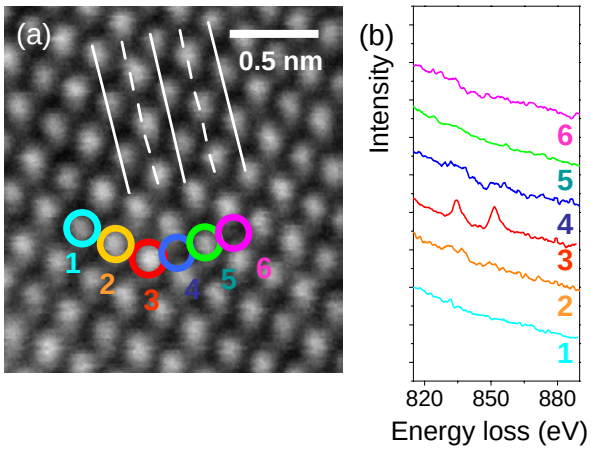

Figure 5. (a) Z-contrast image of $CaTiO_3$ showing traces of the CaO and TiO_2 {100} planes as solid and dashed lines respectively. A single La dopant atom in column #3 causes this column to show slightly brighter than other Ca columns, and EELS from it shows a clear La $M_{4,5}$ signal (b). Moving the probe to adjacent columns gives reduced or undetectable signals. The intensities seen from adjacent columns are caused by beam broadening and can be fitted through dynamical simulations to give an estimate of the depth of the La atom from the specimen entrance surface [Varela *et al.*, 2004].

3D Imaging with single atom sensitivity: The depth of focus is reduced to about 6 nm in the 300 kV STEM after aberration correction, making it possible to optically slice through a (non-channeling) specimen just by changing focus. [Borisevich *et al.*, 2006] Single Hf atoms have been located in 3D within the gate region of a next-generation device structure. [van Benthem *et al.*, 2005]

Future Plans

The above results illustrate the new level of resolution and sensitivity available with aberration correction, but, they also have uncovered numerous issues in imaging physics that need urgent investigation. Optimum microscope conditions become very sample dependent, and we plan a quantitative comparison of image simulations with experiment in 2D and 3D to determine the optimum conditions, for Z-contrast, phase contrast and EELS imaging. Geometric aberrations are no longer the only limit to resolution. The scattering process leading to ADF image formation is highly localised about the atomic site, while images based on core-loss spectroscopy tend to be broader with less contrast because of the additional issues of the non-local nature of the scattering potential. Phase contrast images are intermediate. Fig. 1 was obtained using a probe of FWHM 0.54 Å, but the Si-Si spacing of 0.78Å is only just resolved because of the finite size of the Si atoms. Thermal motion is also important. Detection statistics can also limit resolution,

which in turn are controlled by detector angles. Systematic exploration of these issues in the new era of aberration correction is planned, using a variety of test specimens, including Si, Ge, III/V semiconductors, $SrTiO_3$ and complex oxides.

First, methods will be developed for extracting microscope and specimen parameters directly from experimental images of perfect crystals, then extended to more complex specimens involving interfaces, alloys, superlattices and quantum dots, in order to extract local composition and strain. A series of $InAs_xP_{1-x}$/InP and $InGa_xAs_{1-x}$/GaAs epilayers grown with calibrated As compositions by molecular beam epitaxy will be used for calibration purposes, then applied to various semiconductor quantum wells and superlattices. With crystals aligned to a major zone axis, channeling along the atomic columns opposes the ability to come to a unique sharp focus point inside the material. Although the larger apertures in the next generation of correctors will increasingly overcome this effect, it will not bring 3D atomic resolution. For this purpose, we will investigate the use of a through-focal series of images of the same object in two or more projections. 3D core loss EELS will also be investigated.

The combination of atomic resolution EELS and imaging in transition metal oxides is a very powerful tool to study the chemistry, structure and electronic properties of these materials at the atomic scale. The O K edge and also the L edges of transition metals are well within reach of EELS experiments. The fine structure of these edges is sensitive to the density of unoccupied states around the Fermi level, facilitating the study of the properties and behavior of these systems at the atomic scale. We plan to study the sensitivity of EELS to spin by studying both core and low losses in cobaltites at variable temperatures. We will compare EELS data acquired at room temperature with data obtained after cooling below the spin transition temperature.

We will spatially map these phenomena and nanoscale phase separation in various systems at different temperatures, including spectroscopic imaging of charge carriers in the superconducting state. We already have directly resolved the charge carriers in the chains and planes of YBCO using the fine structure of the O and Cu edges, and will look for any changes on cooling below the superconducting transition. Such systems show numerous novel electronic phenomena at interfaces, and a systematic set of specimens will be investigated.

DOE-sponsored journal publications 2004-2006

Allen, L. J., S. D. Findlay, M. P. Oxley, C. Witte and N. J. Zaluzec, "Channeling effects in high-angular-resolution electron spectroscopy," *Phys. Rev. B*, **73** 094104 (2006).

Borisevich, A. Y., A. R. Lupini and S. J. Pennycook, "Depth sectioning with the aberration-corrected scanning transmission electron microscope," *Proc. Natl. Acad. Sci. USA*, **103**, 3044-3048 (2006).

Borisevich, A. Y., A. R. Lupini, S. Travaglini and S. J. Pennycook, "Depth sectioning of aligned crystals with the aberration-corrected scanning transmission electron microscope," *J. Electron Microsc.*, **55**, 7-12 (2006).

Cosgriff, E. C., M. P. Oxley, L. J. Allen and S. J. Pennycook, "The spatial resolution of imaging using core-loss spectroscopy in the scanning transmission electron microscope," *Ultramicrosc.*, **102**, 317-326 (2005).

Diebold, A. C., B. Foran, C. Kisielowski, D. A. Muller, S. J. Pennycook, E. Principe and S. Stemmer, "Image formation in the high-resolution transmission electron microscope - Authors' response," *Microsc. and Microanal.*, **10**, 399-400 (2004).

Findlay, S. D., M. P. Oxley, S. J. Pennycook and L. J. Allen, "Modelling imaging based on core-loss spectroscopy in scanning transmission electron microscopy," *Ultramicrosc.*, **104**, 126-140 (2005).

Grogger, W., M. Varela, R. Ristau, B. Schaffer, F. Hofer and K. M. Krishnan, "Energy-filtering transmission electron microscopy on the nanometer length scale," *J. Electron Spectrosc. Relat. Phenom.*, **143**, 139-147 (2005).

Hoffmann, A., S. G. E. te Velthuis, Z. Sefrioui, J. Santamaria, M. R. Fitzsimmons, S. Park and M. Varela, "Suppressed magnetization in $La_{0.7}Ca_{0.3}MnO_3/YBa_2Cu_3O_{7-\delta}$ superlattices," *Phys. Rev. B*, **72** 140407(R), (2005).

Kalinin, S. V., S. Jesse, B. J. Rodriguez, J. Shin, A. P. Baddorf, H. N. Lee, A. Borisevich and S. J. Pennycook, "Spatial resolution, information limit, and contrast transfer in piezoresponse force microscopy," *Nanotechnology*, **17**, 3400-3411 (2006).

Lupini, A. R., M. E. Chisholm, K. van Benthem, L. J. Allen, M. P. Oxley, S. D. Findlay, M. Varela and S. J. Pennycook, "Limitations to the measurement of oxygen concentrations by HRTEM imposed by surface roughness," *Microsc. and Microanal.*, **11**, 111-113 (2005).

McBride, J., J. Treadway, L. C. Feldman, S. J. Pennycook and S. J. Rosenthal, "Structural basis for near unity quantum yield core/shell nanostructures," *Nano Letters*, **6**, 1496-1501 (2006).

McBride, J. R., T. C. Kippeny, S. J. Pennycook and S. J. Rosenthal, "Aberration-corrected Z-contrast scanning transmission electron microscopy of CdSe nanocrystals," *Nano Letters*, **4**, 1279-1283 (2004).

Nellist, P. D., M. F. Chisholm, N. Dellby, O. L. Krivanek, M. F. Murfitt, Z. S. Szilagyi, A. R. Lupini, A. Borisevich, W. H. Sides and S. J. Pennycook, "Direct sub-Ångstrom imaging of a crystal lattice," *Science*, **305**, 1741-1741 (2004).

Nellist, P. D., N. Dellby, O. L. Krivanek, M. F. Murfitt, Z. Szilagyi, A. R. Lupini and S. J. Pennycook, "Towards sub-0.5 Ångstrom beams through aberration corrected STEM," in, *Electron Microscopy and Analysis 2003* (2004).

Oxley, M. P., E. C. Cosgriff and L. J. Allen, "Nonlocality in imaging." *Phys. Rev. Lett.* **94** 203906 (2005).

Peng, Y. P., P. D. Nellist and S. J. Pennycook, "HAADF-STEM imaging with sub-angstrom probes: a full Bloch wave analysis," *J. Electron Microsc.*, **53**, 257-266 (2004).

Pennycook, S. J., "*Microscopy: Transmission Electron Microscopy*," p. 240-247 in "*Encyclopedia of Condensed Matter Physics,"* J. Leidl and P. Wyder, Ed., Elsevier Science Ltd., Kidlington, Oxford, 2006.

Pennycook, S. J., M. Varela, C. J. D. Hetherington and A. I. Kirkland, "Materials advances through aberration-corrected electron microscopy," *MRS Bulletin*, **31**, 36-43 (2006).

Rashkeev, S. N., K. van Benthem, S. T. Pantelides and S. J. Pennycook, "Single Hf atoms inside the ultrathin SiO_2 interlayer between a HfO_2 dielectric film and the Si substrate: How do they modify the interface?" *Microelectron. Eng.*, **80**, 416-419 (2005).

Sohlberg, K., S. Rashkeev, A. Y. Borisevich, S. J. Pennycook and S. T. Pantelides, "Origin of anomalous Pt-Pt distances in the Pt/alumina catalytic system," *Chemphyschem*, **5**, 1893-1897 (2004).

van Benthem, K., A. R. Lupini, M. Kim, H. S. Baik, S. Doh, J. H. Lee, M. P. Oxley, S. D. Findlay, L. J. Allen, J. T. Luck and S. J. Pennycook, "Three-dimensional imaging of individual hafnium atoms inside a semiconductor device," *Appl. Phys. Lett.*, **87,** 034104 (2005).

Varela, M., S. D. Findlay, A. R. Lupini, H. M. Christen, A. Y. Borisevich, N. Dellby, O. L. Krivanek, P. D. Nellist, M. P. Oxley, L. J. Allen and S. J. Pennycook, "Spectroscopic imaging of single atoms within a bulk solid," *Phys. Rev. Lett.*, **92,** 095502 (2004).

Varela, M., A. R. Lupini, K. van Benthem, A. Borisevich, M. F. Chisholm, N. Shibata, E. Abe and S. J. Pennycook, "Materials Characterization in the Aberration-Corrected Scanning Transmission Electron Microscope," p. 539-569 in, *Annu. Rev. Mater. Res*, Annual Reviews, v. 35 (2005).

Varela, M., T.J. Pennycook, W. Tian, D.G. Mandrus, S.J. Pennycook, V. Pena, Z. Sefrioui, J. Santamaria. "Atomic scale characterization of complex oxide interfaces". *J. Mat. Sci*. **41**, 4389 (2006)

Wang, S. A. Y. Borisevich, S. N. Rashkeev, M. V. Glazoff, K. Sohlberg, S. J. Pennycook, and S. T. Pantelide, "Dopants Adsorbed as Single Atoms Prevent Degradation of Catalysts", *Nature Materials*, **3** 143-6 (2004)

Phase Reconstruction and Vector Field Electron Tomography

Shakul Tandon, Charudatta Phatak, and Marc De Graef
shakul@gmail.com, cphatak@andrew.cmu.edu, degraef@cmu.edu
Department of Materials Science and Engineering, Carnegie Mellon University,
Pittsburgh, PA 15213

Program Scope

The increasing complexity of today's materials systems must be accompanied by improvements in the methods used to study those materials. In the area of magnetic nano-materials, there is a significant interest in measuring and understanding the magnetostatic interactions between nano-scale elements, whether they be nano-particles for medical applications or patterned elements for magnetic storage applications. The transmission electron microscope (TEM), in particular, one of the modern spherical aberration-corrected instruments, is ideally suited for this kind of analysis, using primarily the Lorentz imaging mode, in which the image intensity is determined to a large extent by the magnetization state of the sample. Analysis of the magnetization configuration requires the determination of the phase of a coherent electron wave after it has passed through and around the sample. In this research program, we are concentrating on three areas of importance:

- computation (prediction) of the magnetic and electrostatic electron wave phase shifts for particles of arbitrary shape and magnetization state;
- determination of the phase of an electron wave, using a through-focus series of images;
- reconstruction (in 3D) of the magnetic induction in and around a small magnetic element, using vector field electron tomography.

The first two areas have been worked on in collaboration with the Brookhaven National Laboratory, the third area involves a collaboration with the Argonne National Laboratory.

The main outcome of this program will be an efficient, accurate technique which can be used in contemporary microscopes for 3D phase reconstruction of magnetic configurations. Such a technique will enable new quantitative observations at high spatial resolution in complex materials systems.

Recent Progress

A significant part of our research has focused on the modeling of the magnetization state of small particles. One could consider this aspect of our work to be equivalent to the efforts that have gone into the simulations of high resolution TEM images in the past; to properly interpret a high resolution image or image series, one must be able to compute these images based on a model for the crystal or defect structure. A comparison of the model with the experimental images then provides validation for the model. In Lorentz microscopy, a similar approach must be followed. If one reconstructs the electron wave phase for a given configuration of magnetic nano-particles, then one must also be able to compute this phase based on a model for the magnetization state of a particle with arbitrary shape.

Every object can be described by its characteristic function, or *shape function*, $D(\mathbf{r})$, a function that takes on the value 1 inside the object and 0 outside. The Fourier transform of this function is known as the *shape amplitude*, $D(\mathbf{k})$. We have discovered that the shape amplitude is, in fact, *the*

central function needed to describe *all* magnetostatic interactions between uniformly magnetized objects. From the shape amplitude one can derive, among others, the following conclusions or relations:

- *The phase of the electron wave is proportional to a planar section through the shape amplitude of the object.* As an electron wave travels through a magnetic material, the phase of this wave changes according to the Aharonov-Bohm theory [1]. For a uniformly magnetized particle of arbitrary shape, the magnetic component of the phase shift can be computed from [2]:

$$\varphi_m(k_x, k_y) = \frac{\mathrm{i}\pi B_0}{\phi_0} \frac{D(k_x, k_y, 0)}{k_x^2 + k_y^2} (\hat{\mathbf{m}} \times \mathbf{k})|_z, \tag{1}$$

  where ϕ_0 is the flux quantum and $\hat{\mathbf{m}}$ the unit magnetization vector. This expression permits the numerical or analytical evaluation of the phase shift for a wide variety of particle shapes, and also lies at the basis of the three-dimensional vector field electron tomography.

- *the demagnetization tensor field of an object is the convolution of the object shape function with the dipolar tensor.* The demagnetization tensor field $N^{\alpha\beta}(\mathbf{r})$ of a uniformly magnetized particle is defined as the proportionality tensor between the magnetization vector $\mathbf{M}$ and the resulting magnetic field (the *fringing field*) $\mathbf{H}(\mathbf{r})$:

$$H^{\alpha}(\mathbf{r}) = -N^{\alpha\beta}(\mathbf{r}) M^{\beta}. \tag{2}$$

  The volume average of this tensor over the volume of the particle is known as the *volumetric demagnetization factor*. The computation of demagnetization factors has for more than a century been a central problem in magnetostatics, with the earliest work going back to Maxwell [3]. It is often stated in magnetism textbooks that the computation of the demag factors can only be carried out for simple shapes, like ellipsoids and cylinders, but is virtually impossible for more complex shapes. In our work, we derived an expression for the Fourier transform of the tensor field, valid *for all particle shapes*, thereby solving a century-old problem. The demagnetization tensor for an object with arbitrary shape is defined as:

$$N^{\alpha\beta}(\mathbf{r}) = \mathcal{F}^{-1}\left[D(\mathbf{k}) \frac{k^{\alpha} k^{\beta}}{k^2} \right], \tag{3}$$

  where $\mathcal{F}$ is the Fourier transform operator, and $\mathbf{k}$ the frequency vector. We have applied this formalism to a number of different shapes, including the well-known ellipsoid problem. Relevant publications are listed at the end of this abstract.

- *the magnetometric tensor field is the convolution of the dipolar tensor with the object cross-correlation function.* Standard dipolar interactions are described by the well known relation for the interaction energy E:

$$E(\mathbf{r}) = \frac{\mu_0}{4\pi} \left[\frac{\boldsymbol{\mu}_1 \cdot \boldsymbol{\mu}_2}{r^3} - 3 \frac{(\boldsymbol{\mu}_1 \cdot \mathbf{r})(\boldsymbol{\mu}_2 \cdot \mathbf{r})}{r^5} \right] = \mu_0 \boldsymbol{\mu}_1 : \mathcal{D}(\mathbf{r}) : \boldsymbol{\mu}_2, \tag{4}$$

  where $\boldsymbol{\mu}_i$ are the dipole moments, and a colon indicates a tensor contraction. We have shown [4] that the magnetostatic interaction between uniformly magnetized objects of arbitrary shape and orientation can be expressed in a similar way:

$$E(\mathbf{r}) = \mu_0 \boldsymbol{\mu}_1 : \mathcal{N}(\mathbf{r}) : \boldsymbol{\mu}_2, \tag{5}$$

where the *magnetometric tensor field* $\mathcal{N}(\mathbf{r})$ is defined by:

$$\mathcal{N}^{\alpha\beta}(\mathbf{r}) = \mathcal{C}(\mathbf{r}) \otimes \mathcal{D}^{\alpha\beta}(\mathbf{r}). \tag{6}$$

The function $\mathcal{C}(\mathbf{r})$ is the cross-correlation of the two particle shape functions: $\mathcal{C}(\mathbf{r}) = D_1(\mathbf{r}) \otimes D_2(\mathbf{r})$. In equation (5), the vectors $\boldsymbol{\mu}_i$ are the total magnetic moments for the complete particle. This novel approach has been used to compute the interactions between uniformly magnetized spheres, rectangular prisms and intersecting rings.

The topics described in the preceding paragraphs represent only a fraction of the results obtained with DOE support. Other topics include: application of shape amplitudes in electrostatic problems, gravitation, and the moment of inertia tensor; shape-induced dipolar ferromagnetism in finite arrays of thin disks; phase diagram of uniformly magnetized rings, including magnetostatic, exchange, and magnetocrystalline interactions; applications of the Transport-of-Intensity formalism to ferromagnetic shape memory alloy; and the demagnetization factors of a fluxgate ringcore.

At present, we are evaluating a number of different theoretical approaches to the determination of the 3D magnetic induction using vector field electron tomography (VFET). We have shown through simulations and an explicit theoretical computation for a magnetic point dipole that 3D tomographic reconstruction of the magnetic induction is possible in principle. The input data for a VFET reconstruction must be obtained using either electron holography, or phase reconstruction based on the Transport-of-Intensity formalism; in either case, reconstructions will only be successful if the microscope on which the data was acquired has a low spherical aberration, much lower than the values commonly available in Lorentz imaging mode. Thus, the availability of modern aberration-corrected instruments will enable the implementation and verification of the VFET algorithms.

On the experimental side, we have nearly completed the construction of a prototype *in-situ* magnetic field holder, based on parallel superconducting wires, and we have initiated the design of a full 360° sample tilt stage for tomographic experiments.

Future Plans

In collaboration with Argonne National Laboratory (Amanda Petford-Long) and the National Institute for Standards and Technology (John Henry Scott), we will begin the experimental validation of the theoretical VFET modeling. This will require acquisition of experimental data sets for two orthogonal tilt axes, using a nearly complete 360° sample rotation, to allow for the separation of the electrostatic and magnetic phase shifts. Initial samples will include a tip of a magnetic force microscope, nano-scale patterned permalloy islands, and colloidal Cobalt nano-particles.

We will evaluate a number of different approaches to the reconstruction of the magnetic induction, using our own algorithms and those proposed by Lade, Paganin and Morgan [5, 6]. In the former, we reconstruct the magnetic induction directly, whereas the latter procedure attempts to reconstruct the divergence-less component of the magnetic vector potential. Once the numerical algorithms have been verified and optimized, we will make them available through a dedicated web site.

References

[1] Y. Aharonov and D. Bohm. Significance of Electromagnetic Potentials in the Quantum Theory. *Phys. Rev.*, 115:485–491, 1959.

[2] M. Beleggia and Y. Zhu. Electron-optical phase shift of magnetic nanoparticles, Part I: Basic concepts. *Phil. Mag. B*, 83:1143–1161, 2003.

[3] J.C. Maxwell. *A Treatise on Electricity and Magnetism, 3rd Ed.*, volume vol. 2. Oxford University Press, 1891.

[4] M. Beleggia and M. De Graef. General magnetostatic shape-shape interactions. *J. Magn. Magn. Mater.*, 285:L1–10, 2005.

[5] S.J. Lade, D. Paganin, and M.J. Morgan. 3-d vector tomography of doppler-transformed fields by filtered backprojection. *Optics Communications*, 253:382–391, 2005.

[6] S.J. Lade, D. Paganin, and M.J. Morgan. Electron tomography of electromagnetic fields, potentials and sources. *Optics Communications*, 253:392–400, 2005.

DOE Sponsored Publications in 2004-2006

- S. Tandon, M. Beleggia, Y. Zhu, and M. De Graef, "On the computation of the demagnetization tensor for uniformly magnetized particles of arbitrary shape. Part I: Analytical approach," *J. Magn. Magn. Mater.*, vol. 271, pp. 9–26, 2004.
- S. Tandon, M. Beleggia, Y. Zhu, and M. De Graef, "On the computation of the demagnetization tensor for uniformly magnetized particles of arbitrary shape. Part II: Numerical approach," *J. Magn. Magn. Mater.*, vol. 271, pp. 27–38, 2004.
- M. Beleggia, S. Tandon, Y. Zhu, and M. De Graef, "On the magnetostatic interactions between nanoparticles of arbitrary shape," *J. Magn. Magn. Mater.*, vol. 278, pp. 270–284, 2004.
- M. Beleggia, S. Tandon, Y. Zhu, and M. De Graef, "On the computation of the demagnetization tensor for particles of arbitrary shape," *J. Magn. Magn. Mater.*, vol. 272, pp. E1197–1199, 2004.
- M. Beleggia and M. De Graef, "General magnetostatic shape-shape interactions," *J. Magn. Magn. Mater.*, vol. 285, pp. L1–10, 2005.
- M. De Graef and M. Beleggia, "Theory of phase-reconstructed vector field electron tomography," *Microscopy and Microanalysis*, vol. 11 (supplement 2), pp. 316–317, 2005.
- M. Beleggia, Y. Zhu, S. Tandon, and M. De Graef, "Shape-induced ferromagnetic ordering in a triangular array of magnetized disks," *App. Phys. Lett.*, vol. 87, pp. 202504, 2005.
- M. Beleggia, M. De Graef, Y.T. Millev, D.A. Goode, and G. Rowlands, "Demagnetization factors for elliptic cylinders," *J. Phys. D*, vol. 38, pp. 3333–3342, 2005.
- M. Beleggia, J.W. Lau, M.A. Schofield, Y. Zhu, S. Tandon, and M. De Graef, "Phase diagram for magnetic nano-rings," *J. Magn. Magn. Mat.*, vol. 301, pp. 131-146, 2006.
- M. Beleggia, M. De Graef, and Y.T. Millev, "The equivalent ellipsoid of a magnetized shape," *J. Phys. D*, vol. 39, pp. 891-899, 2006.
- M. Beleggia, M. De Graef, and Y.T. Millev, "Self-energy and demagnetization factors of the general ellipsoid: A self-contained alternative to the Maxwell-Stoner approach," *Phil. Mag.*, vol. 86, pp. 2451-2466, 2006.
- M. De Graef and M. Beleggia, "The fluxgate ring-core demagnetization field," *J. Magn. Magn. Mat.*, 2006 (in press).

Atomistic Studies of Deformation and Fracture in Materials with Mixed Metallic and Covalent Bonding: Transition Metals and Their Compounds

V. Vitek,
vitek@seas.upenn.edu
Department of Materials Science and Engineering, University of Pennsylvania, Philadelphia, PA 19104

Program Scope

The goal of this research program is generation of knowledge that is needed for the fundamental, atomic level understanding of the deformation and fracture mechanisms in non-magnetic transition metals, specifically Ir, Mo, W, Nb, Ta, as well as in compounds based on these metals, such as $MoSi_2$, Mo_5Si_3, Mo_5SiB_2, Ir_3Nb, Ir_3Zr. The motivation for investigation of these materials is two-fold. First, they are befitting as high-temperature materials, some of which, for example Ir and its alloys, W and molybdenum silicides, have exceptional corrosion resistance. Hence, they are of notable interest to the Department of Energy in the context of energy conversion systems, advanced engines and nuclear energy programs. Secondly, these materials are representative of a broad class of technologically important metallic materials in which the bonding is mixed metallic and covalent and thus atomic interactions depend on both separation of atoms and bond angles. This presents a formidable scientific challenge for atomic level studies of defects, such as dislocations, grain boundaries and other interfaces that govern mechanical and physical properties of materials. In order to tackle this problem we have adopted the bond order potentials (BOPs) that have a sound quantum mechanical basis and are eminently suitable for materials with mixed metallic and covalent bonding [1-3]. Using these potentials we study dislocation core structures and the dislocation glide under the effect of complex applied stresses and employing these results we develop models for plastic deformation and fracture. Such models are essential for advancement of the fundamental understanding of the mechanical behavior of materials that play a crucial role in applications ranging from power generation systems to nanoscale structures, in particular if they are to withstand high temperatures and corrosive environments.

Recent Progress

The BOPs are a real-space semi-empirical description of interactions between the atoms that is based on the tight-binding approximation and for metals studied in this program further rooted in the d-band model. They have now been developed for several transition bcc metals, in particular molybdenum [4] and tungsten [5], the fcc transition metal iridium [6] and $MoSi_2$ [7]. This development encompasses not only construction of the potentials but also thorough testing. These tests include in the first place calculations of the energies of alternative crystal structures and comparison with analogous calculations performed using the DFT based *ab initio* methods. Next the transferability of the BOPs to atomic configurations that deviate significantly from ideal crystal structures is studied by computing the energies along tetragonal, trigonal and hexagonal transformation paths, defined in [8]. For comparison these paths are studied at the same time using an *ab inito* [9-11] method. Finally phonon spectra are evaluated for several symmetrical crystallographic directions and compared with available experiments. Using these potentials we

have investigated dislocation core structure and dislocation glide in molybdenum, tungsten and iridium [4,5,10-14].

In the case of molybdenum and tungsten it is the core and glide of the 1/2[111] screw dislocation that is of principal importance. The calculated structure of the core agrees excellently with that found in the recent *ab initio* calculations [15,16]. An important aspect of the dislocation glide, not appreciated until recently, is the effect of stresses perpendicular to the slip direction that induce very significant tension/compression asymmetries and may even bring about slip on systems with low Schmid factors in preference to those with high Schmid factors [11]. In order to characterize properly the plastic behavior on the scales ranging from nano to macro in the framework of continuum mechanics the corresponding yield criteria must include these effects and the results of atomistic studies lead to formulation of such physically based yield criteria [9-11].

However, the above findings are all based on the results of calculations at 0K. In order to include the effects of temperature and strain rate we need to investigate dislocation propagation via formation of kink pairs. This is done employing a mesoscopic model with the input from atomistic calculations. A functional form of the Peierls potential, in particular its dependence on the applied stress, is constructed so as to reproduce the atomistically found stress dependence of the Peierls stress. Using then the standard dislocation model for kink-pair formation, together with the reaction rate theory, the velocity of screw dislocations is found as a function of the applied stress tensor. For a given strain rate this determines the dependence of the yield stress on temperature and includes fully the orientation dependencies and break down of the Schmid law. This research is in progress and only a preliminary publication is available [17].

In the case of iridium atomistic simulations of the screw dislocation performed using the constructed BOP found a planar core structure that corresponds to dissociation into Shockley partials but also a metastable, non-planar core. Owing to the strong angular character of interatomic bonding in iridium, arising from the partially filled valence *d*-band, the non-planar configuration for the screw dislocation core is unique to iridium and does not exist in other fcc metals. Investigation of transformations between the two core configurations suggests that these transformations represent the basis for a mechanism for cross-slip that neither requires thermal activation nor full constriction of the partials in the primary plane. The associated high rate of cross-slip leads to the creation of high densities of Frank-Read sources and subsequently to a dislocation density that increases exponentially with plastic strain and thus to extremely strong work hardening [13,14]. This dislocation mechanism naturally explains why very pure single crystals and polycrystals of iridium undergo cleavage and/or brittle intergranular fracture at temperatures up to 500°C after extensive plastic deformation, which is in contrast with all other fcc metals [18,19].

Future Plans

Studies of the deformation behavior of bcc transition metals will concentrate on materials that are the structural materials which will play an important role in fusion reactors [20]. These are tungsten and bcc iron and its alloys, in particular Fe-Cr alloys. The latter case represents a major new step since the interatomic potentials must now include the magnetic effects since the bcc structure of iron is stabilized due to magnetism. Development of such potentials has recently been advanced by S. Dudarev and D. Nguyen-Manh of Culham Laboratory, U.K., with whom we have a long-standing extensive collaboration. These advancements employ both the EAM scheme [21] and BOPs. Another important step is the recent development of analytical BOPs by D. G. Pettifor and R. Drautz at Oxford, the group with which we have been collaboration during the duration of this project. These potentials will allow extensive molecular dynamics

calculations and thus studies of interactions between dislocations and point defects produced by irradiation. The latter is the most important phenomenon in nuclear reactors. These atomistic models will be linked with the mesoscopic dislocation theory of the formation of kink pairs, already mentioned in the section on Recent Progress. This will allow advancing a full theoretical treatment of deformation of irradiated materials at finite temperatures and strain rates. Furthermore, we shall investigate the structure and properties of grain boundaries in iridium in order to elucidate the observed intergranular brittleness of this metal in pure state. In this study we compare grain boundary structures and the intergranular cohesion in iridium and copper. The reason is to elucidate the influence of different type of bonding that is practically purely metallic in copper but mixed metallic and covalent in iridium.

At the same time, we shall expand the BOP developed for $MoSi_2$ towards Mo_5Si_3, Mo_5SiB_2. In the former case the *ab initio* calculations of generalized stacking faults that will reveal the positions and energies of stacking-fault-like planar defects are currently in progress. These results will be used in analyses of dislocation dissociations and related structures of dislocation cores and establishment of relationship with mesoscale and macroscale plasticity of these important high-temperature materials.

References

1. D. G. Pettifor, Physical Review Letters **63**, 2480 (1989).
2. D. G. Pettifor, I. I. Oleinik, D. NguyenManh and V. Vitek, Computational Materials Science **23**, 33 (2002).
3. D. G. Pettifor and I. I. Oleynik, Progress in Materials Science **49**, 285 (2004).
4. M. Mrovec, D. NguyenManh, D. G. Pettifor and V. Vitek, Physical Review B **6909**, 4115 (2004).
5. M. Mrovec, R. Gröger, A. G. Bailey, D. NguyenManh and V. Vitek, Physical Review B to be published (2006).
6. M. J. Cawkwell, D. Nguyen-Manh, D. G. Pettifor and V. Vitek, Physical Review B **74**, 064104 (2006).
7. M. J. Cawkwell, M. Mrovec, D. Nguyen-Manh, D. G. Pettifor and V. Vitek, in *Integrative and Interdisciplinary Aspects of Intermetallics*, edited by M. J. Mills, H. Clemens, C.-L. Fu and H. Inui, MRS Symposium Proceedings, Vol. 842 (Materials Research Society, Pittsburgh, 2005), p. S2.8.1.
8. V. Paidar, L. G. Wang, M. Sob and V. Vitek, Modelling and Simulation in Materials Science and Engineering **7**, 369 (1999).
9. V. Vitek, M. Mrovec and J. L. Bassani, Materials Science and Engineering A **365**, 31 (2004).
10. V. Vitek, A. Mrovec, R. Gröger, J. L. Bassani, V. Racherla and L. Yin, Materials Science and Engineering A **387-89**, 138 (2004).
11. R. Gröger and V. Vitek, Materials Science Forum **482**, 123 (2005).
12. D. Nguyen-Manh, M. J. Cawkwell, R. Gröger, M. Mrovec, R. Porizek, D. G. Pettifor and V. Vitek, Materials Science and Engineering A **400-401**, 68 (2005).
13. M. J. Cawkwell, D. Nguyen-Manh, C. Woodward, D. G. Pettifor and V. Vitek, Science **309**, 1059 (2005).
14. M. J. Cawkwell, D. Nguyen-Manh, C. Woodward, D. G. Pettifor and V. Vitek, Acta Materialia, in print (2006).
15. C. Woodward and S. I. Rao, Philosophical Magazine A **81**, 1305 (2001).
16. C. Woodward and S. I. Rao, Physical Review Letters **8821**, 6402 (2002).
17. R. Gröger and V. Vitek, in *Proceedings of the Third International Conference on Multiscale Materials Modelling*, Freiburg (2006), in press.
18. S. S. Hecker, D. L. Rohr and D. F. Stein, Metallurgical Transactions A **9**, 481 (1978).
19. P. Panfilov and A. Yermakov, Journal of Materials Science **39**, 4543 (2004).
20. S. J. Zinkle, Phys Plasmas **12**, 58101 (2005).
21. S. L. Dudarev and P. M. Derlet, Journal of Physics C: Solid State **17**, 7097 (2005).

DOE Sponsored Publications in 2004-2006

Core Structure of Dislocations in Body-Centred Cubic Metals: Relation to Symmetry and Interatomic Bonding, V. Vitek, Philos. Mag. **2004**, 84, 415-428.

Bond-Order Potential for Molybdenum: Application to Dislocation Behaviour, M. Mrovec, D. Nguyen-Manh, D. G. Pettifor and V. Vitek, Phys. Rev. B **2004**, 69, 094115-16.

The Role of Ab-Initio Electronic Structure Calculations in Studies of the Strength of Materials, M. Sob, M. Friak, D. Legut, J. Fiala and V. Vitek, Mat. Sci. Eng. A **2004**, 387-389, 148-157.

Origin of Brittle Cleavage in Iridium, M. J. Cawkwell, D. Nguyen-Manh, C. Woodward, D. G. Pettifor and V. Vitek, Science **2005**, 309, 1059-62.

Theoretical Strength of Metals and Intermetallics from First Principles, M. Sob, J. Pokluda, M. Cerny, P. Sandera and V. Vitek, Materials Science Forum **2005**, 482, 33-38.

Breakdown of the Schmid Law in BCC Molybdenum Related to the Effect of Shear Stress Perpendicular to the Slip Direction, R. Gröger and V. Vitek, Materials Science Forum **2005**, 482, 123-126.

Dislocations in Materials with Mixed Covalent and Metallic Bonding, D. Nguyen-Manh, M. J. Cawkwell, R. Gröger, M. Mrovec, R. Porizek, D. G. Pettifor and V. Vitek, Mat. Sci. Eng. A **2005**, 400-401, 68-71.

A Bond-Order Potential Incorporating Analytic Screening Functions for the Molybdenum Silicides, M. J. Cawkwell, M. Mrovec, Duc Nguyen-Manh, D. G. Pettifor and V. Vitek in "Integrative and Interdisciplinary Aspects of Intermetallics", edited by M.J. Mills, H. Clemens, C-L. Fu, H. Inui, MRS Symposium Proceedings **2005**, Vol. 842, p. S2.8.1-6.

Theoretical Strength, Magnetism and Stability of Metals and Intermetallics, M. Sob, M. Friák, D. Legut and V. Vitek in "Complex Inorganic Solids - Structural, Stability, and Magnetic Properties of Alloys", edited by P.E.A. Turchi, A. Gonis, K. Rajan, and A. Meike, Springer, Berlin **2005**, pp. 307-326.

Interatomic Bonding and Plastic Deformation in Iridium and Molybdenum Silicide, M. J. Cawkwell, PhD Thesis, University of Pennsylvania, Philadelphia 2005.

Construction, Assessment, and Application of a Bond-Order Potential for Iridium, M. J. Cawkwell, D. Nguyen-Manh, D. G. Pettifor and V. Vitek, Phys. Rev. B. **2006**, 74, 064104 - 13.

Atomistic Study of Athermal Cross-Slip and its Impact on the Mechanical Properties of Iridium, M. J. Cawkwell, C. Woodward, D. Nguyen-Manh, D. G. Pettifor and V. Vitek, Acta Materialia **2006**, in print.

Atom-Based Bond-Order Potentials for Modeling Mechanical Properties of Metals, M. Aoki, D. Nguyen-Manh, D. G. Pettifor and V. Vitek, Prog. Mater. Science **2006**, in print.

Bond Screening: A Challenge for Modelling of Intermetallics and Fusion Materials, D. Nguyen-Manh, V. Vitek and A.P. Horsfield, Prog. Mater. Science **2006**, in print.

Effect of Non-Glide stresses on Deformation of BCC Metals at Finite Temperatures, R. Gröger and V. Vitek, in Proceedings of the Third International Conference on Multiscale Materials Modelling, Freiburg **2006**, in press.

Atomic and Electronic Structure of Polar Oxide Interfaces

Marija Gajdardziska-Josifovska*, Michael Weinert*, Scott A. Chambers**
mgj@uwm.edu, weinert@uwm.edu, sa.chambers@pnl.gov
*Department of Physics and Laboratory for Surface Studies, University of Wisconsin
Milwaukee, WI 53201
**Fundamental Science Division, Pacific Northwest National Laboratory, Richland, WA 99352

Program Scope

The problem of surface and interface polarity is especially pronounced in oxides due to the strong ionicity of the metal oxygen bond. This new program is inspired by recent developments in the field of polar oxide surfaces that have found new solutions to the old 'electrostatic catastrophe' problem of polar surface instability. Now that we know that polar oxide surfaces can be stabilized without faceting to neutral planes, we have an opportunity to create hereto unexplored polar oxide interfaces by controlled epitaxial growth of polar oxide films on polar oxide surfaces. This integrated experimental and theoretical research program aims to create such model polar oxide interfaces and to determine their atomic structure and electronic properties. The ultimate scientific goal is to probe the instability of polar oxide interfaces and to develop fundamental understanding of the possible atomic and electronic interface stabilization mechanisms. The applied goal is to establish how the extreme oxide surface polarity can be used as a constraint for the creation of novel oxide and metal nanoscale structures with useful properties for energy applications.

Recent Progress

The polar oxide interface program was initiated in August 2006 under DOE funding. It builds on our recent progress with a proof of principle study demonstrating that oxide surface polarity can have major influence on the growth of polar oxide films. Polar magnetite (111) films were grown on polar magnesia (111) substrates by plasma assisted molecular beam epitaxy. Structural results from transmission electron microscopy and diffraction, and compositional results from x-ray photoelectron spectroscopy, uncovered phase separation with surprising stabilization of Fe nanocrystals under oxidizing conditions. [1] High resolution transmission electron microscopy (HRTEM) and density functional theory were used to study the effect of interface polarity on the atomic and electronic structure of this prototype polar oxide interface. [2] Atomically abrupt interfaces were found to exist between the MgO(111)-substrate and Fe_3O_4 (111) film (e.g. Fig. 1) in regions separated by Fe nanocrystals. While hydrogen was shown to terminate the starting unreconstructed MgO(111) 1x1 surface, [3] modeling and experiment show that H is replaced by Fe during growth (e.g. profiles in Fig. 1). Comparisons of through-focus/through-thickness experimental HRTEM images with calculated images for model interface structures found metal-oxygen-metal (i.e., Mg-O-Fe) interface bonding with octahedral (B) coordination of the first Fe monolayer, rather than the combination of tetrahedral-octahedral-tetrahedral (ABA) stacking also found in Fe_3O_4. First-principles calculations for all the different models found metal-induced gap states in the interface oxygen layer (e.g. Fig. 2). The …4Mg/4O/4**Mg/4O/3Fe$_B$**/4O/Fe$_A$Fe$_B$Fe$_A$…

interface stacking was found to be the energetically most favorable, and effectively screening the MgO(111) substrate surface polarity.

The above study shows that the initial predictions for interface micro-faceting are not supported by experimental observations and first-principles calculations. The data and calculations also exclude mixing of Mg and Fe across the interface, in contrast to the commonly invoked mechanism of cation mixing at compound semiconductor polar interfaces predicted by electrostatic theory.

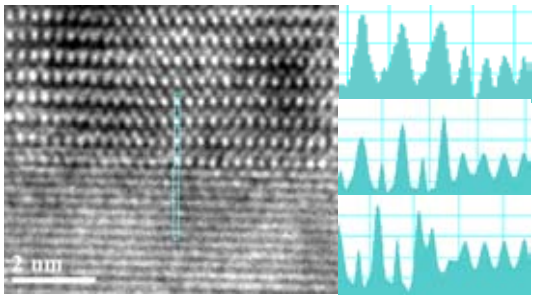

Fig. 1. HRTEM image from the $Fe_3O_4(111)/MgO(111)$ interface in the $[11\bar{2}]$ zone and intensity profiles across interface showing that experiment (top) is better aligned to model with Mg-O-Fe_B interface (middle) than to interfacial hydrogen Mg-O-H-Fe model (bottom).

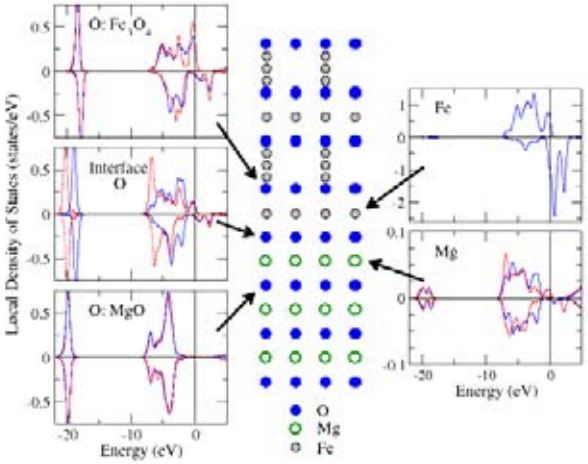

Fig. 2. Calculated local spin-resolved density of states for different atomic sites around the interface for the lowest energy interface model. Majority (minority) spin LDOS are plotted as positive (negative) values. Blue solid (red dashed) lines denote sites with three (one) symmetry equivalent atoms per layer.

Future Plans

While we now know that polar oxide interfaces can be formed, we do not know if they tend to be stabilized by a single dominant mechanism, irrespective of materials combinations and/or differences in formation conditions, or different mechanisms will dominate in different circumstances? To answer this question we plan to study more than one materials system and to explore a wide range of preparation conditions for one of these systems by varying the substrate surface termination, the substrate temperature, and the metal and oxygen flux ratios during growth. The polar MgO(111) and $Al_2O_3(0001)$ single crystal surfaces are the chosen model substrates, and films in the family of iron oxides are grown on these substrates with unreconstructed and reconstructed surface preparations. An initial series of films have now been grown by plasma assisted MBE using a matrix approach for the preparation conditions. Electron microscopy studies of their atomic structure have been initiated, soon to be followed by density functional studies of competing model structures. Of special interest is to uncover if a polar hetero-interface between two oxides (AO/BO) will have an "oxide-like" metal A-oxygen-metal B (A-O-B) interface, a "metal-like" layered (O-A-B-O) or "alloy-like" mixed (O-AB-O) interface? Will the interface have bulk-like in-plane periodicity or will it be reconstructed? Will (ordered or disordered) oxygen vacancies exist at the polar interfaces? Will the interfaces be

atomically abrupt or would there be intermixing concentration gradients across the polar interfaces that extend into the substrate and the film? Will there be charge transfer at the interface? Will the starting surface stabilization mechanism have an effect on the film growth and the resulting interface stabilization? Will the film magnetic properties have any noticeable effects on the interface stabilization mechanism? Are the Coulomb potentials at the interface and in the film good predictors for the winning interface stabilization mechanism? Is it necessary to cancel the polarity in the system, or is minimization sufficient? What is the largest potential gradient that can be supported by any given stabilization mechanism in a given materials system?

As we make progress in the understanding of the polar oxide heterointerfaces, we will address the other extreme in polarity to find what will be the preferred interface structure if a metal film (B) is grown in place of its oxide (BO) on the same polar oxide surface (AO). We will start by comparing and contrasting results from Fe/MgO and Fe_xO_y/MgO interface studies.

There are more questions than answers at this time, typical for a starting phase of a program. The research plan is designed to provide answers that will tease out the physics of polar oxide interfaces.

References

1. Lazarov K, Chambers SA and Gajdardziska-Josifovska M (2003) Polar Oxide Interface Stabilization by Formation of Metallic Nanocrystals. *Phys. Rev. Lett.* **90**, 216108.
2. Lazarov V K, Weinert M, Chambers S A, Gajdardziska-Josifovska M (2005) Atomic and Electronic Structure of Fe_3O_4/MgO(111) Polar Oxide Interface. *Physical Review B* **72**, 195401
3. Lazarov VK, Plass R, Poon H-C, Saldin DK, Weinert M, Chambers SA and Gajdardziska-Josifovska M (2005) Structure of the hydrogen stabilized MgO(111)-(1×1) polar surface: Integrated experimental and theoretical studies, *Physical Review B* **71**, 115434.

DOE sponsored publications in last two years

This new DOE project started on August 14, 2006. There are no publications as yet.

Engineering and Characterizing Nanoscale multilayers for Magnetic tunnel junctions

J. J. Yang, C.-X. Ji, Y. A. Chang,
chang@engr.wisc.edu, jianhuay@cae.wisc.edu, cji@cae.wisc.edu

Department of Materials Science & Engineering, University of Wisconsin, Madison, WI53706

Program Scope

As a new magnetic device of spintronics, magnetic tunnel junctions (MTJs) have attracted considerable attention due to the potential applications in improved magnetic sensors, read heads in the magnetic hard disk drive and especially magnetic random access memories that could simultaneously achieve high speed, high density, and nonvolatility. A MTJ is a nanoscale multilayer consisting of buffer, ferromagnetic (FM), tunnel barrier, antiferromagnetic (AFM) and capping layers. Materials issues play a crucial role in the progress of the MTJ research. Each layer in the nanoscale multilayered stack has their own significance for the performance of MTJs. The objectives of this program are to engineer the nanoscale multilayers primarily via thermodynamic considerations for both fundamental studies and industrial applications of magnetic tunnel junctions (MTJs). The specific goals are to describe the phase changes of sputter-deposited AFM layers, to develop thermodynamically controlled novel approaches for the formation of high quality tunnel barrier layers, to investigate the influence of FM layers on the performance of MTJs and to fabricate sputter-deposited epitaxial MTJs on Si substrate with a MgO tunnel barrier via appropriate buffer layers. Current focus is on the FM layers to specify the origin of the variation of tunneling magnetoresistance (TMR) with the composition of the $Co_{1-x}Fe_x$ FM electrode and to improve the interface and crystal quality of the FM layer for the fulfillment of higher TMR ratio.

Recent Progress

In previous work, we have studied the phase changes of sputter-deposited AFM layers, e.g. NiMn and PtMn, and developed a novel approach to fabricate the tunnel barrier layers, e.g. AlO_x and YO_x by selectively oxidizing the tunnel barrier precursor metal (e.g Al) without oxidizing the adjacent FM layers. We also presented a thermodynamic model to predict the compositions of the tunnel barrier precursor alloys with tendencies to form amorphous phase in the sputter-deposited form.

In the current study, we primarily focused on the FM layer, which according to the well-known Julliere's model directly determines TMR,[1] one of the most important parameters of a MTJ.[2] First, we have made a systematic study of the TMR ratio vs. composition of the $Co_{1-x}Fe_x$ electrode in an AlO_x based MTJ and found significant variation. Based on a model of tunneling dominated by sp states near the Fermi energy,[3] the variation of *ab initio* calculated TMR values reproduce experimental trends with both

composition and structural change. The variation in TMR is attributed to both compositional and structural dependence of the electrode spin polarization, with the large increase in TMR at x=0.17 attributed to the fcc to bcc structural transformation. Relatively weak compositional dependence of the TMR value is found for compositional variation above x=0.17, suggesting that the structural changes dominate the compositional dependence of the TMR in this system. According to the *ab initio* calculation, the P value of the bcc structure is always greater than that of the fcc structure with the same composition, suggesting that the bcc is the preferred structure for higher TMR values.

Next, we carried out some challenging experimental studies to prove the interesting prediction that the bcc (Co,Fe) is superior to the fcc (Co,Fe) as the FM electrodes for MTJs in term of yielding higher TMR ratio. In these studies, we were able to alter the crystal structure of a $Co_{87}Fe_{13}$ electrode from fcc to bcc by engineering the strain of the FM layer via epitaxial growth. The composition of $Co_{0.87}Fe_{0.13}$ is in the fcc-bcc transition composition range,[4] thermodynamically meaning that the Gibbs energy of the fcc phase is close to that of the bcc phase and hence its crystal structure could be readily altered by introducing an extra energy (e.g. strain) caused by adopting different buffer layers in the epitaxial growths. The lattice constants of fcc Cu and bcc Cr are about 0.36 nm and 0.29 nm, less than 4% mismatch with the fcc and bcc $Co_{0.87}Fe_{0.13}$, respectively. Therefore Cu and Cr thin layers were chosen to induce the $Co_{0.87}Fe_{0.13}$ bottom electrode into either fcc or bcc crystal structure. Interestingly, we observed significant TMR ratio difference when we altered the crystal structure, which is a direct experimental evidence of the role of the FM electrode electronic structure in the spin dependent tunneling (SDT). Both experimental and theoretical results suggest that a bcc (Co,Fe) electrode results in a higher TMR ratio than a fcc (Co,Fe) electrode due to the larger spin polarization of the bcc structure. This is also one of the few examples of a clear experimental correlation between crystal structure of the FM electrodes and tunneling properties.[5]

From our studies on the epitaxial growth of $Co_{1-x}Fe_x$ FM layers, we found that the crystal quality and the interface flatness of the epitaxial FM layers could be significantly improved by an in-situ high-temperature (about 400 ^oC) annealing. Accordingly, we successfully achieved over 70% TMR ratio at room temperature in a fairly simple CoFe and AlO_x based MTJ with a structure of Si (001) / Ag fcc (200) / $Co_{84}Fe_{16}$ bcc (200) / AlO_x / $Co_{84}Fe_{16}$ / IrMn / Ag. *This is the highest TMR ratio ever reported with the extensively studied (Co,Fe) and AlO_x based MTJs.*[6] Altering the crystalline orientation of the epitaxial bottom FM electrode may enhance the TMR ratio.[7] We also observed migration of Ag to the surface of the bottom electrode, but its effect on the TMR of a MTJ has not been examined!

Future Plans

Our research plans for the coming year are (1) to identify the role of migrated Ag at the interface of FM and the tunnel barrier on the TMR of a MTJ. We will explore the use of a different buffer without Ag and inserting some other layers to suppress the migration of Ag. (2) to study the crystalline orientation anisotropy of spin polarization of

FM electrodes. Specifically, we will utilize Si substrates with different crystalline orientations for the MTJ fabrication to study the difference in the TMR ratios, from which the information of spin polarization can be extracted.[7] (3) to achieve record high TMR value utilizing amorphous CoFeB electrode for AlO_x based MTJ. It has been shown that amorphous CoFeB with AlO_x barrier can yield TMR value around 70%[8]. With the TiN buffer under the CoFeB, the amorphous structure can be transformed to epitaxial bcc structure without changing the ultra-smooth interface by thermal annealing at 300^{o}C. Thus, it is reasonable to anticipate achieving a very high TMR value for an AlO_x based MTJ because of the near-perfect combination of smooth interface and epitaxial bcc crystal structure! Moreover, the almost atomically flat interface will provide an ideal platform to analyze the true anisotropy property of spin polarization. (4) As noted above, we have demonstrated that the epitaxially grown bcc (Co,Fe) electrode on a Si substrate with an Ag buffer layer in an AlO_x based MTJ yielded over 70% TMR at RT. Moreover, over 200% TMR has been theoretically predicted[9] and experimentally observed[10,11] in MTJs with bcc (Co,Fe) electrodes and a textured or epitaxial MgO tunnel barrier. Because of the close lattice match between bcc (Co,Fe) and MgO with 45^o rotation, *we envision that the formation of a high-quality MgO tunnel barrier on an epitaxial bcc (Co,Fe) electrode grown on a Si substrate as we have done could yield a record high TMR*. In short our on-going effort and proposed research on the magnetic nanostructure help to provide a better understanding of the physics of this class of nanostructures but the novel synthesis of these nano-multilayered structures via sputtering deposition on a Si substrate is also of practical interest for industrial applications.

References

1. M. Julliere, Phys. Lett. **54A**, 225 (1975).
2. J. S. Moodera, L. R. Kinder, T. M. Wong, and R. Meservey, Phys. Rev. Lett.**74**, 3273 (1995).
3. M. Münzenberg and J. S. Moodera, Prys. Rev. B **70**, 060402(R) (2004).
4. M. Wojcik, J. P. Jay, P. Panissod, E. Jedryka, J. Dekoster, and G. Langouche, Z. Phy. B **103**, 5-12 (1997).
5. P. LeClair, J. T. Kohlhepp, C. H. van de Vin, H. Wieldraaijer, H. J. M. Swagten, W. J. M. de Jonge, A. H. Davis, J. M. MacLaren, J. S. Moodera, and R. Jansen, Phys. Rev. Lett. **88**, 107201 (2002).
6. K. Jun, J. H. Lee, K. –H. Shin, K. Rhie, and B. C. Lee, J. Magn. Magn. Mater. **286**, 158 (2005).
7. S. Yuasa, T. Sato, E. Tamura, Y. Suzuki, H. Yamamori, K. Ando, and T. Katayama, Europhys. Lett. **52**, 344 (2000).
8. D. Wang, C. Nordman, J. M. Daughton, Z. Qian, J. Fink, IEEE Trans. Magn. **40**, 2269 (2004).
9. W. H. Butler, X. G. Zhang, T. C. Schulthess, and J. M. MacLaren, Phys. Rev. B **63**, 054416 (2001).
10. S. S. P. Parkin, C. Kaiser, A. Panchula, P.M. Rice, B. Hughes, M. Samant, and S.H. Yang, Nat. Mater. **3**, 862 (2004).

11. S. Yuasa, T. Nagahama, A. Fukushima, Y. Suzuki, and K. Ando, Nat. Mater. **3**, 868 (2004).

DOE Sponsored Publications in 2005-2006

1. *Selective oxidation of an individual layer in a magnetic tunnel junction through the use of thermodynamic control,* P. F. Ladwig, J. J. Yang, Y. A. Chang, F. Liu, B. B. Pant, A. E. Schultz, 2005, APPLIED PHYSICS LETTERS 87, 061901.
2. *Intermixing and phase separation at the atomic scale in Co-rich (Co,Fe) and Cu multilayered nanostructures*, P. F. Ladwig, J. D. Olson, J. H. Bunton, D. J. Larson, R. M. Ulfig, R. L. Martens, T. T. Gribb, T. F. Kelly, M. C. Bonsager, A. E. Schultz, B. B. Pant, Y. A. Chang, 2005, APPLIED PHYSICS LETTERS 87, 12.
3. *Phase transformations in sputter deposited NiMn thin films*, M.-L. Huang, P. F. Ladwig, Y. A. Chang, 2005, THIN SOLID FILMS 478, 137.
4. *Oxidation of tunnel barrier metals in magnetic tunnel junctions,* J. J. Yang, P. F. Ladwig, Y. Yang, C. -X. Ji, and Y. Austin Chang, F. X. Liu, B. B. Pant, and A. E. Schultz, 2005, JOURNAL OF APPLIED PHYSICS 97, 10C918.
5. *The formation of amorphous alloy oxides as barriers used in magnetic tunnel junctions*, J. J. Yang, Y. Yang, K. Wu, Y. A. Chang, 2005, JOURNAL OF APPLIED PHYSICS 98, 074508.
6. *Thermal stability of the interfaces between Co, Ni and Fe based ferromagnets in contact with selected nitrides MN (M = Al, B, Nb, Ta, Ti and V),* Y. Yang, Y. A. Chang, J. J. Yang, C.-X. Ji, P. F. Ladwig, F. Liu, B. B. Pant and A. E. Schultz, 2005, JOURNAL OF APPLIED PHYSICS 98, 053907.
7. *An investigation of phase transformation behavior in sputter-deposited PtMn thin films*, C.-X. Ji, P. F. Ladwig, R. D. Ott, Y. Yang, J. J. Yang, Y. A. Chang, E. S. Linville, J. Gao, B. B. Pant, 2006, JOM 58, 50.
8. *Phase diagram calculations in teaching, research, and industry,* Y. A. Chang, 2006, METALLURGICAL AND MATERIALS TRANSACTIONS B 37B, 7.
9. *Thickness determination of ultra-thin oxide films and its application in magnetic tunnel junctions*, J. J. Yang, Y. Yang, F. Liu, B. B. Pant, A. E. Schultz, and Y. A. Chang, 2006, JOURNAL OF ELECTRONIC MATERIALS, in press.
10. *Realization of over 70% TMR at room temperature for a CoFe and AlOx based magnetic tunnel junction*, J. J. Yang, C. -X. Ji, Xianglin Ke, M. S. Rzchowski, and Y. A. Chang, 2006, APPLIED PHYSICS LETTERS, under review.
11. *Role of the ferromagnetic electrode crystal structure in the spin dependent tunneling*, J. J. Yang et al., 2006, to be submitted to PYSICAL REVIEW LETTERS.
12. *Origin of the variation of tunneling magnetoresistance with the Composition of Co_xFe_{1-x} Electrodes in Magnetic Tunnel Junctions*, J. J. Yang et al., 2006, to be submitted to APPLIED PHYSICS LETTERS.

Structure and Bonding at Surfaces, Interfaces, and Low-Dimensional Solids

Jian-Min Zuo
jianzuo@uiuc.edu
Dept. of Materials Science and Engineering and Materials Research Laboratory,
University of Illinois, Urbana-Champaign, IL 61801

Program Scope

Nanostructures have many applications in energy- and environmental-related applications such as catalyst and energy conversion. These three-dimensional structures are often supported on substrates with surfaces and interfaces. While 2-D flat surfaces have been studied extensively using surface analysis techniques, little is known about 3-D surfaces and interfaces because of the difficulties associated with nanostructure characterization. This program uses multi-pronged approach employing transmission electron microscopy, low energy electron microscopy, electron diffraction and in-situ characterization to develop an atomic-level understanding of structure and bonding at surfaces, interfaces and in low-dimensional solids. Towards this goal, we combined low energy electron microscopy (LEEM) with TEM to study the kinetics of nanostructure growth and investigated nanocluster structure and transformation. The current focus is to develop ultrafast electron diffraction to study transformation dynamics.

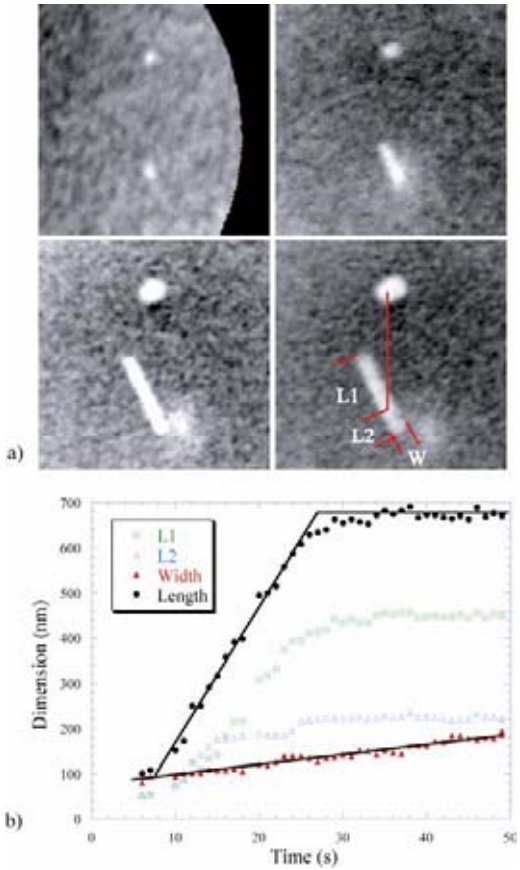

Fig. 1 a) LEEM micrographs of Ag nanowire growth. b) The measured lengths and width of the wire as a function of time. The growth of the wire is asymmetrical with one end (L1) grows 13 times faster than the width.

Recent Progress:

It is commonly believed that lower energy from the competition of surface and strain energies leads the growth of one-dimensional structures such as nanowires. However, energy alone does not explain why wire growth is preferred for some initial islands but not others. In collaboration with Dr. W. Swiech, we examined the growth kinetics of Ag nanowires on Si(100) and the structure of nanowires by in-situ low energy electron microscopy ex-situ TEM observation. Fig. 1 shows the growth of two Ag islands; one grows into a nanowire while the other into a rectangular (in projection) island. The growth processes were captured by LEEM. The measured width and length of the

First Principles Studies of Intergranular Films in Ceramics

Gayle S. Painter[1] and Frank W. Averill[1, 2]
gsp@ornl.gov, faverill@utk.edu
[1]Materials Science and Technology Division, Oak Ridge National Laboratory, Oak Ridge, TN 37831-6114
[2]Center for Materials Processing, University of Tennessee, Knoxville, TN 37996-0750

Program Scope

The crystalline grains in ceramics are often surrounded by amorphous intergranular films (IGFs) that are as thin as 1-2 nm between adjacent grains. The composition of these IGFs is established by the additives (e.g., metal oxides, MeO_x) used to densify the ceramic. These oxide additions also *control* the microstructural evolution and fracture toughness of the ceramic; understanding *how* this occurs is the prime motivation for this project. Although it is recognized that additive selection can give atomic-level control of material properties, processing strategies have remained largely empirical. This program is directed towards providing a more fundamental basis for ceramic design strategies. We seek to understand microchemical interactions, both within the IGFs and at the IGF/grain interface, in terms of the underlying electronic structure, as determined by first-principles studies [using the SCPW (self-consistent partial-wave) cluster method[1]] within local density/gradient corrected approximations to density functional theory (DFT). The general goal of this project is to obtain a basic understanding of the mechanisms by which additives, such as rare earths (RE) and other metal oxides, affect the microstructure and properties of Si_3N_4-based ceramics, with focus on the effects of local coordination and bonding of RE atoms with oxygen and nitrogen, the role of Mg and Al additions, and the effects of O/N ratio on properties of the amorphous phases in the ceramic. Specific goals are defined by collaborations with experimentalists working on synthesis and characterization at the atomic level. In recent work aberration corrected Z-contrast scanning transmission electron microscopy (STEM) imaging was combined with theory to define atomic-level details and an understanding of the selective adsorption of different rare earths (La, Gd and Lu) at β-Si_3N_4 grain surfaces. Current focus relates to processing efforts that seek to enhance ceramic fracture resistance through combinations of additions (RE and Me oxides) that control: (1) viscosity of the IGF, (2) rates of phase transformations of reinforcing grains and (3) grain growth anisotropy. While driven by basic science, establishing principles for the atomic-level control of ceramic properties can be expected to also impact energy issues ranging from power generation (high temperature materials) to energy conservation through increased operating efficiencies and reduced component failure rates.

Recent Progress

Metal oxide additions are well known to affect grain growth morphologies of ceramics: oxides of the rare earths can alter aspect ratios of reinforcing grains in silicon nitride ceramics by nearly an order of magnitude[2]. From a differential binding energy (DBE) model[3], that compared the relative affinities of a given RE with Si for oxygen and

nanowire as a function of time clearly shows that the wire is formed by the difference in growth speeds of different sides of the cluster. The growth diverges after ~10s. Across the wire, the growth proceeds at an almost constant speed of 2.3 nm/s. Along the wire, the overall growth rate is 30.3 nm/s, which is a factor of 13 times faster than the width growth. Interestingly, the length growth stops after ~26 s, while the width continues to grow (for ~110 s, not shown). The growth is asymmetrical with one end of the wire grows faster the other.

To explain the asymmetric growth of Ag nanowires, we suggest that introduction of defects in the form of stacking faults is responsible for breaking of the symmetry of FCC crystals. Fig. 2 shows an atomic model of stacking fault introduction when the growth of Ag island interacts with a kinked surface step. The introduction of a stacking fault creates a ledge on one end of the island, which provides a preferential place for adsorption during growth and desorption during melting. The model is supported by TEM observation, which shows evidence of stacking faults and dislocations in as-grown Ag nanowires.

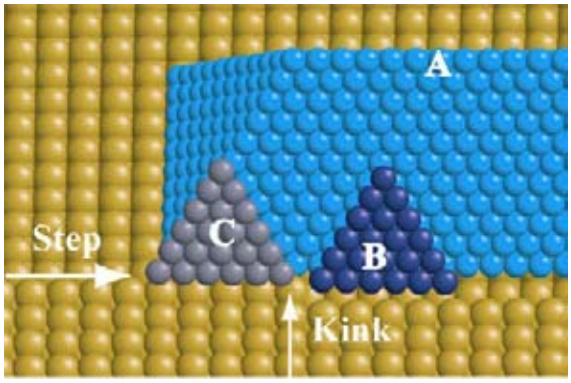

Fig. 2 An atomic model of stacking fault introduction when the growth of an FCC island interacts with a kinked surface step on Si(100) surface.

In another study[1], we studied the interface energetics of nanoclusters. Using Ag on hydrogen terminated Si(100) surface, we have investigated lattice effect on nanoclusters growth and structure. The study follows our previous investigation on the stage of epitaxy formation during cluster growth. On (100) surface, the interfacial interaction competes with the Ag-Ag attraction. Using our UHV TEM, we carried out systematic study of Ag cluster growth and structure. We found that RT deposition stabilizes multi-twinned cluster structure and at higher T (~200 °C), epitaxial clusters are favored. Further, by annealing RT deposited clusters at ~400 °C, almost perfect epitaxial crystalline Ag clusters can be obtained. Epitaxial clusters has the coincidence lattice of Ag(100)||Si(100) and Ag[011]||Si[011] (see fig. 1). The cell is ~1.6 nm in size. The large unit cell suggests that epitaxy is not preferred at the early stage of cluster nucleation and interface effects come in at a late stage of cluster growth, which requires cluster reorientation and crystallization. This study significantly improves our understanding of interface on epitaxial growth.

Future Plans:

With the renewal of MRL at University of Illinois, we are exploring two new directions in the study of surfaces and interfaces. One is interfaces in oxide superlattice with potential for photocatalytic applications. Another is transformation dynamics.

A high-energy ultrafast electron diffraction camera for in-situ characterization is being constructed to investigate solidification of thin-films and supported metal particles at a time resolution of ~1 picosecond using the laser beam pump-probe approach[2,3,4]. The issues to be addressed are supercooling of metal nanoparticles prepared by thermal evaporation and nucleation and growth on flat substrate surfaces. The advantage of nanoparticles is that they can be fully melted and their microstructures can be monitored by electron diffraction *in transmission*. Furthermore, heat conduction through the substrate can be used to control the cooling rate. Information about the structure of both supercooled liquids and the initial crystal structures will be extracted by developing quantitative data analysis algorithms that include local ordering in undercooled liquids, the structure of nuclei and meta-stable phases, crystallization speed, thermal vibrations and crystal orientations. MD simulations will be employed to assist in the diffraction analysis and interpretation of data.

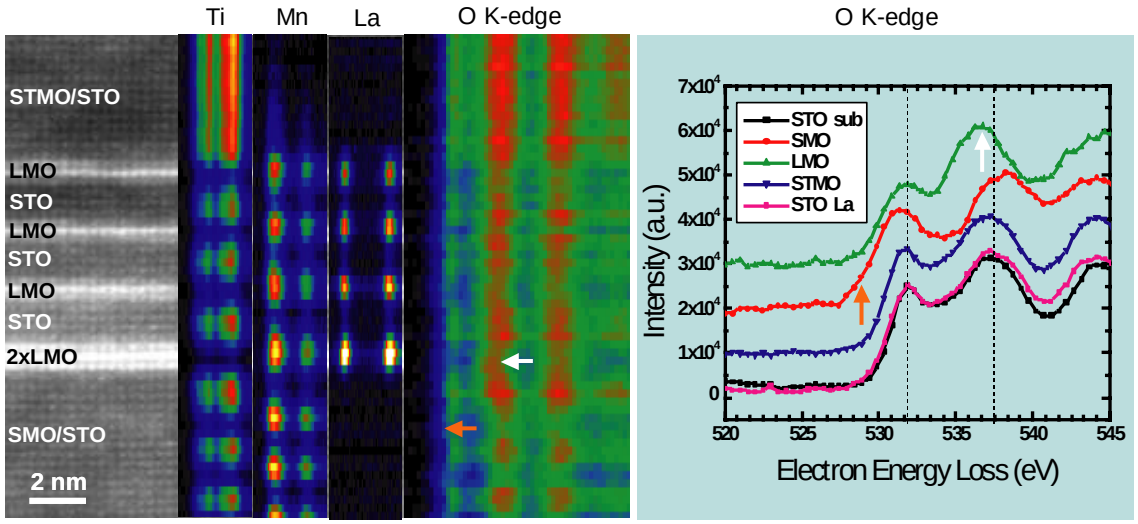

Figure 3. High-resolution Z-contrast STEM and EELS core loss spectroscopy showing precision engineered superlattice of $SrTiO_3$ (STO), $SrMnO_3$ (SMO), $SrTi_{1-x}Mn_xO_3$ (STMO), and $LaMnO_3$ (LMO). Perovskite SMO is stabilized in the superlattice.

Molecular beam epitaxy of oxides is an attractive approach to the systematic study bonding at interfaces. Semiconducting oxides also are potential photocatalyst for energy harvest applications. An example of the kind of atomistic control possible using MBE by Eckstein's group at UIUC is shown in Figure 3. Here three different oxide phases were used to construct an asymmetric tricolor superlattice. The constituent phases are all of the perovskite type, and they bond in a single crystal form even though they have a different A-site atom in each unit cell. The stacking sequence controls the orientation of an asymmetric strain field present in the material, and this leads to asymmetric dielectric response at all temperatures.

The challenge for interfacial characterization is to correlate the electronic structure with interface composition and atomic structure. To address this issue, we propose a research program that combines structural analysis of electron diffraction with local probes of electron imaging and EELS for the study of oxide interfaces and surfaces. Atomic resolution analysis will be achieved using an aberration corrected scanning and

transmission electron microscope with monochromator for high resolution EELS that will be installed in CMM, Fall 2006. This new microscope will provide a sub-Å focused electron probe for direct imaging and electron energy loss spectroscopy at 0.2 eV resolution (the latter to be installed in 2007). The microscope is also equipped with an in-column energy filter, which provides elastic and diffraction intensities for quantitative structure analysis.

To determine the atomic structure of oxide superlattices, we propose to combine electron nanoprobe with precession electron diffraction. The electron precession method developed by Vincent and Midgley[5] averages the diffraction intensities over a range of incident angles. Recent studies[6,7] have shown that dynamic diffraction effect is significantly minimized precession electron diffraction data. This new electron diffraction technique, coupled with nanoprobes, allows us to study local atomic structure, especially the interfaces that dominate the oxide superlattices. Because the intensity is close to kinematical, merging of 3-D data set will be much easier. Structure determination will then be carried out and used to model the electronic structure of the oxide interfaces.

Reference:

1 B.Q. Li and J.M. Zuo, *Phys. Rev. B* 72, 085434 (2005)
2 J. R. Helliwell and P.M. Rentzepis, (Oxford Science Publications, Oxford, UK, 1997).
3 A. M. Lindenberg, J. Larsson, K. Sokolowski-Tinten et al., "Atomic-scale visualization of inertial dynamics," Science **308** (5720), 392-395 (2005)
4 W. E. King, G. H. Campbell, A. Frank et al., "Ultrafast electron microscopy in materials science, biology, and chemistry," Journal of Applied Physics **97** (11) (2005)
5 R. Vincent and P. A. Midgley, *Ultramicroscopy* **53**, 271 (1994)
6 P. A. Midgley, M. E. Sleight, M. Saunders, et al., *Ultramicroscopy* **75**, 61 (1998)
7 C. S. Own, W. Sinkler, and L. D. Marks, *Ultramicroscopy* **106**, 114 (2006)

DOE Sponsored Publications in 2004-2006

1. Zuo, J.M., Measurements of electron densities in solids: a real-space view of electronic structure and bonding in inorganic crystals**,** Reports On Progress In Physics 67, 2053-2103 (2004)
2. Lim, C.W., C.S. Shin, D. Gall, J.M. Zuo, I. Petrov and J.E. Greene, " Growth of $CoSi_2$ on Si(001) by reactive deposition epitaxy", *J. Appl. Phys.* 97, 044909 (2005)
3. W.J. Huang, B.Q. Li and J.M. Zuo, "Diffusion-limited submonolayer pentacene thin film growth on hydrogen-passivated Si(1 1 1) substrates", Surf. Sci. 595, 157-164 (2005)
4. Zuo, J.M. and B.Q. Li, “Nanocluster interfaces and epitaxy: Ag on Si surfaces”, *Z. Metall.* 96, 438-442 (2005).

B.Q. Li and J.M. Zuo, " Structure and shape transformation from multiply twinned particles to epitaxial nanocrystals: Importance of interface on the structure of Ag nanoparticles", *Phys. Rev. B* 72, 085434 (2005)

nitrogen bonding, a qualitative explanation of the different grain growth aspect ratios was obtained from first-principles cluster models using the SCPW. By this measure cations that preferentially attach to the N-terminated grain surface can be distinguished from those that are favored to remain in oxygen-rich glassy volumes. The calculated second energy differentials showed excellent correlation with measured grain growth aspect ratios for several contrasting RE additions. The qualitative explanation of the experimental observations is simple in this model. Rare earths that compete strongly with Si for oxygen bonds experience a weaker driving force for segregation and bonding at the N-terminated grain surfaces than RE that do not. Subsequent STEM confirmed these predictions through direct imaging of RE atoms adsorbed at smooth prism planes of β-Si_3N_4 crystallites in ceramic samples (for RE= La, Gd and Lu.)[4,5] Since crystalline growth on the prism planes is reaction-rate limited, and RE desorption must occur for the attachment of β-Si_3N_4 growth fragments, REs that are strongly adsorbed (such as La) result in higher aspect ratios compared with Lu, which shows less adsorption on the prism planes. Thus the tendency for RE atoms to segregate from the liquid phase is described by the DBE, and the adsorption sites of RE along the nitride prism planes are determined from detailed cluster calculations. The predicted adsorbate structures agree well with STEM imaging from three independent laboratories[6] (typically within a few tenths of an Angstrom), confirming the strong locality of the RE / interface bond[7].

More recent studies addressed the observation of RE ordering in planes parallel to prism surfaces and extending ~5Å *into* the amorphous IGF. This was explained in terms of the calculated RE adsorbate structure[8]. Rare earths adsorb at specific sites on the N-terminated β-Si_3N_4 prism surface with the periodicity of the underlying lattice. The adsorbed RE atoms then serve as a template for N-attachment. For Lu adsorption there is a matching to the structure of a stable c-LuN phase along the [0001] direction. However, this match with the c-LuN phase is broken in the direction *normal* to [0001], and epitaxial growth is inhibited. Thus, LuN-like island structures form with the period of the initial Lu adsorbation. The amorphous nature of the IGF limits the extent of the c-LuN clusters into the IGF.

Future Plans

Work for the future will follow a natural progression to exploit the high accuracy, completeness and flexibility of the SCPW approach with new functionals that are best realizations of DFT. Extension of our studies on ceramics requires further work on the amorphous phases that are present as both IGFs and glassy pockets in ceramics. Long-standing questions persist about the atomistic mechanisms that govern the physical properties of glasses (fragility, hardness, melting points, viscosities), and they require an understanding of the intrinsic nature of bonding within the glassy phase itself. Specifically initial studies will focus on Si-O-N glass properties, for example, network connectivity and composition (O/N ratio and the strengthening effects of N-incorporation into a largely SiO_2 network). Results will serve as a reference for the effects of additions (e.g. Al, RE) introduced by sintering (with alumina, RE oxides). Oxynitride glasses are experimentally well-characterized and have served as study models of the amorphous IGFs in Si-based ceramics, and theoretical work has recently been reported on the glasses[9] and the role of Y-additions.[10] These glasses are also useful materials in their own

right (forming strong, corrosion resistant high melting point glasses). Phenomena occur within the amorphous phases that are critical to ceramic structural performance, particularly at elevated temperatures, e.g. creep behavior with its origin in nanoscale cavitation, and the role of glass transitions[11]. Further studies will focus on the microchemistry of RE-Si-Me-O-N glassy phases (RE = Y, La, Gd, Lu, Sm; Me= Al, Mg), and details about the coordination of RE, Me cations with O and N, and the effects of REs, Me and N/(N+O) ratio on the local mechanical properties of the oxynitride glass. Fundamental questions concerning connectivity will be addressed, such as how local changes in network coordination (e.g., number of bridging oxygens) are affected by cation network formers and modifiers, particularly RE atoms (both larger O/N ratio and RE incorporation increase glass viscosity)[12].

The complexity of ceramic systems has prompted our development of improved first-principles techniques applicable to amorphous mixed-bonding (covalent-ionic) nanoscale volumes. Current focus is on extending the SCPW atomic cluster approach to larger length scales by implementing the order-N ($\mathcal{O}$(N)) divide and conquer (DC) concept of W. Yang[13]. Calculation of the ground state structure and energetics of local regions within amorphous RE-doped oxynitride IGFs sets the stage for addressing phenomena such as growth of the crystalline grains. While identifying growth fragments remains challenging, new SCPW-DC atomic cluster techniques will enable calculation of quantities such as the transition state energies. These can then be used to initiate secondary multi-scale studies, e.g. kinetic Monte Carlo modeling of grain growth and the influence of various rare earth additions.

Future activities will follow the course of this developmental work, not only with regard to areas of application, but also concerning the formulation of the SCPW-DC and its use as a basic component of multi-scale modeling. Here the concepts of the "nearsightedness" of electrons[14] (which has long underpinned atomic cluster models) will be explored and utilized to achieve an optimized $\mathcal{O}$(N) technique complementing, and in some cases interfacing with, techniques based on Bloch states (VASP), Quantum MD, reactive force fields and other multi-scale methods[15].

References

(1) F. W. Averill and G. S. Painter, *Phys. Rev. B* **50**, 7262-67 (1994).
(2) R. L Satet and M. J. Hoffmann, *J. Am. Ceram. Soc*. **88,** 2485-90 (2005).
(3) G. S. Painter, P. F. Becher, W. A. Shelton, R. L. Satet and M. J. Hoffmann *Phys. Rev. B* **70**, 144108-11 (2004).
(4) N. Shibata, G. S. Painter, R. L. Satet, M. J. Hoffmann, S. J. Pennycook and P. F. Becher, *Phys. Rev. B* **72,** 140101-4 (R) (2005).
(5) G. B. Winkelman, C. Dwyer, T. S. Hudson, D. Nguyen-Manh, M. Döblinger, R. L. Satet, M. J. Hoffmann, and D. J. H. Cockayne, *Appl. Phys. Lett*. **87**, 06191, 1-3 (2005).
(6) C. Dwyer, A. Ziegler, N. Shibata, G. B. Winkelman, R. L. Satet, M. J. Hoffmann, M. K. Cinibulk, P. F. Becher, G. S. Painter, N. D. Browning, D. J. H. Cockayne, R. O. Ritchie, and S. J. Pennycook, *J. Mater. Sci.* **41**, 4405-12 (2006).
(7) P. F. Becher, G. S. Painter, N. Shibata, R. L. Satet, M. J. Hoffmann and S. J. Pennycook, *Mater. Sci. Engr'g*, A **422**: 85-91 (2006).

(8) N. Shibata, G. S. Painter, P. F. Becher and S. J. Pennycook, *Appl. Phys. Lett*. **89,** 051908, 1-3 (2006).
(9) S. R. Billeter, A. Curioni, D. Fischer and W. Andreoni, *Phys. Rev. B* **73**, 11539, 1-14 (2006).
(10) W. Y. Ching, J. Chen, P. Rulis, L. Ouyang and A. Misra, J. Mater. Sci. **41**, 5061-67 (2006).
(11) J. C. Mauro and A. R. Varshneya, Am. Ceram. Soc. Bull. **85**, 25-28 (2006).
(12) F. Lofaj, S. Deriano, M. LeFloch, T. Rouxel, and M. J. Hoffmann, *J. Non. Xtal. Solids* **344** 8-16 (2004).
(13) W. Yang, *Phys. Rev. Lett*. **66**, 1438-41 (1991).
(14) E. Prodan, *Phys. Rev*. B**73**, 085108 1-13, (2006).
(15) Handbook of Materials Modeling A & B, S. Yip, ed., Springer, (2005).

DOE Sponsored Publications in 2004-2006

First Principles Study of Rare-Earth Effects on Grain Growth and Microstructure in β-Si_3N_4 Ceramics, G. S. Painter, P. F. Becher, W. A. Shelton, R. L. Satet and M. J. Hoffmann, *Phys. Rev. B* **70**, 144108-11 (2004).

Observation of Rare Earth Segregation in Silicon Nitride Ceramics at Sub-Nanometer Dimensions, N. Shibata, S. J. Pennycook, T. R. Gosnell, G. S. Painter, W. A. Shelton, and P. F. Becher, *Nature* **428**, 730-33 (2004).

Rare Earth Adsorption at Intergranular Interfaces in Silicon Nitride Ceramics: Sub-Nanometer Observations and Theory, N. Shibata, G. S. Painter, R. L. Satet, M. J. Hoffmann, S. J. Pennycook and P. F. Becher, *Phys. Rev. B* **72,** 140101-4(R) (2005).

Direct Observations of Debonding of Reinforcing Grains in Silicon Nitride Ceramics Sintered with Yttria Plus Alumina Additives, P. F. Becher, S. Ii, Y. Ikuhara, G. S. Painter and M. J. Lance, *J. Am. Ceram. Soc*. **88**, 1222-26 (2005).

Atomic Ordering at an Amorphous/Crystal Interface, N. Shibata, G. S. Painter, P. F. Becher and S. J. Pennycook, *Appl. Phys. Lett*. **89,** 051908, 1-3 (2006).

Influence of Additives on Anisotropic Grain Growth in Silicon Nitride Ceramics, P. F. Becher, G. S. Painter, N. Shibata, R. L. Satet, M. J. Hoffmann and S. J. Pennycook, *Mater. Sci. Engr'g*, A **422**, 85-91 (2006).

Convergence properties of the Harris Density Functional and the Self-Consistent Atom Fragment Approximation, F. W. Averill and G. S. Painter, *Phys. Rev. B* **73**, 235125, 1-10 (2006).

Interfacial structure in β-Si_3N_4 sintered with Ln_2O_3, C. Dwyer, A. Ziegler, N. Shibata, G. B. Winkelman, R. L. Satet, M. J. Hoffmann, M. K. Cinibulk, P. F. Becher, G. S. Painter, N. D. Browning, D. J. H. Cockayne, R. O. Ritchie, and S. J. Pennycook, *J. Mater. Sci.* **41**, 4405-12 (2006).

First Principles Theory of the Magnetic State of Nanostructures*

G. Malcolm Stocks[1], Balazs Ujfalussy[1, 2], Markus Eisenbach[1], Aurlian Rusanu[1], D.M.C. Nicholson[3], and Yang Wang[4]
stockgm@ornl.gov, bl@szfki.hu ll, eisenbachm@ornl.gov, rusanua@ornl.gov, nicholsondm@ornl.gov, ywg@psc.edu
[1]Materials Science and Technology Division, Oak Ridge National Laboratory, Oak Ridge, TN 37831
[2] Inst for Solid State Physics H-1525, Budapest, PO Box 49 H-1525 Hungary
[3]Computer Science and Mathematics Division, Oak Ridge National Laboratory, Oak Ridge, TN 37831
[4] Pittsburgh Supercomputer Center, 300 S. Craig Street, Pittsburgh, PA 15213

Program Scope

Driven by the need for ever higher density recording media, smaller and more responsive sensors, and higher energy product permanent magnets, *nanomagnetism*, the science and technology of nanoscale magnetic materials and devices, is currently one of the focii of nanoscience research [1]. A fundamental problem in understanding nanoscale magnetic phenomena is that it is generally not possible to construct simple models based on parameters obtained for bulk systems - neither experimentally nor theoretically. Furthermore, experimental characterization of nanoscale features is also often problematical without sophisticated theory and modeling to interpret experimental results. In this program we develop and apply first principles electronic structure methods to study the magnetic structure of surface and embedded magnetic nanostructures, to relate the magnetic properties to the underlying electronic structure and to interpret experiment. Specifically we use relativistic density functional theory based methods within state of the art surface embedding [2, 3] and order-*N* [4,5] multiple scattering Green's function methods. First principles spin-dynamics [6-8] and the constrained local moment approximation [9-10] are then used to describe non-equilibrium magnetic states and also to optimize moment configurations in highly inhomogeneous materials such as surface and bulk nanostructures. Using these approaches we are able to treat moment formation, the exchange interaction, and magneto-crystalline anisotropy on an equal (electronic) footing which is crucial to obtaining a

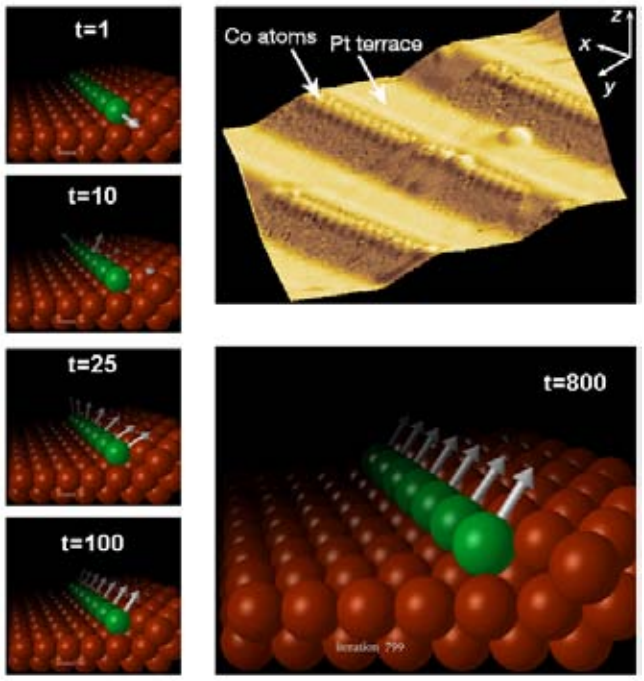

Figure 1: Top right: STM results of Gambardella et al. showing Co-chain at a Pt-surface step edge. Bottom right: Ground-state Co-atom moment orientations calculated using FP-SD (FP-SD time step t=800). FP-SD moment orientation at earlier time steps (t=0, 10, 25, and 100)

* Work performed in collaboration with B. Lazarovits, L. Szunyogh, P. Weinberger and B. L. Gyorffy and sponsored by DOE-OS, BES-DMSE and OASCR-MICS under contract number DE-AC05-00OR22725 with UT-Battelle LLC. The calculations presented in this paper were performed at the Center for Computational Sciences (CCS) at ORNL and at the National Energy Research Scientific Computing Center (NERSC).

proper description of both complex magnetic ground states as well as moment dynamics. This research is part of a more general program of research into the magnetic structure and dynamics of inhomogeneous magnetic materials with the long term goal developing first principles based theories of both intrinsic – magnetic structure, magnetic moment, magnetic anisotropy – and extrinsic[†] – permeability, remenance, coercivity – of properties of magnetic materials.

Recent Progress

We review some of our recent studies of the magnetic structure of surface and bulk nanostructures first principles calculations using first principles electronic structure methods. These studies include calculations of the magnetic structure of three prototypical nanostructures -- short Co and Fe-chains adjacent to a Pt {111}-surface step-edge, a Cr-trimer on the Au {111}-surface, and Fe-chains and impurities in Cu [11].

As illustrative of this work we present some results of studies the angular tilt of the magnetic moments of short Co-chains adjacent to a step edge on the [111]-surface of Pt. As shown in **Fig. 1**, the chains order ferro-magnetically and the Co magnetic moments cant towards the step at an angle of 42^o [12] in quantitative agreement with the experiments of Gambardella et al. who found a ferromagnetic state with a canting angle of 43^o [13]. Computationally the Co-chain together with the Pt-step was treated as an extended impurity embedded in a trough cut in an otherwise perfect semi-infinite Pt-surface in order to create nascent step edges. The semi-infinite surface is treated using a first principle relativistic [Dirac equation] screened KKR (Korringa-Kohn-Rostoker) approach [2] with subsequent embedding of the extended impurity (consisting of the prototypical step and the Co-chain) in the surface using standard impurity embedding techniques [3]. Constrained density functional theory was used to calculate the magnetic state at each time step in the evolution of a semi-classical Landau-Lifshitz equation of motion as the moments were relaxed towards equilibrium. Taken together our work on these highly inhomogeneous surface nanostructures illustrate the need to treat the underlying electronic interactions on a fully self-consistent basis in which the very different energy scales appropriate to exchange coupling and magneto-crystalline anisotropy are treated simultaneously. As a consequence conclusions based on such commonly used approximations as the magnetic force theorem or frozen potential approximation [14, 15] can lead to quantitatively and some qualitatively incorrect results.

Calculating the magnetic properties of nanoparticles from first principles is a daunting task due to the (still) large numbers of atoms in real nanoparticles. Despite this, using a new

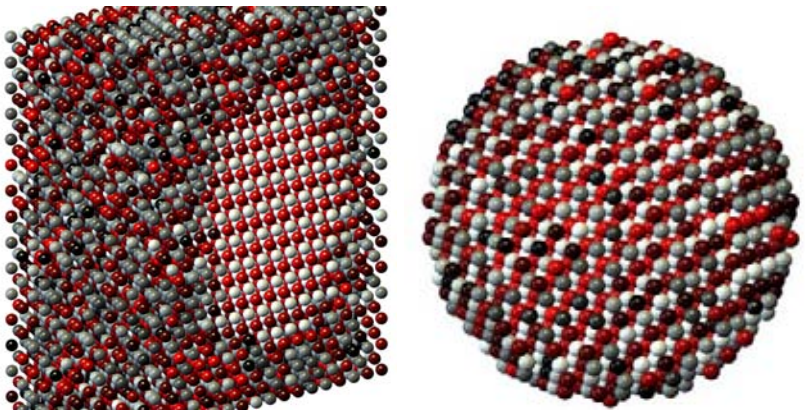

Figure 1: Illustration of the magnetic moment distribution in a ~5 nm L10 ordered iron-platinum particle embedded in a iron-platinum random solid solution alloy. The magnetic moment size is indicated by color depth (darker implies smaller moments) for iron (red) and platinum (silver) atoms.

[†] Often referred to the technical properties of magnetic materials.

implementation of the order-N LSMS method, we are now able to perform [16] calculations of the magnetic structure of embedded and free standing nanoparticles in a size range that is experimentally interesting. As illustrative of our preliminary work with this new code we show in **Fig. 2** a visualization of the magnetic moments associated with L10-ordered FePt nanoparticle (left) that is surrounded by a $Fe_{0.5}Pt_{0.5}$ solid solution (random) alloy. Figure 2 shows two views of the magnetic moment distribution for a 5nm FePt-nanoparticle with the surrounding $Fe_{0.5}Pt_{0.5}$ random alloy (a total of 14,400 atoms). In the interior of the nanoparticle, Fe- and Pt-atoms have their bulk moments. At greater distances from the center, the alloy atoms have reduced magnetic moments (left: cross-sectional view). The nanoparticle itself (right: exterior view) presents a boundary region of one-to-two atoms in which magnetic moments are influenced by the surrounding alloy, while atoms deeper within are unaffected. Taken together calculations of a series of nanoparticles of increasing size – 2.5, 3.86 and 5.0 nm – clearly indicate the need for fully *ab intio* studies in order to describe the subtle moment variations that occur an the surfaces of nanoparticles.

Future Plans

As outlined above, significant progress has been made towards the development of a first principles (FP) theory of the spin dynamics (SD) of itinerant magnets based on a temporal separation between fast electron degrees of freedom (responsible for moment formation) and slow changes in the orientation of local moments [17]. With the addition of the constrained local moment (CLM) model to implement constrained DFT [18] calculation for the non-equilibrium non-collinear moment configuration that results at each time step, FP-SD provides a classical equation of motion for the orientational degree of freedom of the local moments where the effective field driving the motion is obtained from FP. Adding a phenomenological damping term yields a microscopic Landau-Lifshitz-Gilbert (LLG) equation [19]. Based on the foundations provided by these apaches propose to extend and utilize FP-SD within the context of the O[N] LSMS method to study magnetism in complex materials and structures that are of current experimental interest including nanoparticles of ordered and disordered alloys as well as oxides. Using a recently developed full potential version of the LSMS method it will be possible to including the interaction between the magnetic state and structural (atomic) relaxation. In addition we propose to study the response of the magnetization to temperature (superparamagnetic limit) and applied field (switching). Using FP-SD temperature effects can be addressed either by adding a phenomenological damping term to the precessional motion of the moments in the LLG equations or via equilibration of the systems at finite temperature using Monte Carlo methods with subsequent integration of the precession term of the LLG equation (dissipation free or microcanonical simulation).

References

1. J. Kubler, J. Phys.: Condens. Matter **15,** V21 (2003).
2. L. Szunyogh, B. ¶Ujfalussy, and P. Weinberger, Phys. Rev. B **51**, 9552 (1995);
3. B. Lazarovits, L. Szunyogh, and P.Weinberger, Phys. Rev. B 65, 104441 (2002).
4. Yang Wang, G. M. Stocks, W. A. Shelton, D. M. C. Nicholson, Z. Szotek, and W. M. Temmerman, Phys. Rev. Lett. **75** 2867 (1995);
5. M. Eisenbach, B. L. Gyorffy, G. M. Stocks, and B. Ujfalussy, Phys. Rev. B **65** 144424; (2002)
6. V. P. Antropov, et al., Phys. Rev. Lett. **75**, 729 (1995);
7. V.P. Antropov, M. I. Katsnelson, B. N. Harmon, M. van Schilfgaarde, and D. Kusnezov, *Phys. Rev.* B **54**, 1019 (1996).
8. Niu, Q., X. Wang, L. Kleinman, W-M Liu, D. M. C. Nicholson, and G. M. Stocks, *Phys. Rev. Lett*. **83**, 207-210 (1999).

9. G. M. Stocks, B. Ujfalussy, X. Wang, D.M.C. Nicholson, W. A. Shelton, Y. Wang, A. Canning, and B. L. Gyorffy, *Philos. Mag.* B **78**, 665 (1998).
10. B. Ujfalussy, B., X. Wang, D.M.C. Nicholson, W. A. Shelton, G. M. Stocks, Y. Wang, and B. L. Gyorffy, J. Appl. Phys. **85**, 4824 (1999).
11. G. M. Stocks, M. Eisenbach, B. Ujfalussy, B. Lazarovits, L. Szunyogh, and P. Weinberger, *Progress in Materials Science* (2006)
12. B. Ujfalussy, B. Lazarovits, L. Szunyogh, G. M. Stocks, and P. Weinberger, *Phys. Rev. B* **70**, 100404(R) (2004).
13. P. A. Gambardella. Dallmeyer, K. Maiti, M. C. Malagoli, W. Eberhardt, K. Kern, and C. Carbone, *Nature* **416**, 301 (2002).
14. D. G. Pettifor, Communications on Physics, 1, 141 (1976)
15. D. M. C. Nicholson and R. H. Brown, Phys. Rev. B 67, 016401 (2003).
16. Y. Wang, G. M. Stocks, A. Rusanu, D. Nicholson & M. Eisenbach, *Proceedings of the Cray User Group* (2006).
17. B.L. Györffy , et al., *Journal of Physics F-Metal Physics* **15**(6), 1337-1386 (1985).
18. Dederichs, P. H., S. Blügel, R. Zeller, and H. Akai, *Phys. Rev. Lett.* **53**, 2512 (1984).
19. W. F. Brown, *Micromagnetics*, (Interscience, New York, 1963)

DOE Sponsored Publications in 2004-2006 (Selected)

1. *"Quantum Mechanical Simulation of Nanocompiste Magnets on CRAY XT3 "*Yang Wang, G.M. Stocks, Aurelian Rusanu, D.M.C. Nicholson, and Markus Eisenbach, Proceedings of CUG, Editor David J. Gigrich, 2006.
2. *"Ground-state valency and spin configuration of the Ni-ions in nickelates",* L. Petit, G. M. Stocks, T. Egami, Z. Szotek, and W.M. Temmerman, *Phys. Rev. Lett.* 97, 146405 (2006)
3. *"On Calculating the Magnetic State of Nanostructures"*, G. M. Stocks, M. Eisenbach, B. Ujfalussy, B. Lazarovits, L. Szunyogh, and P. Weinberger, *Progress in Materials Science* (in press)
4. *"Linear Scaling Ab-initio Method for Nanoscience"*Yang Wang, G.M. Stocks, Aurelian Rusanu, D.M.C. Nicholson, Markus Eisenbach, and J.S. Faulkner, , HPCNano 2006 Workshop, Editor Jun Ni, *Proceedings of SC06*, IEEE Computer Society Press.
5. *"Epitaxial Stabilization of Ferromagnetism in the Nanophase of FeGe*, Changgan Zeng, P. R. C. Kent, M. Varela, M. Eisenbach, G. M. Stocks, Maria Torija, Jian Shen, and Hanno H. Weitering, *Phys. Rev. Lett.* **96**, 127201 (2006)
6. *"Localization/quasi-delocalization transitions and quasi-mobility-edges in shell-doped nanowires*, Zhong J. X., G. M. Stocks, *Nano Letters* 6, 128 (2006).
7. *Electronic Structure and Exchange Coupling of Mn Impurities in III-V Semionductors*, Schulthess, T.C., W. M. Temmerman, Z. Szotek, W. H. Butler, and G. M. Stocks, Nature Materials **4**, 838-844 (2005).
8. *"Intrinsic volume scaling of thermoinduced magnetization in antiferromagnetic nanoparticles"*, G. Brown, A. Janotti, M. Eisenbach, and G. M. Stocks, *Phys. Rev. B* **72**, 140405 (2005).
9. *"Ab-initio spin dynamics applied to nanoparticles: canted magnetism of a finite Co chain along a Pt(111) surface step edge,"* Ujfalussy, B., B. Lazarovits, L. Szunyogh, G. M. Stocks, and P. Weinberger, *Phys. Rev. B* **70**, 100404(R) (2004).

Author Index

Surface and Interface Science at the Atomic Scale
Participant List

Last Name	First Name	Organization	Phone	Email
Allendorf	Sarah	Sandia National Laboratories	925-294-3379	swallen@sandia.gov
Asta	Mark	University of California, Davis	530-754-8656	mdasta@ucdavis.edu
Averill	Frank	Oak Ridge National Laboratory & The University of Tennessee	865-576-6757	2f9@ornl.gov
Baddorf	Arthur	Oak Ridge National Laboratory	865-574-5241	baddorfap@ornl.gov
Bartelt	Norm	Sandia National Laboratories	925-294-3061	bartelt@sandia.gov
Besenbacher	Flemming	Aarhus University (iNANO)	458-942-3604	fbe@inano.dk
Bhattacharyya	Abhishek	Lehigh University	610-758-4232	abb206@lehigh.edu
Bonnell	Dawn	University of Pennsylvania	215-746-3210	ncharles@seas.upenn.edu
Bowen	Kit	Johns Hopkins University	410-516-8425	kbowen@jhu.edu
Browning	Nigel	University of California, Davis	925-424-5563	nbrowning@ucdavis.edu
Budakian	Raffi	University of Illinois, Urbana-Champaign	217-333-3065	budakian@uiuc.edu
Campbell	Geoffrey	Lawrence Livermore National Laboratory	925-423-8276	ghcampbell@llnl.gov
Carim	Tof	US DOE Office Basic Energy Sciences	301-903-4895	altaf.carim@science.doe.gov
Chambers	Scott	Pacific Northwest National Laboratory	509-376-1766	sa.chambers@pnl.gov
Chandrasekhar	Venkat	Northwestern University	847-491-3444	v-chandrasekhar@northwestern.edu
Chang	Y. Austin	University of Wisconsin	608-262-0389	chang@engr.wisc.edu
Chen	Yok	US DOE Office Basic Energy Sciences	301-903-4174	yok.chen@science.doe.gov
Ching	Wai-Yim	University of Missouri, Kansas City	816-235-2503	chingw@umkc.edu
Crabtree	George	Argonne National Laboratory	630-252-5509	crabtree@anl.gov
Dahmen	Ulrich	Lawrence Berkeley National Laboratory	510-486-4627	UDahmen@lbl.gov
Davis	James	Cornell University	607-254-8965	jcdavis@ccmr.cornell.edu
DeGraef	Marc	Carnegie Mellon University	412-268-8527	degraef@cmu.edu
Eastman	Jeffrey	Argonne National Laboratory	630-252-5141	jeastman@anl.gov
Exarhos	Gregory	Pacific Northwest National Laboratory	509-376-4125	greg.exarhos@pnl.gov
Friedman	Daniel	US DOE Office Basic Energy Sciences	301-903-1048	daniel.friedman@science.doe.gov
Gai	Zheng	Oak Ridge National Laboratory	865-574-1648	gaiz@ornl.gov
Gajdardziska-Josifovska	Marija	University of Wisconsin, Milwaukee	414-229-2925	mgj@uwm.edu
Gersten	Bonnie	US DOE Office Basic Energy Sciences	301-903-3427	bonnie.gersten@science.doe.gov
Goldman	Rachel	University of Michigan	734-644-3599	rsgold@umich.edu
Hamilton	John	Sandia National Laboratories	925-294-2457	jchamil@sandia.gov
Hammel	P. Chris	Ohio State University	614-247-6928	hammel@mps.ohio-state.edu
Hla	Saw-Wai	Ohio University	740-593-1727	hla@ohio.edu
Ho	Kai-Ming	Ames Laboratory	515-294-1960	kmh@ameslab.gov
Horton	Linda	Oak Ridge National Laboratory	865-574-5081	hortonll@ornl.gov
Horwitz	James	US DOE Office Basic Energy Sciences	301-903-4894	James.Horwitz@science.doe.gov
Howe	James	University of Virginia	434-975-4247	jh9s@virginia.edu

Surface and Interface Science at the Atomic Scale
Participant List

Last Name	First Name	Organization	Phone	Email
Jiang	Bin	University of Illinois, Urbana-Champaign	217-265-6815	binjiang@uiuc.edu
Kalinin	Sergei	Oak Ridge National Laboratory	865-241-0236	sergei2@ornl.gov
Kapitulnik	Aharon	Stanford University	650-723-3847	aharonk@stanford.edu
Kelley	Richard	US DOE Office Basic Energy Sciences	301-903-6051	richard.kelley@science.doe.gov
Kim	Judy	Lawrence Livermore National Laboratory	925-424-3712	kim46@llnl.gov
Klie	Robert	Brookhaven National Laboratory	631-344-7709	klie@bnl.gov
Kortan	Refik	US DOE Office Basic Energy Sciences	301-903-3308	refik.kortan@science.doe.gov
Kramer	Matthew	Ames Laboratory/Iowa State University	515-294-0276	mjkramer@ameslab.gov
Kung	Harriet	US DOE Office Basic Energy Sciences	301-903-1330	harriet.kung@science.doe.gov
LaGrange	Thomas	Lawrence Livermore National Laboratory	925-424-2383	lagrange2@llnl.gov
Li	Lian	University of Wisconsin, Milwaukee	414-229-5108	lianli@uwm.edu
Lian	Jie	University of Michigan	734-647-5704	jlian@umich.edu
Liu	Feng	University of Utah	801-587-7719	fliu@eng.utah.edu
Lupini	Andrew	Oak Ridge National Laboratory	865-574-6281	9az@ornl.gov
Manoharan	Harindran	Stanford University	650-723-7263	manoharan@stanford.edu
Marks	Laurence	Northwestern University	847-491-3996	L-marks@northwestern.edu
Marquis	Emmanuelle	Sandia National Laboratories	925-294-3287	emarqui@sandia.gov
McCartney	Martha	Arizona State University	480-965-4558	molly.mccartney@asu.edu
McCarty	Kevin	Sandia National Laboratories	925-294-2067	mccarty@sandia.gov
Medlin	Douglas	Sandia National Laboratories	925-294-2825	dlmedli@sandia.gov
Millunchick	Joanna	University of Michigan	734-647-8980	joannamm@umich.edu
Moler	Kathryn	Stanford University	650-723-6804	kmoler@stanford.edu
Napolitano	Ralph	Ames Laboratory/Iowa State University	515-294-9101	ralphn@iastate.edu
Novotny	Lukas	University of Rochester	585-275-5767	novotny@optics.rochester.edu
Painter	Gayle	Oak Ridge National Laboratory	865-574-5164	gsp@ornl.gov
Parks	Joel H.	Rowland Institute at Harvard University	617-497-4653	parks@rowland.harvard.edu
Pennycook	Stephen	Oak Ridge National Laboratory	865-574-5504	pennycooksj@ornl.gov
Petford-Long	Amanda	Argonne National Laboratory	630-252-5480	petford.long@anl.gov
Plummer	Ward	Oak Ridge National Laboratory & The University of Tennessee	865-574-5503	eplummer@utk.edu
Radmiloic	Velimir	Lawrence Berkeley National Laboratory	510-486-5663	VRRadmilovic@lbl.gov
Ruan	Chong-Yu	Michigan State University	517-355-9200 x2212	ruan@pa.msu.edu
Rühle	Manfred	Max-Planck-Institut für Metallforschung	49-711-689-3520	ruehle@mf.mpg.de
Salmeron	Miquel	Lawrence Berkeley National Laboratory	510-486-6230	mbsalmeron@lbl.gov
Schofield	Marvin	Brookhaven National Laboratory	631-344-3507	schofield@bnl.gov
Sinnott	Susan	University of Florida	352-846-3778	ssinn@mse.ufl.edu
Spence	John	Arizona State University	480-965-6486	spence@asu.edu
Stemmer	Susanne	University of California, Santa Barbara	805-893-6128	stemmer@mrl.ucsb.edu

Surface and Interface Science at the Atomic Scale
Participant List

Last Name	First Name	Organization	Phone	Email
Stocks	Malcolm	Oak Ridge National Laboratory	865-574-5163	stocksgm@ornl.gov
Stumpf	Roland	Sandia National Laboratories	925-294-6114	rrstump@sandia.gov
Sutter	Peter	Brookhaven National Laboratory	631-344-3109	psutter@bnl.gov
Swartzentruber	Brian	Sandia National Laboratories	505-844-6393	bsswart@sandia.gov
Thuermer	Konrad	Sandia National Laboratories	925-294-4564	kthurme@sandia.gov
Tortorelli	Peter	Oak Ridge National Laboratory	865-574-5119	tortorellipf@ornl.gov
Tringides	MIchael	Ames Laboratory/Iowa State University	515-294-6439	tringides@ameslab.gov
Varela	Maria	Oak Ridge National Laboratory	865-574-6287	mvarela@ornl.gov
Vetrano	John	US DOE Office Basic Energy Sciences	301-903-5976	john.vetrano@science.doe.gov
Vitek	Vaclav	University of Pennsylvania	215-898-7883	vitek@seas.upenn.edu
Wang	Cai-Zhuang	Ames Laboratory	515-294-6934	wangcz@ameslab.gov
Wendelken	John	Oak Ridge National Laboratory	865-574-6290	wendelkenjf@ornl.gov
Yang	Jianhua	University of Wisconsin, Madison	608-262-2088	jianhuay@cae.wisc.edu
Yang	Judith	University of Pittsburgh	412-624-8613	jyang@engr.pitt.edu
Zhu	Jane	US DOE Office Basic Energy Sciences	301-903-3811	jane.zhu@science.doe.gov
Zhu	Yimei	Brookhaven National Laboratory	631-344-3057	zhu@bnl.gov
Zuo	Jian-Min	University of Illinois, Urbana-Champaign	217-244-6504	jianzuo@uiuc.edu